

A STUDY OF THE TIN MINERALIZATION AND LITHOGEOCHEMISTRY
IN THE AREA OF THE WEDGEPORT PLUTON,
SOUTHWESTERN NOVA SCOTIA

159
2145
750
Pocket

by

Isobel K. Wolfson

Submitted in partial fulfillment
of the requirements for the degree of Master of Science at
Dalhousie University, Halifax, Nova Scotia, Canada, on
July 20, 1983

COPYRIGHT © ISOBEL K. WOLFSON, 1983

DALHOUSIE UNIVERSITY

DEPARTMENT OF GEOLOGY

The undersigned hereby certify that they have read and recommended to the Faculty of Graduate Studies for acceptance a thesis entitled "A Study Of The Tin Mineralization And Lithogeochemistry In The Area Of The Wedgeport Pluton, Southwestern Nova Scotia"

by Isobel K. Wolfson

in partial fulfillment of the requirements for the degree of Master of Science.

Dated September 15th, 1983

External Examiner _____

Research Supervisor _____

Examining Committee _____

DALHOUSIE UNIVERSITY

Date _____

Author Isobel K. Wolfson

Title A Study Of The Tin Mineralization And Lithogeochemistry In The Area

Of The Wedgeport Pluton, Southwestern Nova Scotia

Department or School Geology

Degree M.Sc. Convocation Fall Year 1983

Permission is herewith granted to Dalhousie University to circulate and to have copied for non-commercial purposes, at its discretion, the above title upon the request of individuals or institutions.

Signature of Author

THE AUTHOR RESERVES OTHER PUBLICATION RIGHTS, AND NEITHER THE THESIS NOR EXTENSIVE EXTRACTS FROM IT MAY BE PRINTED OR OTHERWISE REPRODUCED WITHOUT THE AUTHOR'S WRITTEN PERMISSION.

TABLE OF CONTENTS

	PAGE
LIST OF FIGURES	v
LIST OF TABLES	x
ABSTRACT	xi
ACKNOWLEDGEMENTS	xii
CHAPTER 1 INTRODUCTION	1
1.1 General Statement	1
1.2 Physiography and Surficial Geology	1
1.3 Regional Setting	4
1.4 Previous Work	7
1.5 Economic Geology	9
1.6 Purpose and Methods of Study	10
CHAPTER 2 LOCAL GEOLOGY AND PETROLOGY	13
2.1 Introduction	13
2.2 Metasedimentary Lithologies	24
2.2.1 Meta-pelitic Lithologies	24
2.2.2 Meta-psammitic Lithologies	31
2.3 Plutonic Lithologies	42
2.3.1 Wedgeport Pluton	42
2.3.2 Mafic Dykes	65
CHAPTER 3 ORE PETROLOGY	72
3.1 Introduction	72
3.2 Vein Systems	72
3.2.1 Veins Within Metasediments	73
3.2.1.1 Pre-mineralization Veins	74

	PAGE
3.2.1.2 Main Stage Veins	74
3.2.1.3 Post-mineralization Veins ...	88
3.2.2 Veins Within Pluton	93
3.2.2.1 Pre-greisen Veins	93
3.2.2.2 Greisen Veins	94
3.2.2.3 Post-greisen Veins	98
3.3 Stratiform Mineralization	101
3.3.1 Unmineralized Sulphide Zones	106
3.3.2 Mineralized Sulphide Zones	118
3.4 Cassiterite - Description	129
3.4.1 Stratiform Association	129
3.4.2 Stratiform Sulphide Association ...	130
3.4.3 Stratiform Calcareous Sulphide Association	137
3.4.4 Vein Association in the Metasediments	140
3.4.5 Greisen Association	143
3.5 Cassiterite - Temperature of Formation ...	150
3.6 Cassiterite - Genesis	152
3.6.1 Detrital	153
3.6.2 Main Stage Vein Genesis	156
3.6.2.1 Greisen Veins	157
3.6.2.2 Metasediment Veins	165
3.6.3 Stratiform Mineralization	168
3.6.3.1 Syngedimentary / Diagenetic Origin	169
3.6.3.2 Epigenetic Origin	177
CHAPTER 4 GENERALIZED MODEL OF TIN GENESIS	183
4.1 Introduction	183
4.2 Origin of Tin in Sediments and Magma	183
4.3 Magma Emplacement	185
4.4 Fluid Genesis	186
CHAPTER 5 TRACE ELEMENT LITHOGEOCHEMISTRY	191
5.1 Introduction	191
5.2 Population Partitioning	196

	PAGE
5.3 Discussion	200
5.3.1 Relationship of Elements With Respect to Different Lithologies	214
5.3.2 Relationship of Elements With Respect to Style of Mineralization	216
5.3.3 Relationship of Elements With Respect to Distance From the Pluton	237
5.3.4 Relationship of Elements With Respect to Other Variables	239
5.4 Summary	244
 CHAPTER 6 CONCLUSIONS AND RECOMMENDATIONS FOR FURTHER WORK AND EXPLORATION	 258
6.1 Conclusions	258
6.2 Possible Guides for Tin Exploration	259
6.3 Recommendations for Further Work	261
 APPENDIX I SAMPLE PREPARATION	 264
APPENDIX II ANALYTICAL METHODS	267
APPENDIX III GEOCHEMICAL REFERENCE MATERIALS AND DETERMINATION OF ANALYTICAL ACCURACY AND PRECISION	286
APPENDIX IV PARTITIONING OF POLYMODAL DISTRIBUTIONS	318
APPENDIX V VARIATION OF TRACE ELEMENTS WITH DISTANCE FROM PLUTON	367
SELECTED BIBLIOGRAPHY	385

LIST OF FIGURES

FIGURE	DESCRIPTION	PAGE
	Geology of the study area	Back pocket
1.1	Location of the study area	3
2.1	Scour within meta-argillite	16
2.2	Soft sediment deformation within meta- argillite	16
2.3	Facies change within metasediment	18
2.4	Foliated meta-argillite with elongate pyrrhotite blebs	21
2.5	Ptygmatic quartz veinlets	23
2.6	Mineralized zone displaced by late calcite vein	23
2.7	Crenulated meta-argillite	27
2.8	Chiastolite within carbonaceous meta-argillite	30
2.9	Typical meta-wacke	33
2.10	Na ₂ O:K ₂ O contents of metasediments	35
2.11	Layered calc-silicates	38
2.12	Layered garnet	41
2.13	Calc-silicate nodule	41
2.14	Metasediment-pluton contact	44
2.15	Modal QAP ternary diagram for plutonic lithologies	46
2.16	Normative Qtz-Ab-Or ternary diagram	48
2.17	K ₂ O-Na ₂ O-CaO variation diagram	50

FIGURE	DESCRIPTION	PAGE
2.18	Ferrous/Ferric ratio of monzogranite	52
2.19	F/100-Sn-Li/10 variation diagram	56
2.20	Diversity of monzogranite textures	59
2.21	Effects of mafic dykes upon monzogranite ...	59
2.22	Fresh and weathered monzogranite	64
2.23	"Rusty shear" in monzogranite	67
2.24a	Lamprophyre dyke	71
2.24b	Olivine diabase dyke	71
3.1	Early quartz-arsenopyrite veinlet cut by crenulation cleavage	77
3.2	Main stage veinlets with biotite and iron oxide selvages	77
3.3a	Sulphide-cassiterite veinlet with chlorite- cassiterite selvedge	79
3.3b	Above veinlet in thin section	79
3.4	Veinlet of intergrown pyrite, sphalerite and cassiterite	84
3.5	Veinlet of concentric graphic pyrite after pyrrhotite	84
3.6a	Main stage veinlet cut by later pyrite veinlet	86
3.6b	Stratiform sulphide layer cut by later pyrite veinlet	86
3.7	Chlorite compositions of samples in veins and metasediments	90
3.8	Quartz veinlet barrier to greisen alteration	97
3.9	Greisen in sharp contact with wallrock	97
3.10	Progressive alteration of monzogranite to greisen	100
3.11	Post greisen quartz-kaolinite veinlet	100

FIGURE	DESCRIPTION	PAGE
3.12	Sheared monzogranite	103
3.13	Pyrrhotite disseminations in meta-wacke	105
3.14	Stratiform pyrrhotite in carbonaceous meta-argillite	108
3.15a	Anhedral pyrrhotite altered to graphic pyrite	110
3.15b	Pyrrhotite altered to pyrite and marcasite .	110
3.16	"Shredded-textured" pyrrhotite in biotite meta-wacke	112
3.17	Diagenetic(?) arsenopyrite in coarse meta- wacke	115
3.18a	Blue mineralized zone in drill core	118
3.18b	Blue mineralized zones in thin section	118
3.19a	Stratiform sphalerite-pyrite-chlorite in drill core	120
3.19b	Above mineralization in thin section	120
3.20	Blue mineralized zone displaced by fine veinlet	123
3.21	Carbonaceous calcite layer with cassiterite	123
3.22	Replacement textures in stratiform sulphide zones	127
3.23	Broken zoned cassiterite crystal	132
3.24	Zoned euhedral cassiterite	132
3.25	Zoned twinned cassiterite with colourless overgrowth	134
3.26	Cassiterite aggregate within a microscour ..	136
3.27	Granular cassiterite in a meta-siltstone ...	139
3.28a	Prismatic cassiterite aggregate in a carbonaceous calcite layer	142

FIGURE	DESCRIPTION	PAGE
3.28b	Prismatic cassiterite intergrown with pyrrhotite	142
3.29	Subhedral zoned vein cassiterite	145
3.30	Botryoidal cassiterite in halo adjacent sulphide-cassiterite veinlet	145
3.31a	Late stage spherulitic vein cassiterite	147
3.31b	Acicular vein cassiterite druse on pyrite ..	147
3.32	Subhedral greisen cassiterite	149
3.33	Progression of alteration in greisenized monzogranite	163
5.1	Location map of diamond drill holes sampled for litho-geochemistry	193
5.2	Trace element variation with lithology and mineralization in meta-argillites	203
5.3	Trace element variation with lithology and mineralization in meta-wackes	207
5.4	Trace element variation with lithology and alteration in pluton	211
5.5	Variation of Sb and Bi with As content in veins in the metasediments	219
5.6	Variation of various metals with Sn content in veins in the metasediments	221
5.7	Metal zonation in main stage veins with respect to distance from pluton	224
5.8	Variation of major oxides and minor elements in plutonic samples from study area and other locations	227
5.9	Variation of Sb and Bi with As content in mineralized 'patches'	232
5.10	Variation of Sn and Cu within mineralized 'patches' and greisens	234
5.11	Variation of Sn and Bi within mineralized 'patches'	236

FIGURE	DESCRIPTION	PAGE
5.12	Pseudo-three-dimensional sections of intersecting and parallel drill hole grids ..	242
III-1	Accuracy of trace element analyses	296
III-2	Accuracy of whole rock analyses	302
III-3	Precision of trace element analyses	308
III-4	Precision of whole rock analyses	314
IV-1	Idealized cumulative frequency graph	322
IV-2	Cumulative frequency graph of tungsten in plutonic samples	324
IV-3	Cumulative frequency graphs of 11 elements in three lithologies(33 graphs)	334
V-1	Variation of selected trace elements in two cross-sections(16 figures)	368

LIST OF TABLES

TABLE	DESCRIPTION	PAGE
2.1	Monzogranite, S- and I-type granite characteristics	53
2.2	Major element ratios of monzogranite, 'normal' and 'specialized' granites	54
3.1	Mineralogy of vein systems	80
3.2	Mineral paragenesis in main stage veins	91
3.3	Cassiterite crystal habits and related temperatures of formation	151
3.4	Major mineral and element changes during greisenization	159
5.1	Background and threshold values of lithologies in study area and average values in various other lithologies	201
5.2	Summary of lithogeochemical results	246
II-1	Elements analysed, methods and detection limits	268
II-2	Trace element contents of selected drill core samples	273
II-3	Whole rock geochemistry	282
III-1	Trace element reference standard analyses ...	291
III-2	Whole rock duplicate and reference standard analyses	292
III-3	Trace element duplicate analyses	293

ABSTRACT

Cassiterite and base metal sulphides have recently been discovered in Yarmouth County, southwestern Nova Scotia, in an area of folded and metamorphosed Cambro-Ordovician turbidites of the Meguma Group intruded by the monzogranitic Wedgeport pluton.

Several kinds of tin mineralization occur:

1. rare detrital cassiterite grains in a pelitic 'microscour'.
2. stratiform sulphide-cassiterite replacement bodies in calcareous layers.
3. sulphide-cassiterite veinlets in metasediments with restricted chlorite alteration.
4. rare sulphide-cassiterite veinlets in pluton with restricted greisen alteration.

Cassiterite occurs in several habits:

1. equant - in detrital, stratiform replacement bodies and veins.
2. prismatic - in stratiform replacement bodies.
3. acicular - in veins.
4. botryoidal - in stratiform replacement bodies (rare) and veins.

Geochemical analysis of drill core show that most background values in the metasediments and pluton are low compared to lithologies in the Cornish tin district and specialized ore-bearing granitoids. The sulphide-cassiterite veinlets exhibit a mineralogical and therefore geochemical variation with distance from the pluton: from Mo and W within 2 km of the pluton, to Sn about 3 to 4 km distant, to Pb and Zn about 4 to 7 km distant.

ACKNOWLEDGEMENTS

Much of the thesis could not have been accomplished without the help and support of many people.

Financial support was provided partly by the Dalhousie University Graduate Fellowship for 1980-81 and 1981-82. Further support was obtained from Energy, Mines and Resources Research Agreement Number 10614/81 and the Natural Sciences and Engineering Research Council of Canada Operating Grant A-9036 of Dr. Marcos Zentilli.

Mr. Paul Sinclair of Shell Canada Resources Limited graciously provided accomodation at the East Kemptville base camp and access to more than 11 km of drill core.

Mr. Gordan Brown provided the scores of thin and polished sections with his usual expertise. Mr. Bob MacKay patiently explained and assisted in the wonders of the microprobe. Mrs. Ann Bonhom took on the arduous task of crushing core samples. The many tables were typed by Mrs. Barb Cossar.

Special thanks go to Dr. Marcos Zentilli for his support and many insightful discussions about economic geology and computers.

Much appreciated was the support of my family and the

friendship and support of fellow Dalhousians: Marie-Claude Blanchard who didn't mind 500 lbs of core in our office, and who made shoptalk over coffee and doughnuts an interesting experience-, Anita DeIure, Mark Williamson, Mrs. Armgard Zentilli (for her nourishing feasts), Dr. Barrie Clarke for critically reading part of the thesis, Milton Graves, Phil Hill, and my examining committee, who had to read this thesis maximus.

Last, but not least, thanks are due to Mr. Gregory B. Tucker, draftsperson and husband extraordinaire, who encouraged me in all my endeavors and added a lot to Ma Bell's revenues.

CHAPTER ONE

INTRODUCTION

1.1 General Statement

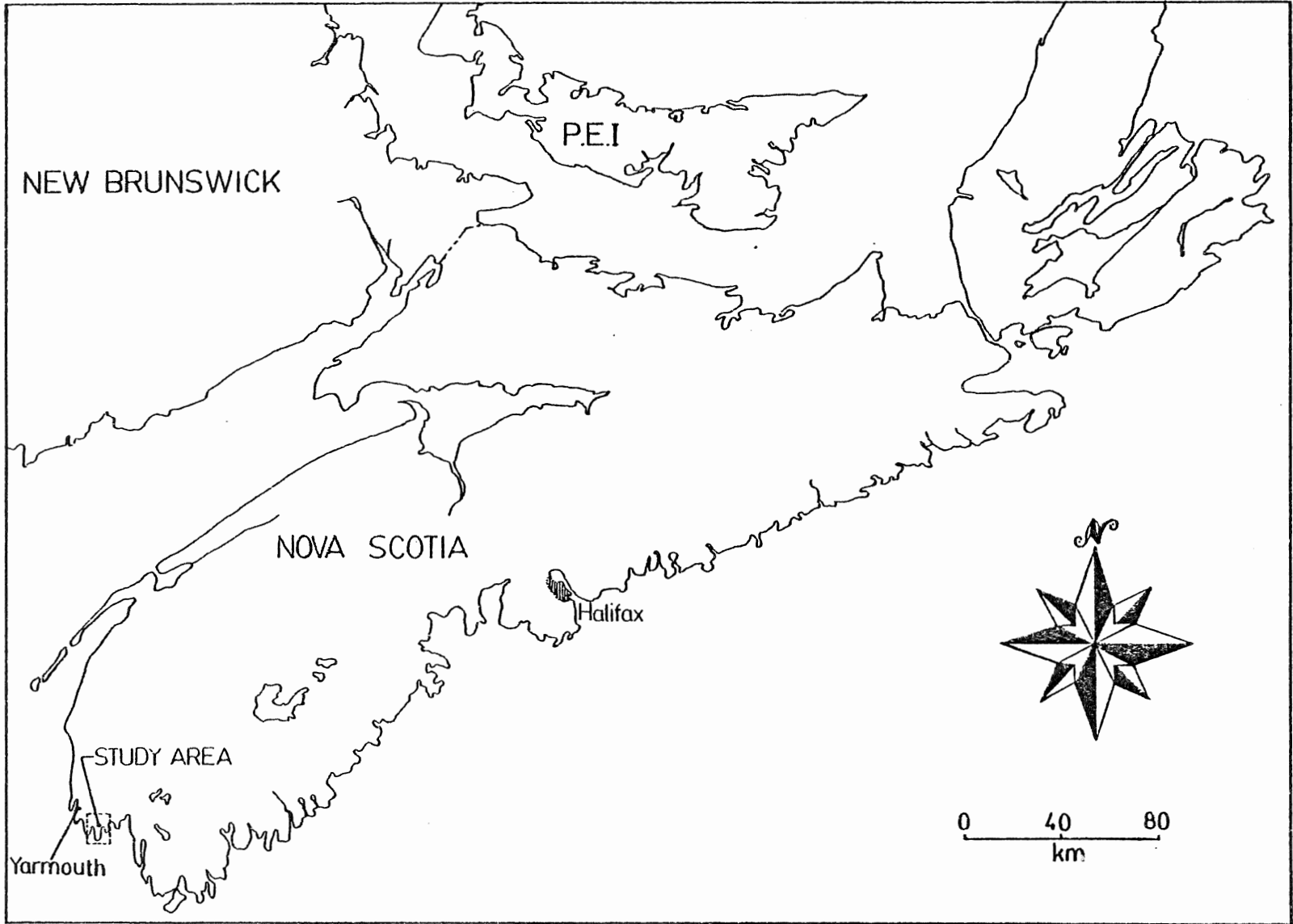
Cassiterite mineralization was discovered in the Wedgeport area in 1976 to 1977 by Millmor Syndicate and Shell Canada Resources Limited. It consists of a veinlet stockwork in the margin of the Wedgeport monzogranite, and both vein and stratiform styles in the surrounding turbidite sequences of the Goldenville Formation. The study area is situated along the coast of southwestern Nova Scotia in Yarmouth County, about 10 km southeast of the town of Yarmouth (Fig. 1.1). It covers an area of approximately 240 km². Access is gained by provincial highway 103 from Halifax to Yarmouth, and secondary paved and dirt roads. Yarmouth is also linked to Halifax by the CNR railway line and by daily air service. Generalized geology of the area is shown in the map in the back pocket of the thesis.

1.2 Physiography and Surficial Geology

The study area is part of the Atlantic Uplands, a low-lying region with rolling hills of up to 50 m relief

Figure 1.1

Location of the study area in
southwestern Nova Scotia.



(Sinclair, 1978); small lakes, swamps and streams occur in between. The coast is a submergent one and is characterized by salt marshes, tidal flats, bays, peninsulas and islands.

Drainage toward the south is controlled by the Tusknet River to the east and the Chebogue and Little Rivers to the west (Taylor, 1967).

Bedrock exposure is limited to the coastline, rivers and lakeshores, with minor occurrences along road and railway cuts. Most of the region is covered by Pleistocene deposits of the Wisconsinan glaciation. Sandy till (up to 18 m in thickness), with boulders (up to 7 m across) of the underlying bedrock is the main type of drift; stratified outwash and ice contact deposits of sand and gravel occur locally (Sinclair, 1978). Two ice lobes may have existed in this area, one moving south-southeast, the other south-southwest (Cant et al., 1978; Taylor, 1967).

1.3 Regional Setting

Tin mineralization is found in both the Goldenville Formation of the Cambro-Ordovician Meguma Group and the Wedgeport pluton. The sediments are part of a thick sequence (at least 10 km; Schenk, 1975) of turbiditic wackes and slates, partly interfingered with, and partly overlain by, the pelitic Halifax Formation. Rare graptolites in both

formations indicate an Early Ordovician period of sediment deposition. K-Ar ages from detrital muscovite in sandstone, provide ages of 476 ± 19 Ma and 496 ± 20 Ma (Harris and Schenk, 1975). The sediments are believed to have been derived from a large, low-lying continental mass of granodioritic and metasedimentary composition; they were deposited by channelized turbidites ('contourites'), overflow turbidites and bottom currents (Schenk and Lane, 1982).

The Meguma Group is overlain, mostly conformably, by Late Ordovician to Early Devonian volcanic rocks and detrital sedimentary rocks of the White Rock, Kentville, New Canaan, and Torbrook Formations (Schenk, 1975).

The Paleozoic strata were subsequently tightly folded and regionally metamorphosed to greenschist, locally almandine-amphibolite facies, during the mid-Devonian Acadian Orogeny (Taylor, 1967). These folds were offset by northwest-trending, mainly sinistral, faults with horizontal displacements of up to 6 km (Harris and Schenk, 1975).

Following these events, the South Mountain batholith and related satellite stocks were emplaced at relatively shallow depths in the crust (about 4 to 10 km; McKenzie and Clarke, 1975), causing local thermal metamorphism (Reynolds et al., 1981). The batholith covers $1/3$ to $1/2$ of western Nova Scotia, outcropping over about $10\,000\text{ km}^2$. The batholith is

predominantly of granodioritic to monzogranitic composition, but parts of it may range from norite and tonalite to syenogranite in composition (McKenzie and Clarke, 1975; Clarke et al., 1980). Stratigraphic relationships indicate that the batholith was emplaced after the Acadian Orogeny, from the mid-Devonian to Early Carboniferous. Age dating of 28 mica samples from the batholith and various northern satellite stocks by K-Ar and $^{40}\text{Ar}/^{39}\text{Ar}$ yield a mean age of 367 Ma (Reynolds et al., 1981). Clarke and Halliday (1980), constructing Rb-Sr isochrons from whole rocks and mineral separates, estimated the age of granodiorite emplacement at 371.8 ± 2.2 Ma and that of adamellite emplacement at 364.3 ± 1.3 Ma. Dating of 14 mica samples from southern satellite stocks (including the Wedgeport pluton) yield younger ages (258-353 Ma). This may be due to either actual intrusion during the Late Carboniferous or to a thermal or tectonic event(s) which partially degassed the rocks or, less probably to protracted cooling to argon blocking temperatures (Reynolds et al., 1981). The Brenton pluton near the study area is a cataclastic granite with foliation parallel to regional schistosity and was believed intruded before or during the Acadian Orogeny; 6 analyses of both biotite and muscovite yield apparent Ar ages of from 314 to 328 Ma, suggesting emplacement during the Late Carboniferous before or during a period of deformation ('Maritime Disturbance').

Analysis of chloritized biotite from the Wedgeport pluton reveals apparent ages of 258 to 175 Ma (Permian to Jurassic) and may be associated with a mineralizing event; the younger ages are probably due to resetting (degassing) by Triassic mafic dykes. Muscovite and biotite from mineralized greisen and pegmatite of the Davis Lake pluton yield ages from 335 to 267 Ma (average of 290 Ma). Biotites from a granitoid body near this pluton give an average age of 272 Ma. These young ages again imply some kind of intrusive, tectonic, or hydrothermal event in the Late Carboniferous to Permian (Reynolds and Zentilli, in prep; Reynolds et al., 1981).

1.4 Previous Work

Prior to 1950, preliminary mapping was carried out by such geologists as C.T. Jackson and F. Alger in 1828, A. Gesner in the first half of the nineteenth century, L.W. Bailey in 1898, E.R. Faribault in the early twentieth century, and S. Powers in 1915 (Taylor, 1967).

Gravity and aeromagnetic maps of southwestern Nova Scotia have been produced by G.D. Garland, and the Geological Survey of Canada in the nineteen fifties (Taylor, 1967); the Nova Scotia Department of Mines and the G.S.C. in 1977 produced airborne gamma ray spectrometric maps covering the South Mountain batholith of southern Nova Scotia (Chatterjee

and Muecke,1982; Sinclair,1978).

R.W Boyle and others in the late fifties analysed water and sediment samples from streams, rivers and lakes of the southwestern part of the province for Cu, Pb and Zn (Taylor,1967).

A more detailed investigation of the geology of the study area was made by Taylor (1967), in which he described the sedimentary Meguma Group, the volcano-sedimentary White Rock Formation, and the various intrusive felsic and mafic rocks; he made a preliminary study of the area's structure and metamorphic characteristics and assembled a list of metal and industrial mineral locations.

Further refinement of the geology was accomplished in the fields of: the Meguma Group (Schenk and Lane,1982; Schenk,1975; Harris and Schenk,1975); the White Rock Formation (Lane,1975; Sarkar,1978); structural geology by Fyson in 1966 and Keppie in 1977 (Cullen,1983); geochronology of intrusions (Reynolds and Zentilli,in prep; Reynolds et al.,1981; Clarke and Halliday,1980) and Meguma Group slates (Reynolds et al.,1973); and metamorphic petrology by Taylor and Schiller in 1966, Muecke in 1973, Keppie and Muecke in 1979, Clarke and Muecke in 1980 (Cullen,1983), and J. Cullen (1983). Pleistocene glacial history has been described by Grant and Gravenor (Sinclair,1978).

1.5 Economic Geology

Only minor exploration took place in the region before 1975. Three small gold occurrences were worked in the late nineteenth and early twentieth centuries. Beryl- and spodumene-bearing pegmatites and veins are found at several localities (e.g. Brazil Lake, Port Joli and Shelburne granodiorites). One very small molybdenite occurrence is near the Jordan River, within a series of quartz veins. Granodiorite, hornblende diorite and quartz diabase were once quarried for building stone. From 1945 to 1960, quartzite beds of the White Rock Formation at Cheggogin Point were quarried for the production of silica brick (Taylor, 1967).

Prior to 1977, prospecting for Cu, Pb, Zn, Sn, W, Ag, and Mo was performed by Chib-Kayrand Copper Mines, Cuvier Mines, Quebec Uranium Mining Corporation and Lacana Mining Corporation (Sinclair, 1978). Discovery of sulphide-bearing boulders in gravel pits by Millmor Syndicate in 1976 resulted in staked claims and subsequent optioning of the property to Shell Canada Resources Limited. In 1978 a tin deposit was discovered about 35 km northeast of Yarmouth, near East Kemptville. Tin, in the form of cassiterite, occurs with various sulphides within a 100 m thick, 500 by 1500 m zone of sericitized and greisenized rocks of the Davis Lake pluton, a part of the South Mountain batholith. By 1982, reserves were

estimated at 38 million tonnes with a grade of 0.2 % Sn and a 0.1 % Sn cutoff grade (Richardson et al., 1982).

Shell Canada Resources Limited undertook an exploration program in the study area, performing airborne and ground geophysical surveys, geologic mapping where possible, geochemical sampling (soil and rock), mineralized boulder tracing, and overburden and diamond drilling. Most diamond drill holes were located over geophysical anomalies. From 1977 to 1978, 80 holes were drilled for a total of about 10 600 m; in 1979 only 8 holes were drilled for a total of about 650 m; and 1980, 3 holes were drilled, totalling about 280 m. The anomalies were found to be due to pyrrhotite and graphite in the metasediments, sulphide stringers in both the metasediments and pluton, and to magnetic mafic dykes. Because of the unsatisfactory results, the company decided against further work in the area (Cant et al., 1978; Cant, 1979; Sarkar, 1980). This area and the East Kemptville deposit are currently owned by Rio Algom Limited.

1.6 Purpose and Methods of Study

Tin and base metal mineralization have only recently been discovered within southwestern Nova Scotia. Subsequent exploration for these metals may be aided by a knowledge of their mode of formation. In an attempt to understand the

genesis of tin and associated metals, the thesis had several basic objectives.

1. To determine the type of tin mineralization. In what form does it occur with respect to veins, sedimentary and igneous host rocks? With what minerals is tin associated? What is its relationship with the pluton?
2. To determine the general type and extent of alteration associated with mineralization.
3. To determine the distribution of a selected group of metals in the metasediments and pluton, and establish background and threshold values for these lithologies.

Because of the limited exposure of both the pluton and country rock (mainly along part of the western shoreline), the thesis is based upon the study of about 11.5 km of drill core. Core logs, drill hole cross-sections and plan maps of all 91 drill holes in the area were studied in order to select core with such features as: vein systems, stratabound mineralization, unmineralized zones, and various structures like foliations, fractures and breccias.

Four weeks were spent sampling the core stored at the base camp of Shell Canada Resources Limited near East Kemptville. Core and reference samples (122 in total) were cleaned, powdered and sent for geochemical analysis to X-Ray

Assay Laboratories Limited in Toronto. Thin and polished sections(almost 200 in total) of relevant samples were made, described and analyzed by microprobe.

This detailed study of tin mineralization in and around the Wedgeport pluton should contribute to the overall understanding of tin genesis in Nova Scotia and assist in subsequent exploration programs.

CHAPTER TWO

LOCAL GEOLOGY AND PETROLOGY

2.1 Introduction

The study area comprises about 240 square km of part of the Lower Paleozoic Meguma Group metasediments with later intrusive monzogranite and basic dykes. Because of the paucity of outcrop, the petrologic study was performed on sections of diamond drill core, using a combination of microscope, microprobe and geochemical methods. All microprobe and chemical analyses are tabulated in the Appendices. Modal compositions were visually determined with the aid of percent comparison charts (Terry et al., 1955).

The core consists of a monotonous metamorphosed sequence of interbedded wackes, siltstones and argillites of the upper members of the Goldenville Formation flysch. Black carbonaceous pelitic layers are also present and may represent coeval, interfingering parts of the Halifax Formation (Schenk, 1975; Harris and Schenk, 1975). Bedding contacts are usually sharp, with minor gradational sequences.

Bedding thickness varies, from less than 1 cm to about 7 m (Taylor, 1967); similar lithologies found along the eastern

shore of Nova Scotia have maximum thicknesses greater than 50 m (Harris and Schenk, 1975). The core generally has thin to medium bedding (3-30 cm).

The meta-wackes and meta-siltstones are commonly structureless, with minor graded bedding, cross-bedding, flutes (Fig. 2.1), and argillaceous rip-up clasts. Minor slump features occur within the pelitic units (Fig. 2.2). Calcareous concretions, metamorphosed to calc-silicate nodules occur within particular psammitic layers and are described by Cullen (1983).

Because the study is based on drill core, continuity of individual layers is unknown. One sample of drill core exhibits a facies change in an open fold (sedimentary slump?), from carbonaceous argillite to biotite meta-wacke (Fig. 2.3).

This sedimentary package was affected by low grade greenschist facies regional metamorphism (Cullen, 1983), folding, intrusion by the Wedgeport pluton (with associated thermal metamorphism to the hornblende hornfels facies), faulting, and intrusion by a series of mafic dykes. Airborne and ground geophysical surveys performed by Shell Canada Resources (electromagnetic, magnetic and induced polarization) plus dip orientations of core and outcrop indicate the presence of several northerly-plunging synclines and anticlines in the study area (Cant et al., 1978).

Figure 2.1

Contact of scoured meta-argillite with upper meta-wacke. Note light coloured current marks rich in ilmenite(altered to leucoxene and rutile) and zircon. Note silver white angular arsenopyrite.

Sample 77-34-86.13

Figure 2.2

Meta-argillite exhibiting contorted soft sediment deformation and linear clusters of pyrrhotite and pyrite.

Sample 80-03-118



Figure 2.3

Facies change within a...
 very much...
 central...
 ...
 biotite...
 ...

Sample 77-11-10-33



Figure 2.3

Facies change within an open fold (sedimentary slump?). Graphitic meta-argillite and central meta-wacke (with green blades of ?) grade laterally to the right into biotite meta-wacke.

Sample 77-31-105.38

The as...
the first...
degrees...
metamorphic...
parallel orientation of...
blebs of...
as a set of...
cleavages...
degrees...
kinked...
Meta-p...
some...
either...
fracture...
to the...
contact...
metamorphic...
development...



The...
narro-...
with...
a pyro...
observed...

The meta-pelitic rocks usually possess two foliations: the first is parallel or at low angles (up to about 40 degrees, depending on location of sample in the folded metasediments) to bedding planes and manifests itself by parallel orientation of phyllosilicate minerals or elongate blebs of pyrrhotite (Fig. 2.4); the second foliation occurs as a set of crenulations which in many places develop into cleavages, and are usually oriented at high angles (50-90 degrees) to the first foliation. Pre-existent veinlets are kinked, ptygmatically folded or broken (Fig. 2.5).

Meta-psammitic lithologies exhibit the first foliation in the same manner as the meta-pelites but the second foliation is either absent or manifested as quartz-calcite-filled tension fractures (but may be of later origin), also at high angles to the first foliation.

The metasediments are in sharp, sometimes parallel contact with the Wedgeport pluton and exhibit thermal metamorphic features such as hornfelsic texture and development of biotite, cordierite, andalusite and garnet. The intrusion dips steeply under the metasediments.

Both metasediments and pluton are faulted, exhibiting narrow (up to about 1 metre wide) shear and breccia zones with associated late stage veins (calcite-quartz-arsenopyrite ± pyrite). Minor displacement, on the order of several cm is observed in drill core (Fig. 2.6); aeromagnetic maps show a

Figure 2.4

Carbonaceous meta-argillite and meta-argillite with metamorphic biotite in bedding planes. Foliated pyrrhotite blebs occur at an angle to bedding.

Sample 77-31-111.97



Foliation
Bedding

Figure 2.5

Meta-argillite cut by early quartz-calcite veinlets, which are both ptlygmatically folded and cut by crenulation cleavage.

Sample 78-10-10

Figure 2.6

Blue mineralized zone in meta-wacke containing fine sulphide hair veinlets and cut and displaced by a late calcite vein.

Sample 77-25-197.8

sniff
nearby
(Culler
are an
north
diab
the p
these
Shell



The
resulting
calcite is
zones



pale
grays
conce
carbo

shift in the position of a pyrrhotite-bearing sedimentary member (Cant et al., 1978) by several hundreds of metres (Cullen,1983). Pre-existent veins are stretched; sulphides are smeared along phyllosilicate grain boundaries.

The lithologies are also cut by northeast- and northwest-, rarely north-trending lamprophyre and olivine diabase dykes. They have roughly the same orientations as the previously described faults and may have intruded along these pre-existent planes of weakness. They were mapped by Shell Resources by airborne electromagnetic surveys and by drill intersections.

The upper 20 to 30 m of the core are weathered, resulting in oxidation of sulphides and dissolution of calcite in veinlets and tension fractures, leaving vuggy zones.

2.2 Metasedimentary Lithologies

2.2.1 Meta-pelitic Lithologies

In drill core, the meta-pelites range in colour from pale greenish grey and greyish green to bluish green to greyish blue to black; this is a manifestation of the concentrations of chlorite, muscovite, quartz, feldspar and carbonaceous material (graphite;Cullen,1983).

Pelitic rocks generally consist of medium to coarse,

silt-sized (averaging 0.03 mm) aggregates of chlorite, muscovite, quartz and feldspar (albitic; in places, potassic), with minor amounts of coarser ilmenite (about 0.1 mm), pyrite and pyrrhotite, finer anhedral to euhedral zircon and sphene (about 0.01 mm), and variable concentrations of extremely fine-grained graphite (≤ 0.003 mm). Several whole rock geochemical analyses are tabulated in Appendix II.

Flakes and needles of chlorite and muscovite are usually tightly intergrown with their long axes defining the foliation. They may be intergrown with roughly equant subangular to subrounded grains of strained quartz and feldspar. Grain contacts range from straight to curved; less commonly they are embayed to sutured lobate. Other pelitic samples have the tectosilicates segregated into silty partings (Fig. 2.7).

Subhedral laths of ilmenite are ubiquitous and are usually partially to wholly altered to rutile or leucoxene, giving the laths a poikilitic appearance (see Stendal, 1982). They parallel foliation and are usually reoriented by crenulation. Ilmenite is a minor constituent of the argillites, but may comprise up to 15 modal percent of some thin layers.

Pyrrhotite is less common in meta-pelitic lithologies. It occurs as elliptical blebs usually oriented parallel to foliation; stress caused pyrrhotite elongation by translation

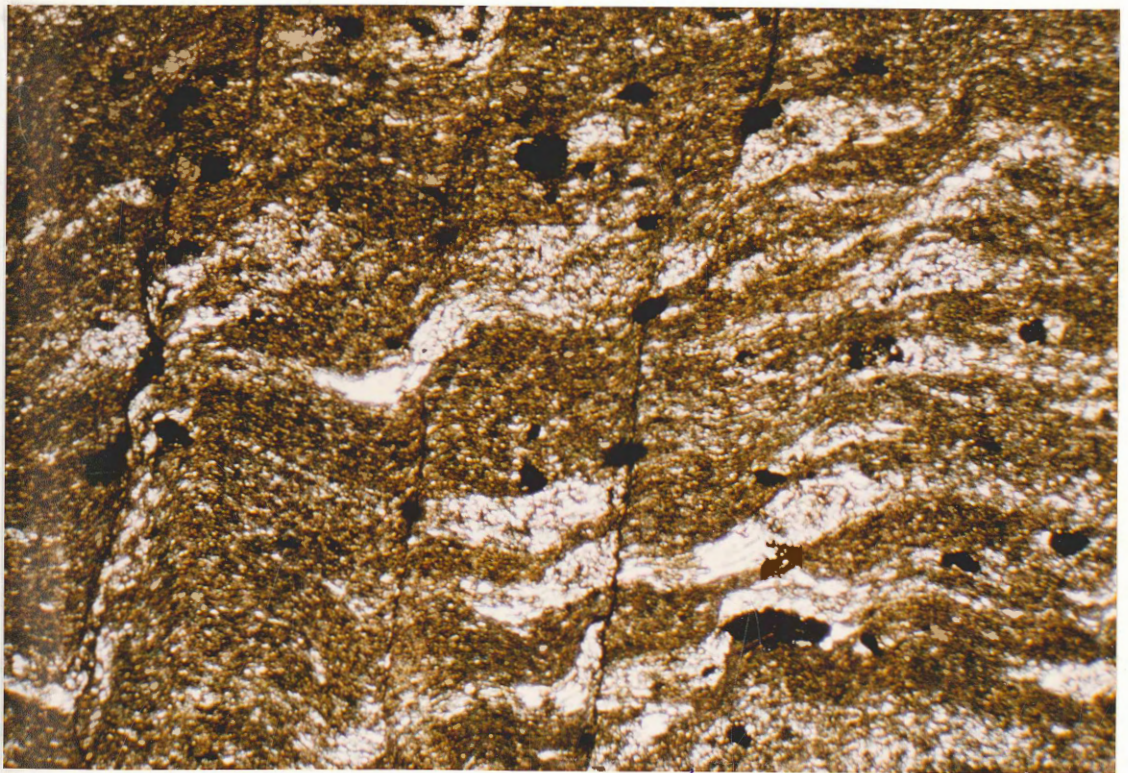
Figure 2.7

Crenulated meta-argillite with silty partings and ilmenite blebs reoriented by crenulation. In places crenulation develops into cleavage.

Crossed nicols.

Long axis of photograph measures 5 mm.

gliding
Graf
and
is found
clusters



spokes
cord
cont
petr
know
aut

gliding along (0001) crystal planes (Ramdohr, 1980; Spry, 1969; Graf et al., 1970).

Darker varieties of meta-pelites contain less chlorite and muscovite, more quartz, carbonate and graphite. Graphite is found as extremely fine disseminations or as linear clusters, forming 'wispy' sheaf aggregates intergrown with the phyllosilicates.

The meta-pelites may become siltier, with decreased phyllosilicate content, and increased concentration of equigranular quartz, forming fine-grained siltstones.

Thermal metamorphism caused overprinting of foliation by such poikiloblastic minerals as: euhedral garnet; subhedral chiastolite retrograded to assemblages of muscovite-quartz-carbonate (Fig. 2.8); euhedral to subhedral blades of carbonate (calcite, dolomite, ankerite); biotite; and chlorite. Round to elliptical aggregates of quartz-chlorite-carbonate are also found, discontinuously rimmed by opaques such as leucoxene and pyrite, and may be altered cordierite 'spots'. One carbonaceous argillite sample contains green poikiloblastic blades of a mineral that has a retrograde assemblage of quartz-chlorite-carbonate; it is not known what the original mineral was (amphibole?).

The most common sulphide mineral within the meta-argillites is pyrrhotite, usually found as blebs, but

Figure 2.8

Slightly sheared carbonaceous meta-
argillite containing contact
metamorphic andalusite(var. chiastolite)
retrograded to muscovite, quartz and
calcite.

Sample 77-31-87.30

se
all
gulf

to give a more

page

arc

blab

fract

conal

felds

Carla

distr

quar

nucc

trac

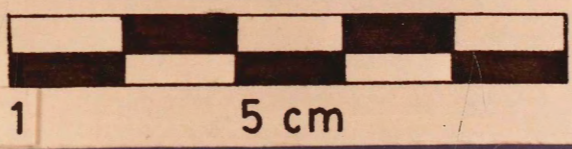
chal

flor

lys

ent

liv



may occur as stratiform layers several cm thick and very slightly foliated. More discussion of this and other sulphides is found in chapter 3.

2.2.2 Meta-psammitic Lithologies

Interbedded with the meta-pelites are pale greenish-grey to greyish-green meta-psammities. They are a fine-grained, massive, indurated rock with rare graded bedding, scours and argillaceous rip-up clasts. These lithologies have both bimodal and unimodal grain size assemblages. The coarser fractions (up to 20 modal percent) of the bimodal samples consist of medium sand-sized (averaging 0.5 mm) quartz and feldspar (usually albitic plagioclase with albite and Carlsbad twinning; less potassium feldspar). They are distributed in a finer (averaging 0.04 mm) silty matrix of quartz, feldspar (up to 25 modal percent), chlorite and muscovite with minor ilmenite, pyrrhotite and carbonate with trace amounts of biotite, zircon, sphene, apatite, chalcopyrite, arsenopyrite and graphite (e.g., Fig. 2.9). Most of the geochemically analysed meta-psammities fall within 'typical' greywacke compositions (Fig. 2.10).

The coarser grains are angular to subrounded and roughly equant; quartz grains are strained.

The matrix (and unimodal meta-psammities) consists of tightly intergrown minerals with embayed to sutured lobate

Figure 2.9

Typical meta-wacke.

PPL

Long axis of photograph measure 8 mm.

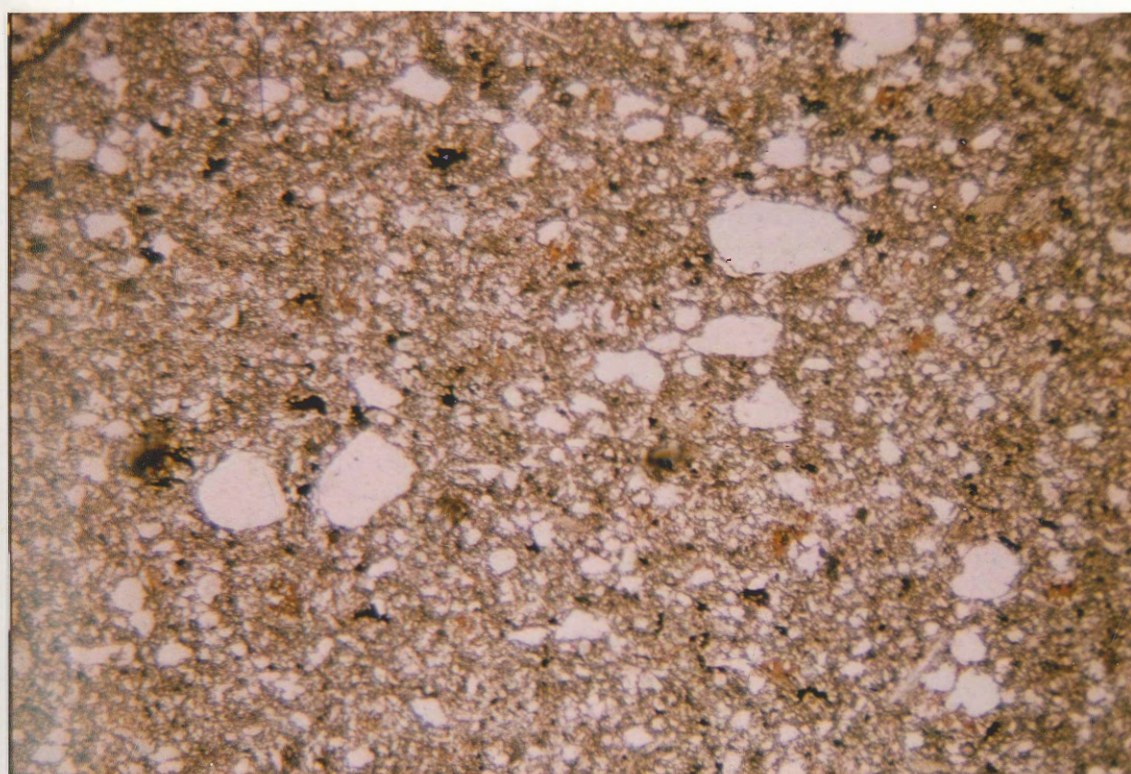


Figure 2.10

Na₂O : K₂O contents in metasediments.

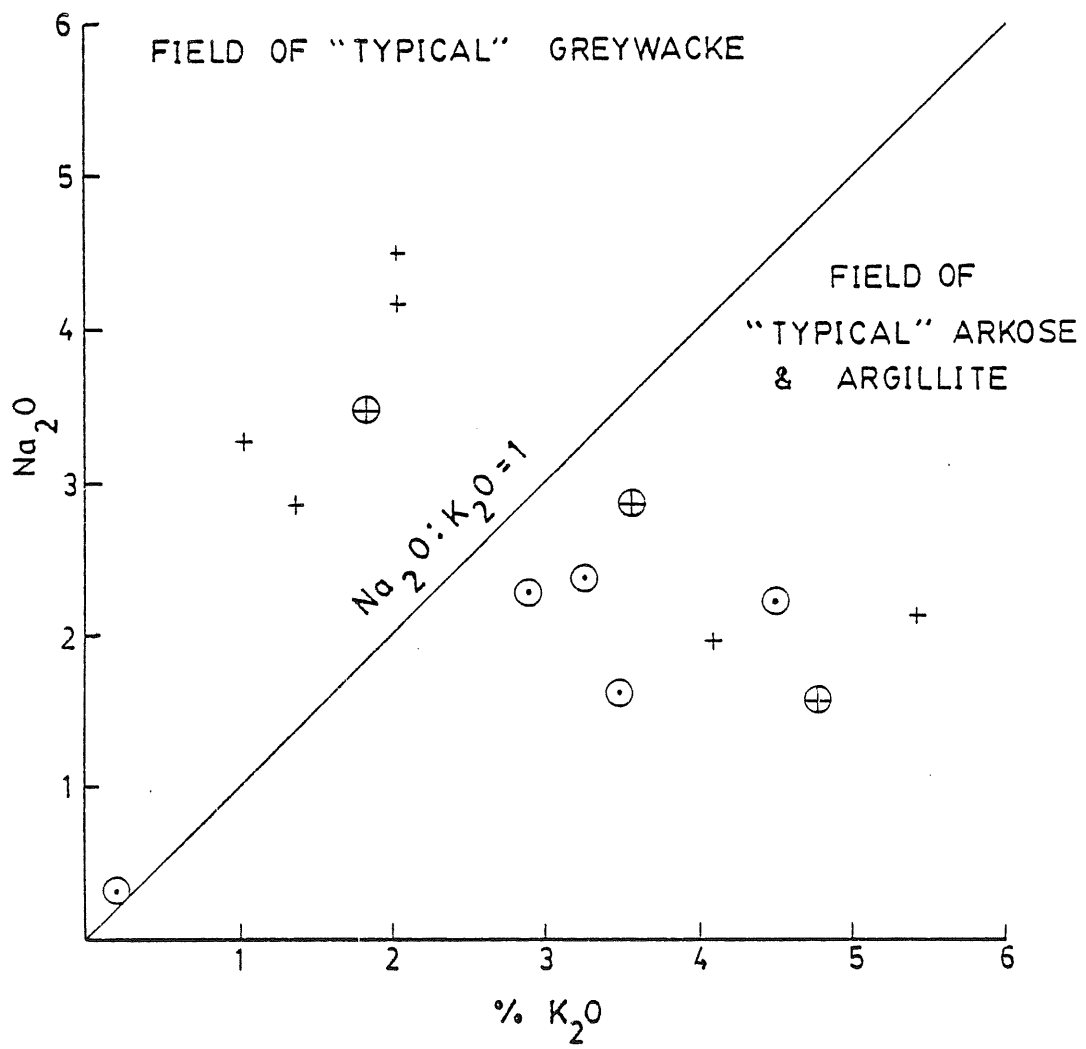
Most meta-wackes plot in the greywacke field; 2 samples have greater amounts of sericite and so plot in the other field.

Meta-argillite which plots near the origin is mineralized.

+ meta-wacke

⊙ meta-argillite

⊕ carbonaceous meta-argillite



grain contacts. Tectosilicates are anhedral, tabular to equant, and are separated by chlorite-muscovite intergrowths. Subparallel orientation of the phyllosilicates and tabular feldspar grains define the linear fabric.

A few meta-psammitic samples appear 'spotted', due to subrounded aggregates of either more (appearing darker) or less (appearing lighter) chlorite and graphite. These may have once been individual clay-rich pellets rolled around by currents and incorporated into sandy layers (Pettijohn, 1975).

Calc-silicate layers also occur throughout the core (Fig. 2.11). They generally have a fine-grained (averaging 0.05 mm) matrix of quartz, with lesser feldspar, biotite and chlorite. This is overprinted by such thermal metamorphic minerals as euhedral garnet, biotite, granoblastic epidote and actinolite, euhedral to embayed carbonate (calcite, dolomite, ankerite) and poikilitic, colloform and massive pyrite.

Several interesting features are found within the meta-psammitic layers:

1. Layers of manganese-rich garnet (Cullen, 1983) in fine sand-sized meta-psammite (Fig. 2.12); this may reflect metamorphosed, originally manganeseiferous sediments. These may have formed by concentration of manganese carbonates or oxides/hydroxides or both during diagenesis or by accumulation

Figure 2.11

Contact metamorphic zones paralleling original layering.

Green zone: actinolite-epidote-garnet-
carbonate-biotite-sphene.

Brown zone: quartz-biotite-epidote-
garnet-sphene-chlorite-
plagioclase-carbonate.

Sample 77-10-44.6

near
el. 157
zone
through
wide
(Zent. II.)

2. Calc
silicate
lithol
in pe
Hodge
disab
subse
envir
el. 19
altri
clays

Purvis (report to Curtis, 1933)



near submarine vents (Whitehead,1973; Germann,1973; Duurama et al., 1976). Apparently, there is a calcareous manganese-rich zone within the upper part of the Goldenville Formation sediments throughout Nova Scotia, and may have formed in response to some widespread synsedimentary, diagenetic or mineralizing event (Zentilli, pers. comm.,1983; Jenner,1982).

2. Calc-silicate layers previously discussed; and calc-silicate nodules (Fig. 2.13) - elliptical to amoeboid metasomatised calcareous concretions within meta-psammitic lithologies. They appear similar to altered limestone nodules in pelitic hornfels of the CanTung tungsten deposit (Dick and Hodgson,1982). Original calcium carbonate may have derived from dissolution of shelly material by acidic intrastratal water and subsequently reprecipitated elsewhere in a less acidic environment within psammitic layers (Schenk,1975; Pettijohn et al.,1972). Additional calcium may have been obtained by albitization of plagioclase (Blatt et al.,1980) during diagenesis. These nodules have been studied in detail by M.F. Purves (cited in Cullen, 1983).

3. Stratiform sulphide zones; these will be discussed in a later chapter.

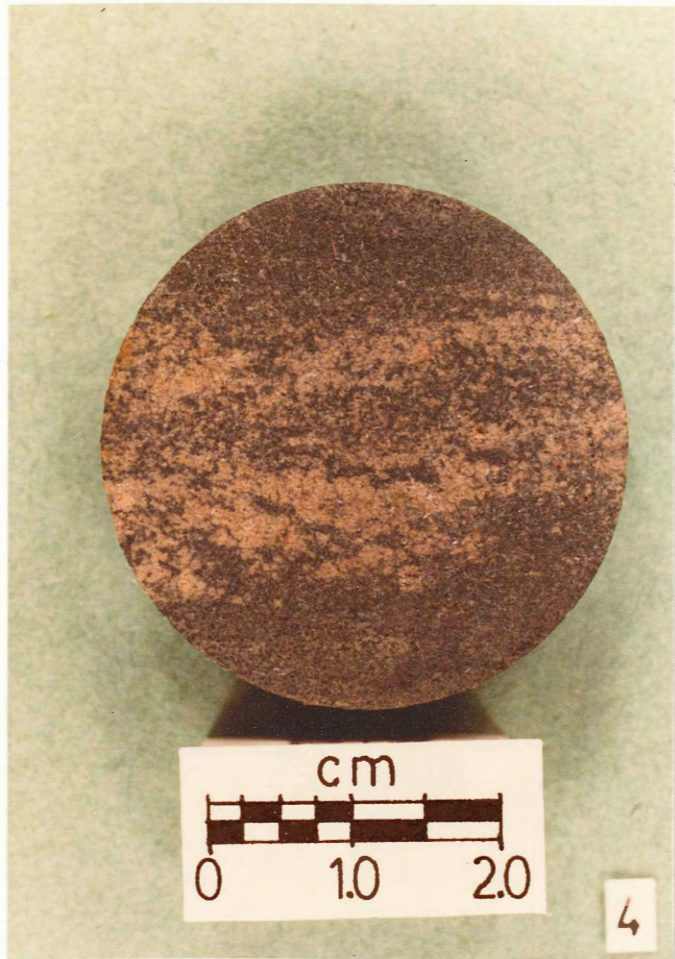
Figure 2.12

Layered manganiferous garnet in meta-wacke. They possibly represent metamorphosed manganiferous sediments.

Sample 77-34-10

Figure 2.13

Metasomatic concretion in meta-wacke. It is an amoeboid body with a white core and rim of quartz, muscovite and zoisite, with a middle green zone of quartz, zoisite and chlorite (Cullen, 1983).



2.3 Plutonic Lithologies

2.3.1 Wedgeport Pluton

The Wedgeport pluton is exposed along a part of the shoreline. It is in sharp contact with the metasediments, which contain minor injections of granitic material (Fig. 2.14). Most of the shoreline comprises monolithic boulders weathered from till.

Samples from the pluton have a modal mineralogy corresponding to monzogranite of Streckeisen's (1976) classification (Fig. 2.15). The samples have normative and oxide contents similar to those of adamellites of the South Mountain batholith (Figs. 2.16 and 2.17). A high ferrous to ferric iron ratio (Fig. 2.18) plus scarcity of opaque minerals, of which ilmenite is the most common, may possibly characterize the pluton as an 'ilmenite series' type (Ishihara, 1981; Takahashi et al., 1980; Ishihara et al., 1979). Geochemically, the pluton appears to be an 'I-type' granite (Chappell and White, cited in Plimer, 1980); mineralogically, it resembles the 'S-type' variety (Table 2.1). Attempts to characterize the pluton geochemically as either potentially ore-bearing or barren have proved disappointing. Selected trace and major element ratios (e.g. Table 2.2, Fig. 2.19) exhibit both 'specialized' (at the margin of the pluton) and 'normal' (the interior of the

Figure 2.14

Wedgeport pluton(left) in sharp contact with metasedimentary country rock. A thin granitic dyke (centre) is injected into hornfelsed meta-wackes.

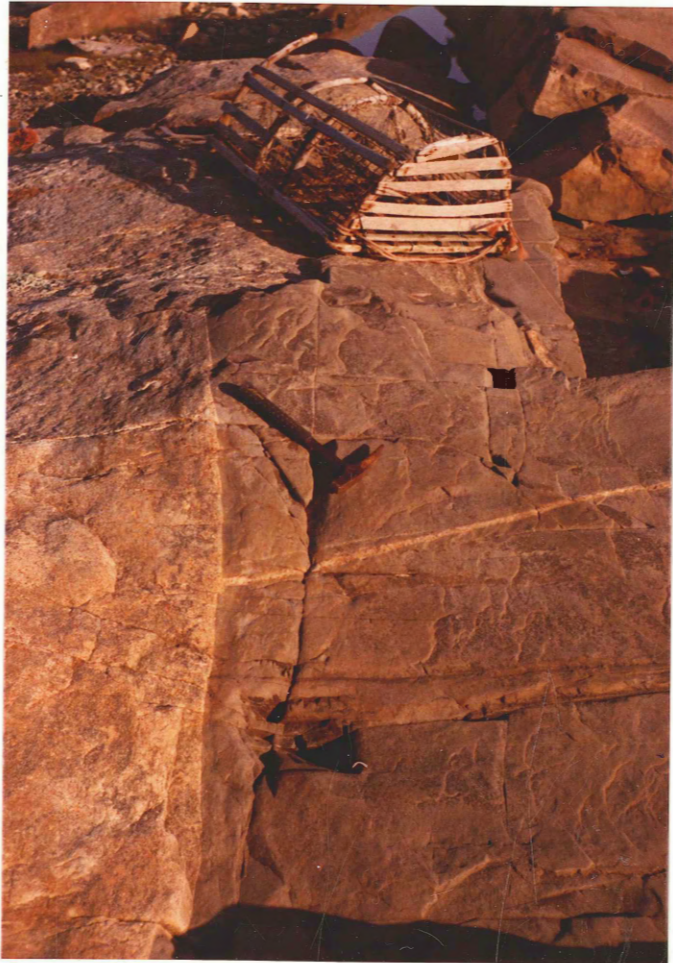


Figure 2.15

Modal QAP composition of plutonic lithologies. All plot within the monzogranite field.

- + Wedgeport pluton
- ⊙ South Mountain batholith adamellites (McKenzie and Clarke, 1975)

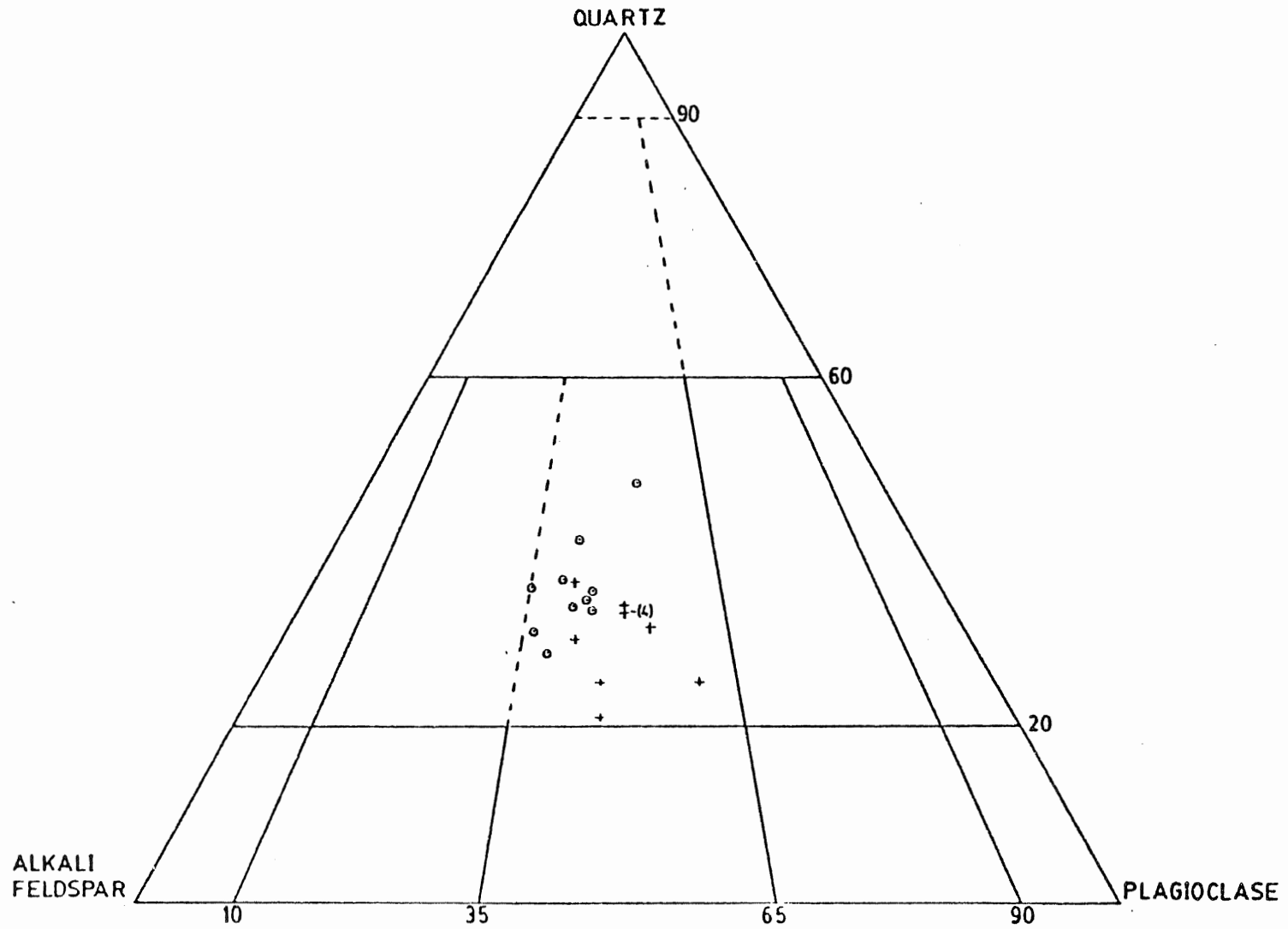


Figure 2.16

Normative quartz-albite-orthoclase diagram. Parallelogram approximately denotes field for adamellite and granodiorite lithologies of the SMB (McKenzie and Clarke, 1975). Greisen sample near the orthoclase apex contains white mica and fluorite with little quartz.

- + monzogranite and greisen samples, this study.
- 2 biotite granites, 1 muscovite-quartz greisen from the Davis Lake pluton, East Kemptville (Chatterjee, 1980).

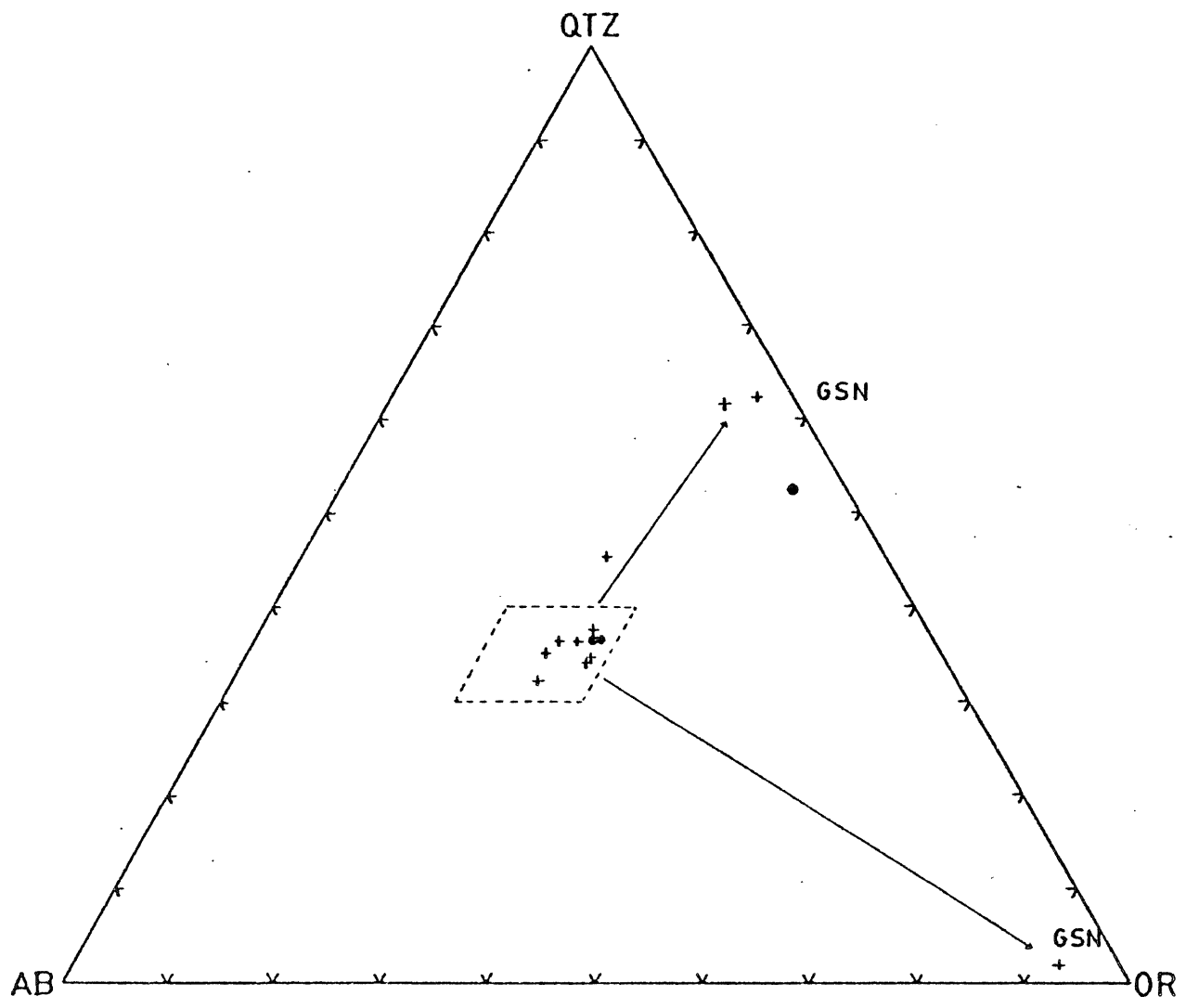


Figure 2.17

K_2O - Na_2O - CaO variation diagram of 11 samples from the pluton. Dotted parallelogram approximately denotes the adamellite field of the SMB; shaded parallelogram approximately denotes the granodiorite field of the SMB (McKenzie and Clarke, 1975). Arrows point to 3 greisen samples adjacent 3 unaltered monzogranite samples, indicating loss of Na_2O and relative increase of K_2O .

+ monzogranite and greisen samples, this study.

● 2 biotite granites, 1 muscovite-quartz greisen from the Davis Lake pluton, East Kemptville (Chatterjee, 1980).

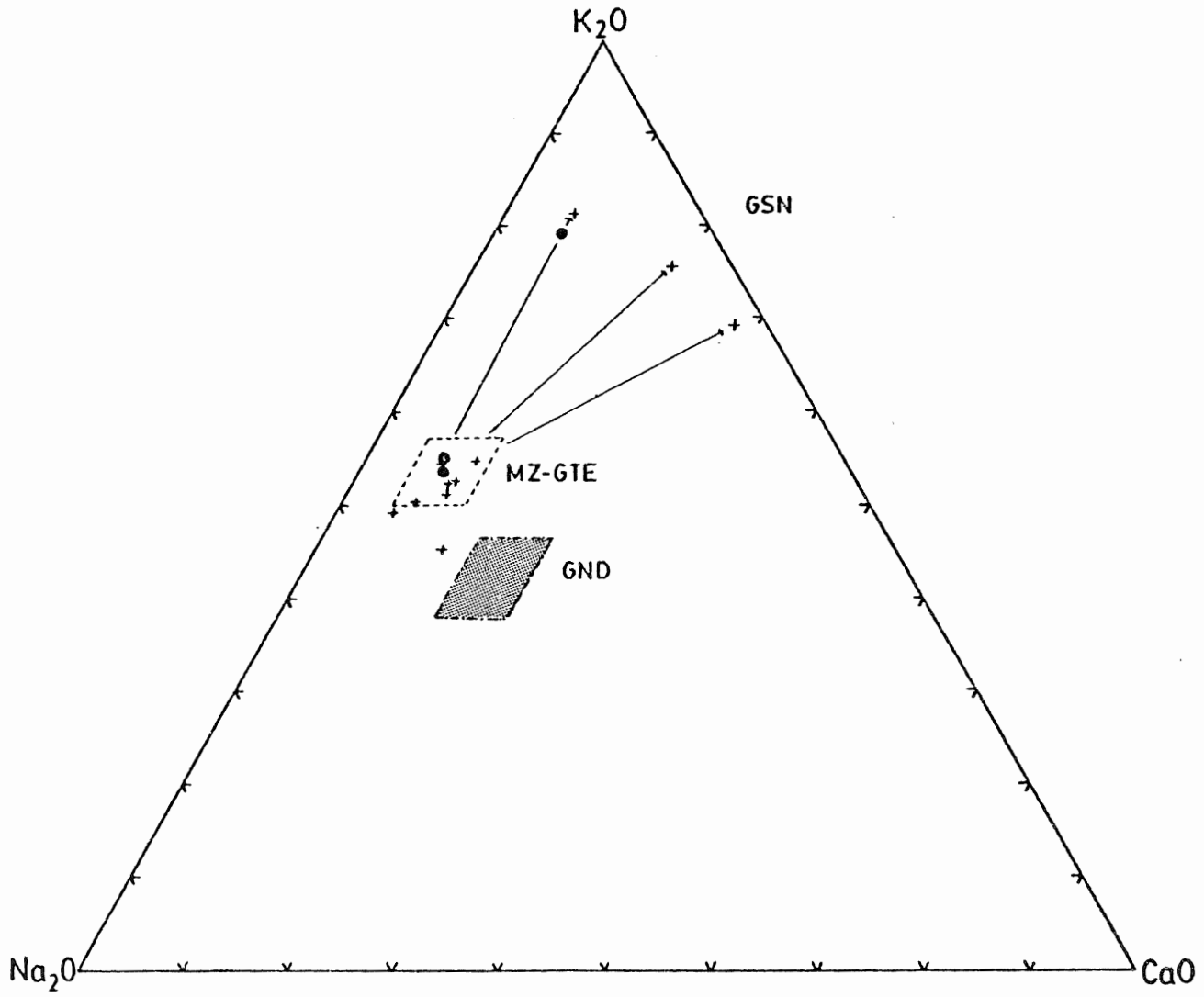


Figure 2.18

Ferrous/Ferric ratio of monzogranite samples. Broken line separates magnetite- and ilmenite-series granitoids of Japan. $\text{FeO}/\text{Fe}_2\text{O}_3$ is roughly 1 to 2 on granite compositions (DI=95-80) and is roughly 2 to 3 on granodiorite (DI=80-60) and tonalite and quartz diorite (Ishihara et al., 1979).

FeO/Fe₂O₃

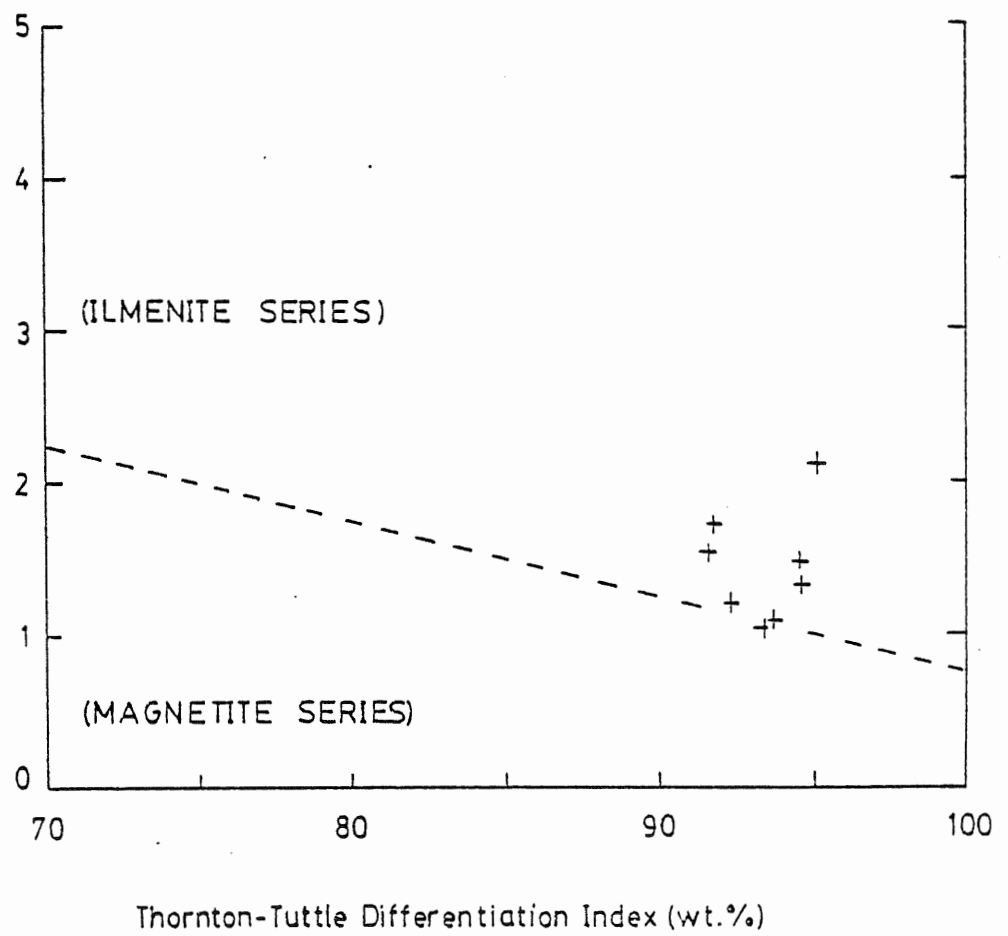


Table 2.1 Properties Of Monzogranite, S- and I-type granites
(from Chappell and White, quoted in Plimer, 1980)

Wedgeport Monzogranite (n=8)	S-type Granite	I-type Granite
Na ₂ O 2.86-4.28%	Na ₂ O < 3.2% in rocks	Na ₂ O > 3.2% in
K ₂ O 4.25-5.07%	with ~ 5% K ₂ O	felsic types
	< 2.2% in rocks	> 2.2% in
	with ~ 2.2% K ₂ O	mafic types
	<u>Molecular Al₂O₃ / (Na₂O+K₂O+CaO)</u>	
0.93-1.06	>1.1(peraluminous)	<1.1
	<u>norm corundum</u>	
0.00-0.45%	> 1%	<1%
	<u>norm diopside</u>	
0.00-1.74%	-	norm di present
Biotite common	Muscovite and Biotite common	Hornblende common

Table 2.2 Major Element Ratios Typical Of 'Normal' and 'Specialized' Granites

	K/Na	K/Rb	Mg/Li
'Normal'	1.2	> 100	270
'Specialized'	1.6	< 100	75
<u>This Study</u>			
Monzogranite (n=8)	1.18-1.78	120-180	14.7-40.97
Greisen (n=3)	7.53-25.5	60-70	4.75-17.5

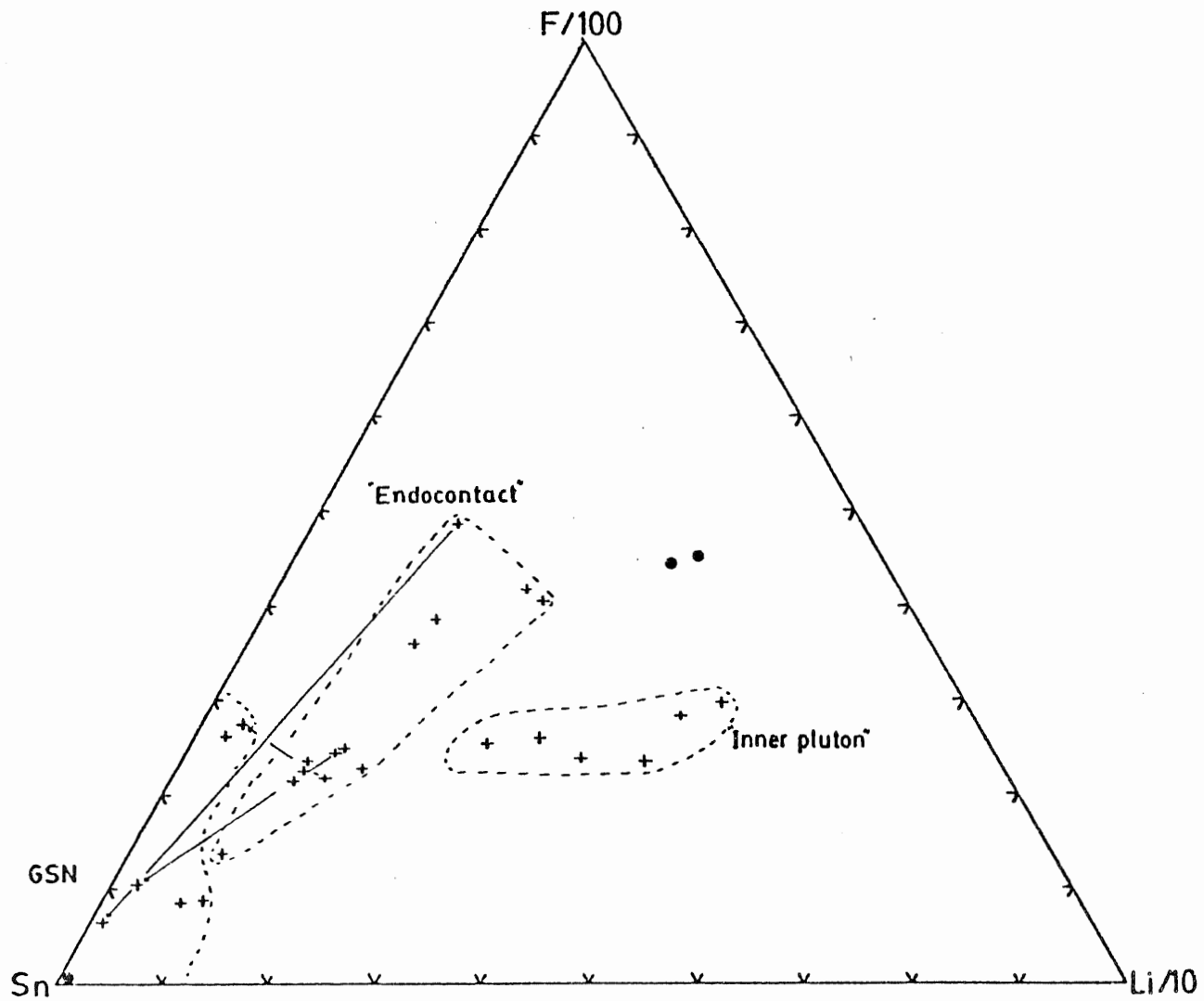
Values for normal and specialized granites are from various authors in Boissavy-Vinau and Roger(1980).

Figure 2.19

Proportions of F, Li and Sn in samples from the Wedgeport pluton (n=25) and the Davis Lake pluton (n=3).

There is a large scatter of data, but there appears to exist a trend towards the Sn axis in altered, sheared and greisenized samples. Samples are grouped according to their positions in the pluton or to their states of alteration. The 3 arrows join barren monzogranite to their adjacent greisenized zones.

- + monzogranite and greisen samples, this study.
- 2 biotite granites, 1 muscovite-quartz greisen from the Davis Lake pluton (Chatterjee, 1980).



pluton) features. Airborne gamma ray spectrometric measurements (Chatterjee and Muecke, 1982) indicate high total radioactivity and high thorium values within the pluton and these appear associated with mineralized intrusions found elsewhere in Nova Scotia (e.g. the tin mineralized Davis Lake pluton).

The samples display a variety of textures throughout the pluton. Fresh material ranges from greyish white with black flecks to a mottled white, grey and black combination. It has a hypidiomorphic granular (granitic) texture, from fine grained equigranular to porphyritic with medium, rarely coarse grained phenocrysts. The endocontact exhibits this diversity of colours and textures - there are no contacts among the different types, rather each type grades into one another. Figure 2.20 shows some examples of this diversity. Samples from the interior of the pluton are less heterogeneous and are generally medium grained with minor coarse phenocrysts.

The monzogranite consists of roughly equal amounts (about 30 modal percent) of fine grained translucent grey (light brown in weathered exposures) quartz, greyish-white (rarely pinkish) microcline and pale greenish-white (rarely pinkish) plagioclase of albite to oligoclase composition. Fine grained black, ragged flakes of biotite comprise up to 10 modal percent; they contain minor inclusions of euhedral,

Figure 2.20

Diversity of monzogranite textures in one drill hole(78-27). Depth increases from left to right: 31.15 m, 68.37 m(near a mafic dyke), and 78.55 m.

Figure 2.21

Effects of mafic dyke intrusion upon monzogranite.

Top: 78-31-30.18 Coarse monzogranite. Pink coloration of microcline; plagioclase remains greenish white.

Bottom: 78-27-70.71 Chloritization of biotite.



zoned zircon prisms, euhedral to subhedral needles of apatite and subhedral laths of ilmenite. Rare fine grained anhedral purplish fluorite, pinkish scheelite, molybdenum, pyrite and pyrrhotite occur throughout the core.

Phenocryst abundances range up to about 15 modal percent and consist of medium (1-5 mm), rarely coarse (up to about 9 mm) grained, round translucent pinkish quartz 'eyes' and subhedral white equant blocks of microcline; subhedral pale greenish-white plagioclase laths are less common.

Quartz is usually slightly strained, showing undulose extinction. Near areas of shear, it exhibits minor subgrain and new grain development. Quartz phenocrysts have minor inclusions of both the feldspars and biotite. Irregular quartz is interstitial to the feldspar crystals.

Microcline occurs as anhedral blocks, rarely as anhedral laths. It is slightly perthitic with bleb and ribbon albitic plagioclase. Cross-hatched or 'tartan' twinning is common. Phenocrysts are poikilitic with quartz and plagioclase inclusions. Rarely, embayed microcline is mantled by plagioclase. It is usually slightly sericitized; near veins microcline is more altered and has a greyish turbid appearance due to the presence of microscopic to submicroscopic fluid inclusions. Near dykes it may take on a rust-brown turbid appearance (presence of iron oxides or hydroxides?) and look pinkish in hand sample (Fig. 2.21).

Plagioclase is found as subhedral to anhedral laths of albite to oligoclase composition. It usually has albite twinning; some phenocrysts have vague normal zoning. Minor microcline and quartz are included within the phenocrysts. Plagioclase suffers a greater degree of alteration, changing to sericite with variable amounts of calcite and rarely epidote, usually within crystal cores. Near dykes it usually becomes a turbid rust brown, appearing pink in hand specimen, although it may remain greenish white.

Biotite occurs as clear brown ragged individual flakes or aggregates of flakes. It usually contains inclusions of zircon, apatite, ilmenite and epidote(?); rarely subhedral pyrite and arsenopyrite crystals and rutile(?) needles. Biotite alters readily to clear, dark green chlorite, even where no alteration is evident in adjacent minerals. Near veins, shears and contact with the metasediments, biotite is altered to a 'shredded' tan aggregate of vermiculite(?) with disseminated iron oxides or hydroxides; included ilmenite is generally altered to blue anatase.

Rare vugs (miarolitic cavities?) are found in some of the core. They are round to elliptical, and up to 3 mm diameter with drusy quartz coatings.

Monzogranite is readily weathered, as seen by the pinkish to rust-brown coloration of both exposed country rock

and upper portions of the drill core, some to 22 m depth (Fig. 2.22).

The core is cut by several stages of veins, several mm to several cm width. Many are of quartz-calcite composition with variable sulphides, fluorite (both purple and green), scheelite, white mica, kaolinite and cassiterite. Alteration envelopes range from slight 'bleaching' immediate the vein (sericitization of feldspars) to greisen zones up to 20 cm in drill core. These vein types will be discussed in a later chapter.

Rare aplite dykes are observed in both core and outcrop. They are thin (several cm), greyish white and aphanitic with assimilated mineral fragments. They are in sharp contact with the monzogranite with no observable alteration effects.

Shears cut the pluton with or without accompanying veins of quartz ± arsenopyrite ± scheelite ± molybdenite ± pyrite. Widths vary from centimetres to several metres over the length of the drill core. In places one may observe a progressive reduction of grain size, destruction of feldspars, orientation of elongate quartz 'eyes' and development of saccharoidal quartz and parallel planes of pale silvery green sericite. Within endocontact samples, euhedral sulphides (principally pyrite; minor chalcopyrite) overprint the shear planes. In shoreline exposures, these

Figure 2.22

Effect of monzogranite weathering.
Sample 78-33

Left: Hematite-stained at 13.73 m.

Right: Unweathered at 46.6 m.



sulphides weather to form iron oxides, producing 'rusty' shear zones (Fig. 2.23).

2.3.2 Mafic Dykes

A series of northeast- northwest- and rare north-trending mafic dykes intrude both the pluton and the metasediments. They are fresh, black, aphanitic with minor vitreous crystals, and are tens of cm thick. Contacts are sharp and reddish brown; little alteration or assimilation of the host rock is observed. Several dykes appear composed of two phases, as if the magma had reintruded planes of weakness. Two types of dykes occur - one a lamprophyre, the other an olivine diabase. Relationships between the two are not known. Such dykes have been described and analysed by Cullen (1983), so will only be given a brief description here.

Lamprophyre dykes (monchiquite?) have a glomeroporphyritic texture, with up to 25 modal percent of clusters of medium grained clinopyroxene and olivine phenocrysts in a fine grained matrix of clinopyroxene, olivine, plagioclase(?), hornblende (kaersutite?), biotite and either a zeolite or feldspathoid (Fig. 2.24a).

Euhedral, zoned and sometimes twinned titaniferous augite laths occur (about 1.5 mm), and may include olivine and magnetite; some have mantles of hornblende. Subhedral to

Figure 2.23

Part of a 'rusty shear' from the western margin of the Wedgeport pluton. The altered monzogranite has a saccharoidal texture; feldspars are completely destroyed. Develops (to the right) into pyrite-(minor chalcopyrite) bearing end of shear, altered to iron oxides.



anhedral olivine phenocrysts (about 1 mm) group with augite; they range from fresh, to totally altered to serpentine, calcite and talc, edged with magnetite. Fine brown laths of hornblende (about 0.15 mm) comprise 10 to 15 modal percent of the lamprophyre. Rare flakes of dark brown and dark green biotite, and fine needles of plagioclase(?) are disseminated throughout. The matrix also contains round amygdales(?) (up to 1.5 mm in diameter) filled either with a feldspathoid or a zeolite (analcite?). Matrix minerals are oriented around these forms; some minerals appear to grow into them.

As the contact with the country rock is approached, the matrix becomes glassy and reddish brown. Adjacent metasediments appear slightly altered (sericitization of feldspars). Within the monzogranite feldspars may be turned pink and biotite may be chloritized (Fig. 2.21).

Trace element analyses (Appendix II) include high fluorine (about 1000 ppm) which probably substitutes for the hydroxyl component of both hornblende and biotite. See Cullen (1983) for their whole rock chemistry.

One sample of an olivine diabase dyke was observed in thin section (Fig. 2.24b). It is relatively unaltered and consists of a fine grained holocrystalline assemblage of euhedral labradorite laths (about 60 modal percent) with undulatory extinction, euhedral augite laths (about 25 modal percent) and minor anhedral olivine altered to serpentine and

talc (about 5 modal percent). Disseminated throughout are fine magnetite and skeletal ilmenite (about 10 modal percent) and a trace amount of brown needles of hornblende(?).

Figure 2.24a

Glomeroporphyritic lamprophyre
dyke. Solitary biotite flake
occurs in centre. Brown hornblende
occurs throughout.

PPL

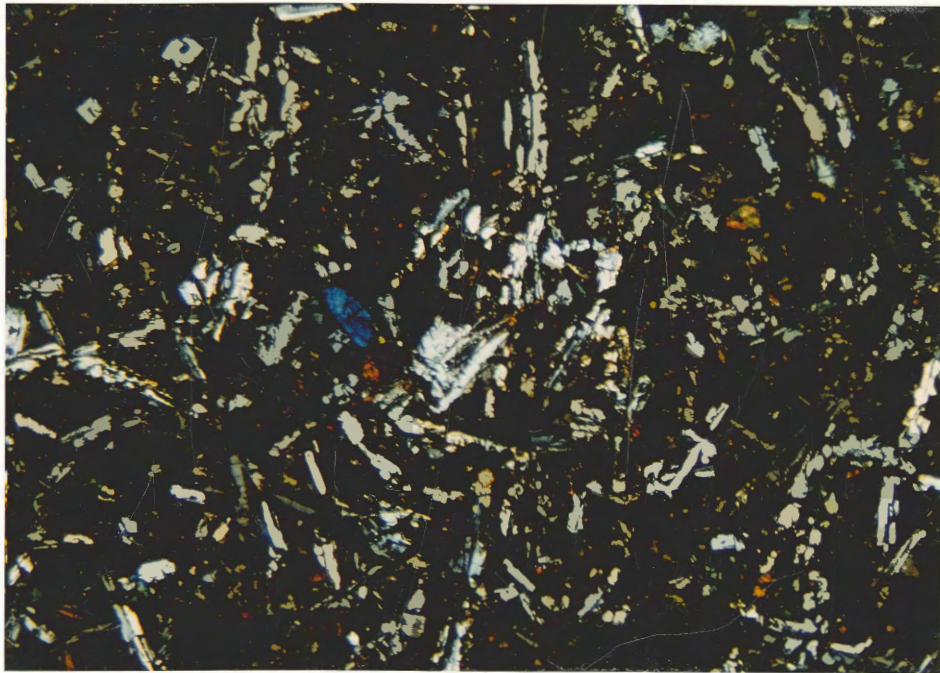
Long axis of photograph measures 3.23 mm

Figure 2.24b

Plagioclase-rich olivine diabase
dyke.

Crossed nicols

Long axis of photograph measures 8.0 mm



CHAPTER THREE

ORE PETROLOGY

3.1 Introduction

Both the metasediments and the Wedgeport pluton are cut by a variety of vein systems of variable orientation and mineralogy, reflecting stress and fluid regimes before and during mineral transport and deposition. A detailed analysis of fracture and vein system orientations is beyond the scope of the thesis; however, their positions with respect to bedding and foliation within drill core have been noted.

Cassiterite mineralization occurs both in veins (mainly within the metasediments) and in thin, sulphide-rich stratiform blue grey to brown 'patches' or zones within the metasediments. The mineralogy, textures and possible modes of genesis of the mineralization will be discussed.

3.2 Vein Systems

Because the vein systems within the metasediments and pluton have somewhat different mineralogies and effects on the host rock, and because relationships between the systems in the two lithologies are not well known, they will be treated separately. Each lithology appears to contain three

main stages of veins: pre-tin, tin, and post-tin. Each stage will be described in terms of its mineralogy and alteration effects on the wall rock. Cassiterite will be described in a later section, incorporating these descriptions in an attempt to develop a possible genetic interpretation of tin mineralization.

3.2.1 Veins Within Metasediments

Relationships among the different veins are not clear as only a small segment of each vein is obtained in drill core. Crosscutting relationships are rare, therefore comparisons were made between the vein and structures within the host i.e., bedding, foliation, crenulation and fractures.

Pre-mineralization veins may parallel bedding, are commonly affected by crenulation (see Fig. 2.5) and cause little, if any alteration of adjacent host rock.

Veins associated with main-stage mineralization crosscut bedding and foliation - some parallel crenulation cleavage - and may have thin, slightly perceptible alteration haloes.

Post-mineralization veins appear related to a late shearing event, which caused fracturing, bleaching, 'smearing' and some displacement of pre-existent veins and mineralized 'patches', concentrations of thin veinlets ('crackle breccia') and minor brecciation infilled with

quartz and calcite.

3.2.1.1 Pre-mineralization Veins

Pre-mineralization veins within meta-argillite are usually affected by crenulation. They are kinked, ptygmatically folded or boudinaged (Fig. 3.1). This vein type within the meta-wackes is at most, slightly offset.

They are usually less than 1 cm wide, and planar in drill core; finer veinlets appear to be anastomosing. Some veins occur at bedding contacts. Intergrown quartz, calcite and chlorite are the principal constituents; muscovite and sulphides (arsenopyrite, chalcopyrite, pyrite, pyrrhotite, sphalerite(?)) are minor or rare. The quartz is commonly strained, forming sub- and new grains. The immediate host rock is bleached (on the order of <1 mm), usually adding sericite and carbonate \pm quartz.

At least two stages of this vein type occur, at times crosscutting each other.

3.2.1.2 Main Stage Veins

This type comprises a variety of widths, orientations, mineral assemblages, and alterations. Widths vary from less than 1 mm to several tens of cm of drill core length (commonly barren quartz); they are usually 0.5 cm or less.

Alteration haloes vary, from slightly perceptible with slight bleaching, to about ten times the vein width. The main alteration types are:

1. Bleaching(common) - destruction of biotite to chlorite(to vermiculite?); sericitization of feldspar; addition of silica, sericite, chlorite and carbonate.
2. Biotitization(uncommon) - development of biotite porphyroblasts adjacent outer selvedge of quartz-calcite-sulphide veinlets (Fig. 3.2); the biotite is later than the regional metamorphic biotite.
3. Chloritization(minor) - development of chlorite ± rare cassiterite around sulphide veinlets (Fig. 3.3).

Main stage veins consist mainly of quartz, carbonate (calcite, siderite), chlorite, pyrite, pyrrhotite and white mica with variable amounts of other sulphides, cassiterite and scheelite. Table 3.1 lists the common vein mineral assemblages. Vein mineralogy changes with distance from the pluton. Near the intrusion (up to about 2 km from its surface projection), rare scheelite, molybdenite and epidote are found. At greater distances, cassiterite and base metals predominate; scheelite is not observed. Cassiterite is a major mineral between 2 and 4 km from the pluton, after which sphalerite and galena become prominent. Arsenopyrite and chalcopyrite are common throughout the study area. This mineral zonation roughly follows that of greisen stockworks above an intrusion, and sulphide-cassiterite deposits described by Shcherba (1970) and Grigoryan (1974),

Figure 3.1

Early quartz-arsenopyrite veinlets
in meta-argillite, cut by crenulation
cleavage.

Sample 78-10-83.55

Figure 3.2

Vein types.

Left: IW-005(77-27-57.7)

Biotite developed around
quartz-chlorite-carbonate-
pyrrhotite-pyrite-chalcopyrite-
galena veinlet in silty meta-
argillite.

Right: IW-054(78-11-97.84)

Arsenopyrite-galena(+ Ag/Bi)-
chalcopyrite-pyrite-marcasite-
carbonate veinlet parallel
crenulation cleavage with no
major wallrock alteration.
A few fine veinlets of
rust brown material(iron
oxides/hydroxides?) offshoot
the veinlet into foliation.

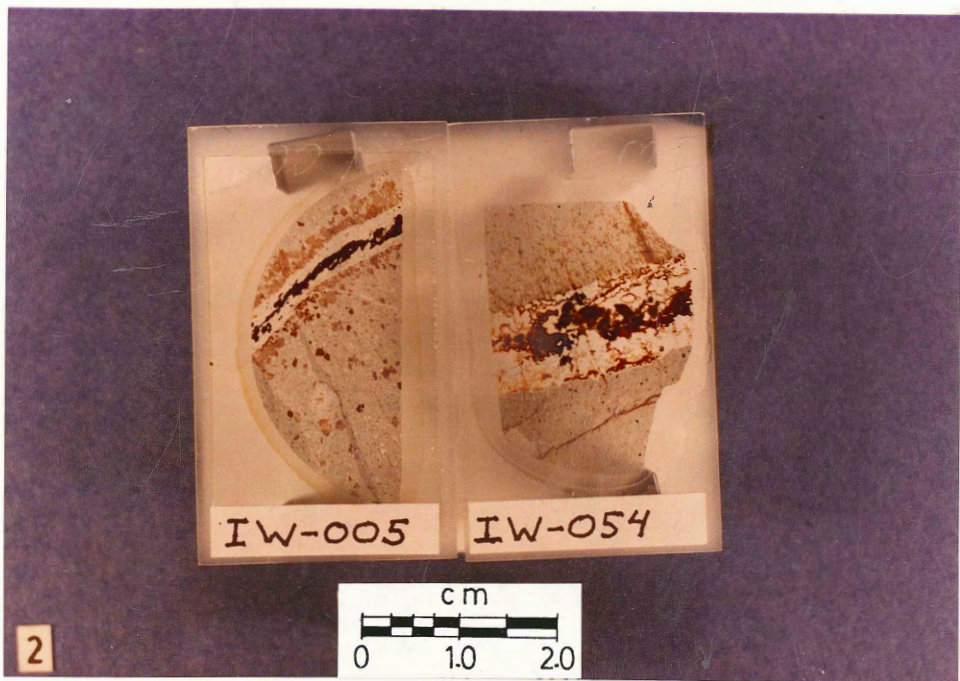


Figure 3.3a

Sulphide-cassiterite veinlets with
a green chloritic alteration zone
within blue-grey meta-wacke.

Sample 77-25-164.77

Figure 3.3b

Thin section of the above sample,
showing detail of sulphide-cassiterite
veinlet and green alteration halo of
chlorite and cassiterite (fine dark
brown spots).



Table 3.1. Mineralogy of Vein Systems

	Metasediments			Pre-Greisen	Pluton Greisen	Post-Greisen
	Pre-Crenulation	Main Stage	Post-Mineralization			
Quartz	X	X	X	X	X	X
Carbonate*	X	X	X			x
Chlorite		X				
White Mica**		x		x	X	x
Pyrophyllite(?)			x			
Pyrite	x	X	.	.	x	x
Marcasite		x			.	.
Pyrrhotite	x	X		.	x	x
Arsenopyrite	x	x	x		x	x
Chalcopyrite	x	x	.			x
Sphalerite	x?	x				
Galena		x				
Silver/Bismuth		.				
Scheelite	
Epidote		.				
Garnet ⁺		.				
Canthite		x			.	
Fluorite				x	X	x
Molybdenum		.		x	x	x
Kaolinite						x

* includes calcite, siderite, dolomite

** may be lithium- or fluorine-bearing

⁺ appears incorporated from matrix

? uncertain

X major vein mineral

x minor vein mineral

.

respectively.

Textures among cassiterite, sulphides and gangue minerals are relatively straightforward. The habits, associations and genesis of cassiterite in this vein type and other settings will be discussed in a later section. Generally, the fine grained sulphides (averaging ≤ 0.5 mm) and cassiterite are found in the middle of the vein within a matrix of quartz, carbonate (usually calcite; minor siderite), chlorite and white mica. Other veins may have sulphides at the selvages instead; others may consist of a patternless intergrowth of all minerals. Mineral contacts are usually straight to curved.

Arsenopyrite occurs as subhedral rhombs and blades, and as massive anhedral grains. It has minor inclusions of pyrrhotite, galena and chalcopyrite. Fine cracks may be filled, and crystal boundaries may be discontinuously rimmed by irregular massive galena, chalcopyrite, pyrrhotite, pyrite and sphalerite. Arsenopyrite may also be rimmed by fine druses of calcite. This sulphide is usually in the middle of the veinlet, but some rhombs are found at vein edges and within the the immediate host rock, grown around phyllo- and tectosilicates.

Pyrite is commonly anhedral and massive, grown around other sulphides, cassiterite and gangue minerals (Fig. 3.4); it also occurs as angular blocks (Fig. 3.5). Gangue and minor

anhedral chalcopyrite and sphalerite may be included in pyrite. Minor pyrite hair veinlets may traverse the earlier sulphide-cassiterite veinlets, crosscutting vein minerals (Fig. 3.6) and the cleavages of phyllosilicates in the wallrock. This is believed to be a later part of the main-stage vein system.

Weathered or altered samples contain round to elliptical, concentric intergrowths of blocky pyrite, marcasite and gangue ('graphic pyrite') (Fig. 3.5). This is a result of pyrrhotite conversion to pyrite and marcasite by loss of iron during low temperature alteration (stoichiometric $2\text{FeS} \rightarrow \text{FeS}_2 + \text{Fe}$; Stanton, 1972); cell volume decreases (from roughly 180 \AA^3 for stoichiometric hexagonal pyrrhotite to 160 \AA^3 for cubic pyrite using cell dimensions from Berry and Mason, 1959), causing the structure to shrink and form cracks. Liberated iron may form oxides, hydroxides or magnetite, staining the surrounding rock (Stanton, 1972). Much of the 'primary' pyrite may in fact be completely altered pyrrhotite.

Pyrrhotite is found as irregular, lobate grains growing around other sulphides (principally arsenopyrite) and gangue minerals. It is rarely observed altering to an assemblage of pyrite (see above description).

Marcasite is rare, and is found as subhedral blades and massive amorphous zones in altered pyrrhotite. Several

Figure 3.4

Part of veinlet containing pyrite, sphalerite and cassiterite intergrowth, with minor chalcopyrite inclusions.

Reflected light, oil immersion.

Long axis of photograph measures 1.08 mm

Figure 3.5

Concentric graphic pyrite (after pyrrhotite) in weathered vein sample.

Reflected light, oil immersion.

Long axis of photograph measures 1.08 mm

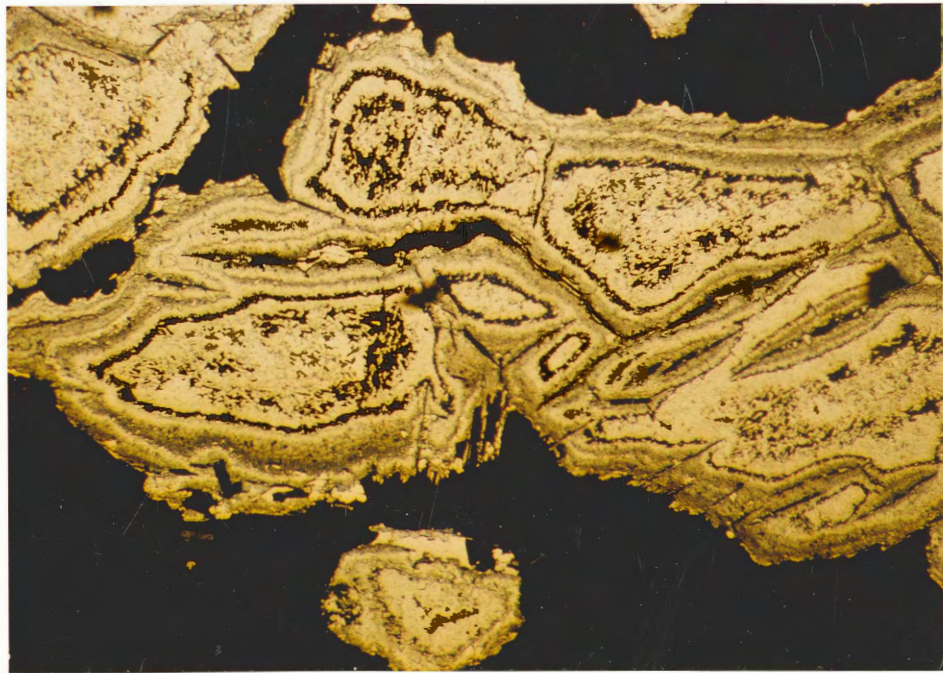
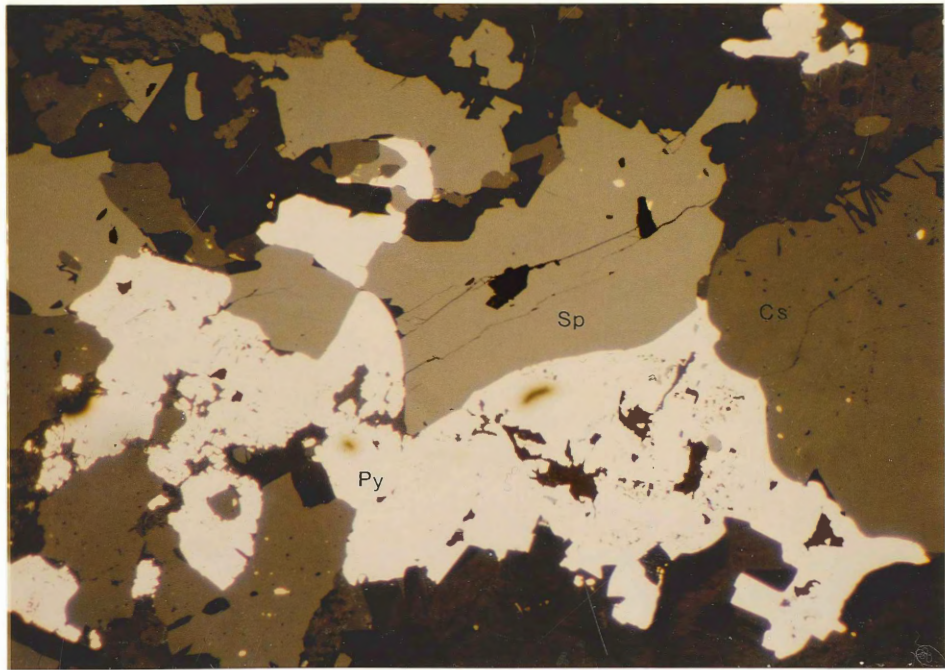


Figure 3.6a

Later pyrite veinlet crosscuts main stage sulphide-cassiterite vein(IW-174); it cuts a sphalerite grain and travels around a cassiterite grain.

Reflected light.

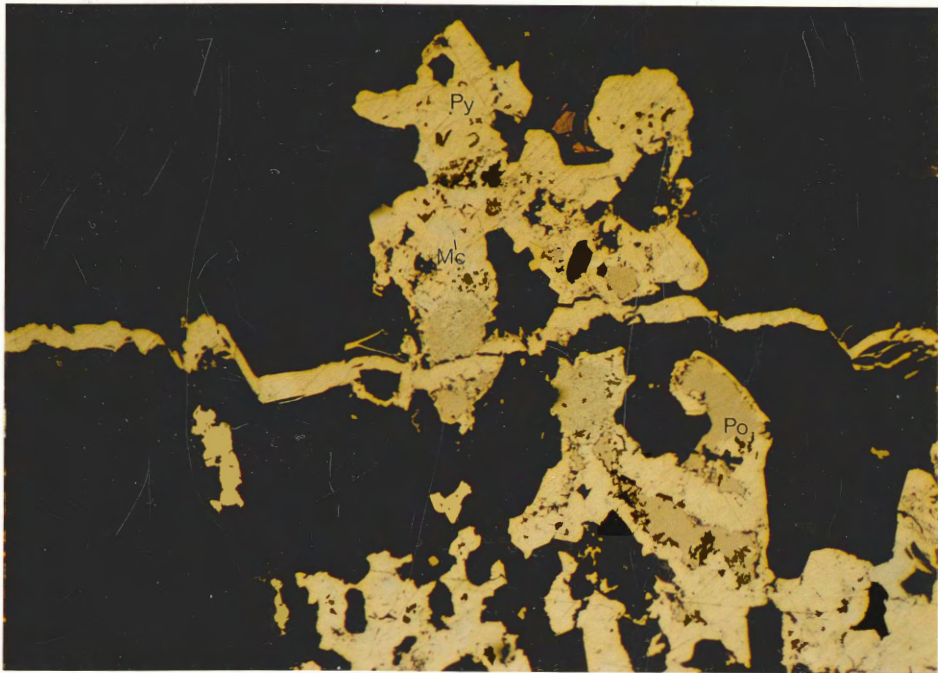
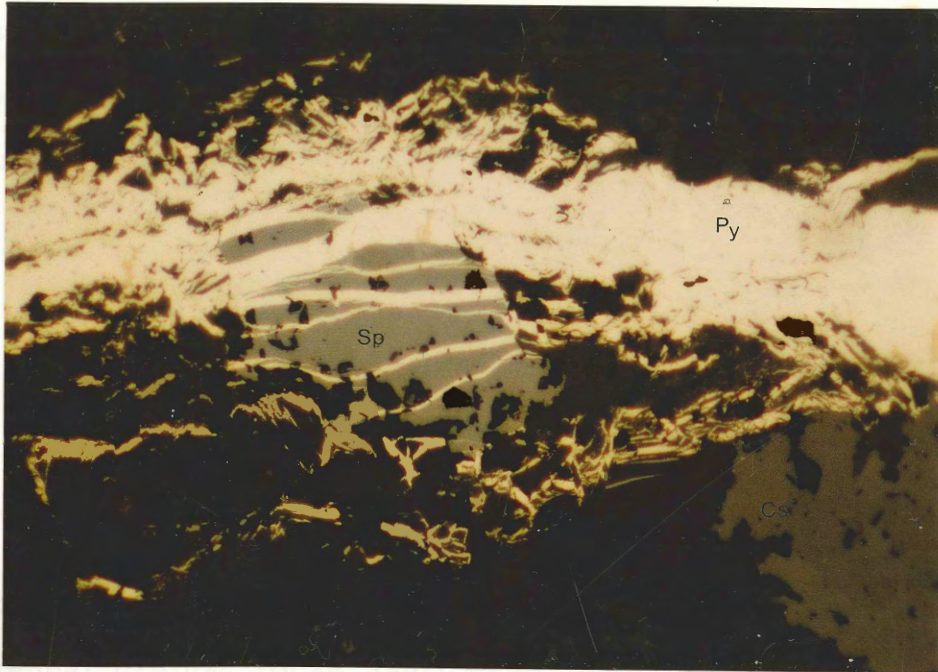
Long axis of photograph measures 0.54 mm

Figure 3.6b

Later pyrite veinlet cuts pyrite and marcasite grains(altered from pyrrhotite) in a stratiform sulphide layer.

Reflected light, oil immersion.

Long axis of photograph measures 1.08 mm



sulphide veins in drill core contain 'vuggy' zones lined with marcasite blades which appear to be a later weathering product.

Sphalerite is a rare to common constituent in the veins. It occurs as anhedral, equant to rectangular grains. The mineral may infill fractures in arsenopyrite and form discontinuous margins around both arsenopyrite and pyrrhotite.

Chalcopyrite is a ubiquitous minor sulphide. It occurs as anhedral grains, forms small exsolution blebs in sphalerite, and is intergrown with pyrite, pyrrhotite, marcasite, sphalerite, galena and gangue; it also mantles pyrrhotite, pyrite, and sphalerite grains.

Galena occurs as anhedral blebs and subhedral to euhedral blocks. It is included in arsenopyrite, fills the fractures of that sulphide, and rims and incorporates arsenopyrite, pyrrhotite, marcasite, sphalerite, and chalcopyrite. A very fine grained, highly reflective mineral is commonly included within galena and may be native silver or native bismuth. Attempts to microprobe several of these grains failed as they were too small.

Scheelite is rare, and is found in quartz-carbonate veinlets near the pluton as flesh-coloured, rectangular anhedral grains.

The gangue consists of granular intergrowths of quartz, carbonate, iron-rich chlorite (see Fig. 3.7) and white mica (muscovite and probably F- and Li-bearing varieties). Two stages of carbonate emplacement are observed in several samples: a minor encrustation of drusy carbonate around sulphides, followed by pyrite and massive carbonate. White mica commonly occurs as discrete flakes, but is also found as radiating spherules intergrown with chlorite and sulphides. Rare garnet is incorporated into the vein.

A possible depositional sequence within the vein system is given in Table 3.2.

Later movement along veins (i.e., along pre-existing planes of weakness) caused elongation of pyrrhotite (parallel to phyllosilicates), strain in quartz (undulatory extinction to formation of sub- and new grains) and incorporation of low temperature acicular cassiterite into new quartz grains. One sample appears to have had regrowth of chlorite into random aggregates and overgrowth of garnet.

3.2.1.3 Post-Mineralization Veins

Identification of this vein type is difficult. The best examples occur where they cut mineralized veins or zones (e.g., Fig. 2.6), but this is relatively uncommon. Brecciated core is tentatively identified as post-mineralization because breccias cut all sedimentary

Figure 3.7

Chlorite compositions of samples in veins and metasediments. Upper field A contains microprobe analyses from 16 chlorite samples in and adjacent to sulphide veinlets. Lower field B contains analyses from 13 chlorite samples in meta-wacke and in stratiform mineralized zones.

(Classification by H.M. Hey, in Deer, Howie and Zussman, 1974)

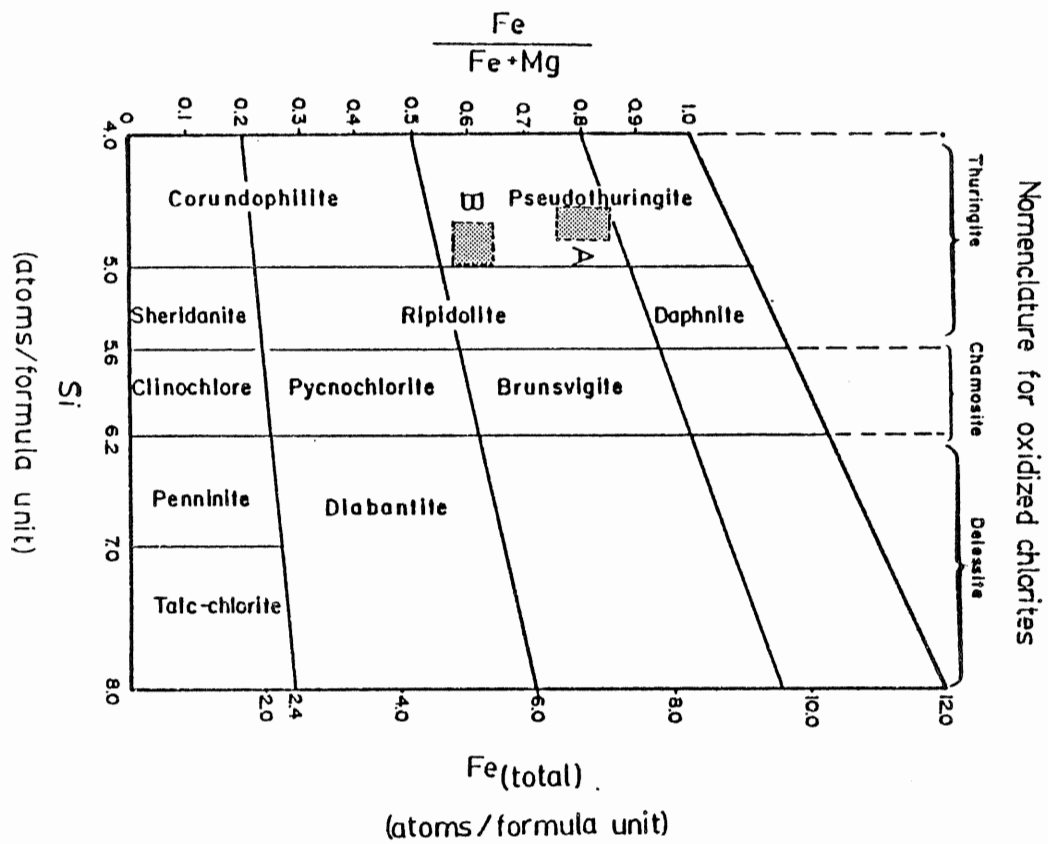


Table 3.2

Mineral Paragenesis in Main Stage Veins

	Early		Late
Scheelite	---		
Molybdenite	---		
Arsenopyrite	_____		
Pyrite		-----	weathered po
Pyrrhotite		-----	
Cassiterite		----- equant	----- acicular
Sphalerite		-----	
Chalcopyrite		-----	
Galena		-----	
Silver / Bismuth		-----	
Druse Carbonate			-----
Main Carbonate			-----
Marcasite			---
Gangue (qtz+chl+mica)		_____	

16

structures and contain only trace amounts of sulphides and no cassiterite; they also are associated with the greatest displacement observed (up to several cm), which is not found in other vein stages.

Widths vary from less than 1 mm to several cm. Veins may occur either singly or in fine networks ('crackle breccia'). Some quartz-calcite tension fractures cut mineralized zones, and therefore belong to this stage; it is not known how these relate to other tension gashes (pre-mineralization?).

Quartz and calcite are the main components; minor arsenopyrite, pyrite and chalcopyrite are disseminated throughout. Several veinlets contain tan spherulitic intergrowths of pyrophyllite(?) and are possibly altered fragments of pelitic wallrock or rock 'flour' formed during brecciation.

Wallrock alteration is variable. Restricted assemblages (≤ 1 mm wide) of muscovite, chlorite and quartz may occur adjacent to the vein and fine hair veinlets may branch from the main vein. Other samples have wide, light hued 'bleached' zones several m in core length, containing intergrown quartz and muscovite aggregates. Several sheared core samples are cut by later quartz-calcite veinlets.

3.2.2 Veins Within Pluton

The endocontact of the Wedgeport pluton is cut by a myriad of thin veinlets; the interior contains minor veining. In contrast with veining in the metasediments, crosscutting relationships are common, and it is sometimes difficult to resolve the various vein stages. As with the metasediments, three main stages of veins exist. Early, pre-greisen quartz veins are usually thin with minor concentrations of other minerals and do not perceptibly alter the adjacent wallrock. Main stage tin-bearing greisen veins are of variable thicknesses and alter the monzogranite country rock from mm to several tens of cm of core length. Late stage quartz veins cut the previous veins, may contain kaolinite and cause little, if any alteration. Later shears may cut any of these veins, and in places have associated quartz-arsenopyrite + scheelite veining.

3.2.2.1 Pre-Greisen Veins

This type of vein is usually thin (≤ 0.5 cm) and is composed of quartz with variable, but minor amounts of white mica, scheelite, purplish fluorite, molybdenum, pyrite and pyrrhotite. Several of these veins usually crosscut each other. Alteration is minimal and comprises fine (several mm) assemblages of quartz and white mica in the adjacent wallrock.

They are not otherwise notable except for their role as

physical barriers to later greisenizing fluids: greisen alteration zones abruptly halt at these pre-existent veins (Fig. 3.8).

3.2.2.2 Greisen Veins

This interesting vein type varies from <1 mm to about 1 cm thick veinlets. A typical greisen vein contains major quartz and minor fluorite, white mica, chalcopyrite, pyrite ± arsenopyrite ± molybdenum ± scheelite ± sphalerite ± a rust brown phyllosilicate (vermiculite??) ± cassiterite.

Alteration is extensive, affecting a zone many times the width of the vein itself. The greisen halo is predominantly a quartz-white mica aggregate containing variable amounts of purplish (in places greenish) fluorite and minor calcite, chalcopyrite, pyrite, pyrrhotite and cassiterite.

Quartz is fine grained (0.25-0.75 mm), commonly anhedral (rarely euhedral), slightly strained and appears to comprise relict quartz 'eyes' of the monzogranite plus silica introduced by greisenization. Fine grained (0.1-0.5 mm) white mica clusters are intergrown with the quartz grains. This phyllosilicate may be lithium-bearing, as evidenced by high lithium concentrations in geochemical analyses of greisen samples. Attempts to identify the mica by X-ray powder diffraction proved disappointing as the d-spacings of muscovite and the lithium-bearing micas (e.g., zinnwaldite,

lepidolite) are very similar.

Anhedral purplish fluorite (usually up to 2 mm in size) has grown around the quartz muscovite aggregate, following their crystal outlines. It comprises from 1 to 10 modal percent of the greisen; rarely it grades into massive fluorite.

Minor anhedral chalcopyrite, pyrite and pyrrhotite (up to about 5 modal percent) are found throughout the greisen and are usually enveloped by or in contact with fluorite. A few opaques are overgrown by calcite.

Minor relict euhedral to subhedral prisms of zircon are disseminated throughout the greisen.

Subhedral cassiterite is rare, both within the greisen vein and its halo, and is usually in close association with fluorite.

Contact between the greisen and monzogranite may be sharp (Fig. 3.9), due either to rapid equilibration ('neutralization') of the greisen fluid with the wallrock or to the presence of a pre-existing quartz vein barrier. The greisen may also be diffuse, changing from a 'true' greisen (quartz-white mica-fluorite assemblage) to an altered ('greisenized') monzogranite, where matrix minerals and their textures are progressively destroyed. Feldspar phenocrysts become rounded and are gradually broken down into mica-rich

Figure 3.8

Leucocratic monzogranite with greisen alteration which stops at pre-existent quartz veinlet barrier.

Sample 79-07-70.66

Figure 3.9

Veinlet with greisen alteration in relatively sharp contact with slightly phenocrystic monzogranite.

Sample 79-08-72.93



aggregates, leaving dark 'ghost' rectangular forms. Quartz phenocrysts appear unaltered and remain as round pinkish 'eyes' in the greisen. This progressive alteration of monzogranite is rarely seen in drill core; usually only individual greisen or slightly altered zones are observed. Fortunately, one such specimen was obtained (Fig. 3.10). It exhibits a gradual change from unaltered material to a 'tan' alteration zone to a 'white' alteration zone to a greisen. The changes which take place during greisenization will be discussed in the cassiterite section.

3.2.2.3 Post-Greisen Veins

Both greisens and unaltered monzogranite are cut by thin (≤ 1 cm) veinlets. They consist of quartz and kaolinite with minor calcite, dolomite and trace molybdenum, pyrite, marcasite, pyrrhotite, arsenopyrite, fluorite, scheelite, chalcopyrite and white mica. Quartz is commonly euhedral and terminated, and is intergrown with the sulphides; kaolinite and the carbonates overgrow these minerals (Fig. 3.11).

Sheared monzogranite may be unmineralized, may cut pre-existent mineralization, or may be mineralized itself. Widths range from < 1 cm to tens of cm (up to 1 m) in drill core. Pre-existent greisens and quartz-scheelite-molybdenite veins may be sheared, although this pre-existence is usually only established in thin section: mineralized quartz veins

Figure 3.10

Phenocrystic monzogranite with alteration zones from 'fresh' to 'tan' to 'white' to greisen proper. Core is cut by later kaolinite veinlets; note displaced feldspar phenocryst (arrow).

Sample 79-08-70.70

Figure 3.11

White and tan altered slightly phenocrystic monzogranite cut by a fine greisen veinlet and a later kaolinite veinlet. Although the latter veinlet appears truncated by a thin veinlet, it actually changes course, following this pre-existent veinlet to the top right.

Sample 79-07-26.30



contain strained quartz and are cut by parallel aggregates of white mica. Some shears have associated quartz veins with variable concentrations of arsenopyrite, scheelite, pyrite and chalcopyrite (Fig. 3.12); others have sulphides (pyrite, pyrrhotite, sphalerite, chalcopyrite) overgrowing the shear planes. Contact with the monzogranite is gradational, exhibiting changes in grain size, orientation and mineralogy. Feldspar and quartz phenocrysts are broken down; newly formed phyllosilicates are oriented in parallel planes.

3.3 Stratiform Mineralization

Many sulphide zones are found throughout the drill core and consist of individual pyrrhotite blebs through to concentrated sulphide disseminations in cm thick beds. They occur in both pelitic and psammitic lithologies (Fig.3.13) within discrete layers, usually in sharp contact with adjacent beds. The thicker, tin-bearing sulphide-rich beds are commonly a distinctive dark blue grey and hence have been termed 'blue mineralized patches'. Description of these concordant zones has been divided into tin-barren and tin-bearing sections.

Figure 3.12

Sheared monzogranite with
quartz-arsenopyrite vein.

Sample 79-07-33.36



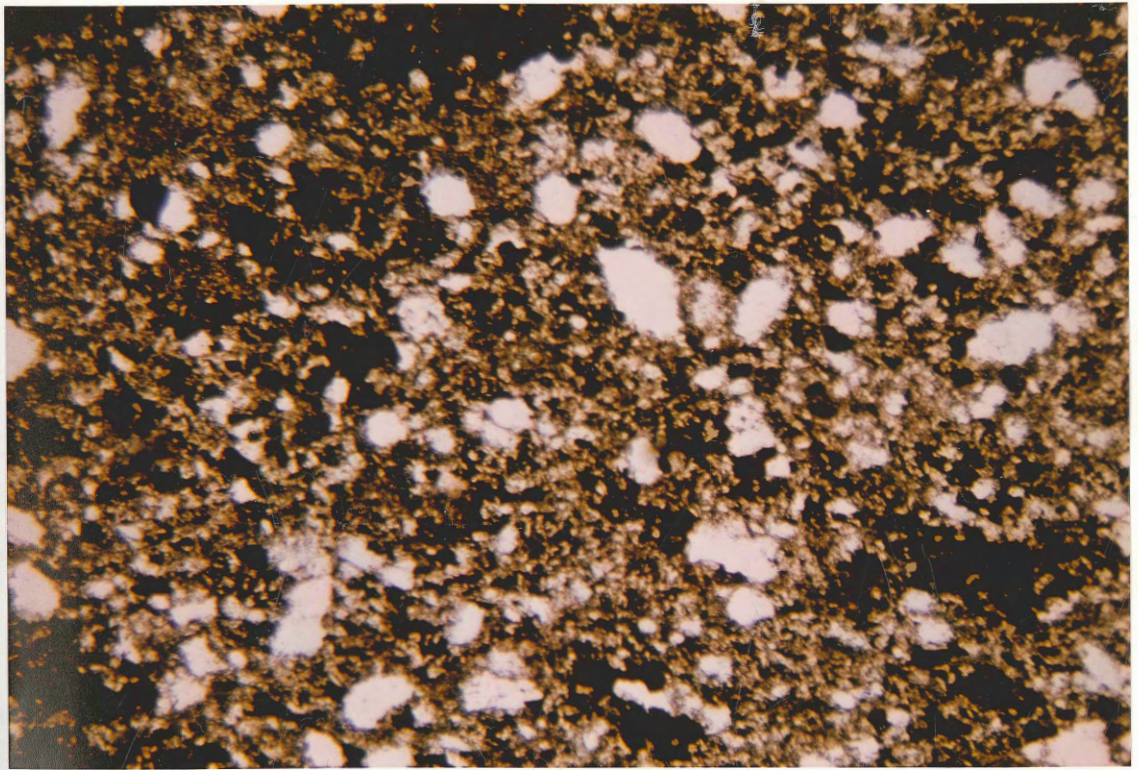
Figure 3.13

Anhedral pyrrhotite disseminated
throughout meta-wacke.

Sample 78-26-117.54

PPL

Long axis of photograph measures 8 mm



3.3.1 Tin Barren Sulphide Zones

This type of mineralization is commonly found as fine-grained elongate blebs of pyrrhotite oriented parallel to foliation; in places they are crenulated. Rarely, layers of almost massive sulphides (pyrrhotite, minor chalcopyrite and arsenopyrite) of several cm thickness occur (Fig. 3.14).

These sulphides consist of anhedral, granoblastic pyrrhotite altering to spotted and massive aggregates of marcasite and pyrite (Fig. 3.15). The sulphides grow around and include all gangue. These larger sulphide layers may in fact represent part of the mineralized sequence, but do not contain any cassiterite.

A number of samples contain 'shredded-textured' sulphides subparallel to the enclosing phyllosilicates (Fig. 3.16); this may indicate an episode of stress after sulphide formation, possibly metamorphic or shear related.

Various authors (e.g., Krauskopf, 1979; Rickard, 1969a,b; Saxby, 1976; and Stanton, 1972b) suggest iron sulphide formation is due to reaction of biogenic sulphur with iron from the sediments. Anaerobic bacteria within organic-bearing sediments reduce seawater sulphate in marine pore water to hydrogen sulphide, and in so doing, produce water and carbon dioxide (Krauskopf, 1979). Iron may become soluble in this reducing environment from detrital iron minerals or iron hydroxides (e.g. goethite) found alone, adsorbed to clays and organic material or coated to clastic

Figure 3.14

Slightly crenulated stratiform
pyrrhotite layer in carbonaceous
meta-argillite. Minor chalcopyrite
and arsenopyrite also occur.

Sample 77-34-233.35

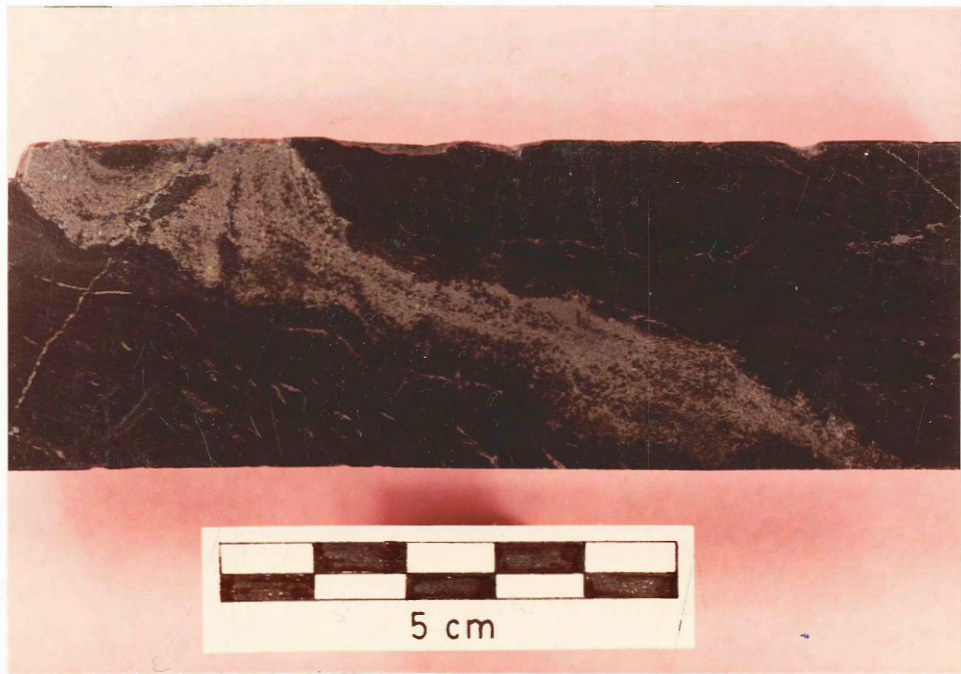


Figure 3.15a

Anhedral grains of graphic pyrite
and marcasite altered from pyrrhotite
within mineralized 'patches'.

Sample 78-12-93.60

Reflected light, oil immersion.

Long axis of photograph measures 1.08 mm

Figure 3.15b

Low temperature alteration of
pyrrhotite to a 'speckled'
assemblage of marcasite and
pyrite to homogenous pyrite.

Sample 77-08-31.45

Reflected light, oil immersion.

Long axis of photograph measures 1.08 mm

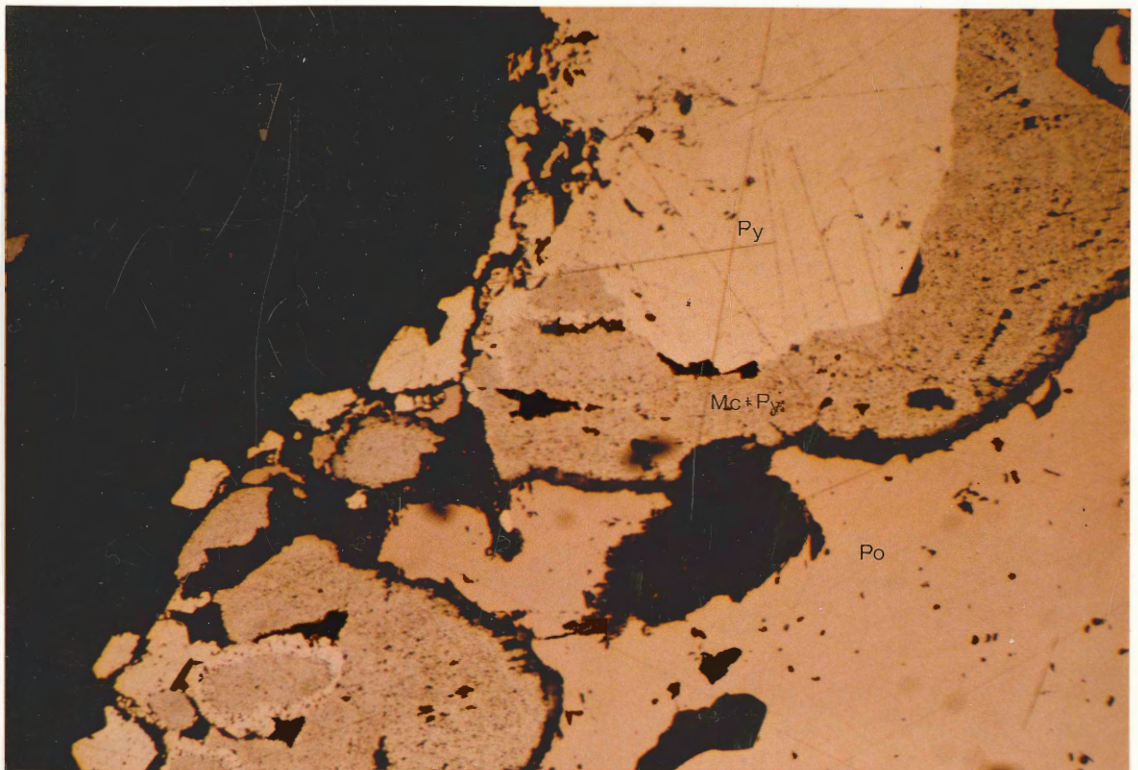
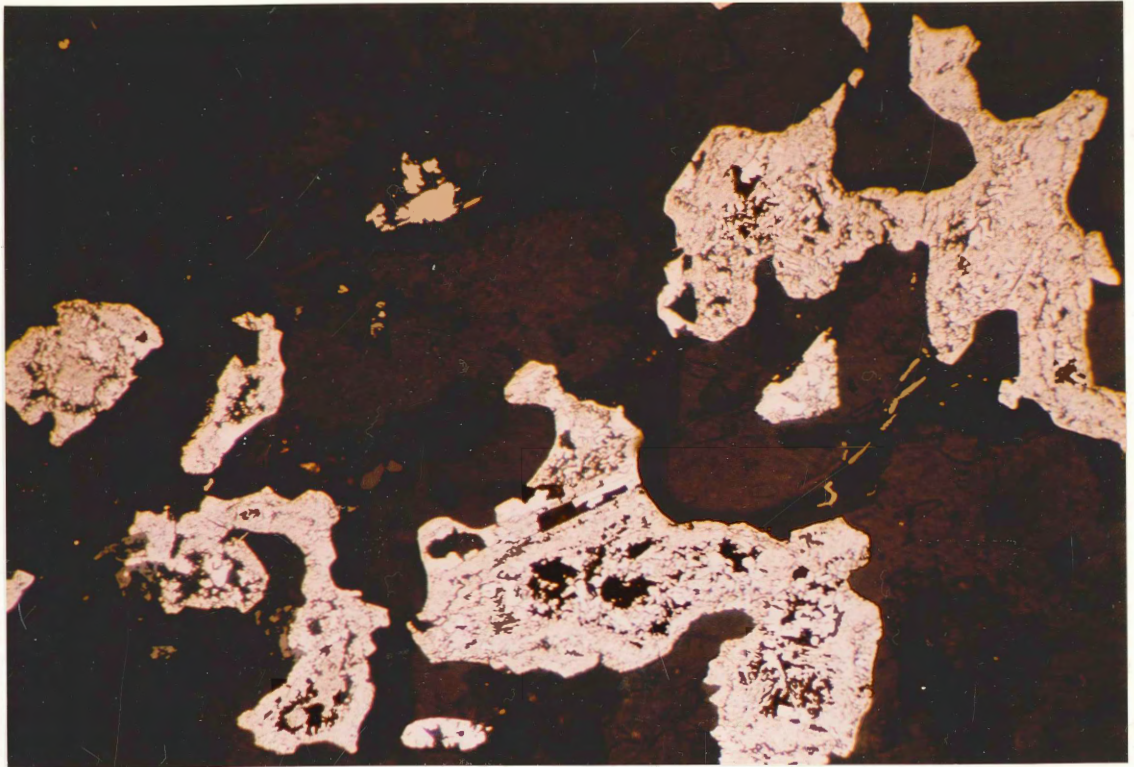
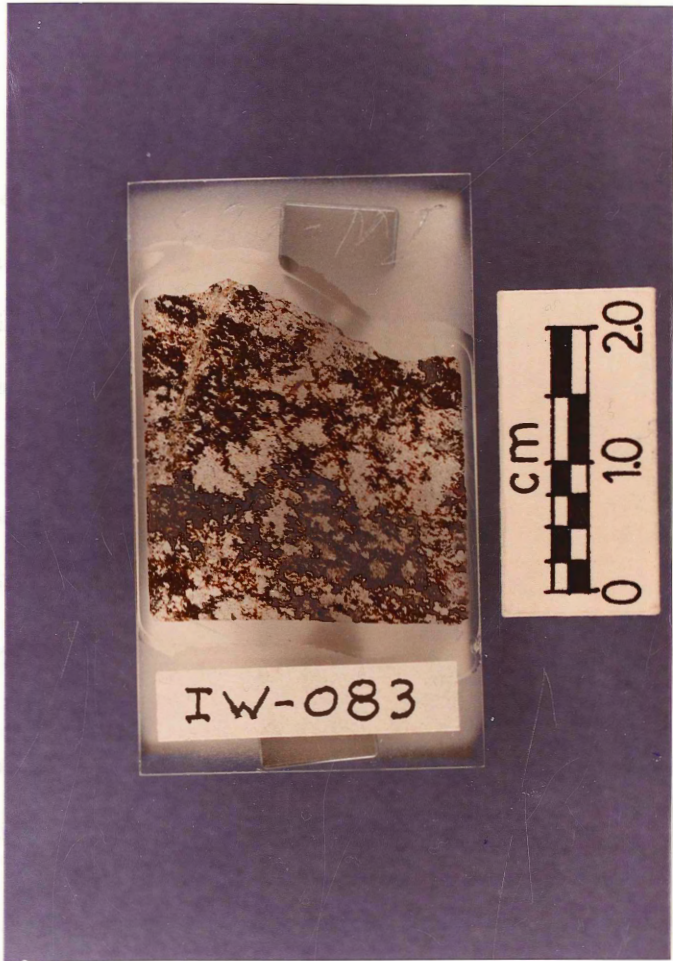


Figure 3.16

Elongate, 'shredded-textured'
pyrrhotite in a biotite meta-
wacke.

Sample 77-05-74.75



IW-083

grains (Love,1969). The first products are soft, dark iron sulphides (e.g. mackinawite, greigite) which may equilibrate to pyrrhotite or incorporate more sulphur from biogenic H_2S or elemental sulphur to form pyrite (Rickard,1969a). Sulphides may form in place in the organic-bearing sediments; the mobile sulphide and metal ions may also be expelled upward during compaction and diagenesis into porous beds to combine there (Vaughan,1976).

An increase in temperature, by compaction, diagenesis and metamorphism may lead to a decrease in sulphur content of pyrite and subsequent conversion to pyrrhotite (Stanton,1972a). Pyrrhotite responds to directed pressure by translation gliding along (0001) crystal planes and thus forms elongate bodies parallel to foliation. The released sulphur from the pyrite may combine with existent iron oxides or hydroxides, iron carbonates or calc-silicates to form 'replacement' or 'sulphidized' iron sulphides (Rose and Burt,1979; Gamble,1982; Love,1969; Kullerud and Yoder,1965; Mookerjee,1981).

Minor chalcopyrite, sphalerite and arsenopyrite found with these pyrrhotite-rich layers may also have formed by the combination of bacterial action, diagenesis and metamorphism (Saxby,1976; Mercer,1976; Love,1969).

Rare samples contain arsenopyrite grains which appear detrital (Fig. 3.17); these angular grains are disseminated

Figure 3.17

Diagenetic(?) arsenopyrite and other sulphides (black) in a coarse meta-wacke in contact with a meta-argillite scour. Current laminations consist of ilmenite and zircon. Steeply dipping lines within meta-argillite are crenulation cleavages.

Sample 77-34-86.13

these

re-

and

the

and

in-

sug-

after

so-

(a)

and

known

has

Pre-

(Ch)

le-

fac-



throughout coarser layers of meta-wackes. Closer examination reveals arsenopyrite to be subhedral with overgrowths of anhedral pyrrhotite, minor chalcopyrite and rare galena; these softer sulphides are compressed around the arsenopyrite and detrital gangue grains. One arsenopyrite grain incorporates a detrital ilmenite lath. This evidence suggests arsenopyrite and the other sulphides formed in situ after sediment deposition and before compression (regional metamorphism?). Little work has been done on arsenopyrite (e.g. Kretschmar and Scott, 1976; Barton and Skinner, 1979) and much of that at high temperatures ($>400^{\circ}\text{C}$) so it is not known if this can occur. However, stratabound arsenopyrite has been described within a sandstone layer in Late Precambrian sediments of the East Greenland Caledonides (Ghisler et al., 1980); euhedral crystals had grown across the laminae, implying a diagenetic to metamorphic (greenschist facies) origin.

3.3.2 Tin Bearing Sulphide Zones

The mineralized 'patches' are usually dark greyish green to dark greyish blue bands (Fig. 3.18). Less commonly they are green, dark and light brown amorphous masses. Rarely, they form dark brownish red and white bands (Fig. 3.19). In drill core the 'patches' have a varied appearance: felty masses rich in phyllosilicates; saccharoidal in the more psammitic zones; or mottled, with light grey, white and

Figure 3.18a

Blue mineralized zone in
meta-wacke.

Sample 77-34-113.73

Figure 3.18b

Two mineralized zones with
thin chloritic haloes.



Figure 3.19a

Sphalerite-pyrite-chlorite
layers in quartz-carbonate
meta-wacke.

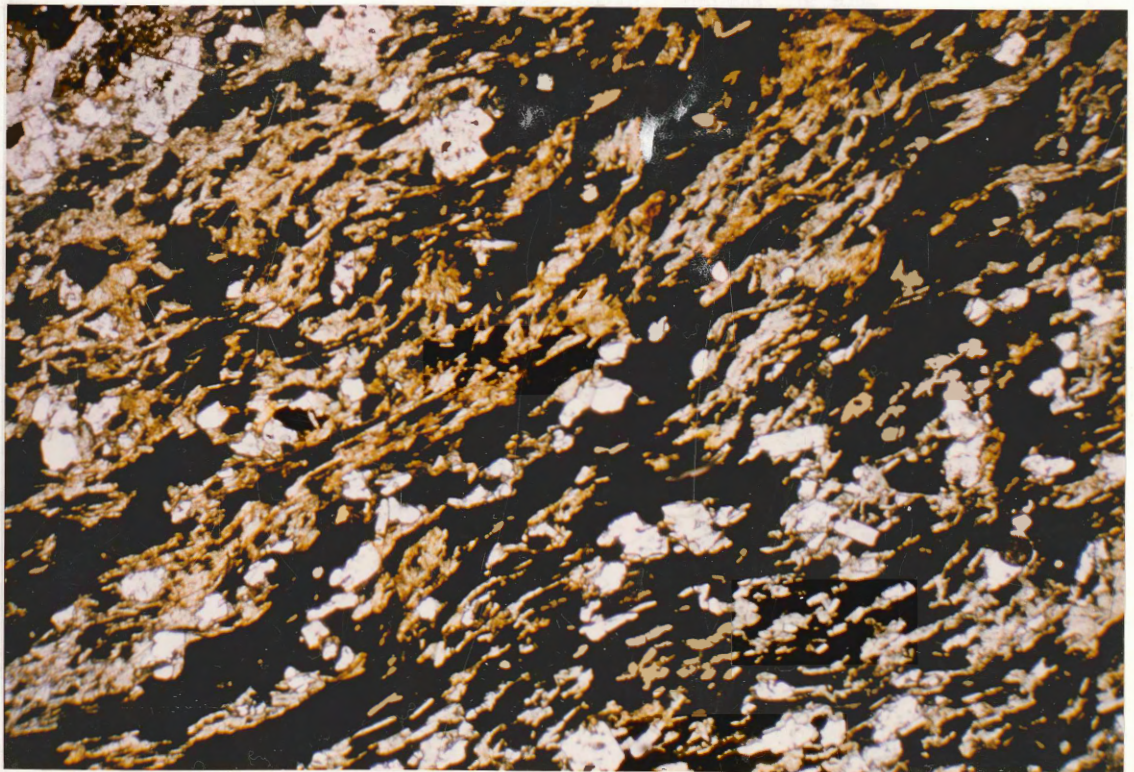
Sample 78-12-13.88

Figure 3.19b

Thin section of above sample.
Elongate sphalerite and pyrite
(opaque) are intergrown with
chlorite and quartz, and are
overgrown by white mica laths.

PPL

Long axis of photograph measures 5 mm



orange stained blebs of carbonate, and irregular disseminations and veinlets of sulphides. They are thin (<1 cm) but rarely attain up to 12 cm length in drill core. The zones are concordant with bedding, with sharp to gradational contacts. Some 'patches' have chlorite and white mica haloes up to 0.5 cm width; one such sample has chlorite that crosscuts the foliation, implying a post-foliation development of these mineralized layers. Their lateral continuity is not known; areas which contain much of this mineralization have these 'patches' at all stratigraphic levels (e.g., see section A in Fig. 5.12). They are pre-faulting, as is evidenced by the crosscutting and displacement of one such zone (Fig. 3.20); therefore they may have formed at the same time as the mineralized veins.

The dark coloration is mainly due to less chlorite and muscovite, and more quartz with disseminated graphite. Mineralization is found in both pelitic and psammitic lithologies, so the gangue mineralogy reflects the host rock. It usually consists of tightly intergrown chlorite, muscovite, quartz, feldspar, and trace amounts of zircon, rutile, sphene and ilmenite. The tectosilicates are granoblastic with lobate to triple point boundaries. The minerals are commonly homogeneously intergrown, although there are 'patchy' growths of: felted chlorite masses; chlorite and quartz; and carbonate. Foliation is defined by parallel orientation of white mica, or vague parallel

Figure 3.20

Blue mineralized zone displaced
by a fine veinlet, and cut by a
quartz-pyrite veinlet.

Figure 3.21

Carbonaceous calcite layer
containing cassiterite
aggregates (arrow).



orientation of graphite.

Graphite occurs as <0.003 mm disseminations to about 0.1 mm needles and wispy aggregates, usually near chlorite. One sample (IW-068) contains vaguely foliated and crenulated graphite wisps and blades in a calcite matrix. It makes up <1 to about 15 modal percent of the mineralized zones. The boundary between mineralized and barren layers is defined, in part, by the concentration of graphite.

Chlorite makes up from 1 to 30 modal percent of the zones, and is found as 0.01 to 0.15 mm anomalous blue needles. It can concentrate at the boundary with unmineralized layers. White mica has about the same form and concentration as chlorite; larger flakes (about 0.45 mm) overprint the matrix.

Carbonate, in the form of calcite, siderite, dolomite or ankerite, occurs throughout the 'patches'. It may form 0.06 to 0.1 mm amorphous blebs intergrown with the matrix, or may form subhedral, equant to tabular, lobate rhombs overprinting the matrix. Inclusions of quartz, muscovite and cassiterite are found. It makes up <1 to 20 (rarely up to 50) modal percent of the zone (Fig. 3.21).

In the more psammitic 'patches' near the pluton, biotite, tremolite (only 1 grain observed) and epidote are also found. Epidote varies from rare to 25 modal percent,

intergrown with, and overprinting the matrix.

Cassiterite and the sulphides comprise from 1 to 30 modal percent of the mineralized zone and occur as clots of grains and fine veinlets. The grains range up to 0.9 mm in size and veinlets are about 0.09 mm wide. Most veinlets are found near the contact with the unmineralized zone, with the graphite and chlorite. They are subparallel to the foliation, following phyllosilicate grain boundaries. The opaques overprint, grow around, or replace the silicates and carbonates.

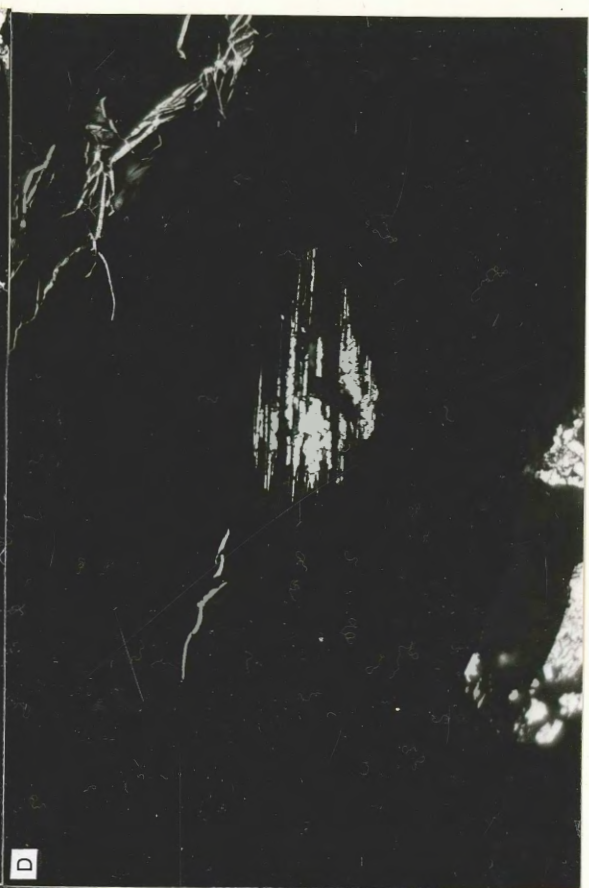
Pyrite is the major sulphide and appears to have been derived from pre-existing pyrrhotite; seen by remnant pyrrhotite within the pyrite (Fig. 3.15). Pyrite is found as anhedral to subhedral, massive to skeletal and graphic textured grains with straight to embayed grain boundaries, following gangue boundaries. Other grains overprint and replace tectosilicates, phyllosilicates (along cleavage planes) and carbonates (from the rim, inwards); see Figure 3.22 for some examples of replacement textures. Many of the grains are on or adjacent to pyrite veinlets, exhibiting a paternoster pattern. This sulphide is intergrown with and replaced by minor chalcopyrite and sphalerite.

Pyrite is also found as individual or bundles of hair veinlets, cutting or outlining silicate and carbonate grains.

Figure 3.22

Replacement Textures in Stratiform Sulphide Zones. All are reflected light, oil immersion.

- A. Detail of poikilitic pyrite (altered from pyrrhotite) inundating cleavage planes of a phyllosilicate, probably biotite. Long axis of photograph measures 0.21 mm.
- B. Pyrite 'atolls' rimming and replacing gangue minerals, probably carbonates. Long axis of photograph measures 1.08 mm.
- C. Detail of partial pyrite replacement of a gangue grain. Long axis of photograph measures 1.08 mm.
- D. Detail of partial pyrite replacement of a phyllosilicate along cleavage planes. Long axis of photograph measures 0.21 mm.



Pyrrhotite varies from less than 1 modal percent in the tin-bearing zones, up to about 40 modal percent in the tin-poor layers. It occurs as anhedral, embayed, polygonal granular and polkilitic grains. This sulphide is intergrown with cassiterite and gangue minerals; it rarely occurs within chalcopyrite, and is partially to completely replaced by pyrite.

Sphalerite is a rare mineral within tin-rich layers (1-2 modal percent), but can attain up to 60 modal percent in tin poor zones. It is usually disseminated, and surrounded by chlorite and white mica. In the richer zones, massive, anhedral sphalerite is intergrown with pyrrhotite partially altered to pyrite; these sulphides are interlayered with chlorite and quartz and are overprinted with white mica (Fig. 3.19). Sphalerite may replace pyrite and may be replaced by chalcopyrite.

Chalcopyrite is a minor sulphide, ranging up to about 1 modal percent. It is associated with pyrite and sphalerite grains. It is grown around, and may replace pyrite, pyrrhotite and sphalerite.

Arsenopyrite is rare, occurring as sub- to euhedral grains surrounded by pyrrhotite.

Cassiterite will be described in detail in the next section, but generally is rare (<1 modal percent), and is

closely associated with the sulphides. It overprints the matrix, and incorporates pyrite, graphite and the phyllosilicates.

A few of these mineralized 'patches' have an adjacent halo of tightly intergrown chlorite and white mica with trace amounts of pyrite, pyrrhotite, chalcopyrite and arsenopyrite.

3.4 Cassiterite - Description

Cassiterite is found in a variety of mineral associations and crystal habits. This diversity appears to be due to the different modes and temperatures of cassiterite formation, and will be discussed further in a later section of the chapter. A summary of the habits and associations of cassiterite is found in Table 3.3.

3.4.1 Stratiform Association

Cassiterite occurs as 0.01 to 0.3 mm sized equant subangular to subrounded grains; several are subhedral (square combination prisms) and have simple twins. The grains are commonly sharply zoned, although the zoning is not always symmetrical: several grains have ragged or broken edges, which may imply a possible detrital origin (Fig.

3.23). One zoned cassiterite grain has a rounded core, a possible relict from an earlier origin (Fig. 3.24).

The grains have a variegated brown coloration, either associated with zoning, or completely random. The core is usually dark brown, lightening outward. Approximately one-half of the grains have colourless ragged rims of cassiterite (Fig. 3.25).

In the only thin section where this particular habit is observed, about 15 modal percent cassiterite occurs in granular aggregates in a pelitic unit. The unit consists of two layers of white mica, chlorite, quartz, minor rutile, graphite and rare chalcopyrite. The aggregates parallel the layering; in one place cassiterite appears to be in a microscour (Fig. 3.26). Cassiterite has also been noted within crossbeds of a Goldenville Formation meta-wacke (A.K. Chatterjee, pers. comm., 1983).

3.4.2 Stratiform Sulphide Association

This type of association is more common, and occurs in the blue to dark green pelitic 'patches'. Cassiterite occurs in two habits: subequant anhedral grains and the more common botryoidal clusters of grains (the so-called 'wood-tin'). The anhedral grains are 0.01 to 0.5 mm in size, of irregular shape with rounded to serrate edges. They are dark brown in

Figure 3.23

Broken zoned cassiterite crystal.
Part of detrital aggregate of
cassiterite.

Sample 78-11-112.4(IW-056)

PPL

Long axis of photograph measures 1.44 mm

Figure 3.24

Zoned euhedral cassiterite with
round core. Part of detrital
aggregate of cassiterite.

Sample 78-11-112.4

PPL

Long axis of photograph measures 0.39 mm

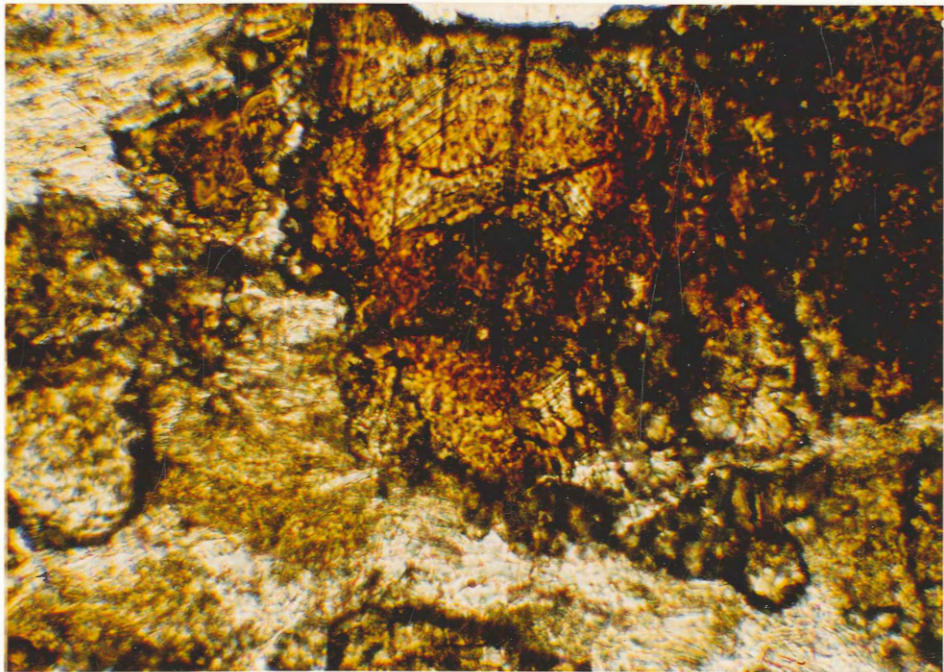
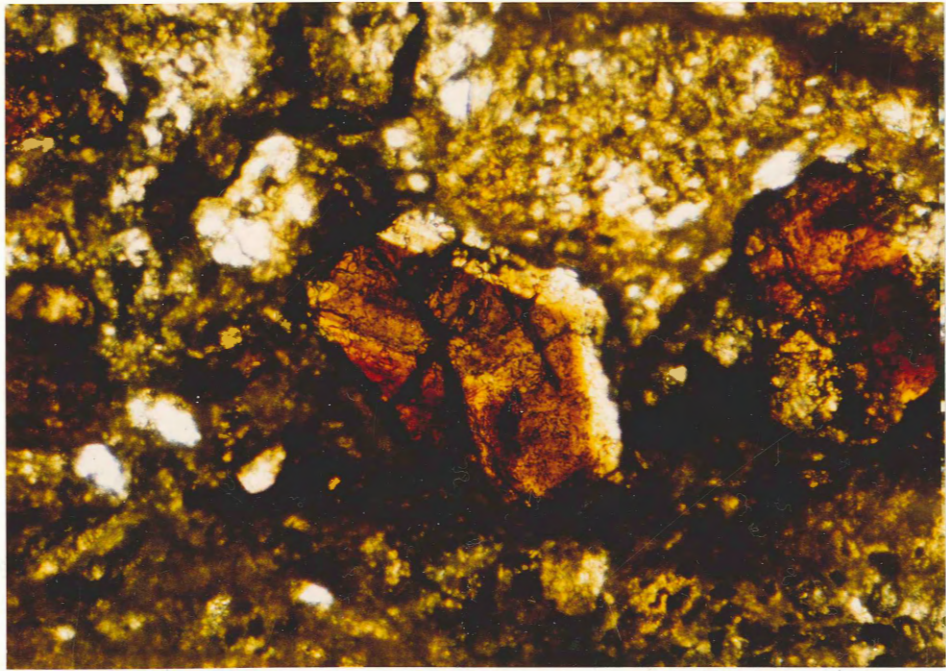


Figure 3.25 Zoned twinned cassiterite with
 ragged colourless overgrowth.

Sample 78-11-112.4

PPL

Long axis of photograph measures 0.39 mm

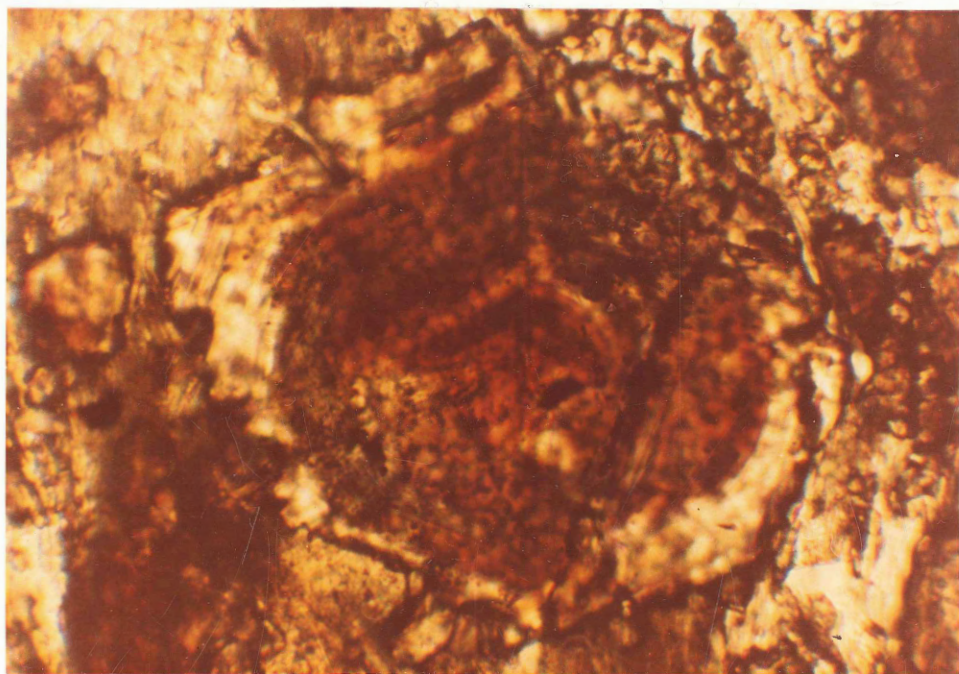


Figure 3.26

Detrital cassiterite in a
siltstone scour. Opaques in
lower layer are ilmenite.

Sample 78-11-112.4

PPL

Long axis of photograph ~ 6.25 mm



the centre, lighten toward the edges, and vary from clear to turbid.

Cassiterite is closely associated with sulphides (pyrite, pyrrhotite, chalcopyrite and sphalerite), ilmenite, rutile, zircon and chlorite. It occasionally partially to completely encloses the sulphides, ilmenite and chlorite. Rarely, it is found without sulphides, within a quartz-biotite-clinozoisite meta-siltstone (Fig. 3.27).

Botryoidal cassiterite occurs as irregular-shaped, rounded or slightly prismatic clusters of grains from 0.003 to 0.2 mm in size, and is dark brown. They usually occur within a groundmass of chlorite and white mica, with or without carbonate, either alone or adjacent the sulphides mentioned previously. They occasionally enclose pyrite, chlorite and white mica, and overprint the groundmass.

Both habits in this association usually comprise less than 1 modal percent in the 'patches', but can attain a maximum of 5 modal percent.

3.4.3 Stratiform Calcareous Sulphide Association

This is an uncommon association, observed in only two thin sections. Cassiterite occurs as 0.05 to 0.1 mm euhedral tetragonal prismatic crystals. They have a variegated coloration: neutral to light brown, with darker brown along

Figure 3.27

Granular cassiterite in biotite-
quartz-clinozoisite meta-wacke.

PPL

Long axis of photograph measures 0.84 mm

crystals

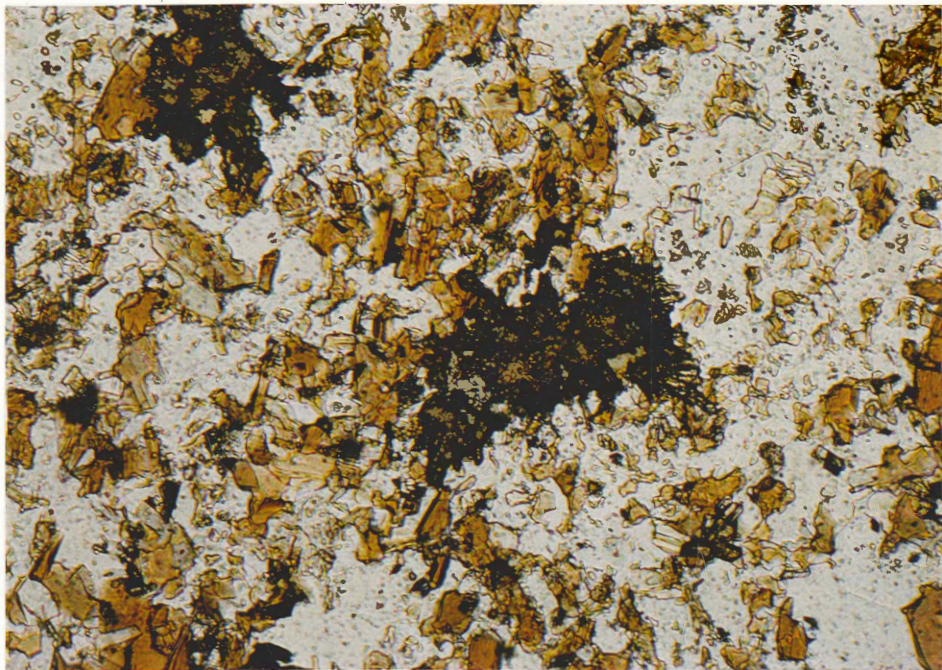
layers

3.26a

a. lower

crystals

layers



crystal edges and microfractures.

In one thin section crystal aggregates occur in a layered graphitic, micaceous calcite-sulphide 'patch' (Fig. 3.28a). The other thin section hosts cassiterite crystals in a linear distribution (boundary layer?) between two calcareous siltstone layers. This type of cassiterite comprises about 1 modal percent of the thin section.

The accompanying sulphides include up to 10 modal percent of pyrrhotite, plus rare pyrite, chalcopyrite and arsenopyrite. They occur throughout the sections and have curved to embayed boundaries (Fig. 3.28b).

3.4.4 Vein Association in the Metasediments

Three habits of cassiterite are displayed within and adjacent to the veinlets of quartz-carbonate-sulphides (pyrite, pyrrhotite, chalcopyrite, ± galena, arsenopyrite, sphalerite). Most cassiterite in the study area is found with this association.

1. Subhedral to anhedral equant crystals (square prisms) up to 1.0 mm in size occur either alone or adjacent to the sulphides in veinlets. They commonly have diffuse colour zonation, defined by a gradual colour change from dark brown in the core to colourless in the rim; few have

Figure 3.28a

Aggregate of prismatic cassiterite in carbonaceous calcite-rich layer (IW-068).

PPL

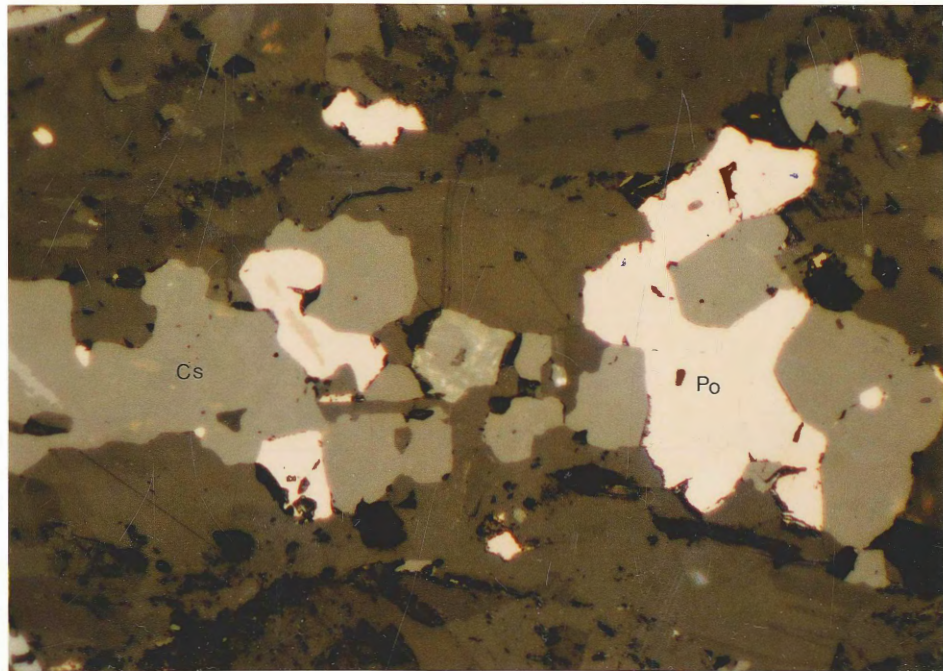
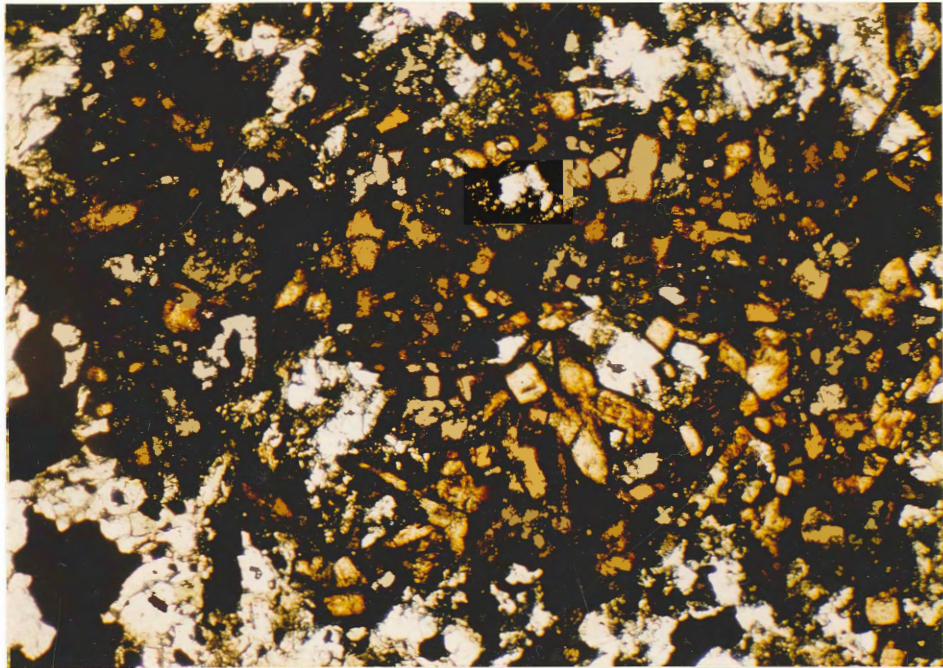
Long axis of photograph measures 3.23 mm

Figure 3.28b

Pyrrhotite intergrown with cassiterite in IW-068. Darker hued patches are remnants of graphite coating.

Reflected light.

Long axis of photograph measures 0.54 mm



oscillatory zoning (Fig. 3.29). Dark to light brown variegated coloration also exists in other crystals.

- ii. Pale to dark brown botryoidal cassiterite up to 0.25 mm in size is disseminated throughout the green chloritic halo surrounding the sulphide veinlets (Fig. 3.30). It is intergrown with chlorite, muscovite, ilmenite and zircon, and occasionally incorporates ilmenite.
- iii. Radial clusters of orange brown to dark brown acicular cassiterite up to 1.25 mm in diameter occur in the veinlets adjacent to late stage carbonate (Fig. 3.31). They form whole or partial spherules and contain variable amounts of inclusions, notably ilmenite, with minor pyrite, pyrrhotite and chalcopyrite. Some form acicular druses on pyrite and pyrrhotite.

3.4.5 Greisen Association

Cassiterite rarely occurs in this association. It is found as light to dark brown, equant, sub- to anhedral crystals up to 0.25 mm in size. It is intergrown with quartz, white mica, fluorite, ± pyrite, pyrrhotite, chalcopyrite. One crystal occurs within a fluorite grain in a greisen zone (Fig. 3.32) and one is found within a greisen veinlet.

Figure 3.29

Subhedral zoned vein cassiterite.

PPL

Long axis of photograph measures 0.84 mm

Figure 3.30

Botryoidal cassiterite in
chlorite alteration halo
adjacent sulphide-cassiterite
vein.

PPL

Long axis of photograph measures 0.39 mm

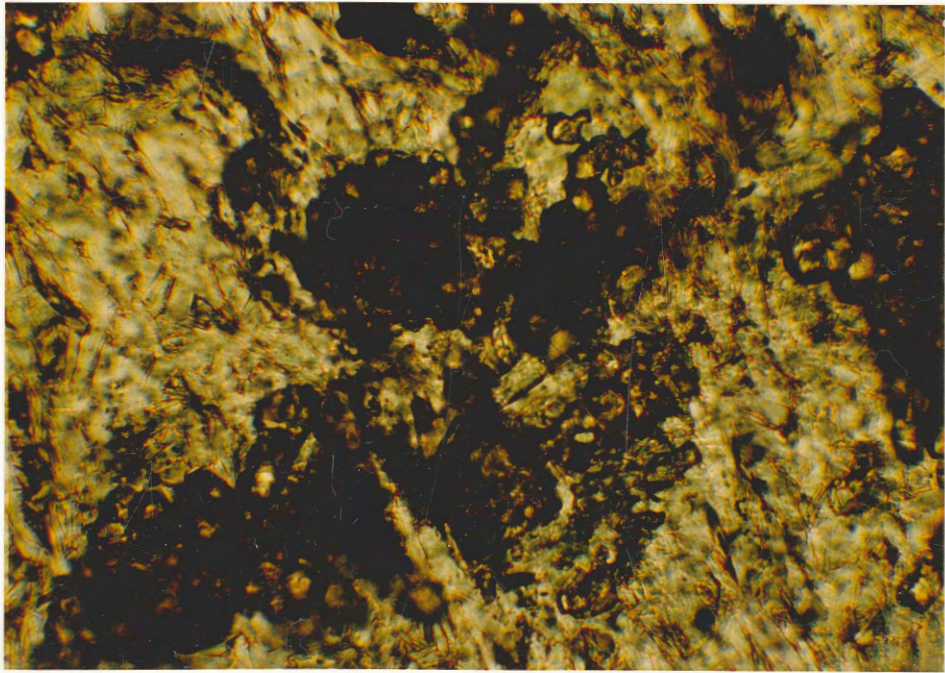
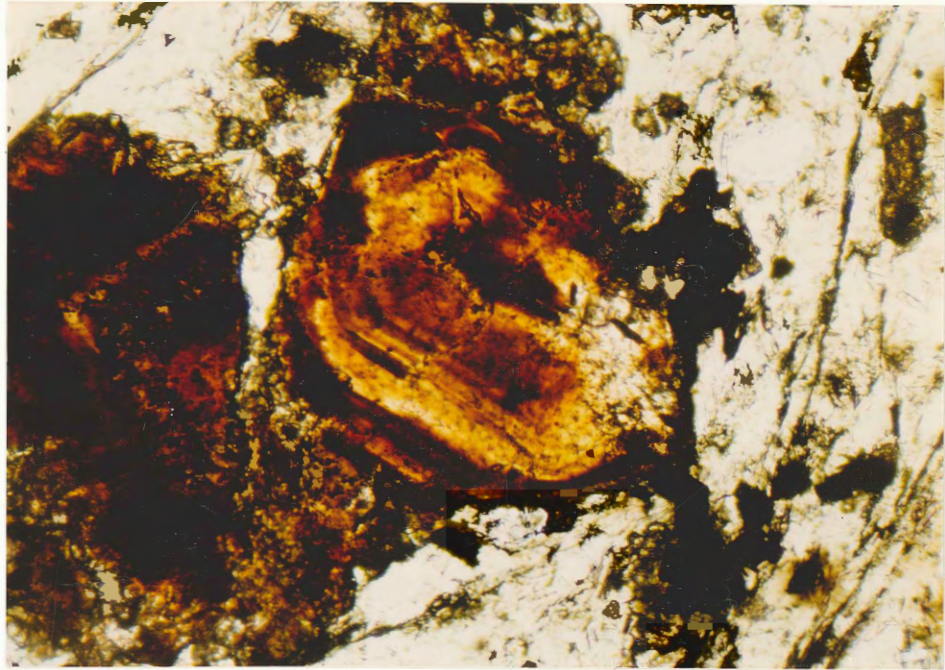


Figure 3.31a

Late stage spherulitic vein
cassiterite.

PPL

Long axis of photograph measures 2 mm

Figure 3.31b

Late stage acicular vein
cassiterite grown around
pyrite.

PPL

Long axis of photograph measures 0.84 mm

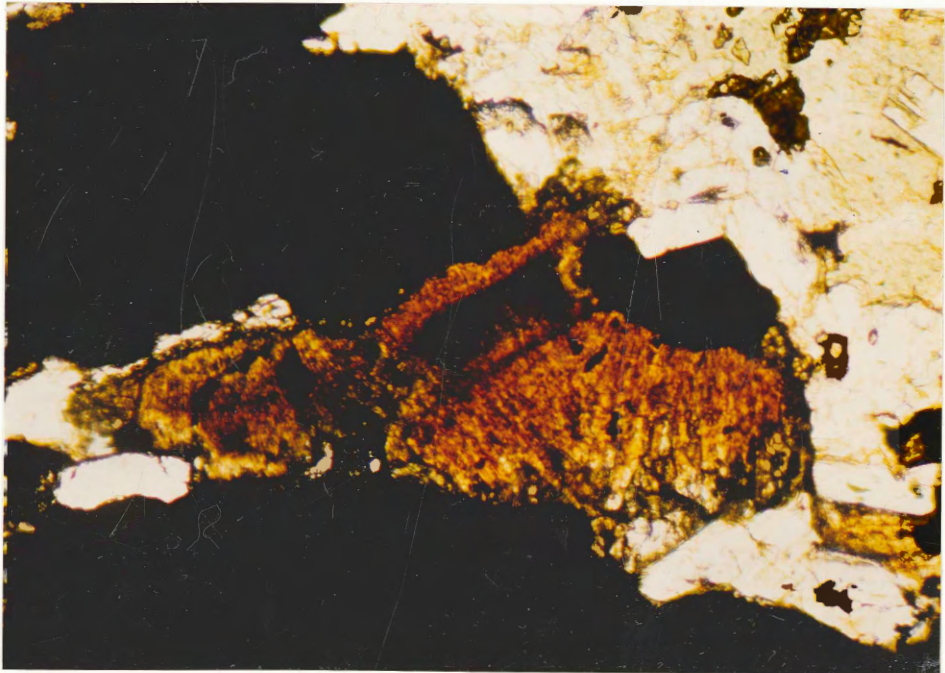
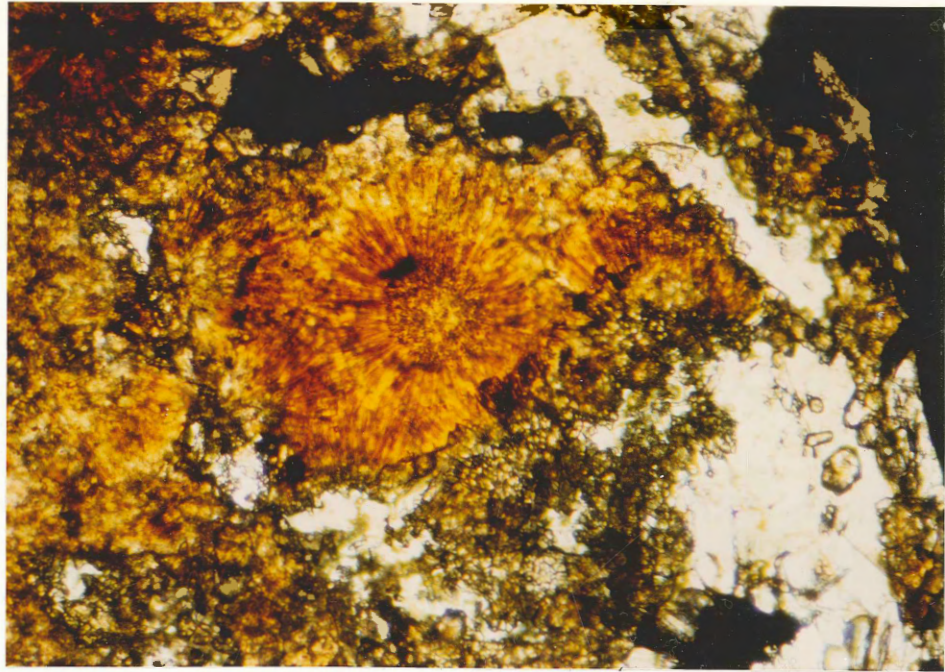
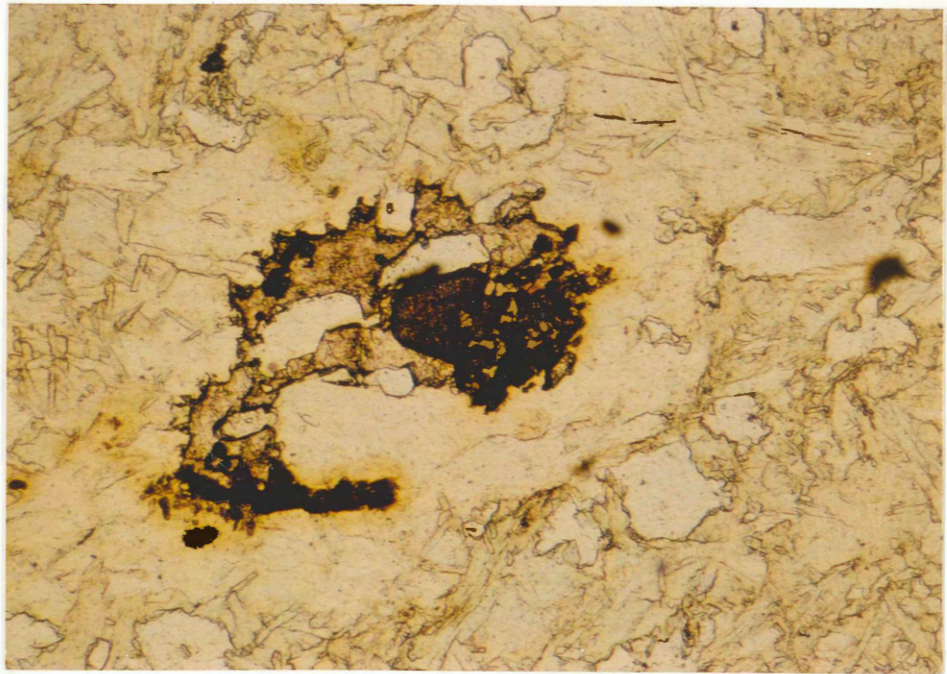


Figure 3.32

Subhedral cassiterite
associated with fluorite,
pyrite and chalcopyrite in
a quartz-white mica greisen.

PPL

Long axis of photograph measures 2 mm



3.5 Cassiterite - Temperature of Formation


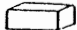


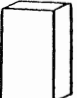

Studies of the formation of cassiterite have shown it to form in the range of approximately 150^o-600^o C (Taylor,1979a; Pan and Ypma,1974; Shneider,1937). The crystal forms of cassiterite can be related to its temperature of formation (Miyahisa,1968; Shneider,1937) and are not influenced by trace element contents (although trace element substitution of Sn⁴⁺ can change the cell volume; Taylor,1979a).

Cassiterite belongs to the tetragonal crystal system and the ditetragonal dipyramidal class. It occurs in a variety of forms, including combinations of prisms, with pyramids, dipyramids without prisms, acicular fibers and botryoidal grains ('wood tin') (Berry and Mason,1959; Taylor,1979a).

In any given deposit, cassiterite characteristically occurs in more than one generation, and in more than one habit, and this diversity serves to assign the minimum relative temperatures of cassiterite formation (Taylor,1979a; Hosking, 1979).

Shneider (1937) and Miyahisa (1968) have measured cassiterite from different deposits and found that cell parameters change with decreasing temperature. This change is manifested by a change from more equant, dipyramidal forms, to more prismatic, acicular forms (Table 3.3).

Table 3.3 Cassiterite Crystal Habits and Related Temperatures of Formation

Habit ^{1,2}	Temperature ¹ and Environment ² of Formation	Cell Parameters ²		Habits in Study Area
		a	c	
	> 600°C	-	-	Equant grains in stratiform association ?Subequant grains in stratiform sulphide association?
	> 500°C	-	-	
 "Isometric" (italics this author)	500°C High temperature type	4.736- 4.739	3.187- 3.190	
	450°C Meso-xenothermal type	4.738- 4.742	3.184- 3.187	
	< 450°C Bolivian volcanic type	4.738- 4.741	3.186- 3.190	Square prisms in stratiform calcareous sulphide association Late stage spherulites in sulphide veins
	≈ at least 150°C	-	-	Botryoids in chloritic haloes adjacent vein and in stratiform sulphide association

1. Shneider, 1937

2. Miyahisa, 1968

N.B. Shneider reports that at high temperatures, the c-axis is compressed and lengthens with decreasing temperature. This is roughly true, although data from Miyahisa show that a also increases. Data from Goncharov and Filatov (1972) roughly indicate an increase in both a and c axis lengths with depth (due to temperature or pressure?).

Botryoidal forms ('wood tin') occur in late stage, high level, lower temperature deposits, and are believed to form by rapid nucleation from highly saturated, possibly colloidal solutions (Taylor,1979a; Hosking,1979; Lufkin,1977; Pan and Ypma,1974; Lebedev,1967; Roedder,1968), flocculating in zones of rapid chemical change, such as in wall rocks adjacent veins (Doucet, quoted in Taylor,1979a).

3.6 Cassiterite - Genesis

The variety of cassiterite crystal habits appears to reflect the temperature and environment of its formation. There appear to be three main stages of genesis: detrital, vein and replacement.

3.6.1 Detrital

The anhedral, equant grains which occur within the pelitic layers have several features which serve to characterize their detrital nature.

1. In the one sample (IW-056), aggregates of cassiterite are restricted to the bottoms of two thin pelitic layers; one layer is a possible scour infill (Fig. 3.26).

2. Many grains in this sample have sharp growth zoning and several such grains have broken edges (Fig. 3.23). These grains could not have grown and been broken in place. No evidence of cataclasis exists, only slight fracturing of the cassiterite with development of brown coloration along the fractures.

One zoned grain has a rounded core (Fig. 3.24), a possible nucleus around which subsequent layers grew. Such zoning is indicative of relatively free growth into fluid-filled spaces with slight changes in the physico-chemical environment (Craig and Vaughan, 1981; Ramdohr, 1980;). The equant habit is indicative of high temperature formation, which could not have occurred under conditions of low grade greenschist facies metamorphism.

3. The cassiterite grains are not associated with any sulphides usually found in the stratiform sulphide

association; there is no evidence of alteration of surrounding host minerals as in all the other associations. There is a slight wrapping of phyllosilicates around the cassiterite, suggesting the grains had existed before or during regional metamorphism (Spry,1969).

This type of cassiterite does not appear to have formed in place; rather it originated in a high-temperature open space (a vein?). Subsequent uplift and erosion liberated the grains and they were transported to a basin. Harris and Schenk (1975) have suggested that the sediments of the Meguma Group were derived from a deeply eroded, cratonic terrain, later sorted on a continental shelf and alluvial plain, and then transported by turbidity currents down submarine channels. It is therefore possible that the cassiterite, eroded from the above terrain could have been winnowed on the continental shelf, transported and then deposited in or along these channels, in scours or on the abyssal plain.

There is no cassiterite in the only other scour infill (Fig. 3.17). This may be because of the scarcity of cassiterite in the first place; finding detrital cassiterite in any concentration would therefore be fortuitous, even in scours. A less likely explanation for the paucity of detrital cassiterite would be its dissolution by intrastratal solution in the more permeable wackes during diagenesis (Blatt and Sutherland,1969; Blatt et al.,1980). Although

detrital cassiterite grains do have ragged edges (Fig. 3.25), the associated ilmenite and zircon (which theoretically should be corroded) do not.

It is beyond the scope of the present study to do more than speculate on the possible origins of detrital cassiterite. Schenk (1975) and Harris and Schenk (1975) have suggested that the source continent consisted of metasedimentary or meta-igneous material of Precambrian age, possibly the present Saharan Shield in northwestern Africa or even a Precambrian shield in northwestern South America. Although stratiform copper, manganese, lead, zinc and uranium mineralization occur in clastic and chemical sedimentary rocks of the 'Infracambrian superieur' of Morocco, no Precambrian tin occurrences have been documented by Michard (1976). Minor tin mineralization in quartz veins occurs in the Moroccan Hercynian Oulmés granite of El Karit in the Meseta with aplites, pegmatites and rare lamprophyres. Minor tin is associated with quartz veins and pegmatites of the Precambrian metamorphic shield of northeastern South America in Brazil; Lower Paleozoic tin deposits are documented in northwestern South America in Bolivia (Taylor, 1979a). These tin occurrences may have either been too young to have been the source of the Meguma detrital cassiterite, or may have been too far removed spatially at the time of erosion (Strong, 1980; Harris and Schenk, 1975), although other resistant minerals such as diamonds have been known to travel

by fluvial and marine processes hundreds of kilometers from their primary source (Sutherland, 1982).

3.6.2 Main Stage Vein Genesis

The transportation and deposition of tin in vein systems have been subject to much study and experimentation (e.g. Smith, 1947; Shcherba, 1970; Cuff in Taylor, 1979a) and the reader is referred to these authors for further details.

Because of the amphoteric nature of stannic oxide (Smith, 1947), it is soluble as both alkali stannates and tin halides and may therefore be transported in, and crystallized from both alkaline and acid aqueous solutions. It is tentatively suggested that both types of solutions played roles in the transportation of tin in veins in both the pluton and the metasediments.

Tin can form a variety of complexes in aqueous solutions; those commonly described in the literature are presented here.

- Acid aqueous solutions - tin soluble as simple ions (Sn^{4+}) (Smith, 1947).
- chloride, fluoride and hydroxide complexes of divalent tin under conditions of acid pH (<7) and low oxygen fugacity (< quartz-feldspar-muscovite buffer) (Taylor, 1979a; Patterson et al., 1981).

Alkaline aqueous solutions - if a high concentration of sulphide ions exist, tin is soluble as an alkali stannic sulphide complex (SnS_4^{4-}) (Smith, 1947).

-alkali complexes of tetravalent tin, such as $\text{Na}_2(\text{Sn}(\text{OH})_6)$, $\text{Na}_2(\text{Sn}(\text{F})_6)$ and $\text{Na}_2(\text{Sn}(\text{OH},\text{F})_6)$ in neutral to alkaline solutions (Taylor, 1979a).
-hydroxy-fluorostannate (Sn^{4+}) complexes of the type $(\text{Na},\text{K})_2[\text{Sn}(\text{OH})_x\text{F}_{6-x}]$ at pH 6-11.75 (Taylor, 1979a)

Changes in the ambient physico-chemical conditions (e.g. P, T, pH, $f\text{O}_2$) lead to the destruction of the complex and deposition of tin as cassiterite, either directly or as a hydroxide, $\text{Sn}(\text{OH})_4$ which then dehydrates to SnO_2 .

A possible model for the transportation and deposition of tin in the study area is presented.

3.6.2.1 Greisen Veins

According to Shcherba (1970), greisenization involves the high temperature ($300^\circ\text{--}500^\circ\text{C}$) alteration of rocks by acid aqueous (\pm vapour) solutions, the residual fluids of a crystallizing granitic intrusion. These fluids are rich in water, silica and such volatiles as F, Cl, S, and C; the concentration of F being much lower than that of H_2O , CO_2 and Cl (Bailey, 1977). They also contain Al, K, Na and Ca. Metals which commonly occur in these fluids are: Sn, Li, W, Mo, B,

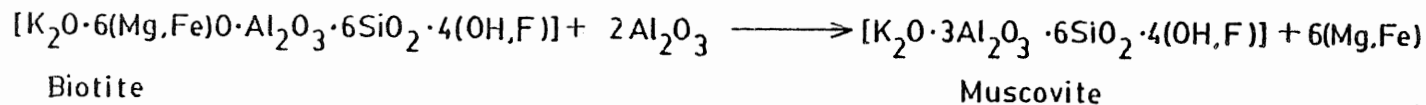
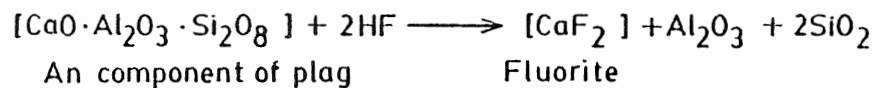
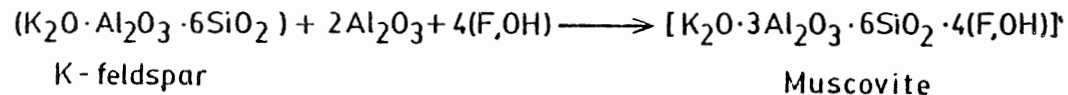
Fe, Mg, Cu, Pb, Zn and As, and are transported as halogen complexes. Salinities, measured in fluid inclusions from greisen deposits range up to about 10 wt. % NaCl equivalent (Charoy and Weisbrod,1974; Kelley and Rye,1979; Taylor,1979a).

Plutonic feldspars and micas are destroyed by these fluids and replaced by variable amounts of muscovite, fluorite, topaz, tourmaline, feldspar, cassiterite, wolframite and sulphides (e.g. chalcopyrite, pyrite and molybdenite). Table 3.4 presents some of the major mineral and element changes which occur during greisenization.

Prior to greisenization, alteration of primary magmatic feldspars to secondary albite or microcline or both is reported to occur (Shcherba,1970; Taylor,1979a). Microscopic examination and microprobe analysis of the feldspars both adjacent to greisens and in optically unaltered monzogranite show the plagioclase to vary in composition from oligoclase-andesine to albite, although there appears to be no pattern to their fluctuating An content. Taylor (1979a) cites from the literature several causes for this diverse feldspar composition:

1. Removal of anorthite component from primary plagioclase. by alkaline solutions (from residual fluids?)
2. Addition of Na₂O and removal of K₂O from potassium feldspar.
3. Albite already primary magmatic.

Table 3.4 Major Mineral and Element Changes During Greisenization



Biotite \longrightarrow Chlorite + Magnetite \longrightarrow Muscovite + Pyrite

Ilmenite \longrightarrow Rutile + Pyrite

Elements brought to greisen zone - Sn W Li Mo Be Cu Pb Zn As Bi REE's Ta Nb P Th Zr
 - Si F Cl B H₂O S CO₂

Elements removed from wallrock - Ca Mg Al(in part) Na

Elements redistributed - K Al Fe Ti

From Mulligan, 1975; Shcherba, 1970

According to these authors, feldspar alteration can be both pervasive and localized, of irregular geometry, and may occur repeatedly, before and after greisenization, as the physico-chemical conditions of the fluid changes with time and location within the pluton. Shcherba (1970) explains that microclinization occurs by conversion of orthoclase to K-anorthoclase to twinned microcline, but not how it happens (possible conversion of monoclinic potassium feldspar to a lower temperature triclinic system during final stages of cooling of the pluton?). J. Logothetis (pers. comm., 1983) suggests that readjustments in major element contents by greisenizing solutions may cause albitization and microclinization. The only unequivocal optical evidence of alteration of the feldspars in the Wedgeport monzogranite is observed in the greisen zones and this is deemed to be caused by the greisenization episode and not by a prior 'alkaline stage feldspathization' episode described by Shcherba (1970). Localized alteration occurs adjacent later shears, mafic dykes and along weathered fractures.

Fresh unaltered monzogranite consists of quartz, slightly sericitized plagioclase and microcline, with accessory biotite containing inclusions of apatite, zircon and ilmenite (Fig. 3.33). In the early stages of greisenization, biotite flakes alter to chlorite(± vermiculite?); possibly ± potassium feldspar ± epidote? (J.

Logothetis, pers. comm.,1983)) and magnetite (+ iron hydroxide?) aggregates, appearing rusty brown or tan in hand specimen. This is the indicator material of the 'tan alteration zone'. Ilmenite alters to anatase; apatite and zircon appear unaffected. Microcline shows slightly greater sericitization and begins to take on a turbid appearance due to a myriad of extremely fine (<0.001 mm) inclusions. Plagioclase is more sericitized, with larger white mica flakes and contains calcite, usually in the crystal cores. Fluorite rarely occurs in this zone.

As greisenization continues, the chlorite breaks down into a light rust-brown hydrous phyllosilicate (vermiculite with iron hydroxide staining?; Craw,1981; Kodama et al.,1982; or epidote grains with subsequent alteration to carbonate?; J. Logothetis, pers. comm.,1983). Plagioclase continues to alter to white mica (possibly lithium-bearing) and carbonate, while microcline becomes more turbid with diffuse grid-iron twinning. The hand specimen now appears a homogeneous milky white ('white alteration zone') with pinkish-grey quartz blebs. Minor fluorite and sulphides may occur in this zone.

In the greisen proper, both feldspars are destroyed, as is the vermiculite(?), possibly due to its instability at temperatures over 300°C (Deer et al.,1974). The zone consists primarily of white mica and quartz, with common to abundant fluorite, rare cassiterite and sulphides.

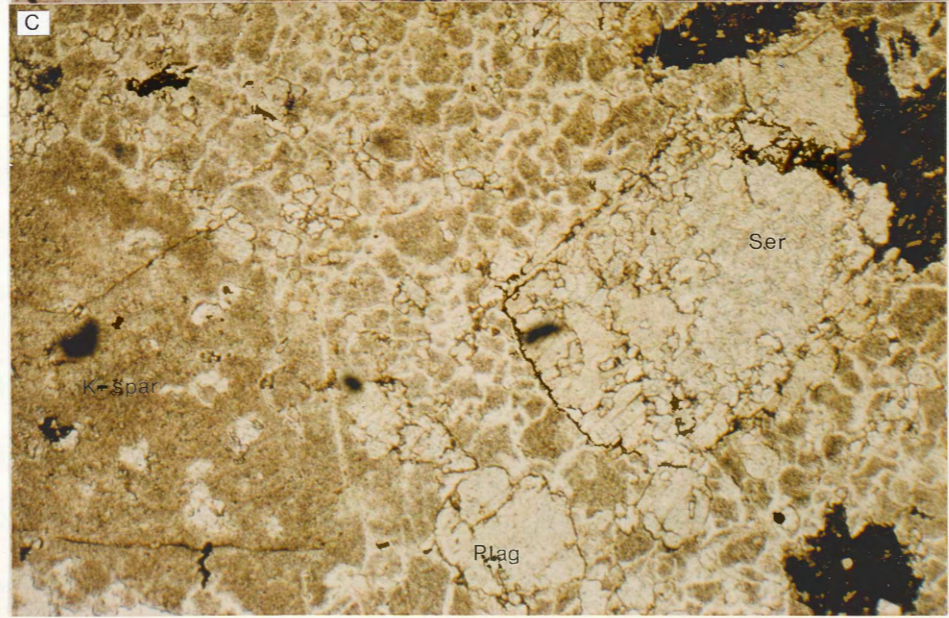
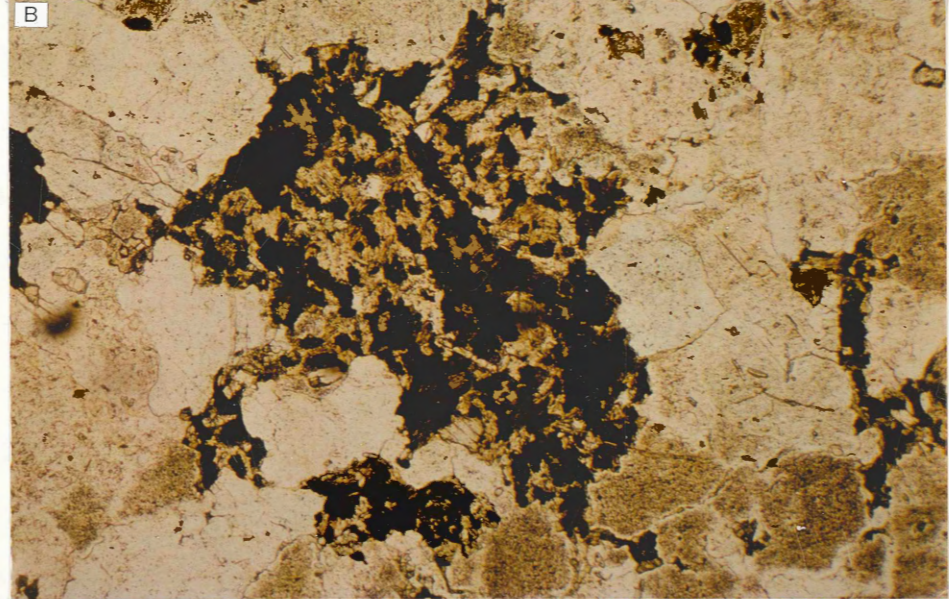
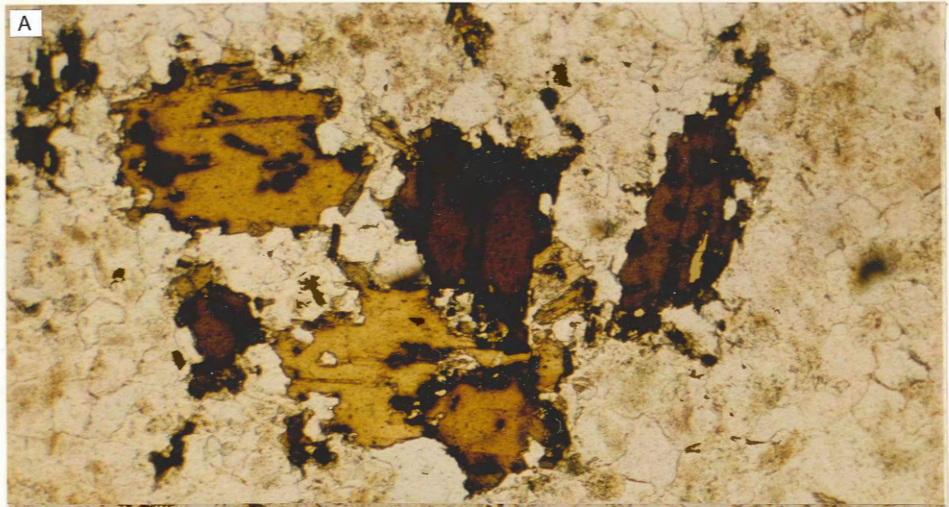
Figure 3.33

Progression of alteration in greisenized monzogranite.

Sample 79-08-70.70

All PPL; long axis of first two photographs measures 3.23 mm; last one measures 4.9 mm.

- A. Unaltered zone; biotite flakes are clear and include apatite, zircon and ilmenite. The surrounding feldspars are slightly sericitized.
- B. 'Tan alteration zone'; biotite flake has altered to a chlorite-vermiculite(?) aggregate containing iron and titanium oxides (ilmenite to anatase). Microcline becomes turbid; plagioclase remains clear.
- C. 'White alteration zone'; biotite flakes completely alter to oxide and vermiculite(?) assemblages. Microcline becomes more turbid; grain boundaries become diffuse. Plagioclase remains clear but becomes sericitized.



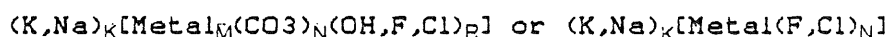
Greisenization begins with acid leaching of the granitic wallrock. The acid fluids may either be 'primary' residual solutions of a crystallizing granitic intrusion or may result from the breakdown of alkaline fluids: a rapid decrease in P or T or both destroys complexes, thereby freeing halogens and causing the pH to decrease (Shcherba,1970). These acid fluids break down the feldspars and biotite, adding and removing various constituents. Fluorine tends to react with calcium released from destroyed plagioclase, forming fluorite; F may also substitute for OH in the white micas of a greisen. Removal of F from the fluid destroys whatever complexes it held with tin and the tin may either precipitate as cassiterite or recombine to form other complexes. The close association of cassiterite and sulphides with fluorite (Fig. 3.32) suggests that fluorine probably aided in metal transport. Evidence for transport of tin by other complexes, such as chlorides or hydroxides, is more difficult to ascertain because such elements form few independent minerals, and are instead incorporated in other minerals or in fluid inclusions. The subhedral equant habit of cassiterite suggests it precipitated at a relatively high temperature ($\geq 450^{\circ}\text{C}$?) (Shneider,1937).

Removal of F also decreases the activity of the fluids, and this, in combination with the addition of alkali metals from the leached silicates, causes the fluids to become more alkaline (Shcherba,1970; Tischendorf,1973).

The paucity of cassiterite within the greisens of the study area suggests either a low initial concentration of tin in the residual fluids, or the persistence of tin in solution by complexing with alkali metals (+ sulphide ions) introduced by greisenization. The greisen zones in the pluton are rather narrow (on the order of cm) and usually in sharp contact with fresh or incompletely altered monzogranite. This implies relatively rapid equilibration (neutralization) of acid fluids with the wallrock, removing large amounts of alkalis from the silicate minerals. As tin-halogen complexes break down and the halogens are incorporated in the greisen minerals (fluorite, white micas), tin may be able to form complexes with the now abundant alkali metals and remain in solution (now alkaline) instead of precipitating as cassiterite. It may also be possible that other halogen complexes would be more stable under these changing conditions (chloride complexes) and keep tin in solution (Patterson et al., 1981).

3.6.2.2 Metasediment Veins

These alkaline fluids may enter the metasediments via fracture systems and react with the wallrock. Metals may be carried in such alkali complexes as:



(Shcherba,1970), and, if enough sulphide ions are available, as alkali-metal-sulphide complexes (Smith,1947; Stanton,1972a; Barnes,1979). Shcherba (1970) and others believe that since Cl is more mobile than F, it is able to travel beyond the greisen in solution and is therefore the more important carrier of tin in complexes; F tends to be readily fixed within the greisen zones as F-bearing minerals. Geochemical analyses seem to bear this out: greisen vein samples in the pluton show enrichment of F relative to unmineralized monzogranite, while those of sulphide-cassiterite veins in the metasediments show F concentrations at or near background levels. Chlorine analyses were unusable as all values were below the detection limit of 50 ppm.

Changes in the physico-chemical conditions (e.g. decrease in P, T and pH, dilution of fluids, increase in the fugacity of oxygen) can result in destruction of the complexes and precipitation of metals and gangue minerals (Barnes,1979). Deposition of metal sulphides(in this case mainly pyrrhotite, pyrite and chalcopyrite) decreases the sulphide ion content of the alkali-thio-metal complex, leading to precipitation of tin as cassiterite with the sulphides. The subhedral, equant habit of this type of cassiterite may indicate a relatively high temperature of formation ($\geq 450^{\circ}\text{C}$?) (Shneider, 1937). Fluid inclusion studies, however, point to lower formation temperatures ($\sim 350^{\circ}$

C) of cassiterite-sulphide veins (Jackson et al.,1979). Carbonate and later acicular cassiterite overgrow the previous minerals as the fluid cools and complexes continue to break down - the acicular habit indicates a lower formation temperature (<450°C) (Shneider,1937). Quartz, minor accessory white mica and chlorite form within the vein; iron-rich chlorite and botryoidal cassiterite surround the vein, forming a thin alteration halo, again implying rapid equilibration of the fluids. Formation of the phyllosilicates and quartz accounts for most of the other constituents of the fluid; Na may enter feldspars in the country rock, or remain in solution with Cl and other material in fluid inclusions. Botryoidal cassiterite is considered a late-stage, low-temperature (at least 150°C; Shneider, 1937) tin oxide, formed by rapid nucleation of saturated solutions (Taylor,1979a).

The relationship of these fluids with cassiterite-absent veins is not known. They exist farther from the pluton and at shallower depths than the tin-bearing veins. They may be extensions of the same vein system; fluids are depleted in tin, but still contain such metals as Cu, Pb, and Zn in complexes whose solubility products are exceeded at lower pressures and temperatures.

3.6.3 Stratiform Mineralization

A major problem in dealing with stratiform mineralization is the mode of its formation. Two schools of thought exist on this issue: this type of mineralization forms as a result of syngenetic or diagenetic processes; or, it forms as a result of epigenetic processes, in this case by replacement. This section will deal with these two genetic models in terms of formation of the stratiform zones.

To determine the possible origin of these 'patches', a number of questions must be answered, namely:

1. What was the original habit of tin and how was it mobilized?
2. Where is tin deposited (unconsolidated sediments, sediment-seawater interface, consolidated sediments)?
3. Under what conditions is tin deposited and does this process noticeably affect the surrounding host?
4. If the tin is indeed an early precipitate (i.e., synsedimentary or diagenetic) will it and its associated host rock be affected by subsequent metamorphic events?

An attempt will be made to qualitatively answer these questions for each genetic interpretation.

3.6.3.1 Symsedimentary / Diagenetic Origin

In this model, tin is somehow mobilized from pre-existing sediments, transported in a hydrothermal fluid with other metals and ionic complexes, and deposited in higher level unconsolidated sediments or onto the seafloor.

The most common form of tin within these sediments is detrital cassiterite; it is possible that tin ions or their complexes were adsorbed to clastics or organics, or had formed organo-metallic complexes (Saxby,1976).

Mobilization of tin may prove difficult. If it is adsorbed onto particles or forms organo-metallic complexes, compaction and resultant dewatering of the fluid-rich turbidites may be sufficient to strip the tin from its substrate. Cassiterite is harder to deal with as it is considered a stable resistate. However, another such resistant mineral, zircon can be dissolved by intrastratal solution (Blatt and Sutherland,1969). This may have occurred with cassiterite, but evidence for this is poor - only one sample contains detrital cassiterite, and it occurs within a pelitic layer (detritus in less permeable shales may not be subject to this process; Blatt and Sutherland,1969). The cassiterite is subrounded with irregular edges and this may be more due to abrasion during transport, rather than solution by pore water. Zircon is found throughout the metasediments and exhibits no demonstrable corroded edges, even within coarser (and thus more permeable) psammitic

layers. Mobilization of tin by dissolution is therefore not considered likely.

If, for the sake of argument, corrosion did take place, what conditions are necessary for this process? Most studies (see Cuff, in Taylor, 1979a) deal with formation of cassiterite at high temperatures ($> 250^{\circ}\text{C}$) and under various chemical conditions. Diagenesis is thought to take place at temperatures ranging from several degrees below 0°C to about $250^{\circ}\text{--}300^{\circ}\text{C}$ (Hanor, 1979). Smith (1947) determined that cassiterite was stable in, and crystallized from, sodium stannate(IV) solutions from room temperature up to at least 450°C . Barsukov and Kuril'chikova (quoted in Taylor, 1979a) reported that tin can be transported as hydroxy-fluorostannate complexes in the temperature range of $25^{\circ}\text{--}400^{\circ}\text{C}$ and pH range of 6-11.75. Patterson et al. (1981) calculated from thermodynamic data, dissociation equilibrium constants of divalent tin complexes of Cl, OH and F, at temperatures from 25° to 350°C . Tin concentrations in solutions containing such complexes would be small at low temperatures (< 10 ppm).

If cassiterite can precipitate from low-temperature solutions, it may be possible to dissolve cassiterite by such fluids. According to the above authors, tin is soluble in a variety of pH's (because of its amphoteric nature); at neutral pH, cassiterite is insoluble.

Can sedimentary formation water dissolve cassiterite?

Various authors (e.g., Blatt et al.,1980; Mookerjee,1981; Pettijohn et al.,1972; Hanor,1979; Bischoff et al.,1981) have listed the diverse physico-chemical characteristics of hydrothermal brines derived by sediment diagenesis and the reader is referred to their works. Generally, pore water chemistry changes in response to mineral-ion-fluid reactions during diagenesis. Clay layers within shale units can act as semi-permeable membranes and, driven by pressure differentials with depth, can effectively 'salt sieve', leaving certain ions behind in the pore fluid. Increase in salinity is attributed to this process. Reaction of clay and feldspar minerals to chlorite and calcite to dolomite depletes pore fluid of magnesium and increases H⁺ ion concentrations for further reaction with host sediments. Potassium, calcium, silica, CO₂ and metal concentrations within interstitial water increase by dissolution of various mineral species. The chlorinity of sandstone porewater increases; shale pore water is dominated by HCO₃ and SO₄ ions (Hanor,1979). Chlorine concentrations range up to 7.61 molal with a median of 2.48 molal (compare to modern seawater of 0.535 molal Cl; Blatt et al.,1980). Seawater sulphate is reduced to bisulphide ions by bacterial action.

Compaction of shales at shallow depths (0 to 100 m) results in the expulsion of 75 percent of their pore water; sandstone requires burial to about 3 km before this amount of

fluid is expelled. This compaction would displace shallower waters out of the basin and not produce hot saline brines (Hanor,1979). It is necessary for the fluid to remain at depth to heat up and react with coexisting sediments to form a brine capable of mobilizing and transporting metals. Large amounts of fluid within rapidly deposited turbidites may be trapped by overlying shale units of low permeability. As subsequent layers are deposited, the increased weight causes deeper fluids to be overpressured. Growth or block faulting provides a means of rapid egress (Morganti,1981); fluids may also migrate through more permeable strata laterally to a fault zone or angular unconformity (Cathles,1981).

Studies by Bischoff and others (1981) indicate hot brines (200^o-350^o C; 500 bars) are capable of leaching metals from greywackes with little change in bulk rock composition. Long and Angino (1982) found that low temperature (25^o-90^o C), low pressure (<400 atm) fluids are capable of leaching metals from shales. In both studies, increase of temperature or ionic strength of the fluid, or both effectively increases the leaching capability of the fluids. At low temperatures (25^o C) tin is more chemically active than iron in a system with iron in excess (Krauskopf,1979) and so it is possible cassiterite may be leached in addition to iron and other base metals during reaction with low temperature brines.

The brines move rapidly up the fault conduits and cool;

they may mix with shallower formation waters or may even reach the sediment-seafloor interface before minerals precipitate. In the study by Bischoff and others (1981), metal-Cl complexes within high temperature brines (350°C) dissociate below 200°C, at which temperature metal sulphides precipitate and reaction of K-rich brines with sediment produces extensive potassic or sericitic alteration. Lower temperature, lower salinity fluids cause the same effects, but at a lesser magnitude; at temperatures less than 200°C, few sulphides coexist with metals unless the fluid has a low pH (<7) (White, 1981). Gross solution chemistry of brines after reaction with greywacke samples appears similar to that of hot submarine springs, namely hot acidic saline fluids enriched in Ca, K, H₂S and metals (including tin) and depleted in Mg and sulphate (Edmond, 1982).

Stratabound tin deposits have been documented throughout the world (e.g., Mulligan, 1975; Lehmann and Schneider, 1981), but are usually associated with volcanic lithologies: e.g., Precambrian cassiterite-bearing Pressnitz Series of the Erzgebirge and equivalent beds in the IZERA Mountains in Czechoslovakia and Poland; the polymetallic massive sulphide deposits of Canada, including Kidd Creek and Brunswick Mining with byproduct cassiterite and stannite; and possibly the sedimentary complex of the Belitung district of Indonesia. Hutchinson (1979, 1980, 1982) suggested that the Tasmanian stratabound, stratiform tin deposits are of exhalative

origin, one of the reasons being the close association of ore within submarine mafic volcanics. This idea has been disputed by Solomon (1980) and Patterson (1981,1982), who believe these deposits are of replacement type. Plimer (1980) describes a 'typical' stratiform submarine exhalative tin deposit as consisting of extremely fine cassiterite (<0.001 mm) associated with pyrrhotite ± carbonate or quartz-tourmaline rocks within a thick deep water sequence of pelites, carbonates, calc-silicates, cherts and mafic volcanics. Thermal energy, supplied by the volcanics, was sufficient for fluid circulation and associated leaching of tin from the sediments; cassiterite and other metals were deposited at the sediment-seawater interface. Below this deposit is a zone of K enrichment and Na depletion, whereas Mn is enriched in the sediments surrounding the deposit, all due to fluid-sediment interaction.

Stratiform tin-bearing deposits not associated with volcanic lithologies are less common, or are not recognized as such. The Sullivan Mine of British Columbia is a polymetallic base metal sulphide deposit within argillaceous meta-siltstones and quartzites. Cassiterite occurs near the outer edge of the orebody's pyrrhotite core. Mineralization occurred at the sediment-seawater interface, where hydrothermal brines were expelled from feeder conduits. Continued activity caused tourmalinization of footwall rocks and albitization of hanging wall rocks; the feeder zone

itself suffered chloritic alteration.

Subsequent low grade regional metamorphism may readjust mineral assemblages in several ways in addition to general coarsening of grains and formation of 'typical' metamorphic mineral suites; this has been described in detail by Mookherjee (1981). The isograd of pyrite to pyrrhotite and sulphur is found within the chlorite zone of the greenschist facies; if the released sulphur cannot escape, sulphide-sulphide, sulphide-silicate, sulphide-carbonate or sulphide-oxide reactions may take place, forming new minerals. Softer minerals may flow into cracks and fractures. Metals within carbonaceous material may migrate into iron sulphide grains. Movement of material (except CO₂ and H₂O) across lithological boundaries is restricted to the higher metamorphic grades. Cassiterite is not affected by low grade metamorphism (Plimer, 1980). Non-sulphide metal-bearing zones may be transformed into layers containing distinctive mineral species, e.g., Mn-carbonate-bearing layers metamorphosed to layers containing Mn-garnet.

This discussion is made in an attempt to show that tin may be of a syngenetic or diagenetic origin. However, applying this model to the mineralized zones in the study area meets with a number of difficulties:

1. Scarcity of cassiterite (only one sample obtained) exhibiting unequivocal solution textures, plus no evidence of

solution of other minerals in supposedly once permeable psammitic layers. As cassiterite is believed to be the major tin-bearing mineral, it does not appear likely tin was mobilized in the first place.

2. No clearcut alteration zones attributable to this model except for the layered Mn garnet. Other restricted alteration zones can be attributed to metamorphism, later veining and shearing.
3. Proximity of these mineralized 'patches' to a fold hinge, which acts as a locus for structural weakness and can therefore act as a conduit for epigenetic fluids. Similar favourable layers (containing carbonate, calc-silicate nodules) far from this hinge (100's of m) do not show this type of mineralization, implying its structural control. Limited study of this area does not show any evidence of diagenetic growth or block faulting.
4. Proximity of these mineralized zones to an intrusion containing tin-bearing greisens and which produced the tin-sulphide veins in the adjacent metasediments; arguments have been made (Plimer, 1980; Hutchinson, 1979, 1980, 1982) to the effect that existence of a granitic body does not preclude a prior synsedimentary origin.
5. No volcanics within the sedimentary sequence which would

have added thermal energy to drive the hydrothermal brine system. Evolution of a sedimentary basin with no additional heat source may not have been enough to provide the necessary temperatures (>200°C) for metal mobilization and transport (White, 1981).

6. Existence of a chloritic alteration halo adjacent a mineralized zone in which chlorite and white mica needles crosscut pre-existent foliation, therefore implying a post-metamorphic event.
7. Sulphide replacement textures can be explained just as easily by an influx of ore fluids from the pluton, replacing pre-existent minerals. One does not have to resort to desulphurization of pyrite to produce sulphide minerals from gangue. Individual pyrrhotite blebs in the study area have been elongated, but do not show vein forms or replacement textures. Other 'shredded-textures' in the sulphides are attributed to late shearing of sulphides within ductile phyllosilicate layers.

3.6.3.2 Epigenetic Origin

In contrast to a syngenetic origin, these mineralized layers may form by reaction of magma-derived, ore-bearing fluids with chemically reactive host rocks. Tin may precipitate directly from the solutions as cassiterite, or form the oxide as a consequence of destruction of earlier

tin-bearing calc-silicate minerals.

Skarn formation has been recently described by Einaudi and others (1981) and Rose and Burt (1979) and the reader is referred to these works for further information. Detailed description and interpretation of tin-bearing skarns have only been published in the past few decades (e.g., Patterson and Solomon, 1981; Lehmann and Schneider, 1981; Dobson, 1982; Nekrasov, 1971; Shcherba, 1970; El Sharkawi and Dearmann, 1966). The findings of these authors will be used to discuss the formation of tin-bearing skarns in relation to the stratiform mineralization of the study area.

According to Einaudi and others (1981), there are three main stages in the genesis of a skarn deposit:

1. Isochemical contact metamorphism in response to magma intrusion. Groundwater is expelled, local reaction skarns occur and a widespread (km scale) zoned thermal aureole (hornfels) is formed in the surrounding country rock. Calcareous shales are metamorphosed to their equivalent, unmineralized calcium aluminum silicate layers.
2. Metasomatism of calcareous country rock by reaction with high temperature (400° - 650° C) magmatic hydrothermal fluids along permeable zones (e.g. beds along stock and fault boundaries; sedimentary contacts). This produces an 'igneous metasomatic skarn' and can affect up to hundreds of metres of host rock. The skarn may be conformable or

crosscut bedding. The resultant calc-silicate mineralogy depends on both the protolith and the fluid chemistry. Sulphide mineralization is minor at this stage of skarn development (usually pyrrhotite, bornite, chalcopyrite and sphalerite). Metasomatism may also occur locally ('reaction skarn') on the order of mm to several metres, and is concordant with bedding. It is due to reaction between chemically incompatible layers (e.g. limestone and shale) in moderate to high grade metamorphic terrains. Ore is not usually found in this type of skarn.

3. Low temperature alteration and sulphide deposition. Early formed hornfels and skarn (containing metals in silicate and carbonate crystal structures) are subject to hydrous alteration by lower temperature (300°-450° C) mixed fluids of magmatic and meteoric origins. Alteration patterns are influenced by local structure, and usually crosscut earlier skarns. Calc-silicate minerals are leached of their calcium, and are replaced by silicate-carbonate-oxide-sulphide assemblages. Neutralization of hydrothermal fluids by carbonate host rocks, decreasing temperature and increasing Eh cause sulphides to precipitate, replacing earlier minerals.

In this highly simplified evolution of skarn, tin may precipitate in the last two stages, either as a major tin mineral (e.g. cassiterite or stannite) or as a tin-bearing

calc-silicate, sulphide or aluminoborosilicate (e.g. garnet, axinite, idocrase or epidote), possibly substituting for iron in the mineral structure.

Several types of tin-bearing skarns have been described (Einaudi et al., 1981; Nekrasov, 1971) - magnesian skarns, calcic skarns, and replacement deposits. Their mineral compositions and stages of mineralization are a reflection of the changing physico-chemical conditions of the fluid (Eh, pH, T, activities of S, F, B, fO_2 , fCO_2) as it reacts with the carbonate wallrocks. Primary minerals are destroyed and replaced by new minerals, which in turn are replaced by later phases. Tin-bearing phases which are destroyed release tin to the fluids. It may be reprecipitated as cassiterite or stannite in association with chlorite, carbonate, quartz and sulphides. The depositional sequence of tin and sulphide minerals is similar to that of cassiterite-sulphide vein deposits (Nekrasov, 1971). Cassiterite, chlorite and quartz are deposited first, followed by arsenopyrite and pyrrhotite; these sulphides may be replaced by sphalerite, chalcopyrite, stannite, loellingite and vallerite. Bismuth minerals, galena and siderite are the last minerals deposited.

In contrast to this step by step development of contact metasomatism, reaction and magmatic hydrothermal metasomatism (skarn) and retrograde alteration with ore deposition, there is another way in which to form stratiform tin deposits.

Contact metamorphic calcareous lithologies are replaced by relatively low temperature hydrothermal fluids from intrusions; there is no intermediate skarn formation (Einaudi et al.,1981). Oxides (principally magnetite) or sulphides (mainly pyrrhotite) predominate. In the sulphide replacement deposits, cassiterite occurs in a carbonate gangue with pyrrhotite and minor stannite, arsenopyrite and pyrite; this may be followed by calcite, fluorite, chalcopyrite, galena and sphalerite (Einaudi et al.,1981).

The Renison Bell cassiterite-sulphide deposit in Tasmania is considered a carbonate replacement type (Taylor,1979b; Patterson et al.,1981; Einaudi et al.,1981). Dolomite beds were replaced at about 350°C at low fO_2 ($\sim 10^{-31.5}$ atm; probably controlled by CO_2-CH_4 reaction), low fS_2 (10^{-11} - $10^{-12.5}$ atm) and low pH (3.9-5.4). Tin was transported as a divalent chloride complex. Dolomite replacement resulted in pH increase, causing ore deposition. Replacement assemblages include cassiterite, massive pyrrhotite, arsenopyrite, minor chalcopyrite, iron oxides, quartz, tourmaline, talc, tremolite, magnesian siderite and fluorite. Layers of pyrrhotite parallel to bedding may represent original carbonate-rich layers in the siliceous sediments (Patterson et al.,1981).

Comparison of the blue 'patch' mineralogy (section 3.3.2) with the above descriptions shows this type of

mineralization to be of the lower temperature replacement origin. There are none of high temperature calc-silicate minerals (e.g. calcium pyroxene, amphibole, garnet) indicative of skarn formation. Cassiterite and sulphides appear to have replaced original carbonates within thin calcareous layers. Carbonate and phyllosilicates are rimmed and corroded; later carbonate, muscovite and chlorite overgrow the sulphides. Fluids which caused this probably leached the immediate surrounding host of boron and some copper (see lithogeochemistry section) and formed restricted chlorite and muscovite haloes.

The layered sphalerite in one sample (Fig. 3.19) and higher zinc contents in 'patches' far from the pluton may be equivalent to the 'distal facies' zinc replacement skarn (Einaudi et al., 1981) - zinc may remain in solution over a greater range of conditions, and thus be precipitated far from its source, either in veins or in replacement layers.

According to A.H. Clark (pers. comm. 1983), these blue 'patches' resemble the replacement tin-bearing 'carbonas' of Cornwall.

CHAPTER 4

GENERALIZED MODEL OF TIN GENESIS

4.1 Introduction

The tin prospect of the study area comprises a variety of styles of cassiterite mineralization. Detailed description of these styles, as presented in this thesis, suggests both a syngenetic and an epigenetic origin: detrital cassiterite deposited within turbidites, and cassiterite precipitated in veins and associated replacement layers.

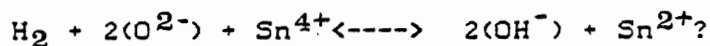
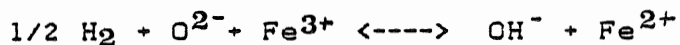
Based on these descriptions and a review of the current literature, an interpretation of this mineralization will be attempted.

4.2 Origin of Tin in Sediments and Magma

Cassiterite and other clastics were eroded from a low-lying continental mass (Schenk, 1975). Because of its zoned, equigranular habit, cassiterite probably derived from a relatively high-temperature source; possibly from Precambrian tin-bearing veins. Cassiterite was deposited within scours and crossbeds.

Partial melting of these cassiterite-bearing carbonaceous turbidites may lead to a melt of low oxygen

fugacity (below the quartz-magnetite-fayalite buffer) (Lehmann,1982) and low SO₂fugacity (Burnham and Ohmoto,1980). In such a magma, tin may exist in its divalent state rather than its tetravalent state (Lehmann, 1982). This is a possible analogue of the reduction of iron by hydrolysis in a felsic melt (Burnham, 1979) where,



Divalent tin is larger than its tetravalent counterpart; about 0.93 Å vs 0.69 Å respectively, for these octahedrally-coordinated ions (Cotton and Wilkinson, cited in Taylor,1979a). Because of its low oxidation state, relatively large radius and relatively high electronegativity, Sn²⁺ tends to be excluded from the crystal lattices of rock forming minerals, becoming concentrated in residual fluids.

Mulligan (1975) states that Sn⁴⁺ may also exist in the magma. It is a very minor network-forming element in a silicate melt and can form three-dimensional bonds with oxygen ions. However, the dominant network-forming elements, silicon and aluminum, have much stronger bonds with oxygen, thereby excluding tin from these complexes; it remains a free ion to be concentrated in residual fluids. Tetravalent tin may substitute for Ti⁴⁺ and Fe³⁺ in ferromagnesian minerals, and is therefore concentrated in such accessory minerals as ilmenite, rutile, magnetite, sphene, biotite and hornblende (Mulligan,1975; Lehmann,1982).

4.3 Magma Emplacement

According to McKenzie and Clarke (1975), the adamellites (monzogranites) of the South Mountain batholith were emplaced at pressures of about 1 to 2 kb, equivalent to about 4 to 8 km depth. Hornblende-hornfels thermal metamorphic assemblages in the study area indicate P-T conditions of 1 to 3 kb (about 4 to 10 km depth) and 550° to 700° C (Cullen, 1983).

Marsh (1982) has discussed two theories of magma emplacement. The magma body may rise buoyantly as a diapir; wallrock flows plastically around the magma with minor fracturing, giving rise to concordant contacts. Magma may also ascend by stoping the wallrock. Because of the thermal stresses set up, blocks can spall off and sink through the magma. The country rock suffers little deformation, and the magma may exhibit unassimilated xenoliths.

According to Shell Canada's mapping, the Wedgeport pluton cuts several fold hinges of the metasediments. Its contact with the country rock on the western shore outcrop is concordant with bedding. There is no clear evidence of xenoliths in the pluton. Accordingly, the pluton may have been emplaced by either method, although such a high crustal level of emplacement (4-10 km depth) implies ascent by wallrock stoping.

4.4 Fluid Genesis

Burnham (1979) and Burnham and Ohmoto (1980) have discussed how an aqueous fluid evolves and is released from a cooling magma body.

In one of their examples, a granodioritic magma is emplaced and cools. The margin of the pluton has cooled and crystallized first, and has an inner coating of water saturated interstitial melt. As magma cools and crystallizes, the water remains in the melt. The water is of low diffusivity and will tend not to move any great distance, remaining in this lining. A further decrease in pressure and temperature oversaturates the melt, causing separation of volatile bubbles (known as 'second boiling'). Evolution of this vapour phase is accompanied by an increase in volume (of this phase), which can produce stress on the outer crystalline margin. This margin behaves in a brittle manner at shallow depths and will tend to be fractured by the expanding volatiles. At deeper levels, total pressure is greater, resulting in less volume expansion (and therefore less mechanical energy) of the volatiles. Less fracturing takes place, and few or no void spaces (miarolitic cavities) are formed.

Early fractures are lengthened by the fluid phase outward from the inner lining ('hydraulic fracturing'). This decreases the fluid pressure, causing crystallization of the

inner magma; the water saturated liner withdraws deeper into the magma body.

Mineral precipitation heals the fractures and isolates the melt system. Continued cooling of the magma begins the above process all over again.

Initial water content of a magma influences its depth of crystallization, and therefore its depth at the stage of vapour separation and extent of subsequent wallrock fracturing. An initial melt with greater than 2 wt % water will be able to evolve enough vapour at second boiling to cause extensive fracturing at pressures less than 2 kb (~ 8 km depth). An 'ideal' magma to generate sufficient ore-bearing fluid would have an initial water content of 2 to 4 wt % ; this would result in vapour phase separation at 2 to 6 km depth before the magma becomes totally crystalline. Higher water contents restrict magma emplacement to deeper crustal levels which would not allow extensive wallrock fracturing. Lower water content restricts the amount of vapour released on second boiling, resulting in little or no fracturing of the wallrock.

Strong (1980) noted that biotite granites usually do not have enough initial water to concentrate lithophile elements, but are too water-rich to reach shallow crustal depths and leach metals from the country rock.

According to Burnham and Ohmoto (1980), a granodioritic magma with an initial water content of 2.7 wt % will only cause sufficient wallrock fracturing at depths of less than 5 km. Shallow magma emplacement (< 10 km) appears to be one of the criteria for hydrothermal ore genesis.

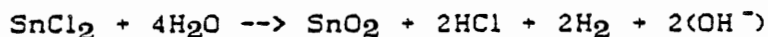
The evolved aqueous phase contains lithophile elements and chloride complexes of alkalis, chalcophile metals, hydrogen and calcium. The chloride content of these fluids determines their ability to transport metals; a total chlorine content of greater than 0.3 molal is necessary. Ilmenite series magmas evolve fluids containing CO₂ and CH₄ in nearly equal proportions, low total sulphur content (SO₂ and H₂S) and low oxygen fugacity.

These fluids precipitate small amounts of sulphides (mainly pyrrhotite) and larger quantities of oxides, such as cassiterite. According to Patterson and others (1981), divalent tin may be transported as a chloride complex. Other authors (e.g. Barsukov, in Taylor, 1979a) suggest tetravalent tin transport as a hydroxy-fluorostannate complex, although divalent tin could conceivably be carried in this way; i.e. (Na,K)₂[Sn(OH)_xF_{4-x}]. Smith (1947) also suggests divalent tin transport as a sulphide complex.

Reaction of such chloride-rich fluids with feldspathic wallrock results in potassium and hydrogen metasomatism (potassic and phyllic alteration), hydrolysis of SO₂ to H₂S

and H_2SO_4 and production of HCl from metal chloride complexes, leading to precipitation of the metals.

Reaction of these fluids with carbonate rocks leads to destruction of HCl by decarbonation ($\text{CaCO}_3 + 2\text{HCl} \rightarrow \text{CaCl}_2 + \text{H}_2\text{O} + \text{CO}_2$). This results in destruction of the metal chloride complexes and precipitation of metal sulphides and oxides, replacing the carbonates (Burnham and Ohmoto, 1980). For example,



Study of the Wedgeport monzogranite reveals the western shore contact margin (endocontact) to be porphyritic with several generations of veinlets and some shear zones. This may represent the chilled carapace described by Burnham (1979) and Burnham and Ohmoto (1980). The pluton either did not initially contain sufficient water or did not reach shallow enough crustal depths (2-6 km?) to cause extensive fracturing by an evolved aqueous phase. The endocontact was breached by minor fractures, allowing formation of early veinlets containing quartz and carbonate with rare scheelite (fluid with high activity of CO_2 ?). Healing of fractures began the process again, causing fracture formation either along previous planes of weakness or in other orientations. A mid stage in this evolution produced fluids of low oxygen fugacity and low sulphur content which caused greisen formation, sulphide-cassiterite veins and replacement zones

within the country rock. Sulphide mineralogy is a reflection of the changing physico-chemical conditions outwards and upwards from the pluton. It may be possible that a later evolved fluid (containing radioactive elements ??) caused the shearing in the pluton and consequent movement in the country rock.

CHAPTER FIVE

TRACE ELEMENT LITHOGEOCHEMISTRY

5.1 Introduction

The lithogeochemical survey was performed to identify those elements associated with tin mineralization and to study their dispersion patterns to discover possible indicator elements ('pathfinders') for use in subsequent exploration programs in similar geological settings.

Specific drill core samples were analysed for a selection of 13 elements typically associated with tin deposits (Table II-1). Results of the 122 analyses are tabulated in Appendix II.

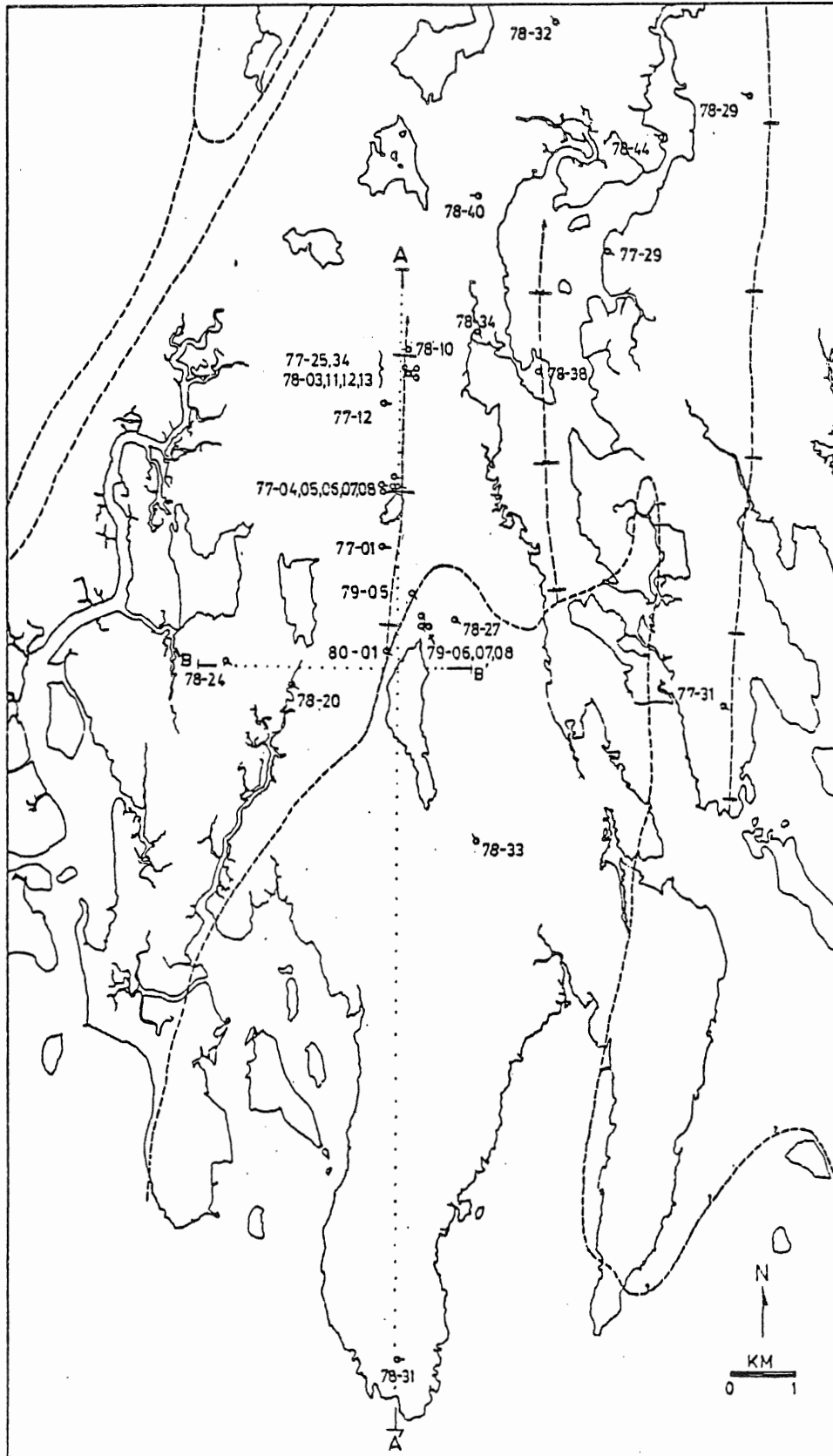
Geochemical dispersion patterns are based upon a number of factors which must be taken into account during any lithogeochemical survey (Levinson, 1974):

1. Different mobilities of elements in solution.
2. Porosity and permeability of country rock, be it primary (e.g. pore space) or secondary (e.g. fractures).
3. Possibility of fluids reacting with the country rock.

Certain elements remain in solution over a wide range of

Figure 5.1

General base map of study area
showing location of diamond drill
holes samples and 2 cross-section
lines A-A', B-B'.



physico-chemical conditions (hence are 'mobile') and therefore are observed over a greater volume of rock than other, less mobile elements. These more mobile elements associated with mineralization may be used as pathfinders, as they may have a greater possibility of discovery than the element of economic interest.

For ore-bearing fluids to pass through the country rock, permeability must exist. Extensively fractured host rock enables these fluids to travel longer distances from their source, creating wider geochemical dispersion patterns.

Fluids reacting with the country rock may precipitate minerals characteristic of certain deposits and may be used as guides in exploration, e.g., reaction with calcareous rocks producing metalliferous skarns.

Levinson (1974) describes from Hawkes several geochemical patterns which may occur: extensive penetration of rock by fluids producing an areal pattern; migration of fluids from an ore body during or just after its formation, along fractures, creating leakage haloes; reaction and alteration of adjacent wallrock with solutions producing wallrock patterns.

One of the objectives of the geochemical study was to search for the existence of these patterns and try to relate them to the tin mineralization. The sampling procedure was

established to select drill core with observable mineralization as well as unmineralized ('barren') material from a variety of locations and depths. This was to determine several characteristics of the study area:

1. Relationship of elements with respect to different lithologies (meta-argillites, meta-wackes, monzogranite) to compare their mean ('background') and anomalous (above 'threshold') values.
2. Relationship of elements with respect to different styles of mineralization: greisens, sulphide veins and stratabound zones ('patches').
3. Extent of trace element dispersion from the mineralization; for this reason samples adjacent the mineralization were obtained, on the order of several centimetres to several metres distant.
4. Relationship of elements in the meta-sediments with respect to distance from the pluton. A series of samples were obtained at increasing distance from the surface projection of the pluton and at various depths.

After the drill core samples were selected they were cleaned, powdered and sent to X-Ray Assay Laboratories

Limited (Toronto) for analyses. Appendices I, II and III describe sample preparation and analytical methods with their precision and accuracy estimates.

5.2 Population Partitioning

To adequately interpret the metal distribution in the mineralized samples, a comparison is made with that in the unmineralized core. The distributions are assumed to result from either the 'normal' processes of geochemical dispersion in the metasediments and the pluton (e.g. sedimentation, metamorphism, anatexis, diffusion in a melt) or the mineralizing event(s) and not from a secondary dispersion by later chemical weathering. Most samples were chosen free of relatively late fractures with recognizable oxidation products; all sample surfaces were ground to remove the effects of recent weathering.

Separation of the data set of each element in each lithology into background and anomalous populations was accomplished graphically by means of cumulative frequency plots, which depict the general form of each population. The graph is constructed in such a way that points of a single population will form a straight line; deviations from linearity represent combinations of populations (Sinclair, 1974; Parslow, 1974). These populations are separated by the partition method explained by Sinclair (1974) and summarized in Appendix IV along with the

cumulative frequency diagrams of the analysed samples. The procedure arbitrarily chooses threshold values between background and anomalous populations. Because other methods of choosing threshold values are also arbitrary (see Levinson,1974; Parslow,1974), this particular method is believed to be just as satisfactory. Sinclair (1974) notes that although a minimum of 100 values should be used to construct a cumulative frequency graph, fewer values can be dealt with using the plotting percentage technique of Koch and Link (1970). Such computations were performed on the small data sets (see Appendix IV for an example) and the differences in the final values between the two methods were not large enough to warrant the use of the latter technique. Furthermore, the geochemical analyses were performed on a selected sampling of lithologies, from known unmineralized to known mineralized material, so as to estimate background and anomalous populations. Manipulation of these small data sets by Sinclair's method serves to define further the backgrounds and thresholds.

Several attempts were made to obtain the best possible groupings of metasedimentary sample data; e.g. group all metasedimentary analyses together, all unmineralized sample analyses together, etc. It became evident that grouping the metasediments according to their lithologies ('pre-partitioning' into meta-pelitic and meta-psammitic samples) facilitated interpretation of the cumulative

frequency graphs. It also established different background and threshold values for several elements (e.g. Sn, Cu, Zn). This is important if further exploration in the area is planned, as an anomalous value in one lithology may only be of secondary importance in another; more time, effort and money would need to be expended to perform follow-up examination (and possible rejection) of these spurious anomalies. It is easier to first establish background and threshold values of the two lithologies; it is also relatively easy to distinguish the two lithologies in hand sample so no extra effort need be expended.

Several difficulties were encountered in population partitioning:

1. Values below the detection limit. To continue population partitioning with a large enough data set, values one order of magnitude lower than the detection limit were substituted during mathematical manipulations. This can cause erroneous cumulative frequency curves and therefore, inaccurate background and threshold values. An example of this is observed in molybdenum values in the metasediments; most are below the detection limit of 0.5 ppm. Use of 0.05 ppm instead results in one or two populations with an interpolated background of 0.4 ppm which is not a valid estimate. Care must be taken in the subsequent interpretation of such results.

2. Gentle slopes of the cumulative frequency curves create difficulty in selection of inflection points and can cause inadequate partitioning of the data set.
3. Insufficient number of analyses to give a continuous (i.e. 'smooth') range of values. This can produce a rapid change in slope, giving the impression of the existence of two or three populations where in fact only one or two exist.
4. Existence of two inflection points (implying three populations) complicates partitioning as a limited number of data points are available for the partitioning equation. At least three points per population are desirable and this is not always possible when more than one inflection point occurs. When this happens, points are obtained from the cumulative frequency curve, which may produce errors in final background and threshold values.

Once the background and threshold values were acquired, they were compared with the data set and their corresponding lithologies to determine possible causes for their trace element distributions. Background and threshold values of the elements in the three lithologies, average values in tin-bearing rocks of Cornwall, of the nearby Davis Lake pluton, and of the so-called 'specialized' and 'normal' granites, as well as the clarkes of shale, sandstone and

granite are listed in Table 5.1. A summary of the results of analyses of each element in each lithology is found in Table 5.2. Plots of element distributions with respect to lithologic type or mineralization type are found in Figures 5.2 to 5.4 and are discussed in the tabulated summary. It is important to keep in mind the small sample sizes; even though an adequate estimate of background and threshold values was obtained, comparison of trace element contents among this selection of lithologies is believed to be limited.

It is also necessary to realize the importance of analytical control. Duplicate and reference standard samples were included in the sample batch to evaluate the precision and accuracy of the analyses performed by X-Ray Assay Laboratories Limited. Details are shown in Appendix III. Precision (reproducibility of analyses) ranged from poor to excellent; accuracy (closeness to 'true' or accepted concentrations) ranged from very poor to acceptable. The analyses appear to be relatively precise, but not too accurate. In other words, the results may be considered 'valid' within the data set but are not to be taken as absolute ('true') values.

5.3 Discussion

Assuming the analyses and population partitioning are valid, the following observations of geochemical distribution can be made.

Table 5.1 Background and Threshold values in the lithologies of the study area and average values in various other lithologies.

All values in ppm	Metapelitic Rocks (n = 23)	Metapsammite Rocks (n = 51)	Monzogranite (n = 25)	Davis Lake 1 Biotite Granite (n = 2)	Cornish 2 Metasediments, Granite (Avg. min-mix)	Plumoseitic 3 Rare-Metal Granitoids	"Specialized" Granite	"Normal" Granite	Shale	Clarke's 5 Sandstone	Granite	
<u>Sn</u> Background	3.5	18	8	16.5	10-17	17-58	6.3	30 ± 15	1-8	4	0.X	3
Threshold	100	180	48									
<u>M</u> Background	7.5	5	12	-	4-5	20-30	4.1	7 ± 3	1-2.7	2	1.6	2
Threshold	60	19	65									
<u>Mn</u> Background	0.4*	0.4*	4	-	-	-	1.4	4 ± 2	<1-2.5	3	0.2	2
Threshold	5	9	32									
<u>As</u> Background	11.5	18	4.5	-	12-30	26-65	-	-	-	15	1	1.5
Threshold	100	160	70									
<u>Cu</u> Background	36	10	4.5	4.5	30-59	4-9.5	-	-	-	50	X.	10
Threshold	250	365	135									
<u>Pb</u> Background	4.5	7	8.5	-	14-51	13-44	30	-	-	20	7	20
Threshold	50	120	15.5									
<u>Zn</u> Background	80	110	26	40	112-245	39-63	57	-	-	100	16	40
Threshold	275	330	76									
<u>Sb</u> Background	0.54	0.44	0.3	-	-	-	-	-	-	1	0.0X	0.2
Threshold	2.0	1.45	0.6									
<u>Bi</u> Background	0.42	1.65	5.4	-	-	-	-	-	-	0.18	-	0.1
Threshold	3.5	10	100									
<u>Li</u> Background	30	52	45	186	-	-	97	200 ± 100	36 ± 5-150	60	15	30
Threshold	100	100	80									
<u>F</u> Background	410	470	730	4000	-	-	3000	3700 ± 1500	250-1500	740	270	735
Threshold	900	1000	1550									

Values from:

*Background values unreliable; near or at detection limit

¹Chatterjee, 1980

Dashes (-) denote unavailable data.

²Jackson, 1979³Tauson, 1974⁴Tischendorf, in Hosking, 1979⁵Taylor in Levinson, 1974 and Turekian and Wedepohl, 1961
with order of magnitude estimates in form of X

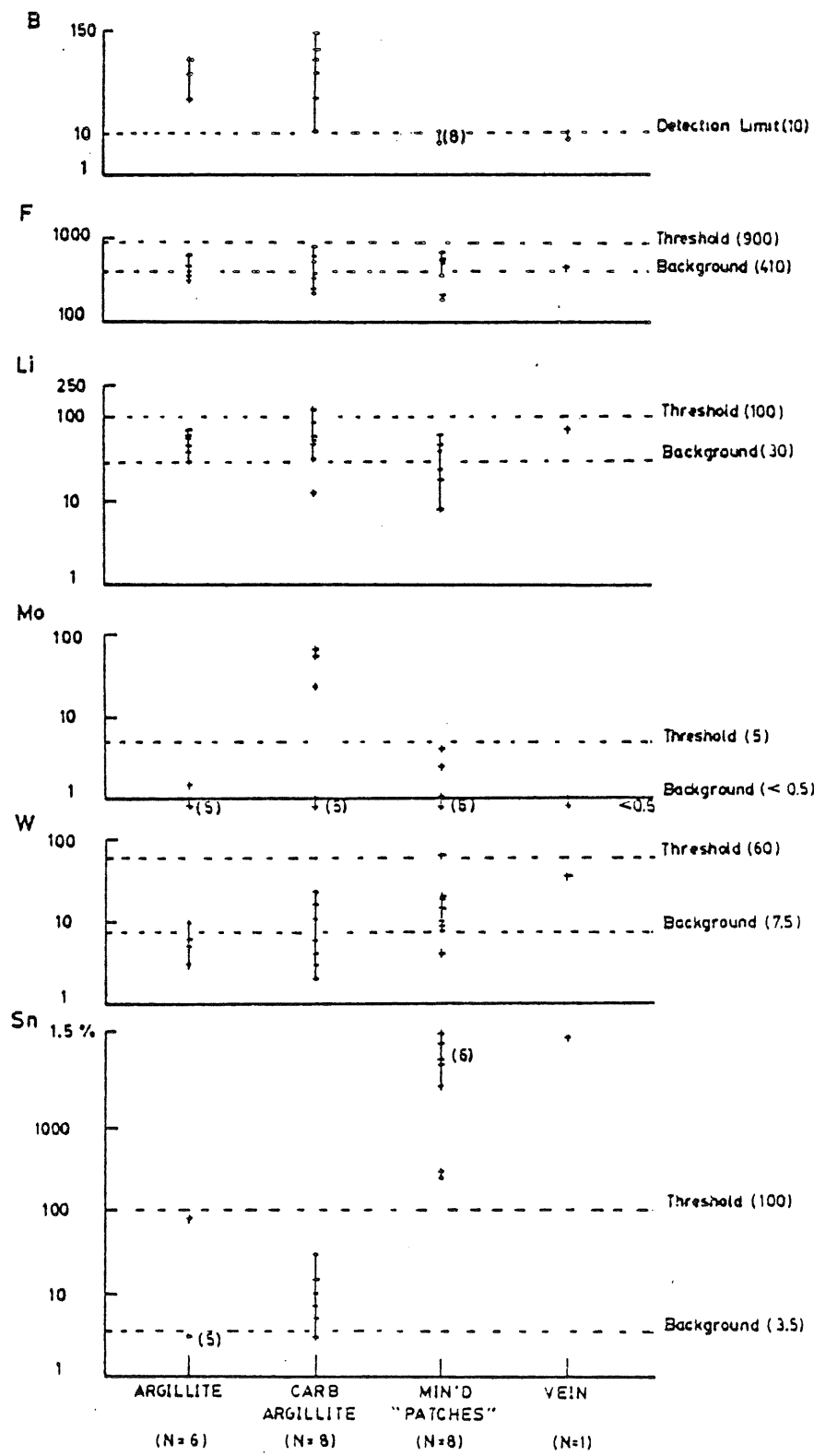
Figure 5.2

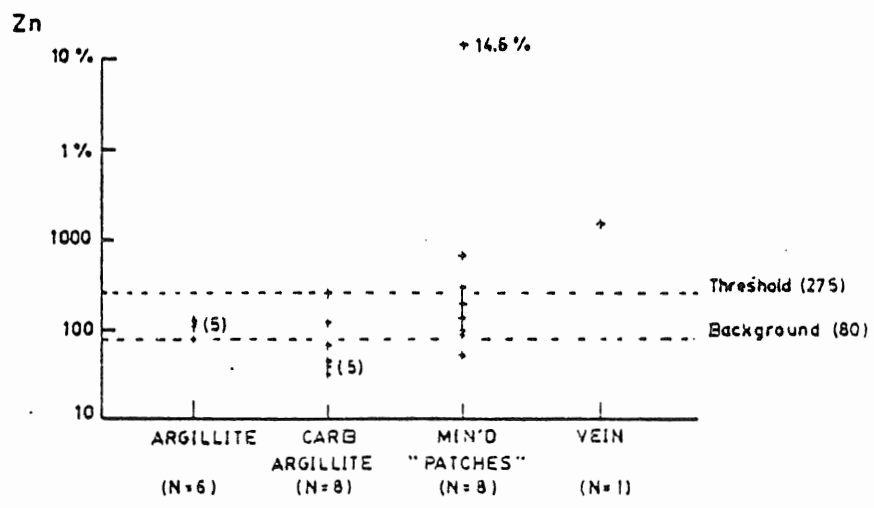
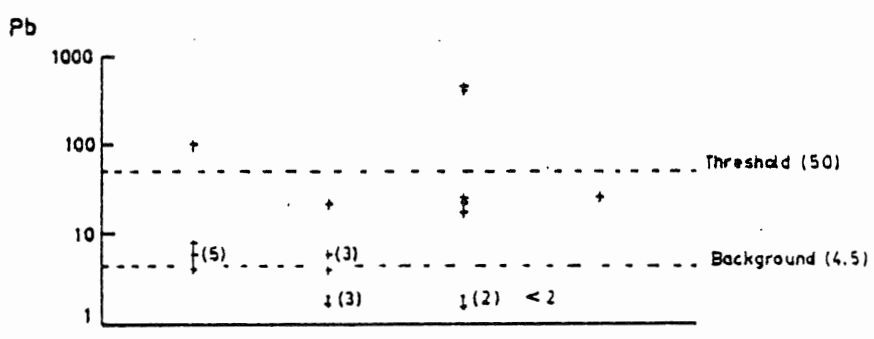
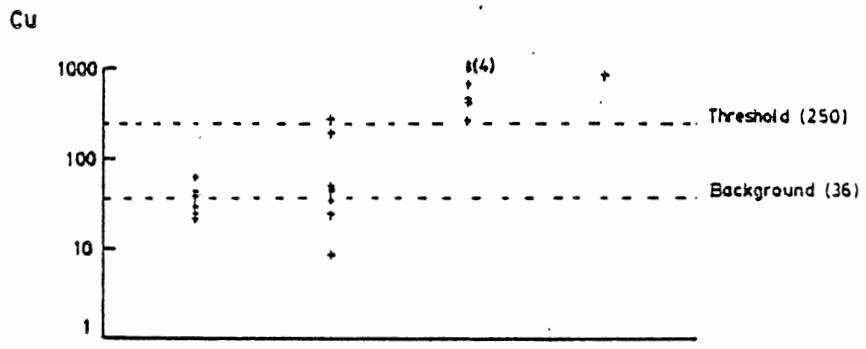
Trace element variation with
lithology and mineralization
in meta-argillites.

Values in ppm unless otherwise noted.

Carb Argillite - carbonaceous argillite

Min'd "Patches" - stratiform mineralization





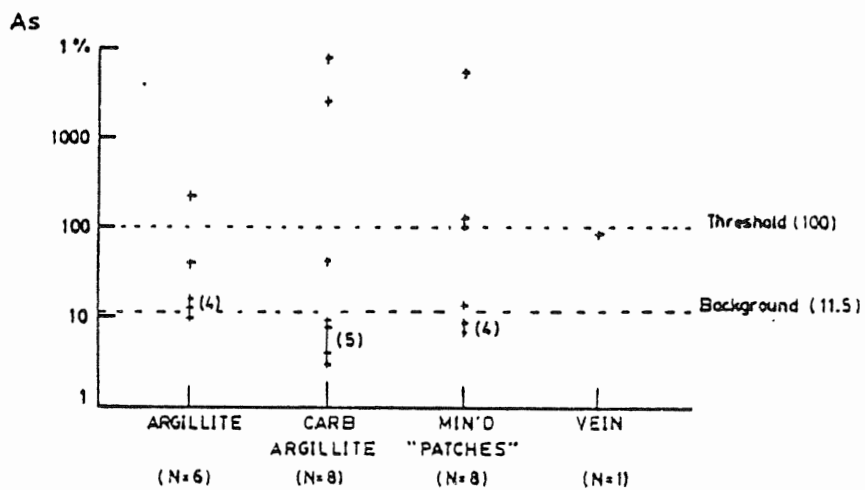
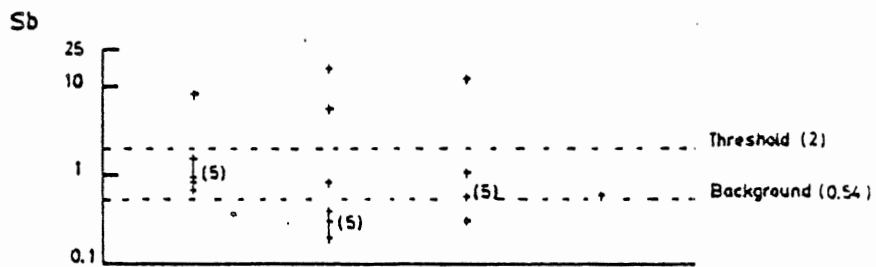
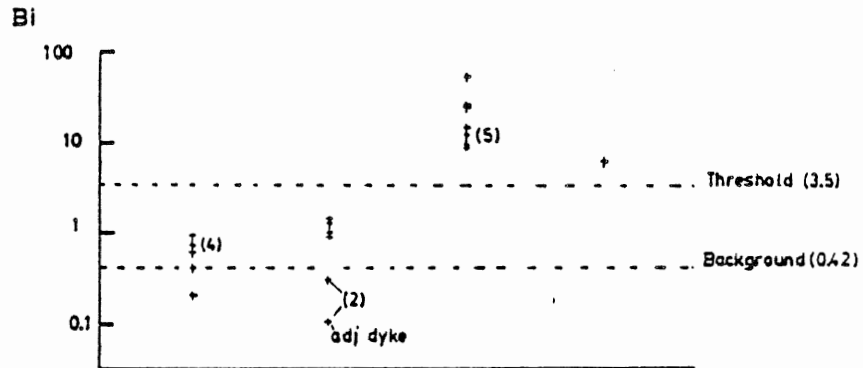


Figure 5.3

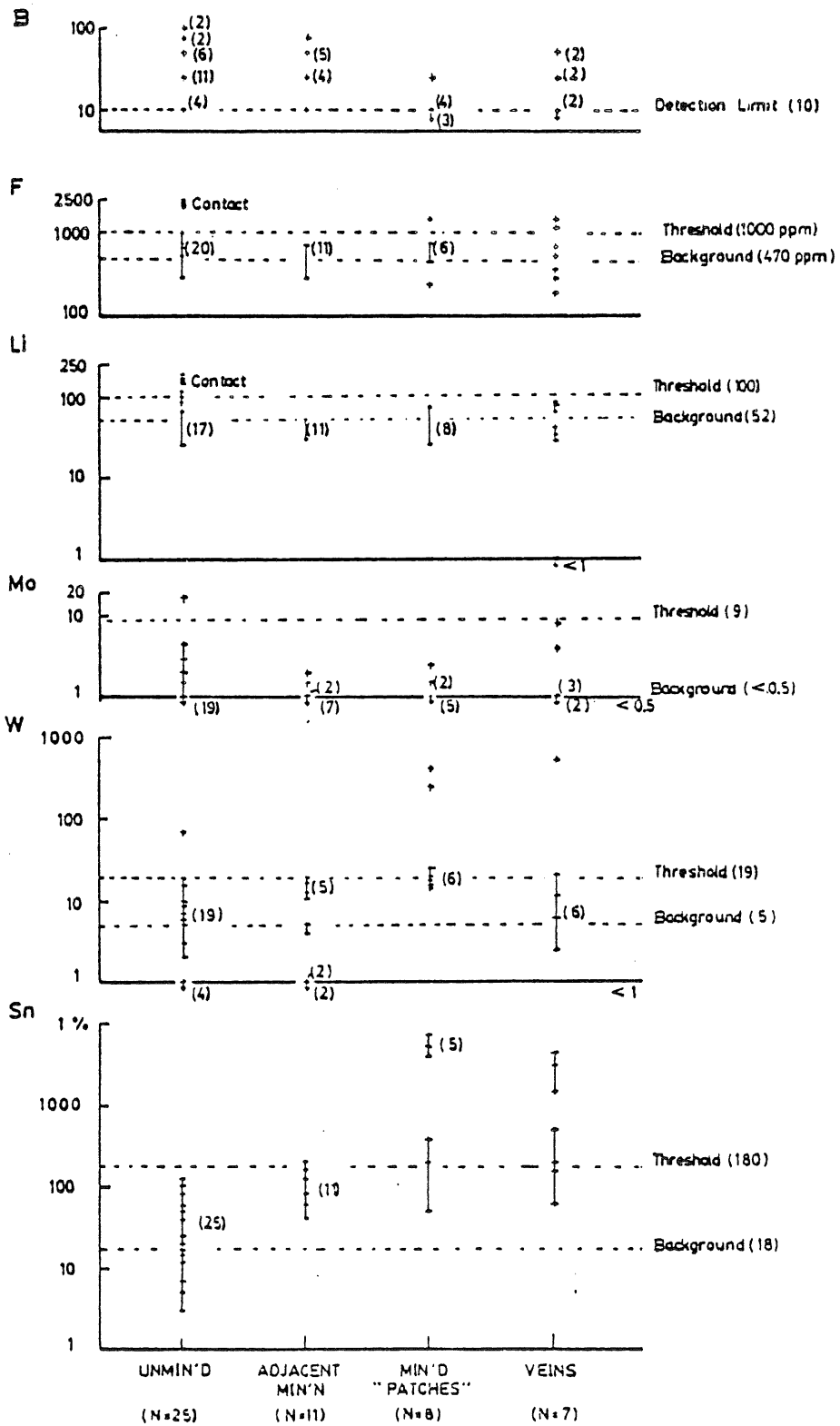
Trace element variation with
lithology and mineralization
in meta-wackes.
Values in ppm unless otherwise noted.

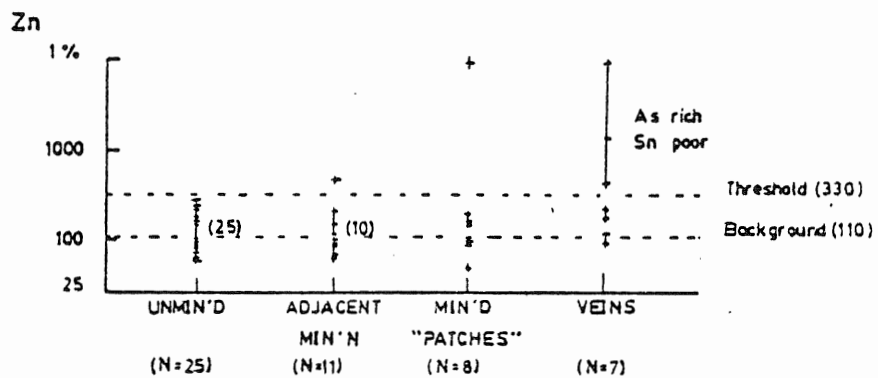
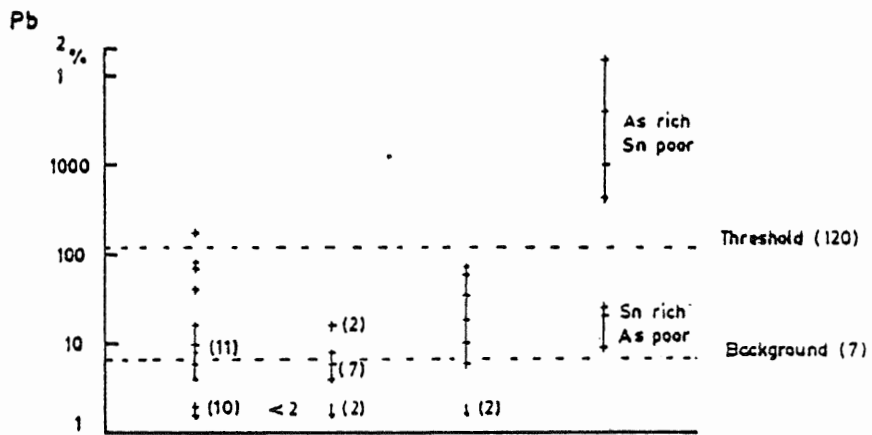
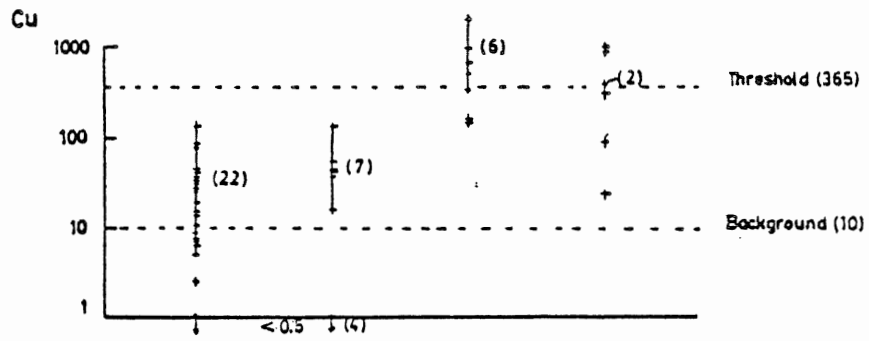
Unmin'd - unmineralized samples

Adjacent Min'n - barren samples adjacent
mineralization

Min'd "Patches" - stratiform mineralization

Contact - refers to those samples in or
near the contact with the
pluton in DDH 79-05, 80-01





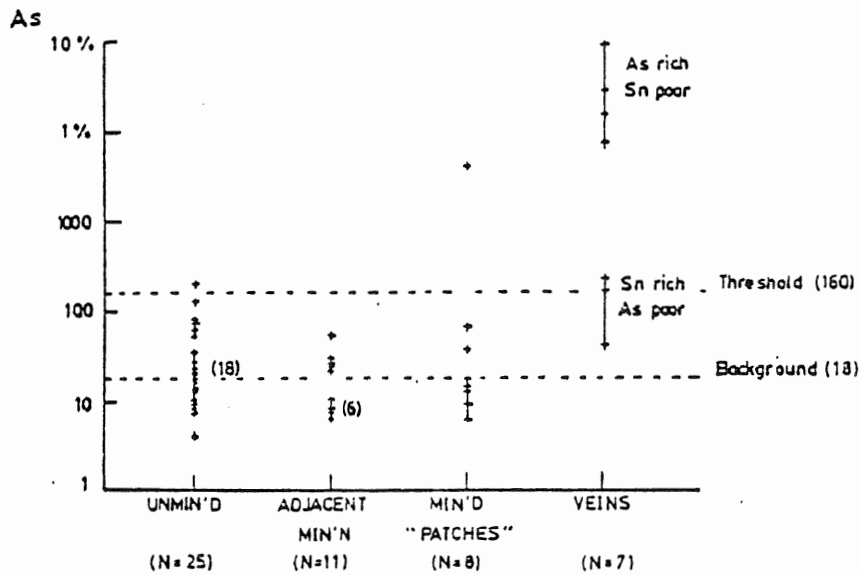
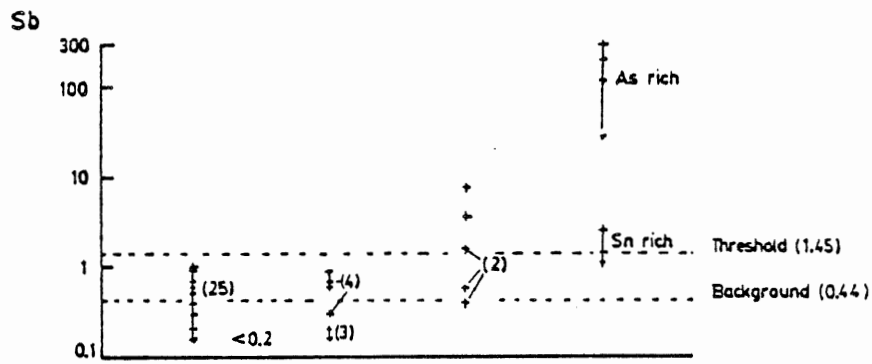
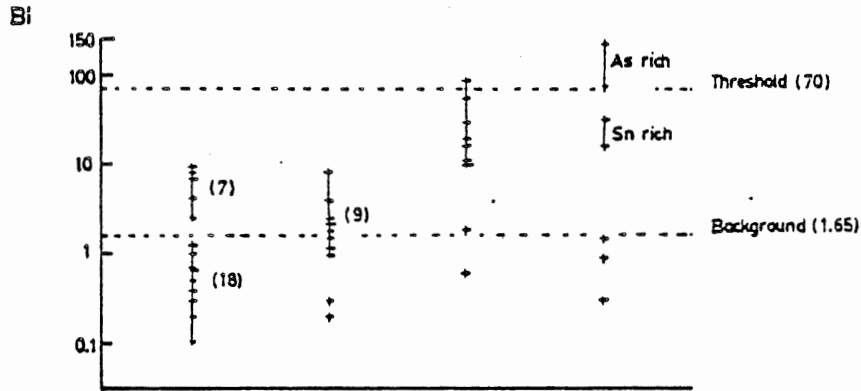


Figure 5.4

Trace element variation with lithology and alteration in pluton. Values in ppm unless otherwise noted.

Non pheno - non-phenocrystic monzogranite

Sl. pheno - slightly phenocrystic monzogranite(1-5 modal %)

Pheno - phenocrystic monzogranite (>5 <75 modal %)

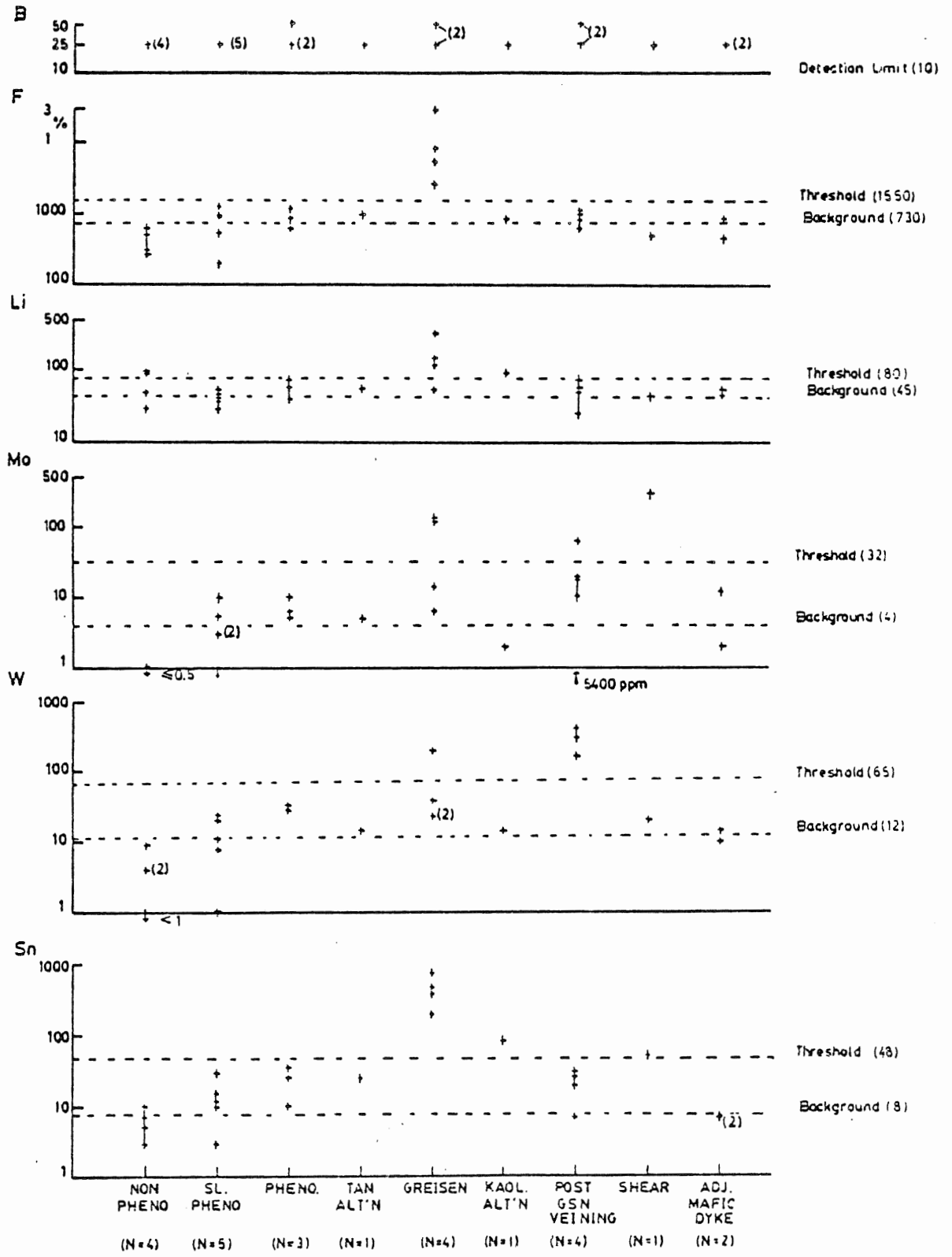
Tan alt'n - sample adjacent greisen with tan-coloured alteration

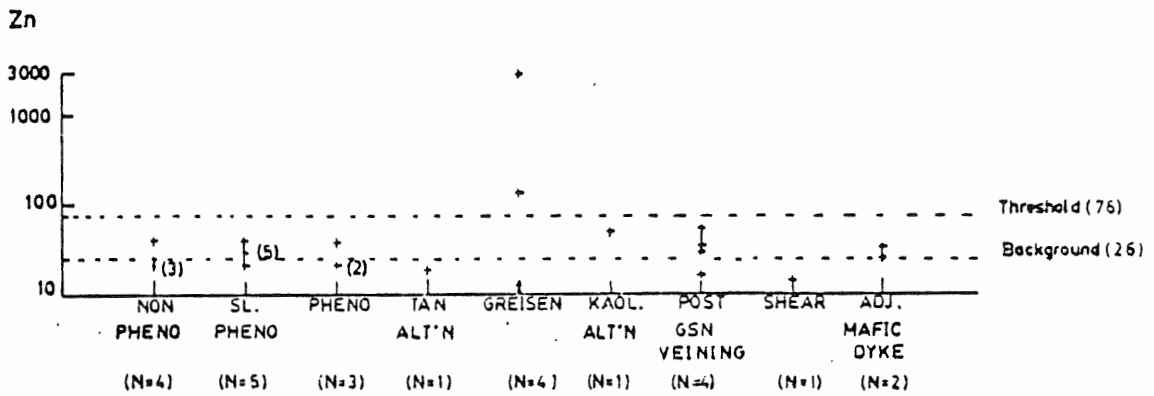
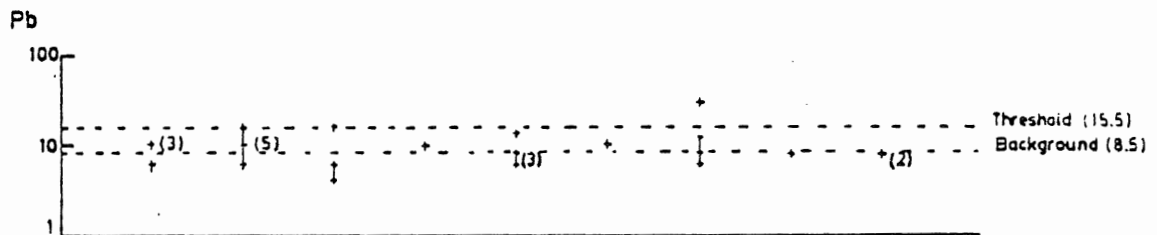
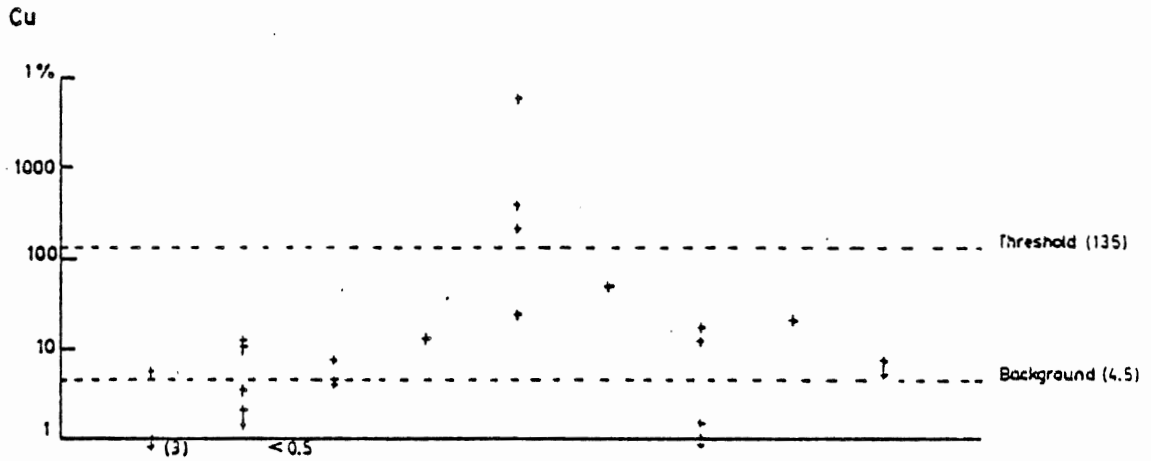
Kaol. alt'n - sample with kaolinite vugs and veinlets

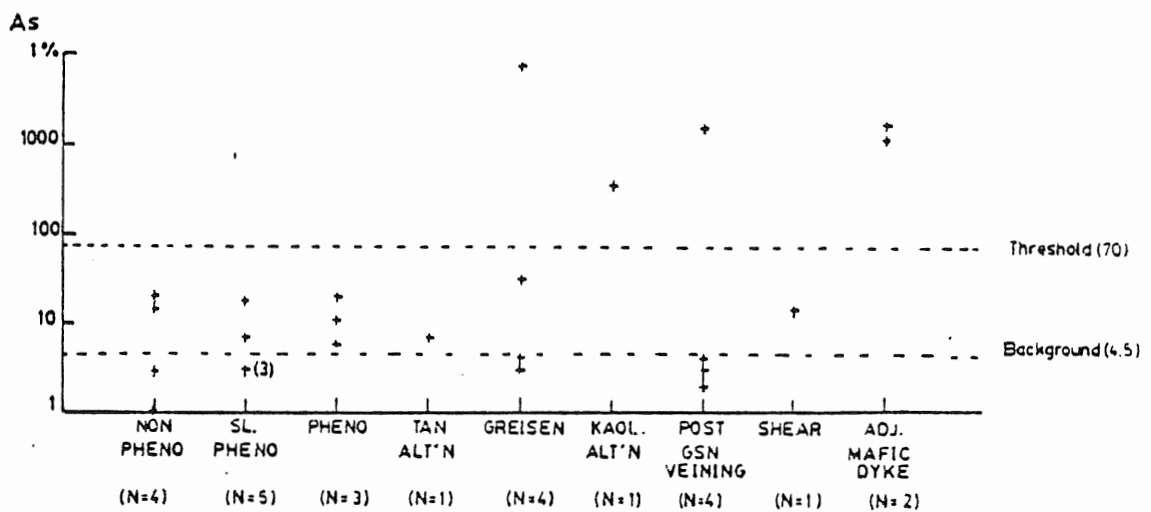
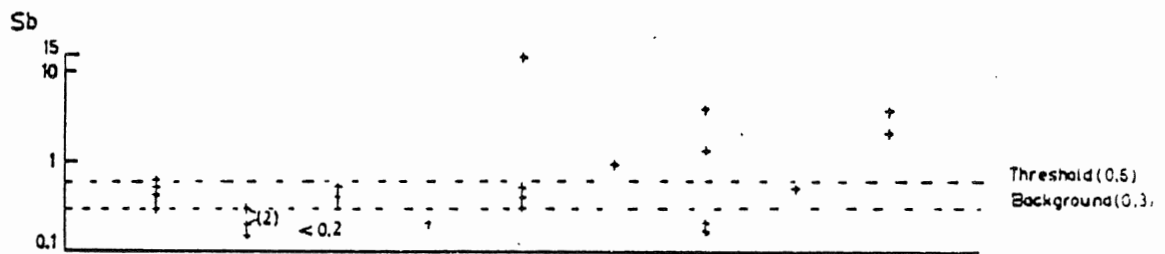
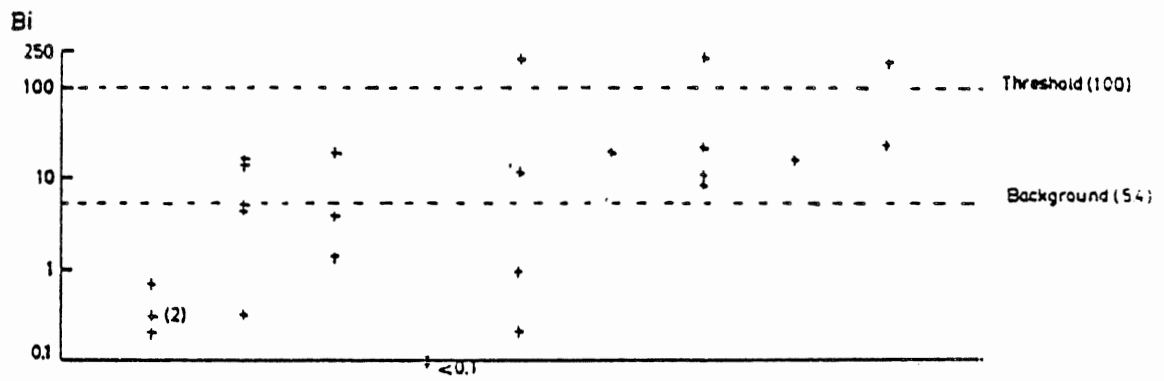
Post gsn veining - samples with those quartz veinlets which cut greisen zone

Shear - sheared monzogranite containing a pre-shear quartz veinlet containing scheelite, molybdenite and chalcopyrite

Adj. mafic dyke - 2 samples(78-27) adjacent a mafic dyke







5.3.1 Relationship of Elements With Respect to Different Lithologies

Trace element distributions were compared within each lithology, i.e., among gross mineralogical types arbitrarily established in each rock group. For example, meta-psammitic samples were classified on both mega- and microscopic features such as presence of biotite, feldspar and carbonate, as well as by grain size; meta-argillites were typed by presence of carbonaceous material; samples from the pluton were grouped arbitrarily by the presence of phenocrysts (none, 1 to 5 modal percent, greater than 5 modal percent), presence of greisens, alteration, veinlets, shears or mafic dykes. Obviously the meagre number of samples precludes any definite conclusions about trace element distribution within each lithology; however, a rough estimate of the ranges may be inferred. Accordingly, there appear to be no major differences in trace element contents among the various unmineralized meta-psammitic samples. Within meta-pelitic samples, wider ranges of metal contents are observed in the carbonaceous meta-argillites, due either to slightly greater number of samples or to primary sedimentological differences; organic-rich sediments appear relatively enriched in metals, by adsorption or by forming metallo-organic or chelate compounds (Krauskopf, 1979). Both metasediment types have relatively high contents of molybdenum, tungsten, lithium and

fluorine in samples close to the pluton, implying possible addition of these elements from the intrusion. Background values of both lithologies are similar except for those of tin, copper, zinc and bismuth; the meta-pelitic samples have a higher copper background, and the meta-psammitic samples have higher backgrounds in the other elements. This may be due to the presence of discrete metal-bearing particles, minerals with those metals in solid solution, or 'sorption of those metals or their complexes to particular mineral grains.

Arsenic has a long paragenesis, occurring principally as arsenopyrite in sediment disseminations (detrital or diagenetic?), in pre-crenulation veinlets, in main-stage mineralization veins and patches, and in post-mineralization veins and breccias.

Determination of variations within plutonic samples is more difficult as consideration must be taken of sample location within the pluton (endocontact vs. the interior) and of the ubiquity of metal-rich veinlets which may go unnoticed but cause high trace element analytical results. Therefore, only general conclusions are made. No major differences in trace element contents exist in samples of different crystallinities, although the non-phenocrystic samples (of the interior of the pluton) usually have slightly lower ranges than those samples with phenocrysts. Two

unmineralized samples adjacent a mafic dyke (DDH 78-27) contain biotite with inclusions of arsenopyrite, causing high concentrations of arsenic, antimony and bismuth. This has not been observed in any of the other plutonic samples and may be due to the mafic dyke intrusion, although it is not known how this occurs.

5.3.2 Relationship of Elements With Respect to Style of Mineralization

(i) Sulphide-Cassiterite Veins

Certain mineral assemblages are associated with the sulphide-cassiterite veins in the metasediments and this is reflected in the trace element distributions. Two main types of veins exist: tin-rich (> 1000 ppm), arsenic-poor and arsenic-rich (> 1000 ppm), tin-poor. Tin-rich veins have relatively high concentrations of copper and bismuth due to the existence of cassiterite and chalcopyrite; the high bismuth content may be due to native bismuth, solid solution within such minerals as native silver or galena, or to presence of unobserved rare bismuth sulphides or sulphosalts. Veins rich in arsenic have relatively high contents of lead, zinc, antimony and bismuth. Bismuth content within the two vein types is not clear - both types have background and anomalous concentrations. A plot of bismuth against arsenic (Fig. 5.5) appears to show a negative correlation with several deviations, whereas that of bismuth

against tin shows no correlation (Fig. 5.6). Bismuth therefore seems to occur in other forms not associated with arsenic or tin mineralization. Most of the arsenic-rich veins have a higher range of fluorine content than the tin-rich veins.

There appears to be a chemical and physical relationship between the two vein types. Chemically, there is a positive correlation between tin and copper, and a negative relationship between tin and arsenic, lead, zinc and antimony (Fig. 5.6). Physically, tin-copper-rich veins occur deeper in the country rock and closer to the pluton than the relatively shallow, more distant arsenic-rich veins with their more 'mobile' base metals and fluorine. Figure 5.7 gives a rough metal pattern observed in this vein system. The two vein types are not observed together in drill core, so their relationship is only inferred; however, there is a mineralogical (and therefore elemental) zonation in the major veins in the metasediments surrounding the pluton. Veins close to the pluton are relatively rich in tungsten and molybdenum (in the form of scheelite and molybdenite, respectively). Tin, zinc and lead become dominant farther from the intrusion. Arsenic and copper, of variable concentrations, are ubiquitous. Shallower and more distant veins show a decrease in tin and an increase in the other base metals. This type of zonation has been described by Grigoryan (1974), and may be of use in exploration, to

Figure 5.5

Variation of Sb and Bi with As content in veins in the metasediments.

Sb is proportional to As content. Bi, with a few exceptions, shows a negative correlation.

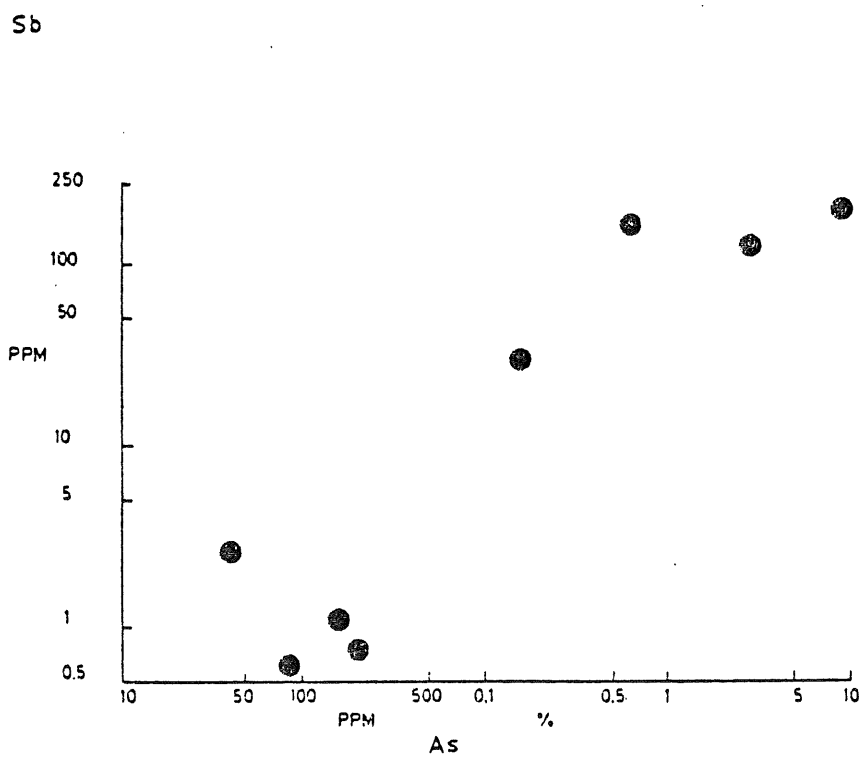
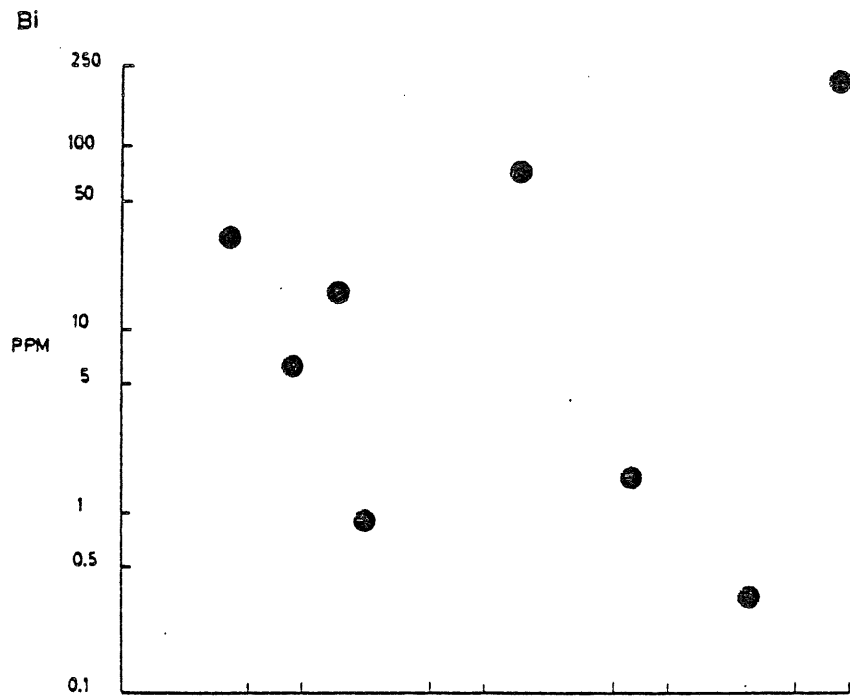
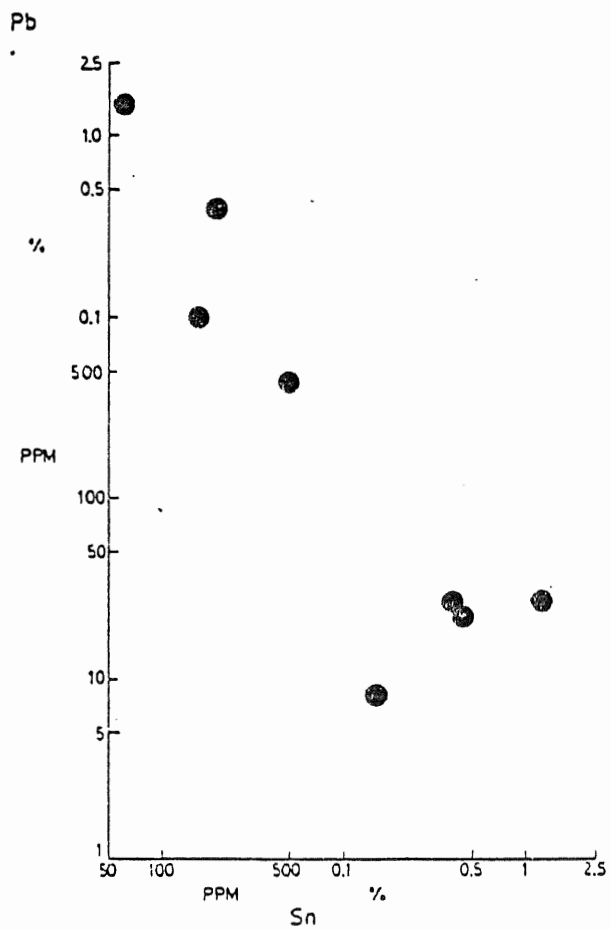
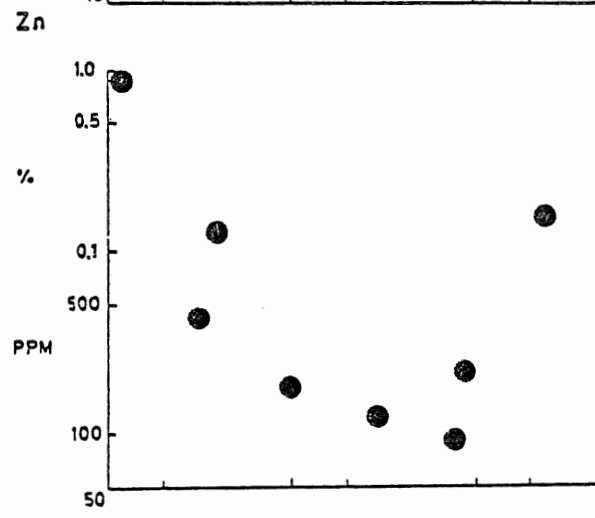
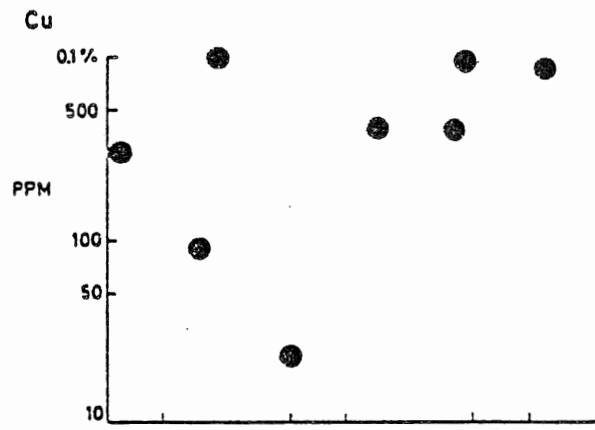


Figure 5.6

Variation of various metals with Sn content in veins in the metasediments.
Note the antipathetic relationship of As, Pb and Zn (with one exception) with Sn. Relationship with Cu and Bi is not as clear.



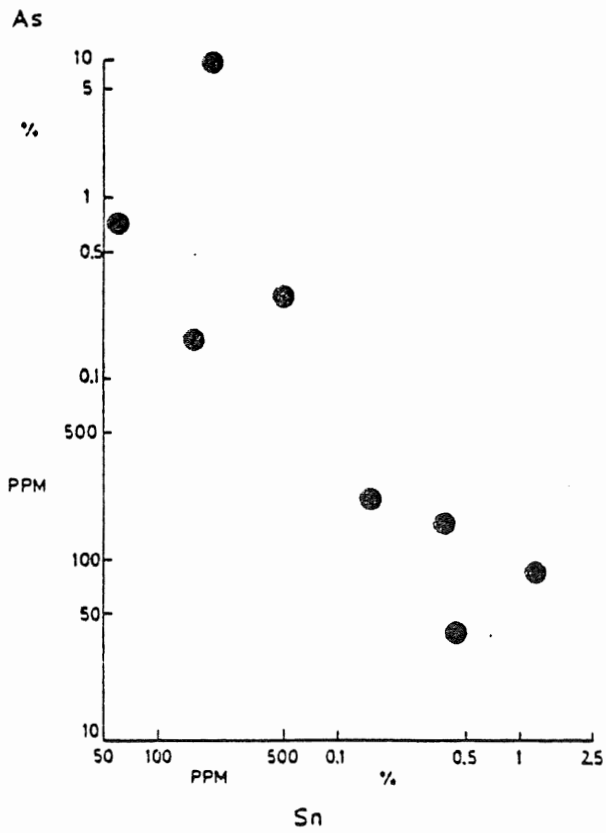
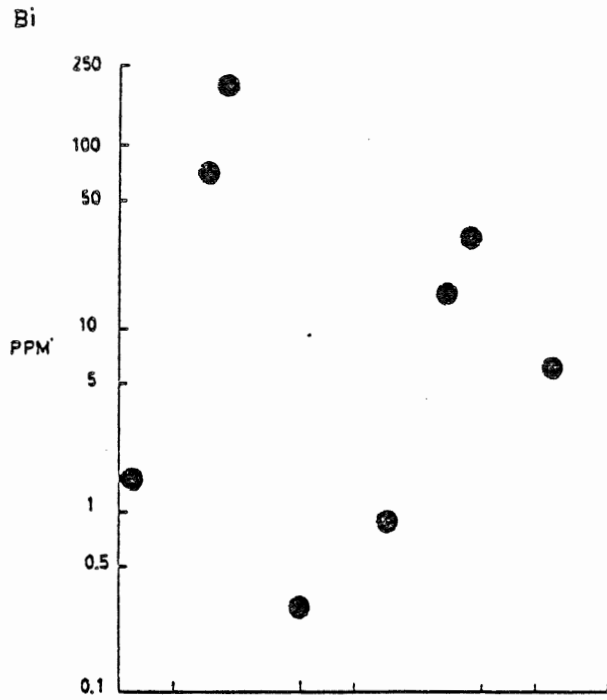
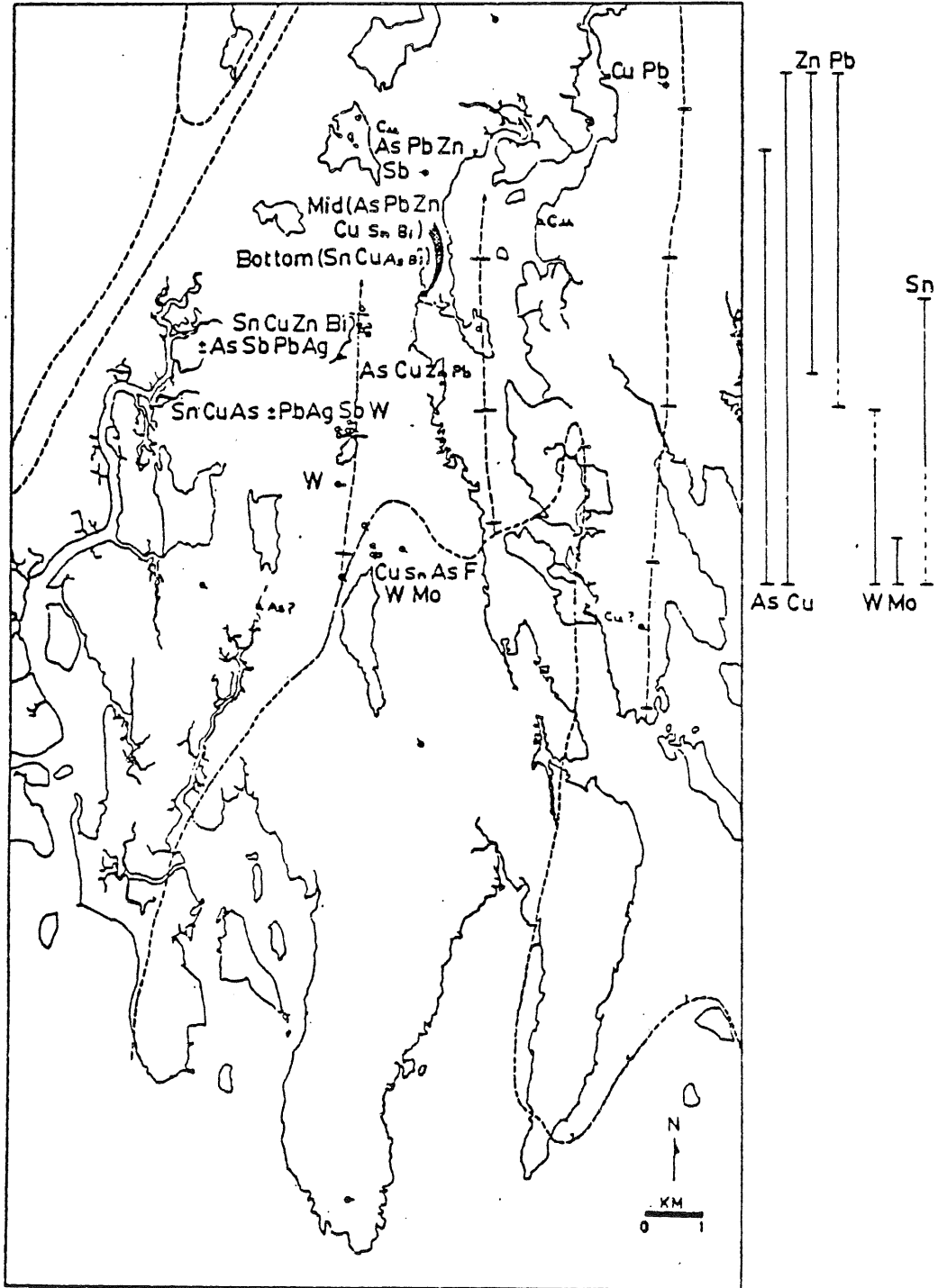


Figure 5.7

Plot of metals commonly occurring in mineralized vein systems in both the pluton and surrounding metasediments. There is a pattern of metal concentration from the pluton outwards and upwards, from W and Mo to Pb and Zn; As and Cu are ubiquitous; Sn has an intermediate range (~ 3-5 km from pluton).

Lower case metals have relatively lower abundances.

"Mid" refers to those metals occurring in veins at "middle" depths of 50-100 m in DDH 78-34. "Bottom" refers to those metals occurring in veins at "bottom" depths greater than 100 m in DDH 78-34.



indicate possible directions and depths for further geochemical or geophysical work.

The veins are rather thin (commonly on the order of mm) and have relatively narrow alteration haloes (mm to several cm). There has been no wide mineralogical or geochemical response associated with these veins. If a stockwork of such veins occurred within a small volume of rock, the geochemical effects may be enhanced to such an extent as to produce a broader, noticeable response, but this has not been observed.

(ii) Greisen Veins

Greisen veins and their associated haloes are relatively high in tin (about 200-800 ppm) with respect to the rest of the pluton, although low compared to sulphide-cassiterite veins. The greisens are also relatively high in tungsten, copper, lithium, fluorine, total iron and rubidium; they have wide ranges of molybdenum, arsenic, zinc and bismuth - this is probably due to multiple-stage, cross-cutting veinlets containing molybdenite, arsenopyrite, sphalerite and scheelite. Both sodium and strontium are depleted in the greisens (Fig. 5.8).

Contact of the greisen with the monzogranite varies from sharp to gradational. Trace element contents of unaltered samples adjacent greisens show either no change or a slight

Figure 5.8

Variation of several major oxides(in %) and minor elements(in ppm) in plutonic samples from study area and two other granitoid bodies.

Greisens have higher concentrations of Fe_2O_3 (total) and Rb(addition of sulphides and white mica); they are relatively depleted in Na_2O , Sr and K/Rb(destruction of feldspars).

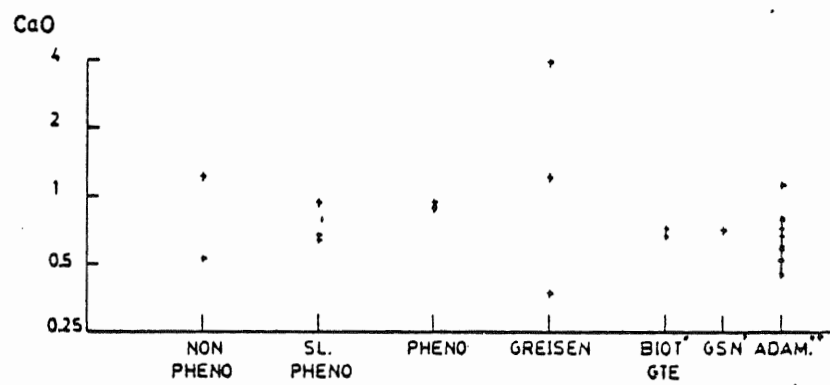
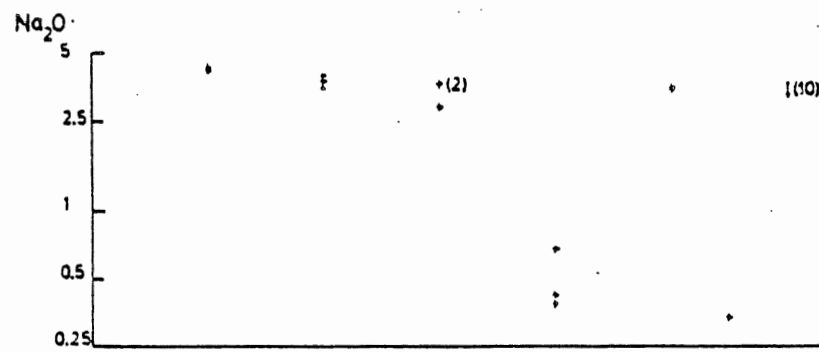
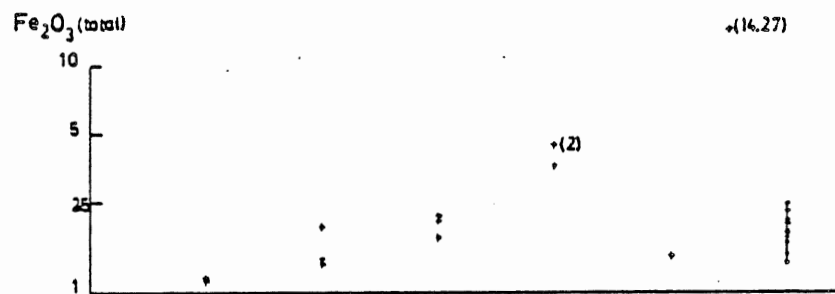
Non pheno - non-phenocrystic monzogranite

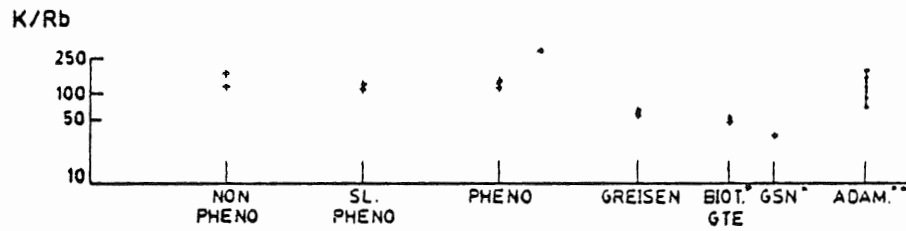
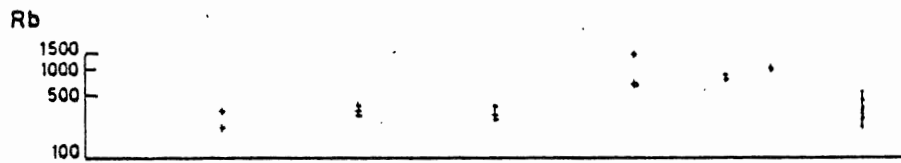
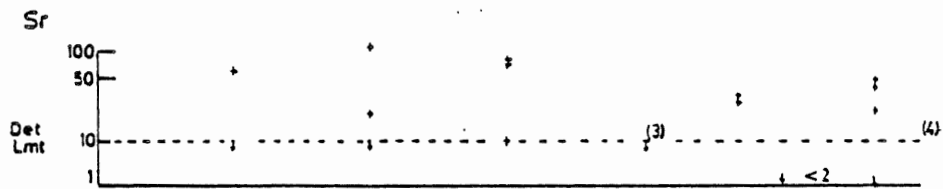
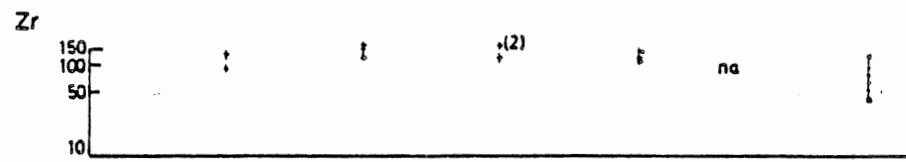
Sl. pheno - slightly phenocrystic monzogranite(1-5 modal %)

Pheno - phenocrystic monzogranite (>5 <75 modal %)

*Biot gte - biotite granite and greisen samples from the Davis Lake pluton, East Kemptville (Chatterjee, 1980)

**Adam - adamellite from part of the South Mountain batholith (McKenzie and Clarke,1975)





enrichment in tin and fluorine. One sample of slightly altered monzogranite (tan alteration adjacent greisen) is relatively enriched in copper and depleted in antimony and bismuth (addition of chalcopyrite, removal of arsenopyrite?).

As with veins in the metasediments, greisens do not have a wide zone of influence - usually several cm, rarely up to about 20 cm. Trace element contents have a narrow zone of enrichment around each greisen vein, e.g., see Figure 5.10 for variation of tin and copper in greisens and their adjacent country rock. Unless there is a concentration of such veins to produce a broad geochemical effect, they cannot be traced geochemically. If the overlying country rock had behaved in a more ductile fashion, with less fracturing, the ore-bearing 'greisen' fluids may have instead remained within the apical parts of the intrusion, 'ponding' against the country rock, forming broad greisen zones of economic interest.

(iii) Stratiform Mineralization

The stratiform patches are relatively enriched in tin, copper and bismuth, due mainly to the presence of cassiterite and chalcopyrite; bismuth may occur in the form of sulphides or sulphosalts, as submicroscopic inclusions in the other sulphides, or as solid solutions within native silver or galena. All boron analyses are below the detection limit (10

ppm) (leaching effect?). Other element distribution patterns are not as distinct: tungsten contents have a slightly higher range, with larger values in samples close to the pluton; zinc contents are similar to those of unmineralized samples, with the exception of two samples containing much sphalerite; meta-psammitic samples have a higher range of antimony contents but they are not always directly related to arsenic content (Fig. 5.9) as observed in veins - perhaps Sb substitutes for other elements, e.g., Fe, Sn⁴⁺, Ti³⁺⁴⁺ instead of existing as a sulphosalt within arsenopyrite. Sb analyses are also not very precise (see Appendix III for accuracy and precision estimates).

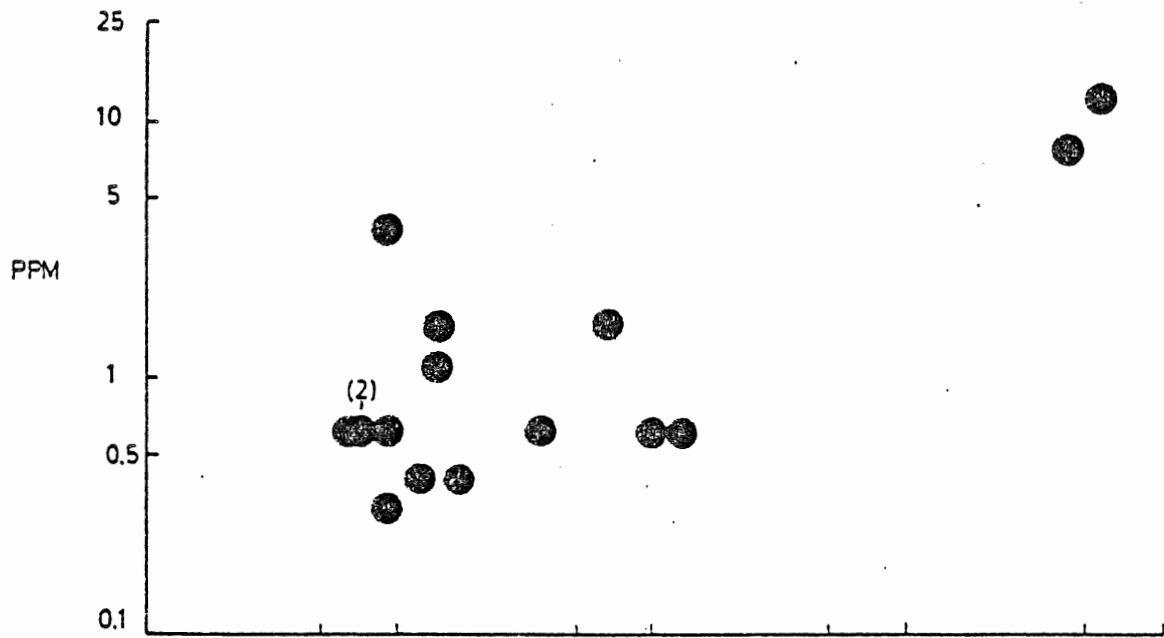
Samples adjacent psammitic mineralized zones show slightly elevated tin contents. Copper contents are ambiguous: seven of the eleven adjacent samples are in the upper ranges of the normal population; the other four samples are below the detection limit of 0.5 ppm (leaching effect?). Figures 5.10 and 5.11 show the variation of tin and copper, and tin and bismuth in mineralized patches and their adjacent zones. Other elements show no significant observable changes. Figures 12a,b show cross-sections of parts of the study area containing tin mineralization but show no clear-cut geochemical haloes.

Again, a restricted geochemical dispersion exists around the mineralization. No widespread halo occurs which would be

Figure 5.9

Variation of Sb and Bi content with As in mineralized 'patches'. There is no apparent relationship of the two elements with As (some increase of Sb with As).

Sb



Bi

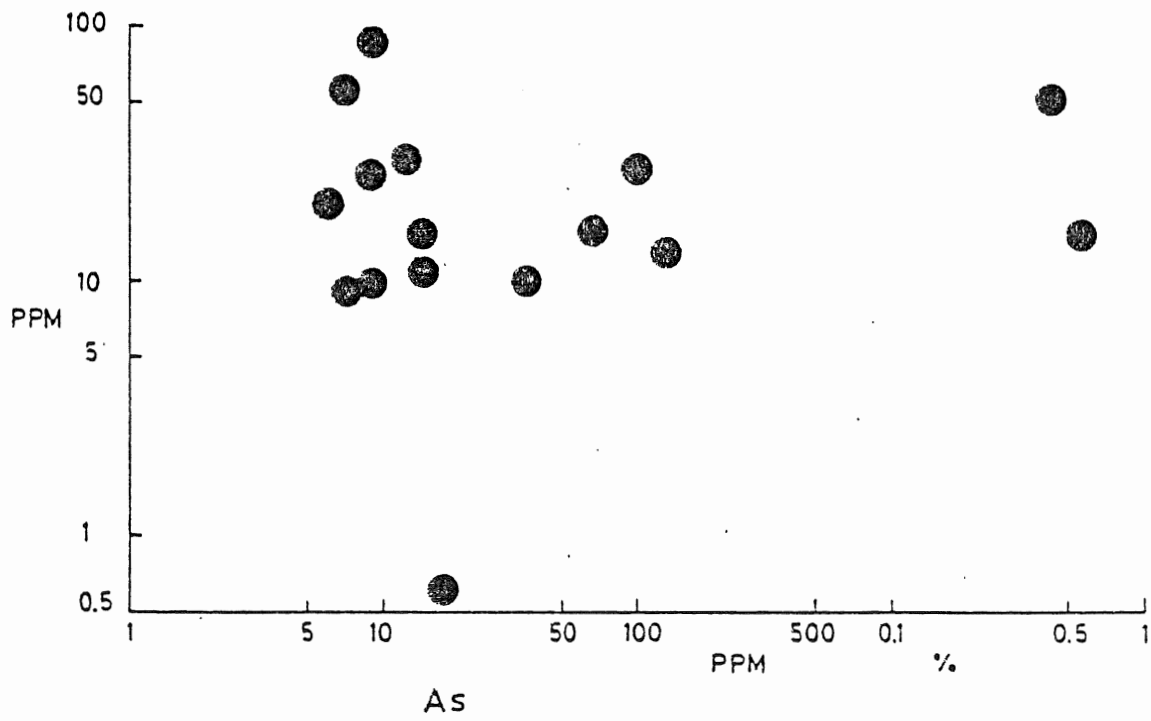


Figure 5.10

Variation of Sn and Cu within mineralized 'patches' and greisens, and their respective adjacent unmineralized zones. The sharp decrease in both elements indicates their restricted ranges in both mineralization types.

- Mineralized 'patch'
- Barren sample adjacent 'patch' (cm to m distant)
- ▲ Greisen
- △ Barren sample adjacent greisen (cm to m distant)

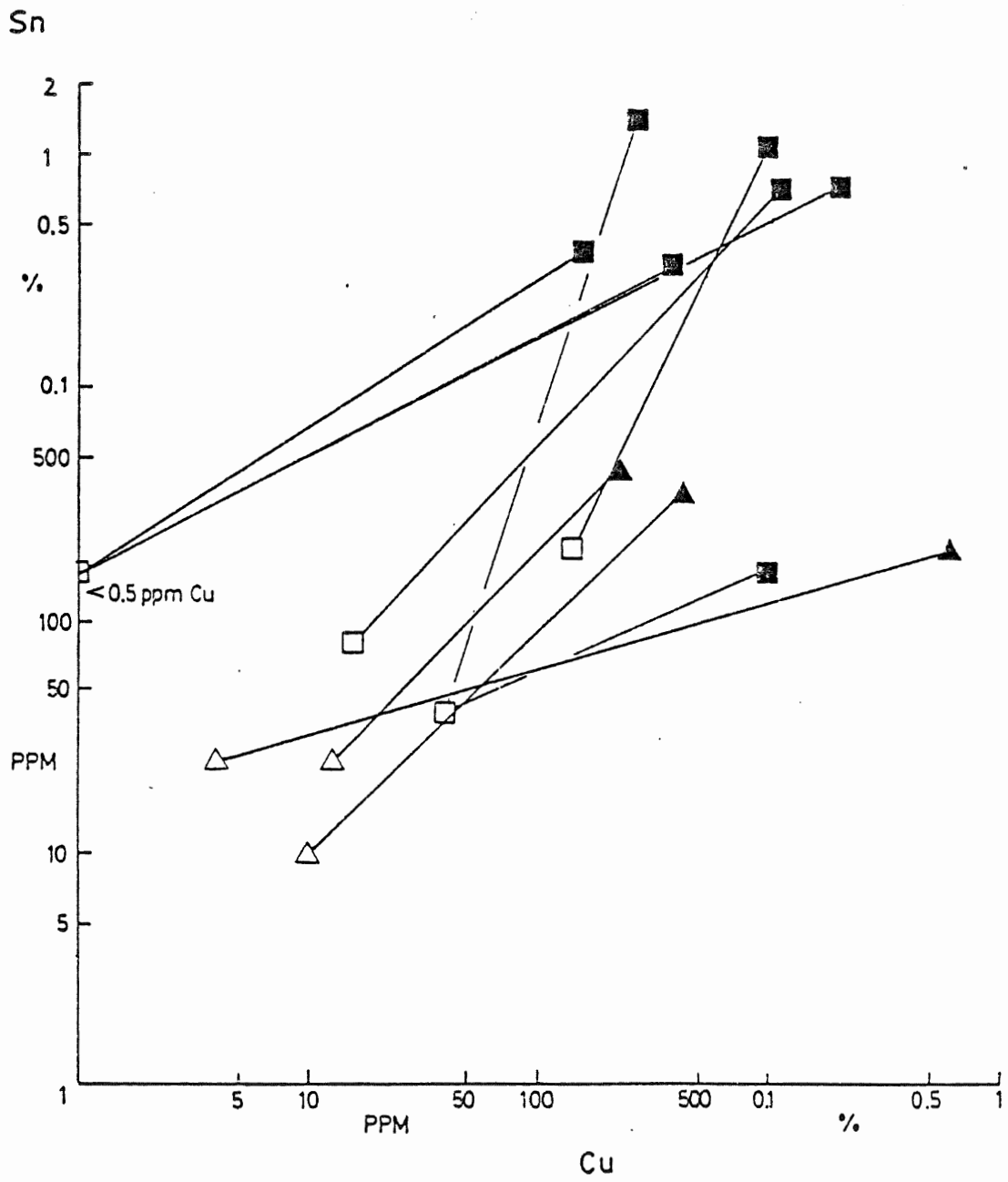
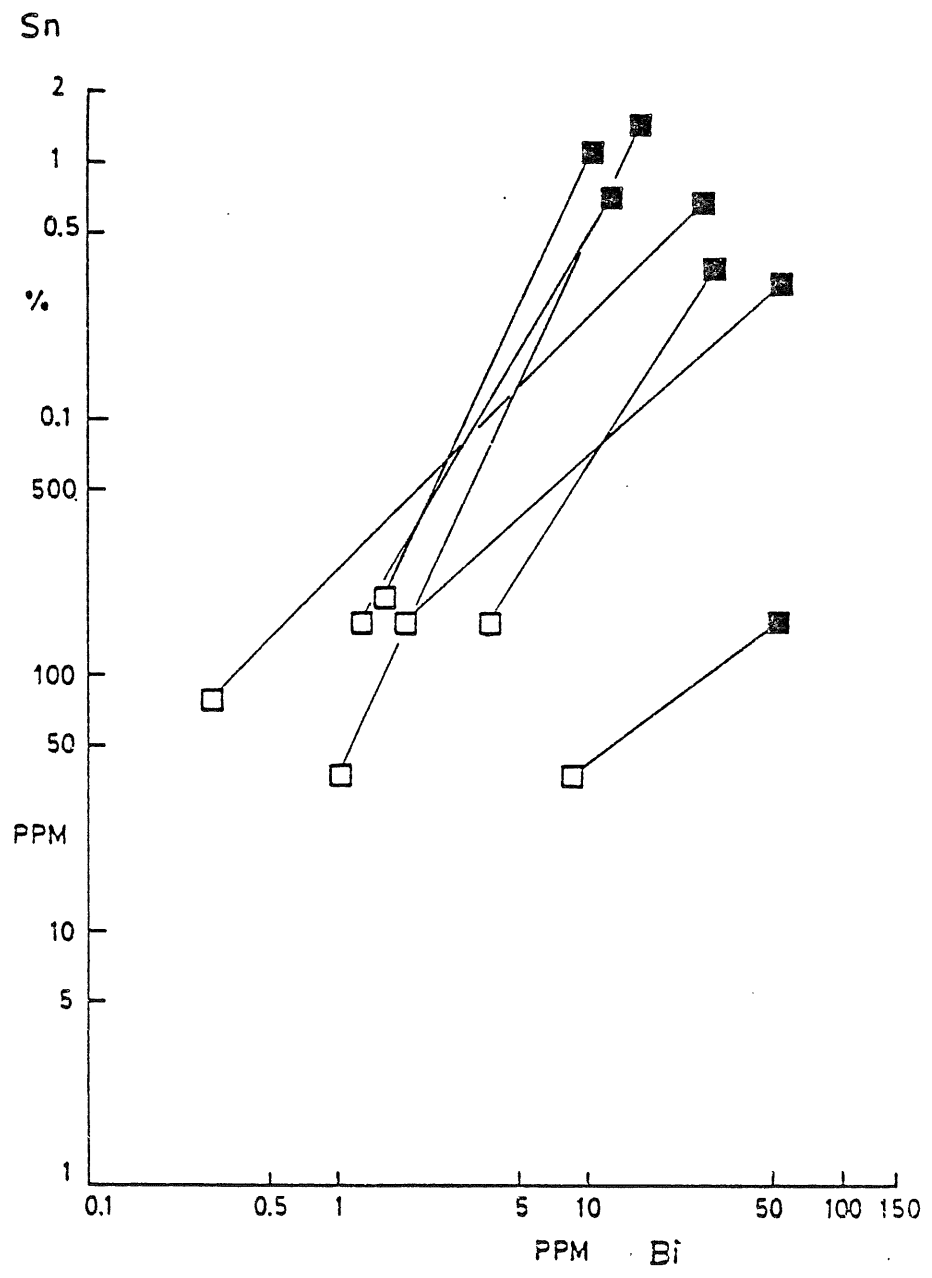


Figure 5.11

Variation of Sn and Bi within mineralized 'patches' and their adjacent unmineralized zones. There is a sharp decrease in both elements from mineralized to unmineralized samples, indicating the restricted extent of these elements.

- Mineralized 'patch'
- Barren adjacent samples
(cm to m distant)



of use in a geochemical exploration program.

5.3.3 Relationship of Elements With Respect to Distance From the Pluton

Establishment of a trace element zonal pattern in any region can aid in subsequent geochemical exploration programs. Once position in any 'zone' is known, one can travel toward the ore-bearing zone with some degree of confidence.

Based on the present study, the mineralizing event(s) exerted no broad geochemical influence upon the country rock. Vein and stratabound mineralization are of limited lateral extent, with only a few cm of altered wallrock. Rarely, veinlets in the pluton have relatively wide greisen alteration haloes.

Because of the restricted nature of the mineralization, an attempt was made to investigate trace element distribution in mineralized samples at various distances from the pluton. Two cross-sections were made: one roughly follows a fold hinge from the metasediments to the pluton (A-A'); the second cuts regional foliation (B-B'). Sample point locations from each diamond drill hole were translated onto the plane of each cross-section. The cross-sections were arbitrarily divided into 'top', 'middle', and 'bottom' zones, representing depths of, respectively, 0 to 50, 50 to 100, and

more than 100 metres. This was to look for trace element variation with depth. Several of these cross-sections are shown in Appendix 5. There appears to be little variation in trace element content in unmineralized metasedimentary samples, either with depth or with distance from the intrusion. Small variations in their concentrations may be due primarily to their lithology (pelitic vs. psammitic), so no definite conclusions can be made about geochemical dispersion in barren metasedimentary country rock. Relatively high contents of some trace elements in unmineralized samples occur close to or adjacent the pluton and appear caused by metalliferous veinlets (containing tungsten, fluorine, lithium and copper). Zinc decreases slightly with depth. Arsenic is ubiquitous, disseminated in the metasediments and within several stages of veins as arsenopyrite. Bismuth is erratic, and is related to both arsenic and tin.

Within the pluton, there is a slight decrease in trace element content in the interior. This may result from primary differentiation or the absence of metal-bearing veinlets found in the endocontact.

Few analyses were made of vein samples in areas of the cross-sections, so interpretation includes megascopic and microscopic presence of the metal-bearing minerals. There is a metal zonation within vein systems from the pluton into the

metasediments and this was discussed in a previous section of this chapter.

Trace element distribution within stratabound mineralized patches appears regular. There is little change with depth or distance from the pluton, except where cut by veinlets bearing tungsten, molybdenum, lithium and fluorine. Zinc content appears to increase with distance from the intrusion in two samples - possibly related to higher zinc content in distant parts of the vein system? Arsenic is erratic because of its common occurrence throughout the area.

5.3.4. Relationship of Elements With Respect to Other Variables

Trace element distribution may vary with other factors such as stratigraphy and secondary dispersion processes. Due to time and monetary constraints, it was not possible to perform a study of these types of element distribution.

It is conceivable trace element concentrations vary with depth or lateral extent in the sedimentary package. The geochemical study has been simplified by assuming there is little variation in trace element concentrations with depth or lateral extent.

Mafic dykes in the area do not change the trace element

patterns in the host rock. Several samples adjacent the dykes were analysed and only the arsenic content in two monzogranite samples increased. Arsenopyrite was included in the biotite flakes - it is not known how this occurred, as arsenic contents in the dykes are low.

Chemical weathering of the country rock can disperse the trace elements at surface, along fracture systems, or through breccia produced by late shearing. Examination of some core proved difficult because of weathering effects from storage at surface - iron sulphides became oxidized. Clean core with fractures or breccia zones usually show little oxidation and it was assumed that little secondary dispersion took place; however as a precautionary measure these cores were not sampled. Some mineralized patches show elongate, 'shreddy'-textured sulphides, as if they had been stretched out by later movement, possibly the late-stage shearing event. It does not appear these chlorite- and sulphide-rich zones fractured cleanly with a minimum of rock powder ('gouge') to permit movement of fluids to disperse any elements. Other, more brittle, barren psammitic layers are well brecciated with later infillings by calcite, quartz and minor sulphides; a restricted bleached zone and rarely, a stockwork of veinlets ('crackle breccia') surrounds this breccia. Dispersion of elements appears limited.

Figure 5.12

Pseudo-three-dimensional sections of two mineralized area with tin concentrations of sampled core (in ppm except where noted). See Fig. 5.1 for drill hole locations.

A. Intersecting drill hole grid

▣ Mineralized 'patch'

+ Unmineralized core

△ Mineralized vein

adj -unmineralized sample
adjacent mineralization

78-12 -diamond drill hole

Boxes with two numbers indicate a mineralized 'patch'(higher value) with an adjacent sample. Inset depicts general bedding and crenulation(˘) orientation.

B. Parallel drill hole grid

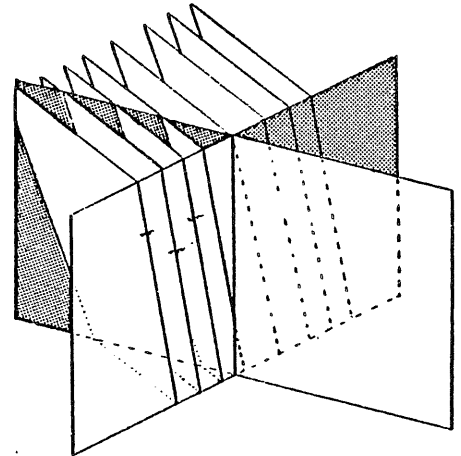
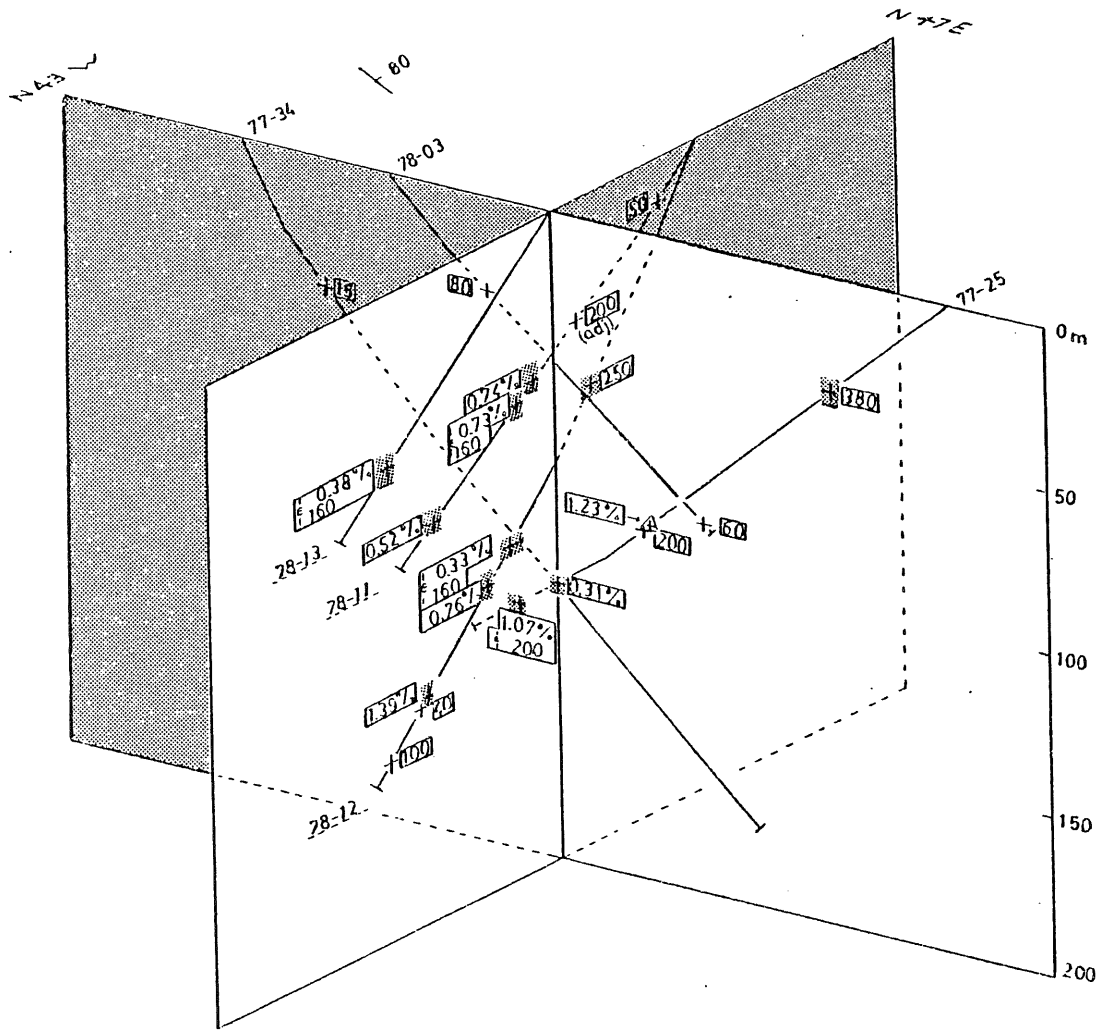
Same symbols as above, plus

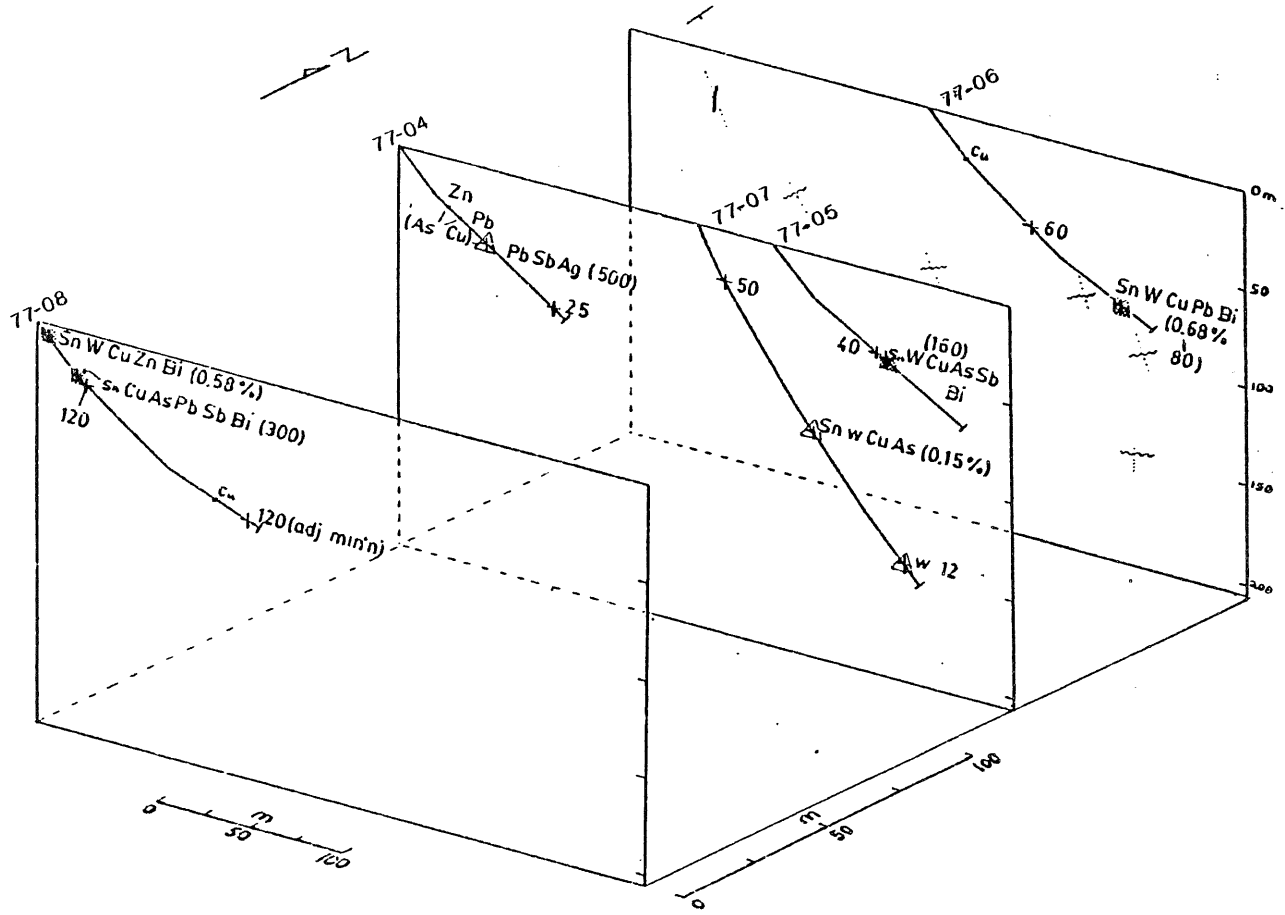
Sn -relatively high amount of mineral containing this metal

sn -relatively low amount of mineral containing this metal

. sample location described but not geochemically analysed

˘˘˘ general bedding orientation





5.4 Summary

A group of barren and mineralized diamond drill core was analysed for 13 trace elements. Chlorine analysis was disappointing as most were below the detection limit (50 ppm). Boron analyses were not much use as the values were multiples of 10 and 25; however they proved useful in the mineralized samples, as all values were below the detection limit (10 ppm).

Analytical control was erratic: precision was adequate, but accuracy was not. The analyses may be useful for comparisons within the sample group, but are not to be considered 'true' values.

Background values between pelitic and psammitic samples are similar for most trace elements, with a few exceptions (Sn, Cu, Zn, and Bi). This may be due to primary sedimentologic factors. Element contents are similar to or lower than the average values found in Cornish tin-bearing metasediments, and the clarkes of shale and sandstone (Table 5.1). Trace element background values of plutonic samples are lower than those usually associated with 'specialized', tin-bearing granitoids. Accordingly, the Wedgeport pluton is not considered a major tin-bearing intrusion.

Alteration haloes around mineralization are limited (wallrock pattern of Hawkes, in Levinson, 1974) and therefore lithogeochemical exploration is of little use in terms of

discovering trace element haloes. However, there is a metal zonation within the main-stage vein system, from the pluton, outwards. Accurate determination of the stage of a vein and its mineralogy may aid in tracing the more economic members of the system.

Table 5.1 SUMMARY OF LITHOGEOCHEMICAL SURVEY

ELEMENT	Meta-pelitic Samples (n=23)	Meta-psammitic Samples (n=51)	Monzogranite (n=25)
Sn	<p>2 Populations:</p> <p>Anomalous(>100 ppm) All known mineralized samples</p> <p>Background(<100 ppm) All known unmineralized samples</p> <p>No significant differences in background [Sn] between meta-argillite and carbonaceous meta-argillite. In mineralized patches a positive correlation exists among Sn, Cu, and Bi; all B values at or below detection limit(10 ppm). Relationship with other elements less clear. Background and threshold are lower than those of meta-psammites. May be due to small data set or to primary sedimentological differences, i.e., Sn as cassiterite more likely occurs in psammitic layers (rarely in pelitic scours).</p>	<p>3 Populations:</p> <p>Anomalous(>180 ppm) Mineralized samples</p> <p>Intermediate (<180 >128 ppm) Mineralized samples and samples adjacent mineralization</p> <p>Background(<128 ppm) All known unmineralized samples, plus several samples adjacent mineralization; 1 in a mineralized patch; 1 in a vein.</p> <p>No significant differences in background [Sn] among meta-psammitic lithologies(wacke +/- biotite, feldspar, carbonate). In mineralized patches a +ve correlation exists between Sn and Cu;less so with W,Sb, and Bi; most B values at or below detection limit. In veins a +ve correlation exists between Sn and Cu; a -ve correlation between Sn and As,Pb,Sb and Zn. Other relationships less clear.</p>	<p>3 Populations:</p> <p>Anomalous(>48 ppm) Greisens; 1 sample with kaolinite alt'n; 1 sheared sample</p> <p>Intermediate(<48 >15 ppm) Samples adjacent greisens, cut by several vein stages; unmineralized samples</p> <p>Background(< 15 ppm) Unmineralized samples and 1 adjacent greisen</p> <p>No apparent distinction in [Sn] based on presence or absence of phenocrysts. Endocontact background samples have a higher range(7-35 ppm) than those in the interior of the pluton(3-10 ppm). May be due to: small data set; presence of a myriad of Sn-bearing veinlets in endocontact; primary differentiation of magma.</p>

Table 5.1 cont'd.

ELEMENT	Meta-pelite	Meta-psammite	Monzogranite
W	<p>1 Population: usually assume upper 2 1/2% anomalous until proven otherwise (Sinclair, 1974), i.e., 60 ppm threshold.</p> <p>Similar values occur in min'd and barren meta-pelites (2-23 ppm); slightly higher [W] in carbonaceous and min'd meta-argillites. Higher [W] near pluton.</p>	<p>2 Populations:</p> <p>Anomalous (>19 ppm) 10 min'd patches and veins; 1 sample adjacent min'n</p> <p>Background (<19 ppm) Mostly unmin'd (22/40 samples); 11/40 adjacent min'n; 7/40 are min'd patches and veins</p> <p>Slightly higher values occur in min'd patches and zones adjacent min'n. Higher values occur in samples near pluton-possibly cut by scheelite-bearing veinlets.</p>	<p>2 Populations:</p> <p>Anomalous (>65 ppm) 1 greisen and all samples with non-greisen veining</p> <p>Background (<65 ppm) All other samples, including 3/4 greisens</p> <p>High W values appear related to non-greisen scheelite bearing quartz veinlets. Similar values exist for different phenocryst concentrations; [W] increases from non-phenocrystic to phenocrystic samples. W values in greisen slightly higher than unmin'd samples; 23-38 ppm vs. <1-24 ppm respectively. Endocontact samples have higher values than interior samples; 8-24 ppm vs. <1-9 ppm, respectively.</p>

Table 5.1 cont'd.

ELEMENT	Meta-pelite	Méta-psammite	Monzogranite
Mo	<p>2 Populations:</p> <p>Anomalous(>5 ppm) 3 unmin'd carbonaceous meta-argillites near the pluton (1 is adjacent a mafic dyke)</p> <p>Background(<5 ppm) 16/23 samples below detection limit (0.5 ppm) including min'd patches and vein; 4/23 are <5 and >0.5 ppm (3 are min'd patches; 1 is barren)</p> <p>In population partitioning, value of 0.05 ppm (1 order of magnitude lower) was used for all values below detection limit, producing an interpolated background of 0.4 ppm. Use this value with caution. Mo content appears related to pluton proximity.</p>	<p>1 Population:</p> <p>Most high Mo values associated with veins, either near pluton with molybdenite +/- scheelite, or containing arsenopyrite and other sulphides(?). [Mo] in min'd patches erratic (<0.5-2.5 ppm) and cannot be correlated with [Sn]. 35/51 values < 0.5 ppm, so 0.05 ppm was used in population partitioning, giving an interpolated background of 0.4 ppm. Use this value with caution. Mo content appears related to pluton proximity.</p>	<p>2 Populations:</p> <p>Anomalous(>32 ppm) In samples cut by veinlets containing molybdenite +/- scheelite</p> <p>Background(<32 ppm) In unmin'd, altered, and greisenized samples.</p> <p>Most low values are from interior pluton samples; endocontact samples are higher in [Mo] and are also cut by stockwork hair veinlets bearing molybdenite +/- scheelite. Greisen Mo values are ambiguous-appear to depend on presence of non-greisen veinlets.</p>

Table 5.1 cont'd.

ELEMENT	Meta-pelite	Meta-psammite	Monzogranite
As	<p>3 Populations:</p> <p>Anomalous(>100 ppm) 1 vein; 2 min'd patches; 1 barren sample with disseminated arsenopyrite; 1 barren sample with pre- crenulation arsenopyrite veinlet.</p> <p>Intermediate(<100 >16 ppm) 1 min'd patch; 3 barren samples</p> <p>Background(<16 ppm) 5 min'd patches; 9 barren samples</p> <p>Arsenic has erratic distri- bution in metasediments, patches and veins. Have to know its stage in paragenetic sequence before using As in exploration.</p>	<p>2 Populations:</p> <p>Anomalous(>160 ppm) 6 veins; 1 min'd patch and 1 barren sample with dissem- inated arsenopyrite.</p> <p>Background(<160 ppm) Includes barren and mineralized samples, samples adjacent min'n and 1 vein.</p> <p>Appears to be an anti- pathetic relationship between Sn and As in veins and patches. Those veins with [As] >7000 ppm have [Sn] <500 ppm and are at shallower depths farther from the pluton. Low [As] (<220 ppm) in veins have high [Sn](>1500 ppm) and are found closer to the pluton at deeper levels.</p> <p>May use Sn-As content in veins as exploration guide.</p>	<p>2 Populations:</p> <p>Anomalous(>70 ppm) 3 samples(barren; greisen; kaolinite alt'n) cut by arsenopyrite-bearing hair veinlets; 2 sam- ples adjacent mafic dykes contain biotite with inclusions of arsenopyrite(?).</p> <p>Background(<70 ppm) All other samples, both barren and mineralized; actually all <30 ppm.</p> <p>Arsenic content ap- pears related to syn- & post-greisen veining.</p>

Table 5.1 cont'd.

ELEMENT	Meta-pelite	Meta-psammite	Monzogranite
Cu	<p>2 Populations:</p> <p>Anomalous(>250 ppm) All mineralized patches, 1 vein and 1 carbonaceous meta-argillite adjacent a mafic dyke and the pluton.</p> <p>Background(<250 ppm) All barren samples; 1 carbonaceous meta-argillite (190 ppm) is near pluton and contains chalcopryrite within pyrrhotite.</p> <p>There exists a definite gap between mineralized and unmineralized samples. Get interested in values >125 ppm.</p>	<p>2 Populations:</p> <p>Anomalous(>365 ppm) 8 mineralized patches; 3 'high Sn', 1 'high As' veins.</p> <p>Background(<365 ppm) All barren samples; samples adjacent mineralization; 3 mineralized patches and 3 'high As' veins.</p> <p>No major differences between unmineralized samples and those adjacent mineralization. In adjacent mineralized samples there is a gap between very low values (<0.5 ppm) and those above background(possible leaching effect?).</p> <p>High [Cu] (<150 >70 ppm) may be due to chalcopryrite or Cu solid solution in the ubiquitous pyrrhotite blebs. Good correlation of Sn and Cu, but restricted range of Cu in patches precludes its use as a pathfinder. Try veins.</p>	<p>2 Populations:</p> <p>Anomalous(>135 ppm) 3 greisens</p> <p>Background(<135 ppm) All other samples, including 1 greisen</p> <p>Those samples adjacent to greisens, are greisenized, cut by non-greisen veinlets and are sheared, have high Cu values higher than the background. Interior pluton samples are on average lower than the endocontact samples;<0.5-5.5 ppm vs. 1.5-35 ppm, respectively. May be due to ubiquity of veining in the endocontact. Both greisen and non-greisen vein samples have erratic Cu values, possibly because of low sample size.</p>

Table 5.1 cont'd.

ELEMENT	Meta-pelite	Meta-psammite	Monzogranite
Pb	<p>2 Populations:</p> <p>Anomalous(>50 ppm) 2 mineralized patches; 1 barren sample</p> <p>Background(<50 ppm) All other samples</p> <p>Pb distribution erratic; gives a poor population split. Higher values >15 ppm) associated with mineralized patches, 1 vein, 1 pre-crenulation arsenopyrite veinlet and 1 barren sample. Pb usually in galena, often associated with arseno- pyrite.</p>	<p>2 Populations:</p> <p>Anomalous(>120 ppm) 4 'high As-low Sn' veins, 1 barren sample</p> <p>Background(<120 ppm) All other samples</p> <p>Most values <23 ppm (39/51 samples); higher values (<90 >23 ppm) include 3 mineralized patches, 1 'high-Sn low-As' vein and 3 barren samples (1 near pluton with rare mo- lybdenite on fracture surface). 2 barren samples from 1 drill hole (78-29) contains relatively high [Pb] (40 & 170 ppm); not known why. Not much difference between mineralized and un- mineralized samples. In veins, there is a +ve correlation be- tween Pb and As; a -ve correlation between Pb and Sn.</p>	<p>2 Populations:</p> <p>Anomalous(>15.5 ppm) 1 sample adjacent a greisen; 1 cut by non-greisen veining; 1 barren sample</p> <p>Background(<15.5 ppm) All other samples</p> <p>Pb values are erratic with respect to litho- logic types and miner- alization; higher values appear related to post- greisen veinlets (contain- ing arsenopyrite, molyb- denite and scheelite).</p>

Table 5.1 cont'd.

ELEMENT	Meta-pelite	Meta-psammite	Monzogranite
Zn	<p>2 Populations:</p> <p>Anomalous(>275 ppm) 3 mineralized patches and 1 vein</p> <p>Background(<275 ppm) All other samples</p> <p>Little difference among meta-argillites, carbonaceous meta-argillites and mineralized patches: Meta-argillite - narrow cluster of values (79-130 ppm) Carbonaceous meta-argillite - wider range of values (41-260 ppm) Mineralized patches-(54-680 ppm and 14.6%) Vein('high Sn-low As' type)- 1500 ppm</p>	<p>2 Populations:</p> <p>Anomalous(>330 ppm) 3 veins of 'high As-low Sn' type; 1 mineralized patch; 1 sample adjacent mineralization.</p> <p>Background(<330 ppm) All other samples</p> <p>Little difference among various psammitic types or between mineralized and barren samples. Veins high in As have high Zn contents.</p>	<p>1 Population:</p> <p>Most values(21/25) <41 ppm. 2 anomalous values exist in greisen zones(140 & 2900 ppm)</p> <p>Little difference among different granitoid types. [Zn] in greisen erratic-may be due to cross-cutting post-greisen veinlets.</p>

Table 5.1 cont'd.

ELEMENT	Meta-pelite	Meta-psammite	Monzogranite
Sb	<p>2 Populations:</p> <p>Anomalous(>2.0 ppm) 1 mineralized patch; 2 carbonaceous meta-argillites with pre-crenulation arsenopyrite; 1 meta-argillite</p> <p>Background(<2.0 ppm) All other samples. 17/23 samples <1.0 ppm</p> <p>[Sb] appears tied to [As]; those samples with arsenopyrite have higher Sb contents.</p>	<p>2 Populations:</p> <p>Anomalous(>1.45 ppm) 4 veins of 'high As-low Sn' type; 1 'high Sn' type; 4 mineralized patches.</p> <p>Background(<1.45 ppm) All other samples. 25/51 samples <0.5 ppm</p> <p>No major observable differences among various psammitic types; both wacke and calcareous wacke values are less than background(<0.44 ppm)-may be due to low sample size. High [Sb] in mineralized patches and veins tied to [As].</p>	<p>2 Populations:</p> <p>Anomalous(>0.6 ppm) 1 greisen(with arsenopyrite-bearing veinlet); 1 sample with kaolinite alteration; 2 with non-greisen veining; 2 samples adjacent mafic dyke(with arsenopyrite in biotite flakes)</p> <p>Background(<0.6 ppm) All other samples</p> <p>Slightly phenocrytic samples have lower Sb contents than other unmineralized samples; not known why. High [Sb] tied to [As].</p>

Table 5.1 cont'd.

ELEMENT	Meta-pelite	Meta-psammite	Monzogranite
Bi	<p>2 Populations:</p> <p>Anomalous(>3.5 ppm) All mineralized patches & the Sn-rich vein</p> <p>Background(<3.5 ppm) All unmineralized samples</p> <p>There is a definite difference between mineralized and barren samples.</p>	<p>1 Population:</p> <p>Most(7/8) mineralized samples have higher Bi contents(>10 ppm) than the other samples. No observable differences among various psammitic types or between unmineralized & adjacent mineralized samples(restricted range).[Bi] erratic with respect to 'high As' & 'high-Sn' type veins.</p>	<p>1 Population:</p> <p>Lower Bi content in non-phenocrytic samples (interior pluton). Tan altered sample below detection limit(<0.1 ppm). Other samples have wide spreads of values. Bi does not appear related to Sn mineralization as in the metasediments.</p>

Table 5.1 cont'd.

ELEMENT	Meta-pelite	Meta-psammite	Monzogranite
Li	<p>2 Populations: (Possibly 1)</p> <p>Anomalous(>100 ppm) 1 carbonaceous meta- argillite adjacent pluton</p> <p>Background(<100 ppm) Rest of data set</p> <p>Little difference between pelitic types. Tightly grouped(31- 70 ppm). Exceptions:sample with pre-crenulation arseno- pyrite veinlet(89 ppm); 1 sample adjacent mafic dyke(13 ppm). Mineralized patches - values spread out(8-59 ppm)</p>	<p>1 Population: Most values (35/51) <60 ppm. High [Li] usually occurs near the pluton. One high value(100 ppm) found in a 'barren' sample in a DDH with other high trace element contents(78-29). Primary cause? Little difference among psammitic types, be they barren or mineralized.</p>	<p>2 Populations:</p> <p>Anomalous(>80 ppm) 3 greisens; 1 kao- linite alteration; 2 non-phenocrystic barren samples from the interior pluton(78-31)(?).</p> <p>Background(<80 ppm) Rest of data set. 10/25 samples <49 ppm.</p> <p>Restricted range of Li in greisens. Little difference among non-greisen samples;usually in range of 26-80 ppm.</p>

Table 5.1 cont'd.

ELEMENT	Meta-pelite	Meta-psammite	Monzogranite
F	<p>1 Population:</p> <p>Carbonaceous meta-argillites have wider spread(100-820 ppm)than meta-argillites(320-630 ppm). Mineralized patches not different(360-660 ppm)except for 2 samples(190 & 200 ppm); not known why. Highest value(820 ppm)found in barren sample adjacent pluton(80-01).</p>	<p>2 Populations:</p> <p>Anomalous(>1000 ppm) 4 barren samples and 1 mineralized patch, all adjacent the pluton(79-05; 80-01); 2 'high As' type veins.</p> <p>Background(<1000 ppm) Rest of data set. 41/51 samples <760 ppm. Little difference among various psammitic types or mineralized patches. [F] in veins not clear cut: 3/4 'high As' > 'high Sn' types; 670-1500 ppm vs. 280-530 ppm respectively.</p>	<p>2 Populations:</p> <p>Anomalous(>1550 ppm) All 4 greisens</p> <p>Background(<1550 ppm) Rest of data set</p> <p>Slight differences among various types of non-greisen samples. Interior pluton samples have a slightly lower range than endo-contact samples. Greisens have 'classic' high F contents, but are of restricted range.</p>

Table 5.1 cont'd.

ELEMENT

B Population partitioning not performed as all values are multiples of 10 or 25 (10, 25, 50, 75, 100 and 150 ppm). This does not appear 'natural'. Little difference among meta-pelitic and meta-psammitic lithologies, except in mineralized patches of both rock types - at or below detection limit of 10 ppm. Due to leaching?

Cl Not performed as most values below detection limit of 50 ppm.

CHAPTER SIX
CONCLUSIONS AND RECOMMENDATIONS FOR
FURTHER WORK AND EXPLORATION

6.1 Conclusions

Mineral and geochemical study of the Wedgeport pluton and adjacent metasedimentary host rocks has provided the following impressions concerning the genesis of tin mineralization in the area.

1. Tin as cassiterite, occurs in several habits and mineral associations, reflecting variable conditions of its formation. It is a rare detrital mineral within Cambro-Ordovician Meguma metasediments; it rarely occurs within greisen veins in the pluton; it occurs as a minor to common mineral within sulphide veinlets and stratiform sulphide replacement bodies in the metasediments.

2. Partial melting of carbonaceous, cassiterite-bearing metasediments produced a low fO_2 , ilmenite-series melt with divalent tin (and other lithophile elements) concentrated within a later evolved aqueous phase(s). Tin may have been transported as chloride and fluoride complexes. Fracturing of the pluton margin provided a means of escape for this phase. Healing of the fractures by mineral precipitation and refracturing by later aqueous phases resulted in several

generations of veinlets. Sulphide-cassiterite precipitation occurred in a 'middle' stage of vein formation, after barren quartz veinlets and before quartz-kaolinite veinlets and shears. These ore-bearing fluids caused limited greisenization within the pluton margin. They then travelled through fractures near or along an anticlinal fold hinge; sulphides and cassiterite precipitated in veins and replaced calcareous layers within the metasediments. Apparently there was insufficient initial water in the melt to generate economically significant amounts of ore-bearing fluid.

3. Mineralization is found in a zonal sequence away from the pluton, reflecting the changing physico-chemical conditions of the fluid(s) as it travelled through, and reacted with the metasediments (e.g. P, T, fO_2 , fS_2 , pH, Eh, wallrock chemistry).

4. Alteration effects associated with mineralization within both the pluton and metasediments are restricted - no broad geochemical or mineralogical halo is observed.

6.2 Possible Guides for Tin Exploration

1. Ilmenite series granitoids appear associated with tin deposits (Ishihara, 1981) and those containing biotite or biotite-muscovite may have contained sufficient water to evolve a separate aqueous phase of adequate volume to carry ore metals. The characteristics used to recognize such

Intrusions are (Ishihara, 1981):

- magnetic susceptibility below 1×10^{-4} emu/g
- low bulk $\text{Fe}_2\text{O}_3/\text{FeO}$ ratio
- magnetite and ilmenite content < 1 vol. %
- contains accessory pyrrhotite (look for limonite staining on weathered surfaces)

Possibly look for these intrusions in carbonaceous sediments, which were supposedly assimilated to produce such melts.

2. The Wedgeport pluton and granitic bodies associated with known mineralization (e.g. East Kemptville deposit in the Davis Lake pluton; New Ross-Vaughan Complex in the South Mountain batholith) contain high total radioactivity and high thorium values (Chatterjee and Muecke, 1982). Airborne gamma ray spectrometric measurements may serve to locate potential ore-bearing intrusions (Yeates et al., 1982).

3. Mineralization within the study area is structurally controlled - in fracture systems and replacement layers within a fold hinge. Such axial structures may therefore be of interest in the location of this type of mineralization. Tin mineralization at the East Kemptville deposit is controlled along an irregularly-shaped contact ('inflection contact') of the Davis Lake pluton with the Goldenville metasediments (Richardson et al., 1982). In European and some Tasmanian deposits, mineralization is found in apical zones ('cupolas') of an intrusion, in contact with impermeable

country rock. Therefore, it would be of benefit to investigate any granite-country rock contacts.

4. Some of the tin mineralization occurs in sulphide-cassiterite replacement bodies of calcareous metasediments. It may be of interest to look for such beds adjacent relevant plutons in structurally prepared ground(e.g. fold hinges, intrusive contacts).

5. Pyrrhotite is the major sulphide in veins and replacement layers. It gives a good magnetic and electrical response and could be of use in geophysical exploration. Unfortunately, this mineral also occurs in tin-barren graphitic layers.

6. If mineralized veins and replacement layers have been found, it is possible to use the mineralogical and geochemical zonation of the vein systems to locate the tin-bearing sections.

6.3 Recommendations for Further Work

Much of the work accomplished within this thesis has been of a qualitative nature. A more quantitative investigation of the mineralization in this area would serve to define the parameters of ore genesis more rigorously. These include:

1. Fluid inclusion studies of the different vein stages

to obtain estimates of gross salinities and filling temperatures; possibly use the latest techniques (lasar?) to obtain fluid chemistry.

2. Age dating of unaltered and mineralized samples of the pluton to obtain better estimates of time of emplacement and time of mineralization. Studies of various mineralized plutons (Reynolds and Zentilli, in prep.) point to a Hercynian mineralizing event, which may have implications in future mineral exploration. Possibly dating of the lead in galena-bearing veins would further tighten age of mineralization.

3. A search for coexisting sulphide minerals in vein and replacement bodies to obtain estimates of temperatures of equilibrium.

4. A study of sulphur isotopes in veins and in mineralized and unmineralized layers; are there any differences?

5. A study of the tin concentrations in the ferromagnesian minerals of the pluton. Are there appreciable amounts in these minerals, as is indicated in other plutons (e.g. Nigerian Younger Granite, Erzgebirge plutons)? The microprobe can only analyse for elements in concentrations as low as 500 ppm, which is too high for tin in such minerals (more in the 10's ppm range).

6. A study of the reactions between ore-bearing fluids and wallrocks to get a better understanding of mass exchange.

7. A study of the 'rusty shears' within the pluton. They apparently contain radioactive minerals (Cullen pers. comm.,1982) and are the probable cause of the high values obtained in airborne gamma ray spectrometric measurements (Chatterjee and Muecke,1982). They are therefore an integral part of the evolution of mineralization in the study area.

APPENDIX I
SAMPLE PREPARATION

1. Remove surface drill marks and weathering effects by drill-mounted garnet paper. Blow away ensuing dust. Drill core should be of a lighter hue, with a clean smooth surface.
2. Split core into approximately 1 cm cubes. Discard any pieces with saw marks or marker labels. Clean the splitter with brush and air hose.
3. Reduce the sample further into mm-sized pieces by a ceramic jaw crusher. Preclean crusher with a portion of the sample and discard the crushed result. After crushing clean with nylon brush and air hose.
- 4a. Grind crushed sample in a ceramic shatterbox. Preclean sample holder with an aliquot (about 10 ml) of the sample. Run the machine for about 1 minute. Discard the powder and blow out holder with the air hose.
- 4b. Place a larger aliquot (about 30 ml) of the sample in the holder and run for about 8 minutes. Check resul-

tant powder - if small granules are evident (i.e. > 0.5 mm), sample must be ground a further 5 minutes. If in doubt, sieve a portion of powder to check its size. For ease of acid digestion, sample powders were -200 mesh.

4c. Transfer powder onto a clean folded sheet of paper.

Pour powder from sheet into a labelled 40 ml polyethylene vial.

4d. Clean holder after use by these steps:

- i. Air blow holder.
- ii. Run an aliquot (about 10 ml) of silica gel for about 1 minute and discard powder. Air blow again.
- iii. Wash out shatter box - 5 rinses with tap water
 - 1 rinse with distilled water
 - 1 rinse with alcohol
- iv. Air blow dry inside and outside of holder. The steel rim will rust if left damp and can cause sample contamination.

Sources of Contamination:

1. Dust is a major problem during sample preparation and may result in appreciable contamination. Rigorous

cleaning between each stage may decrease this effect.

2. Remnant marker, drill and saw marks; remnant powder and chipped material from splitter jaws, jaw crusher and shatter box.
3. Excessive grinding may oxidize ferrous iron, producing decreased FeO contents (Jeffery and Hutchison, 1981).

APPENDIX II

ANALYTICAL METHODS

Powders of 122 samples were analysed for 13 trace elements by various methods (Table II.1) by X-Ray Assay Laboratories Limited in Toronto, Ontario. Of these, 13 were duplicate samples and 6 were reference samples. Powders of 30 additional samples were sent for whole rock analyses by XRF, and of these, 3 were duplicates and 2 were reference samples.

The following outlines the analytical methods used by the laboratory (J.H. Opdebeeck, X-Ray Assay Laboratories, written communication, 1982).

Tin Determination by Emission Spectroscopy(EMS)

Low concentrations of tin are determined using a 0.1g sample, mixed with graphite and burned in a direct current arc. The spectrum is photographically recorded and interpreted using a densitometer. For small samples with greater than 50 ppm tin, 0.1g of sample is fused with 0.7g of lithium metaborate (LiBO_2) in a graphite crucible, and the melt is dissolved in 5% HNO_3 . The solution is run on a direct-current plasma emission spectrometer. Calibration in both setups is done on synthetic standards. Larger samples with values above 50 ppm are determined by x-ray fluorescence

Table 11-1 Elements Analysed, Methods and Detection Limits

Element	Method*	Detection Limit (ppm except where noted)
Su (ppm)	EMS	3.000
Su (%)	XRF	0.010%
W	NA	1.000
Mo	DCP	0.500
As	NA	1.000
Cu (ppm)	DCP	0.500
Cu (%)	XRF	0.010%
Pb (ppm)	DCP	2.000
Pb (%)	XRF	0.010%
Zn (ppm)	DCP	0.500
Zn (%)	XRF	0.010
Sb	NA	0.200
Bi	FAA	0.100
Li	AA	1.000
F	SIE	100.000
B	DCP	10.000
Cl	XRF	50.000
FeO (%)	Wet Chemical	0.100%
WRG-Major Oxides (%)	XRF	0.010%
WRG-Minor Elements (Cr,Rb,Sr,Zr)	XRF	10.000

*EMS - Emission Spectroscopy

XRF - Wavelength Dispersive X-ray Fluorescence Spectrometry

NA - Neutron Activation

DCP - Direct-Current Plasma Emission Spectrometry

FAA - Flameless Atomic Absorption Spectrometry

AA - Atomic Absorption Spectrometry

SIE - Selective Ion Electrode.

spectrometry using a Philips PW 1410 sequential x-ray fluorescence spectrometer interfaced to a Digital PDP 11/40 computer.

Tungsten, Arsenic and Antimony Determination by Neutron Activation(NA)

Powders are irradiated in a high density neutron flux, producing isotopes of elements contained in the sample. A multi-channel gamma spectrometer determines element concentrations.

Molybdenum, Copper, Lead and Zinc Determination by Direct-Current Plasma Emission Spectrometry(DCP)

Samples are prepared by the acid soluble procedure. Sample powders (0.25g) are digested with 2 ml of HNO₃ for 1/2 hour in a water bath, then 1 ml of HCl is added and digestion continues a further 2 1/2 hours; test tubes are agitated at regular intervals. Samples are made up to volume with a lithium buffer. A high temperature argon plasma is used to excite the elements in solution and the spectrum is analysed by a direct-current Spectrametrics plasma emission spectrometer using an echelle grating interfaced to a microprocessor. Higher values (in the percent range) are analysed by the XRF method.

Bismuth Determination by Flameless Atomic Absorption Spectrometry

Samples are prepared by the acid soluble procedure and solutions are run on an atomic absorption spectrometer where the flame has been replaced by a heated quartz tube. Bismuth hydride is formed using sodium borohydride and is emplaced within the furnace containing the quartz tube.

Lithium Determination by Atomic Absorption Spectrometry

Sample powders are digested by HF and H₂SO₄ (total metal digestion method) followed by HCl to redissolve any residue. Solutions are run through the atomic absorption spectrometer.

Fluorine Determination by Selective Ion Electrode

Sample powders (0.25g) are fused with NaOH in a nickel crucible for 15 minutes at 650°C. The resultant solid is dissolved in an ammonium citrate buffer solution. A fluoride-selective ion electrode determines the fluoride concentration in solution. The electrodes are used in association with reference electrodes and the reference samples are run with every batch.

Boron Determination by Direct-Current Plasma Emission Spectrometry

Sample powders (0.05g) are fused with KOH in a nickel crucible and the resultant solid is dissolved in 5% HCl. The solution is run on a direct-current emission spectrometer.

Chlorine Determination by X-Ray Fluorescence Spectrometry

Sample powders (4g) are mixed with 4 g of sand and 2 binder pellets and are pressed into pellets. The analysis is performed on a sequential x-ray fluorescence spectrometer. Peak and background readings are taken using a germanium crystal.

Whole rock major and minor element determinations are performed by x-ray fluorescence spectrometry; FeO, by wet chemical methods.

The analyses are calibrated on synthetic standards and reference samples; in house standards and previously analysed samples are run as controls of the digestion procedures.

Rock Coding for Lithochemistry

Explanation

Major rock classification; in this case, a metasediment } 111 } Average grain size; in this case, medium silt-sized
 Type of metasediment; in this case, a graphitic argillite

I METASEDIMENTARY ROCKS 100 SERIES

(a) Type	(b) Size
<u>10</u> Argillite	<u>1_0</u> Fine Silt (0.004-0.0156 mm)
<u>11</u> Graphitic Argillite	<u>1_1</u> Medium Silt (0.0156-0.0312 mm)
<u>12</u> Calcareous Argillite	<u>1_2</u> Coarse Silt (0.0312-0.0625 mm)
<u>13</u> Siltstone	<u>1_3</u> Fine Sand (0.0625-0.25 mm)
<u>14</u> Biotite Argillite	<u>1_4</u> Medium Sand (0.25-0.5 mm)
<u>15</u> Wacke	<u>1_5</u> Coarse Sand (0.5-2.0 mm)
<u>16</u> Feldspathic Wacke	
<u>17</u> Calcareous Wackes (±Feldspar)	
<u>18</u> Biotite Feldspathic Wacke	
<u>19</u> Biotite Wacke	

II VARIATIONS IN METASEDIMENTARY ROCKS

<u>3</u> Sulphide Vein Zone	} Type and size variations as above
<u>4</u> Sulphide Disseminated Zone	

III MONZOGCRANITE 500 SERIES

(a) Type	(b) Size (if porphyritic, 'size' indicates phenocryst size)
<u>50</u> Nonporphyritic	<u>5_0</u> Fine (<1 mm)
<u>51</u> Slightly Porphyritic (<5 modal % phenocrysts)	<u>5_1</u> Medium (1-5 mm)
<u>52</u> Porphyritic (>5, <75 modal % phenocrysts)	<u>5_2</u> Coarse (>5 mm)

IV ALTERED MONZOGCRANITE 600-900 SERIES

<u>6</u> Tan Alteration	} Type and size variations as above
<u>7</u> Greisen Alteration	
<u>8</u> Kaolinite Alteration	
<u>9</u> Sheared Monzogranite	
<u>900</u> Mafic Dyke	

Table 11-2 Trace Element Contents of Selected Drill Core Samples (Metasediments)

DDH	78-32	78-29	78-29	78-44	78-44	78-44	78-40	78-40	77-29	77-29	78-38	78-38	78-38
Depth (m)	19.8	57.72	80.3	29.10	59.94	100.0	83.6	132.	68.30	99.50	30.18	68.5	129.22
Rock Type*	100	164	164	163	164	164	102	352	184	184	164	164	164
Values in ppm except where noted													
Sn	3	50	60	3	12	3	3	60	5	7	20	50	20
W	3	5	6	2	5	5	9	6	6	3	3	3	1
Mo	<0.5	<0.5	<0.5	<0.5	<0.5	<0.5	<0.5	8.0	<0.5	2.0	<0.5	1.0	3.0
As	13	12	50	13	17	8	39	7100	19	12	10	23	19
Cu	29.0	31.0	9.0	84.0	7.5	44.0	23.0	310	33.0	5.0	15.0	2.5	1.0
Pb	6	40	170	<2	4	4	4	1.44%	10	4	6	16	8
Zn	110.	270.	230.	97.0	70.0	98.0	79.0	0.90%	86.0	80.0	57.0	61.0	55.0
Sb	7.9	0.7	0.6	0.6	0.2	0.6	1.5	280	0.4	0.3	0.2	0.2	0.5
Bi	0.9	1.0	9.1	0.4	0.2	0.2	0.2	1.5	0.2	0.1	0.7	1.3	0.7
Li	60	42	100	51	48	63	38	<1	65	54	27	36	60
F	470	460	720	480	400	480	420	190	320	300	360	500	540
B	50	25	25	25	10	50	75	<10	50	50	50	50	75
Cl	50	100	50	50	<50	<50	<50	<50	50	<50	<50	<50	<50

* Table of definitions on previous page.

Table 11-2 (Cont'd) Trace Element Contents of Selected Drill Core Samples (Metasediments)

DDI	78-34	78-34	78-34	78-10	77-34	77-34	78-03	78-03	77-25	77-25	77-25	77-25	77-25
Depth (m)	72.16	75.61	109.24	93.5	48.30	154.90	44.18	132.0	53.88	132.10	135.58	186.25	186.35
Rock Type ^a	354	364	364	110	110	422	100	164	455	301	163	412	173
Sn	200	160	0.33%	30	15	0.31%	80	60	380	1.23%	200	1.07%	200
W	550	<25	12	16	6	10	6	1	16	34	5	9	4
Mo	1.0	<0.5	1.0	<0.5	<0.5	2.5	<0.5	<0.5	<0.5	<0.5	1.5	<0.5	0.5
As	90000	15000	160	7500	2600	130	220	10	17	86	8	9	6
Cu	1000	89.0	400	48.0	24.0	400	41.0	140	160	860.	<0.5	95.0	140.
Pb	4090	1000	26	22	<2	26	8	<2	60	26	16	<2	4
Zn	1300.	440.	91.0	260.	120.	89.0	120.	120.	0.96%	1500.	220.	680.	480.
Sb	200.	29.0	1.1	16.0	5.8	0.6	0.7	0.7	0.4	0.6	0.3	0.6	0.2
Bi	220	72.0	16.0	1.3	0.9	13.0	0.6	0.2	0.6	6.2	1.1	9.7	1.5
Li	43	83.0	35	89	60	46	56	34	70	72	47	46	38
F	1200	1500	530	630	650	660	630	410	650	450	690	500	420
B	25	30	10	25	100	10	50	50	<10	<10	75	<10	10
Cl	<50	<50	<50	<50	<50	<50	<50	<50	50	150	50	50	<50

Table 11-2(Cont'd) Trace Element Contents of Selected Drill Core Samples (Metasediments)

DDH	78-11	78-11	78-11	78-11	78-11	78-11	78-12	78-12	78-12	78-12	78-12	78-12	78-12
Depth (m)	19.3	58.6	77.45	85.45	85.45	123.6	70.25	118	118	130.27	163.3	166.3	183.67
Rock Type*	164	163	432	432	132	452	423	422	153	453	423	164	164
Sn	50	200	0.74%	0.73%	160	0.52%	250	0.33%	160	0.76%	1.39%	40	100
W	10	19	21	19	13	15	4	14	11	25	19	11	7
Mo	<0.5	<0.5	<0.5	<0.5	<0.5	1.5	<0.5	1.0	0.5	<0.5	4.0	2.0	<0.5
As	34	6	66	14	7	36	9	7	25	6	14	6	7
Cu	<0.5	55	510	2000.	<0.5	670	670	430	<0.5	1000	260	41.0	140
Pb	6	<2	34	6	4	70	<2	22	4	18	18	8	2
Zn	170.	100.	98.	150.	85.0	93.0	14.6%	100.	100.	110.	54.0	90.0	77.0
Sb	0.6	0.9	1.6	1.6	0.3	0.6	0.3	0.6	<0.2	0.6	1.1	0.2	0.5
Bi	0.2	2.1	16.0	11.0	1.2	10.0	26.0	56	1.8	20.0	15.0	1.0	1.0
Li	40	46	45	63	31	27	8	40	39	30	18	53	42
F	440	540	460	740	450	490	190	560	570	550	430	610	680
B	25	25	10	<10	25	10	10	10	50	10	10	50	100
Cl	<50	<50	50	<50	<50	<50	<50	50	50	<50	50	<50	<50

Table II-2 (cont'd) Trace Element Contents of Selected Drill Core Samples (Metasediments)

Depth (m)	78-13	78-13	77-12	77-12	77-06	77-06	77-06	77-04	77-04	77-07	77-07	77-07
Rock Type*	472	172	900	311	183	422	184	311	184	184	394	183
Sn	0.38%	160	15	0.45%	60	0.68%	80	500	25	50	0.15%	12
W	20	17	7	6	<1	64	1	<25	3	5	21	2
Mo	1.5	<0.5	2.0	4.0	<0.5	<0.5	<0.5	<0.5	<0.5	<0.5	1.0	<0.5
As	12	28	8	40	59	100	49	28000.	26	74	220	190
Cu	150.	<0.5	40.0	940.	27.0	1100.	16.0	23.0	38.0	15.0	410.	25.0
Pb	10	6	4	22	16	430	6	430.	4	<2	8	2
Zn	170.	150.	95.0	220.	240.	200.	150.	180.	150.	89.0	120.	91.0
Sb	0.4	0.3	0.2	2.5	0.6	0.6	0.3	120.	<0.2	0.9	0.7	1.0
Bi	30.0	4.0	0.2	32.0	0.1	27.0	0.3	0.3	0.5	0.5	0.9	4.2
Li	41	38	30	65	41	40	35	75	60	37	29	51
F	240	680	1100	280	340	540	340	670	410	340	350	680
B	10	25	10	25	25	<10	50	10	25	25	50	100
Cl	<50	<50	50	<50	<50	100	<50	<50	50	50	<50	<50

Table II-2(Cont'd) Trace Element Contents of Selected Drill Core Samples (Metasediments)

DEH	77-05	77-05	77-08	77-08	77-08	77-08	77-08	77-01	77-01	78-24	78-24
Depth (m)	71.93	74.5	7.6	31.34	36.37	117.5	136.7	80.1	173.35	44.75	91.8
Rock Type*	183	433	422	403	183	Qtz vein	183	163	163	102	100
Sn	40	160	0.5%	300	120	3	120	20	17	3	3
W	1	250	20	8	<1	2	<1	70	2	3	3
Mo	<0.5	<0.5	<0.5	<0.5	<0.5	1.5	<0.5	<0.5	<0.5	<0.5	1.5
As	21	4200	7	5500	7	12	23	120	4	13	16
Cu	43.0	1000.	1100.	1000.	14.0	1.5	36.0	38.0	77.0	39.0	60.0
Pb	4	<2	24	460	70	14	16	<2	<2	4	100
Zn	68.0	110.	300	140.	180.	25.0	67.0	97.0	100.	110.	130.
Sb	0.6	7.8	0.6	12.0	0.4	0.3	0.7	0.4	0.2	0.7	0.9
Bi	8.2	52.0	9.1	15.0	9.0	3.4	1.0	0.3	8.2	0.4	0.7
Li	38	34	59	24	29	2	34	88	99	31	48
F	280	620	360	200	290	130	280	1000	700	320	420
B	50	<10	<10	10	25	50	25	75	50	50	25
Cl	<50	<50	50	<50	<50	200	<50	<50	<50	50	<50

Table 1F-2(Cont'd) Trace Element Contents of Selected Drill Core Samples (Metasediments) -

DDH	78-20	78-20	78-20	77-31	77-31	77-31	77-31	77-31	77-31
Depth (m)	53.88	86.67	104.68	55.61	55.61	59.90	60.16	78.94	115.79
Rock Type*	110	110	194	900	110	900	110	112	141
Sn	5	10	5	3	7	3	3	3	3
W	4	3	<1	4	2	3	6	11	5
Mo	<0.5	<0.5	<0.5	4.5	0.5	3.5	55.0	23.0	<0.5
As	8	8	21	4	9	12	3	4	10
Cu	34.0	44.0	39.0	62.0	270.	64.0	8.5	45.0	21.0
Pb	<2	6	<2	2	4	46	<2	6	6
Zn	43.0	68.0	57.0	88.0	42.0	190.	32.0	45.0	120.
Sb	0.3	0.2	0.2	0.7	0.3	0.3	0.2	0.4	0.8
Bi	1.0	0.3	0.1	0.2	0.1	5.4	0.1	0.3	0.7
Li	52	61	41	32	13	51	32	50	70
F	350	550	440	820	230	820	260	370	360
B	100	150	25	10	10	10	50	75	50
Cl	<50	<50	<50	100	<50	50	<50	<50	50

Table 11-2(Cont'd) Trace Element Contents of Selected Drill Core Samples (Contact and Endopluton)

DDH	79-05	79-05	79-05	79-05	79-05	79-05	79-05	80-01	80-01	80-01	80-01	80-01	80-01	80-01
Depth (m)	15.07	51.60	53.48	54.0	63.08	63.08	81.54	24.3	37.2	47.68	51.25	52.0	76.0	85.85
Rock Type*	183	183	154	511	611	700	521	110	433	193	194	920	522	521
Sn	40	15	15	15	25	460	10	5	50	7	80	50	35	20
W	<1	9	19	8	15	24	34	23	430	3	16	21	29	5400
Mo	<0.5	4.5	17.0	3.0	5.0	6.5	10.0	65.0	2.5	1.5	<0.5	280.	5.0	10.0
As	16	13	17	3	7	4	6	42	9	71	9	14	11.0	2
Cu	18.0	7.0	6.5	2.0	13.0	220.	4.0	190	340	11.0	80.0	20.0	4.5	17.0
Pb	<2	<2	6	10	10	6	16.	6	<2	82	<2	8	6	30
Zn	170.	97.0	110.	21.0	18.0	11.0	38.0	41.0	47.0	220.	250.	14.0	21.0	30.0
Sb	0.4	0.3	0.2	<0.2	0.2	0.3	0.3	0.8	3.7	0.9	0.3	0.5	0.5	1.3
Bi	2.6	0.5	6.8	4.4	<0.1	0.9	1.4	1.4	88.0	4.3	0.7	16.0	20.0	210.
Li	160	150	120	28	59	150	76	130	76.	190	170	46	41	50
F	2400	2500	2300	520	1000	5400	1200	820	1500	2000	2200	500	620	830
B	10	10	10	25	25	50	50	50	25	25	25	25	25	50
Cl	<50	<50	<50	<50	<50	<50	<50	<50	<50	50	<50	<50	<50	<50

Table 11-2(Cont'd) Trace Element Contents of Selected Drill Core Samples (Endopluton)

DB#	79-06	79-06	79-06	79-06	79-07	79-07	79-08	79-08	79-08	79-08	78-27	78-27	78-27	
Depth (m)	10.45	48.24	52.0	85.33	70.66	70.66	36.22	55.62	72.93	72.93	68.19	68.37	73.55	
Rock Type*	521	509	700	511	511	711	511	800	521	721	501	501	511	
Sn	25	30	760	7	10	360	12	80	25	200	7	7	30	15.4
W	170	390	38	300	24	23	11	14	18	190	14	10	20	17.4 (787)
Mo	3.5	19.0	14.0	63.0	5.5	130.	10.0	2.0	6.5	120.	12.0	2.0	3.0	
As	3	1500	3	4	3	30.	3	370	20	7400.	1600	1100	18	
Cu	<0.5	12.0	23.0	1.5	10.0	430.	3.5	46.0	4.0	0.60%	7.0	5.0	12.0	
Pb	12	8	8	6	16	8	10	10	4	14	8	8	6	
Zn	54.0	35.0	13.0	16.0	30.0	2900.	31.0	49.0	21.0	140.	25.0	35.0	39.0	31
Sb	0.2	3.8	0.5	<0.2	0.3	0.4	0.3	0.9	0.4	14.0	3.7	2.2	0.2	
Bi	8.7	22.0	0.2	11.0	16.0	12.0	5.0	19.0	4.0	210	24.0	190.	14.0	
Li	74	57	330.	26	37	55	40	93	57	120	56	47	53	49
F	960	1100	2.80%	610	1300	2500	900	850	860	8100	440	840	960	880
B	25	25	25	50	25	50	25	25	25	25	25	25	25	
Cl	<50	50	<50	<50	<50	<50	<50	<50	<50	<50	50	100	<50	

230

Table 11-2 (Cont'd) Trace Element Contents of Selected Drill Core Samples (Endopluton)

Depth	78-33	78-33	78-33	78-31	78-31
Depth	13.73	46.6	73.33	9.4	71.75
Rock Type*	501	501	511	501	501
Sn	5	3	3	10	7
W	9	4	1	<1	4
Mo	0.5	<0.5	0.5	1.0	<0.5
As	15	20	7	3	1
Cu	5.5	<0.5	1.5	<0.5	<0.5
Pb	6	10	10	10	10
Zn	21.0	21.0	29.0	40.0	25.0
Sb	0.4	0.6	0.2	0.5	0.3
Bi	0.7	0.3	0.3	0.3	0.2
Li	30	49	48	97	92
F	270	310	230	620	500
B	25	25	25	25	25
Cl	<50	<50	<50	<50	<50

Table II-3 Whole Rock Geochemistry (Meta-argillites)

DDH	77-25	77-34	78-24	77-31	77-31	78-10	77-31	78-20
Depth (m)	132.10	48.30	92.	78.94	115.79	93.5	60.16	53.88
Rock Type	301	110	100	112	141	110	110	110
Values in wt.%								
SiO ₂	31.8	55.8	57.5	52.3	60.4	46.5	66.6	61.9
TiO ₂	0.76	1.02	0.95	1.22	0.83	1.21	0.68	1.00
Al ₂ O ₃	14.3	19.4	18.0	19.6	17.1	23.4	16.4	15.7
Fe ₂ O ₃ *	3.2	2.04	1.64	2.07	1.71	3.4	0.88	1.84
FeO	31.8	7.5	6.8	5.5	5.9	7.2	1.1	5.5
MnO	0.42	0.17	0.14	0.06	0.14	0.24	0.02	0.12
MgO	3.98	3.88	3.14	2.42	3.33	4.31	1.18	2.92
CaO	0.19	0.52	2.88	0.42	2.19	1.08	0.39	3.17
Na ₂ O	0.26	1.63	2.28	2.22	2.37	1.56	2.85	3.46
K ₂ O	0.20	3.49	2.90	4.51	3.26	4.79	3.57	1.83
P ₂ O ₅	0.09	0.14	0.14	0.18	0.13	0.18	0.11	0.15
L.O.I.	7.08	4.16	4.23	10.00	2.54	5.62	6.77	1.62
TOTAL	94.08	99.75	100.60	100.5	99.90	99.49	100.55	99.21
Trace Elements (in ppm)								
Rb	0	140	110	140	120	170	120	120
Sr	0	90	200	130	240	100	150	280
Cr	130	130	140	160	100	170	100	120
Zr	110	180	140	260	170	220	210	230

*Fe₂O₃ = Fe₂O₃ (total) - FeO

Table II-3 (Cont'd) Whole Rock Geochemistry (Meta-wackes)

DDH	78-29	77-25	77-06	77-04	78-20	79-05
Depth (m)	80.3	135.08	74.70	105.9	104.68	51.60
Rock Type	164	163	183	184	194	183
SiO ₂	42.6	65.3	66.4	46.9	66.7	69.3
TiO ₂	1.21	0.78	0.85	1.54	0.86	0.71
Al ₂ O ₃	23.0	13.6	14.3	21.5	13.9	13.6
Fe ₂ O ₃ *	2.6	1.61	1.40	4.73	0.92	1.24
FeO	9.5	6.6	5.0	4.9	4.9	3.8
MnO	0.22	0.19	0.11	0.20	0.14	0.09
MgO	5.93	2.28	2.36	2.91	2.40	2.00
CaO	2.54	1.83	1.68	2.79	3.56	2.19
Na ₂ O	1.96	2.85	4.16	2.11	3.26	4.49
K ₂ O	4.08	1.36	2.04	5.43	1.03	2.03
P ₂ O ₅	0.19	0.13	0.14	0.22	0.13	0.13
L.O.I.	5.47	2.70	1.39	5.31	1.16	0.85
TOTAL	99.3	99.23	99.83	98.54	98.96	100.5
Trace Elements (in ppm)						
Rb	220	110	140	220	50	220
Sr	110	150	250	240	310	290
Cr	180	120	110	180	110	100
Zr	190	140	170	210	140	110

Table 11-3 (Cont'd) Whole Rock Geochemistry (Monzogranites)

DDH	79-06	79-07	78-27	78-33	78-31	79-05	80-01	79-08
Depth (m)	85.30	70.66	78.55	46.6	72.0	81.45	85.85	72.93
Rock Type	511	511	511	501	501	521	521	521
SiO ₂	76.60	76.70	75.40	76.70	75.00	74.60	78.20	74.80
TiO ₂	0.14	0.12	0.20	0.09	0.20	0.22	0.17	0.23
Al ₂ O ₃	12.60	12.30	12.40	12.80	13.40	13.20	10.7	12.9
Fe ₂ O ₃ *	0.60	0.54	0.95	0.38	0.75	0.76	0.83	0.84
FeO	0.8	0.8	1.0	0.8	0.9	1.3	0.9	1.3
MnO	0.02	0.02	0.04	0.03	0.03	0.03	0.04	0.03
MgO	0.11	0.09	0.36	0.14	0.29	0.23	0.16	0.27
CaO	0.64	0.67	0.93	0.52	1.21	0.93	0.89	0.90
Na ₂ O	3.92	3.49	3.73	4.16	4.28	3.60	2.86	3.59
K ₂ O	4.60	4.98	5.07	4.51	4.51	4.99	4.54	4.69
P ₂ O ₅	0.04	0.03	0.06	0.03	0.07	0.09	0.05	0.07
L.O.I.	0.77	0.93	0.70	0.62	0.23	0.77	1.00	1.23
TOTAL	100.84	100.67	100.84	100.78	100.87	100.72	100.34	100.85

Trace Elements
(in ppm)

Rb	300	370	330	320	220	360	270	300
Sr	20	0	110	0	60	70	10	80
Cr	40	30	30	40	50	30	40	40
Zr	150	120	160	90	130	160	120	160

CIPW Norms

Quartz	34.37	35.54	31.97	33.45	29.79	31.82	42.35	33.32
Orthoclase	27.19	29.53	29.95	26.63	26.51	29.53	27.03	27.85
Albite	33.14	29.60	31.51	35.14	35.98	30.47	24.36	30.49
Anorthite	2.91	3.14	2.10	2.38	4.00	4.03	2.96	4.02
Diopside	0.00	0.00	1.74	0.00	1.25	0.00	0.98	0.00
Hypersthene	1.05	1.09	0.83	1.41	0.85	2.03	0.67	2.05
Magnetite	0.87	0.78	1.38	0.55	1.08	1.10	1.21	1.22
Hematite	0.00	0.00	0.00	0.00	0.00	0.00	0.00	0.00
Ilmenite	0.27	0.23	0.38	0.17	0.38	0.42	0.33	0.44
Apatite	0.09	0.07	0.14	0.07	0.16	0.21	0.12	0.16
Corundum	0.10	0.02	0.00	0.20	0.00	0.40	0.00	0.45

Table 11-3 (Cont'd) Whole Rock Geochemistry (Greisens)

DDH	79-05	79-06	79-07	Biot. porphyritic gte from Pine Hill - Renison Bell area, Tasmania (Patterson et al, 1981) (avg. 6 analyses)
Depth (m)	63.08	52.0	70.66	
Rock Type	700	700	711	
SiO ₂	76.10	49.60	75.30	73.04
TiO ₂	0.14	0.13	0.13	0.36
Al ₂ O ₃	12.0	27.5	11.9	13.34
Fe ₂ O ₃ *	2.58	2.42	2.05	} 2.14 Total iron as FeO
FeO	1.0	2.0	2.4	
MnO	0.03	0.06	0.04	0.08
MgO	0.16	0.26	0.16	0.66
CaO	1.20	3.85	0.37	1.98
Na ₂ O	0.38	0.42	0.67	2.76
K ₂ O	4.88	9.59	4.51	5.23
P ₂ O ₅	0.05	0.07	0.04	0.11
L.O.I.	2.08	4.54	2.62	1.05
TOTAL	100.6	100.44	100.19	100.75
Trace Elements (in ppm)				
Rb	630	1410	650	
Sr	0	0	0	
Cr	40	30	40	
Zr	120	110	140	
CIPW Norms				
Quartz	53.31	1.31	53.33	30.79
Orthoclase	29.30	59.15	27.34	30.88
Albite	3.26	3.71	5.81	23.91
Anorthite	5.71	19.44	1.61	7.80
Diopside	0.00	0.00	0.00	0.82
Hypersthene	0.40	2.31	3.05	4.57
Magnetite	2.96	3.66	3.05	
Hematite	0.58	0.00	0.00	
Ilmenite	0.27	0.26	0.25	0.68
Apatite	0.12	0.17	0.10	0.26
Corundum	4.09	10.00	5.47	0.00

APPENDIX III

GEOCHEMICAL REFERENCE MATERIALS AND

DETERMINATION OF ANALYTICAL ACCURACY AND PRECISION

In an attempt to assess the accuracy of the analytical results a set of 5 samples of known trace element content and a set of 2 samples of known major oxide content were randomly placed in the sample batch (Tables III-1 and III-2).

Problems exist with such reference materials in that a wide range in values exists in the analyses among laboratories. Because of this uncertainty the values obtained by such laboratories are termed 'usable' or 'recommended', meaning they may be used with caution and not as exact concentrations. Most of the variability in the analyses appears to stem from inter-laboratory bias and a set of guidelines is used to determine the 'usefulness' of a laboratory's results (Abbey,1980).

The reference samples used for trace element analysis include:

1. Silica gel - this was essentially used as a 'blank' sample on the premise that it contained insignificant trace element concentrations and this is shown

in the results. Actual trace element contents are not known.

2. GSE - one of a series of 4 artificial glass reference standards containing 46 trace elements and made by Corning Glass Works. This sample contains the 46 elements at concentration levels of about 500 ppm each. The 'accepted values' are defined as the medians of the analyses by different laboratories (Meyers et al.,1976). Because analyses for Mo, Cu, Pb, Zn and Bi involve acid digestion, these elements were not totally liberated in the digestion process and therefore give low values. These were not used in accuracy calculations.

3. NIM-L - one of a set of 6 igneous rocks from South Africa, this sample is a lujavrite (a coarse-grained nepheline syenite) from the Pilanesberg Alkaline Complex. The means and medians of the sets of results are used in the published values (Abbey, 1980; Steele et al.,1978). This sample was submitted in duplicate to assess the precision of the analysis.

4. SY-2 - a syenite sample from the Canadian Certified Reference Materials Project (Abbey,1980).

5. TLG-1 - a scheelite ore sample that is useful only for the analysis for tungsten.

Two reference samples used for the whole rock geochemical analysis are:

1. NIM-G - a granite from the Bushveld Complex in the Transvaal, South Africa (Abbey,1980; Meyers et al.,1978).

2. QMC-M2 - a pelite from the Queen Mary College, United Kingdom (Abbey,1980).

The accuracy of an analysis is a measure of the 'correctness' of a result or how close the observed result is to the 'true' or recommended result. Put another way, it reflects the absolute error of a measurement and is the difference between the measured value and the true value of the element being analysed, where

$$\text{Accuracy} = [1 - |(X-T)/T|] * 100\% \quad \text{where } X = \text{observed value} \\ T = \text{'true' value}$$

In this study, accuracy was determined graphically by obtaining the vertical difference between the sample value furthest from the ideal value (slope = 1); these graphs are shown in Figures III-1 and III-2. Results are plotted on log-log graph paper, where results of analyses are plotted

against the recommended or 'usable' values documented in various publications (e.g. Abbey, 1980). A 45° line is drawn - if the analyses were carried out satisfactorily, the points should lie on or very near this line (analysed values = recommended values). Minor deviations may be expected due to procedural errors. Limits of ± 10% (and in some graphs, ± 25%) are marked off on the graph parallel the 45° line.

Of the 13 trace elements analysed, 2 were not plotted: chlorine, because all values were below the detection limit of 50 ppm, and bismuth, because no reliable 'usable' values could be obtained from the literature for the above samples. Of the remaining 11 elements, analytical control ranged from acceptable to poor (e.g. Mo accuracy for 3 samples ranged from +117% to +183%).

Analytical control of whole rock analyses of the 2 samples fares much better, as most are within ± 10%. The graphs do not include those samples which have no known element content. 'Known' values include those with question marks, which are considered by the originating laboratories to be inadequate to recommend as usable values; however, because of the low number of samples, they were included for comparison purposes.

The precision (reproducibility) of the analyses was checked by sending duplicate samples for both trace element and major oxide analyses (Tables III-2 and III-3). Duplicate

sample values for each element and oxide are plotted (Figs. III-3 and III-4) and precisions are determined graphically as well. Precision of trace element and whole rock analysis ranged from fair to excellent. Poor analytical results may be due to inadequate homogenization of sample powder prior to analysis (causing fluctuating results), inadequate analytical technique, or low element concentration within the samples.

Table III-1 Trace Element Reference Standard Analyses*

Sample	Silica Gel "Blank"	GSE	Recommended Value	SY-2	Recommended Value	NIM-L	Duplicate	Recommended Value	TLG-1 for W only	Recommended Value
Values in ppm.										
Sn	<3	300	440	5	4	3	3	77	20	-
W	3	510	420	1	-	8	9	<20??	890	830
Mo	<0.5	12.0	500	6.5	3?	7.0	8.5	3?	54.0	-
As	6	490	450	19	18	4	3	<15??	25	-
Cu	<0.5	16.0	500	2.0	5	10.0	11.0	13	330.	-
Pb	<2	16	500	92	80	56	62	43	100	-
Zn	1.0	15.0	500	110	250	360	350	400	140.	-
Sb	0.3	490	470	0.5	0.2	0.3	0.3	0.3?	3.7	-
Bi	0.3	1.2	480	1.0	-	0.5	0.7	<3??	24.0	-
Li	<1	470	480	83	93	45	39	48?	15	-
F	140	260	300	3600	5100	2800	2600	4400	480	-
B	25	400	500	75	85?	10	10	<20??	10	-
Cl	<50	NSS	800	NSS	130?	NSS	NSS	1300	<50	-

GSE - Trace element glass standard from the USGS. Low values of some elements due to insufficient dissolution from their glass matrix.

SY-2 - Syenite, from Canadian Certified Reference Materials Project.

NIM-L - Lujavrite (a trachytic ophidolite-bearing nepheline syenite from the Pilaesberg Alkaline Complex), from the National Institute of Metallurgy, South Africa.

TLG-1 - Scheelite ore; used for tungsten only.

Recommended values are tabulated in Abbey (1980), Meyers et al. (1976) and Steele et al (1978). Values with question marks are considered by the original laboratories to be inadequate to recommend as usable values.

Table III-2 Whole Rock Duplicate and Reference Standard Analyses

DDH Depth (m) Rock Type	78-10 93.5 110	Duplicate	79-06 85.30 511	Duplicate	79-08 72.93 521	Duplicate	NIM-G (gran- ite)	Rec- ommended Value	QMC-M2 (Pelite)	Recommended Value
Values in wt. %										
SiO ₂	46.3	46.5	76.6	76.0	74.8	74.8	76.2	75.70	46.9	48.86?
TiO ₂	1.22	1.21	0.14	0.15	0.24	0.23	0.10	0.09	0.68	0.72
Al ₂ O ₃	23.3	23.4	12.6	12.8	13.0	12.9	12.2	12.08	23.7	23.97?
Fe ₂ O ₃ *	3.2	3.4	0.6	0.58	0.73	0.84	0.75	0.6?	3.08	2.31?
FeO	7.4	7.2	0.8	1.0	1.4	1.3	1.2	1.30	6.2	6.30?
MnO	0.24	0.24	0.02	0.02	0.03	0.03	0.01	0.02	0.24	0.26
MgO	4.22	4.31	0.11	0.23	0.26	0.27	0.01	0.06?	2.37	2.45
CaO	1.08	1.08	0.64	0.68	0.89	0.90	0.80	0.78	1.72	1.75
Na ₂ O	1.57	1.56	3.92	3.88	3.59	3.59	3.72	3.36	1.38	1.40
K ₂ O	4.80	4.79	4.60	4.64	4.66	4.69	5.07	4.99	8.13	7.90
P ₂ O ₅	0.18	0.18	0.04	0.04	0.08	0.07	0.01	0.01	0.54	0.50?
L.O.I.	5.62	5.62	0.77	0.77	1.00	1.23	0.47	-	3.08	-
TOTAL	99.13	99.49	100.84	100.79	100.68	100.85	100.54	-	100.02	-
Trace Elements (in ppm)										
Rb	150	170	300	330	300	300	310	320	270	-
Sr	110	100	20	30	60	80	0	10	180	-
Cr	170	170	40	40	40	40	40	12	60	-
Zr	210	220	150	140	180	160	270	300	90	-

*Fe₂O₃ = Fe₂O₃ (Total) - FeO

NIM-G - Granite from the Bushveld Complex in the Transvaal (Steele et al., 1978)

QMC-M2 - Pelite, from Queen Mary College, U.K. (Abbey, 1980)

Question marks are used for values considered uncertain or inadequate by the original laboratories.

Table III-3 Trace Element Duplicate Analyses.

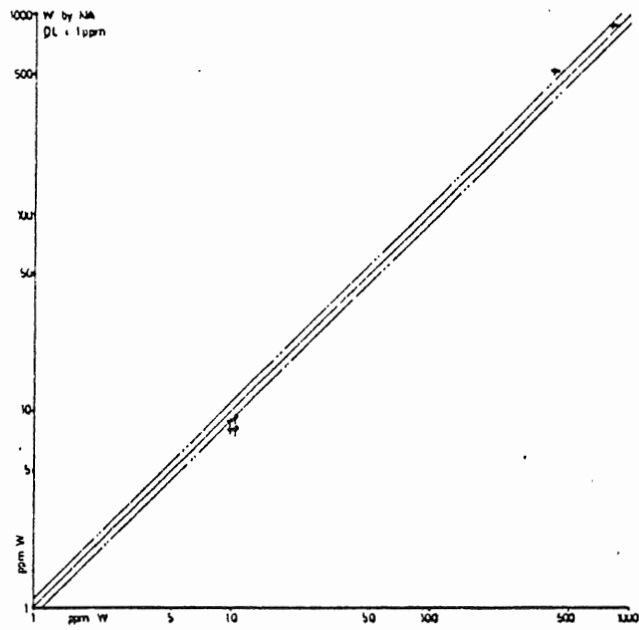
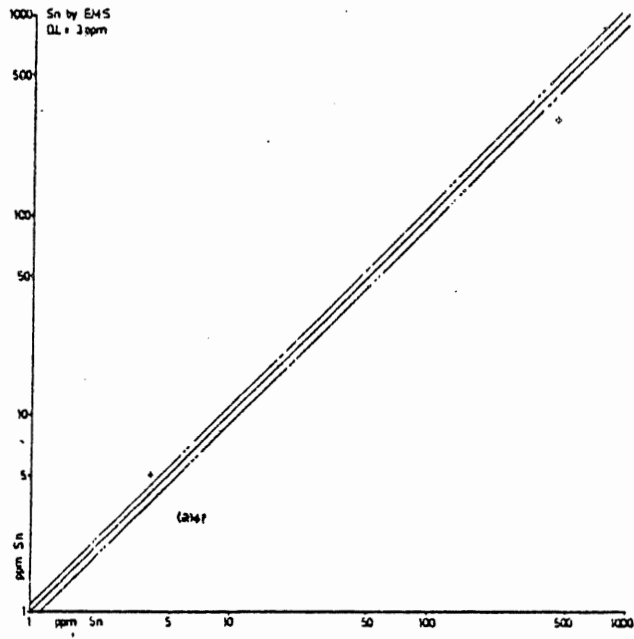
DDI Depth (m) Rock Type	78-44 100 164	Duplicate	78-29 57.72 164	Duplicate	77-25 132.10 301	Duplicate	78-10 93.5 110	Duplicate	78-11 85.45 432	Duplicate	78-12 118 153	Duplicate
Values in ppm except where noted												
Sn	3	3	50	50	1.23%	1.30%	30	25	0.73%	0.74%	0.33%	0.36%
W	5	6	5	6	34	35	16	16	19	17	14	10
Mo	<0.5	<0.5	<0.5	1.0	<0.5	<0.5	<0.5	<0.5	<0.5	<0.5	1.0	1.0
As	8	9	12	12	96	81	7500	8500	14	15	7	7
Cu	44.0	50.0	31.0	30.0	860.	960.	48.0	36.0	2000.	2000.	430	450.
Pb	4	2	40	42	26	28	22	28	6	16	22	22
Zn	98.0	100.	270	290	1500	1500	260	230	150	160	100	88
Sb	0.6	0.2	0.7	0.7	0.6	0.9	16.0	19.0	1.6	1.7	0.6	0.6
Bi	0.2	0.2	1.0	1.0	6.2	8.2	1.3	2.0	11.0	15.0	56.0	70.0
Li	63	62	42	51	72	81	89	61	63	42	40	51
F	480	560	460	480	450	420	630	670	740	590	560	610
B	50	50	25	25	<10	<10	25	25	<10	25	10	10
Cl	<50	50	100	<50	150	<50	<50	50	<50	<50	50	100

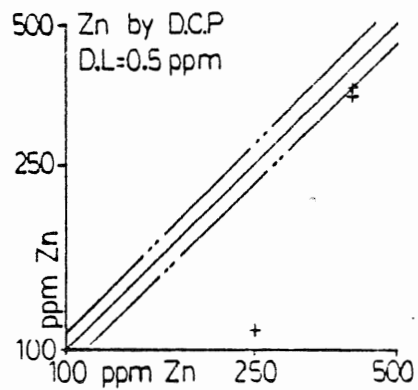
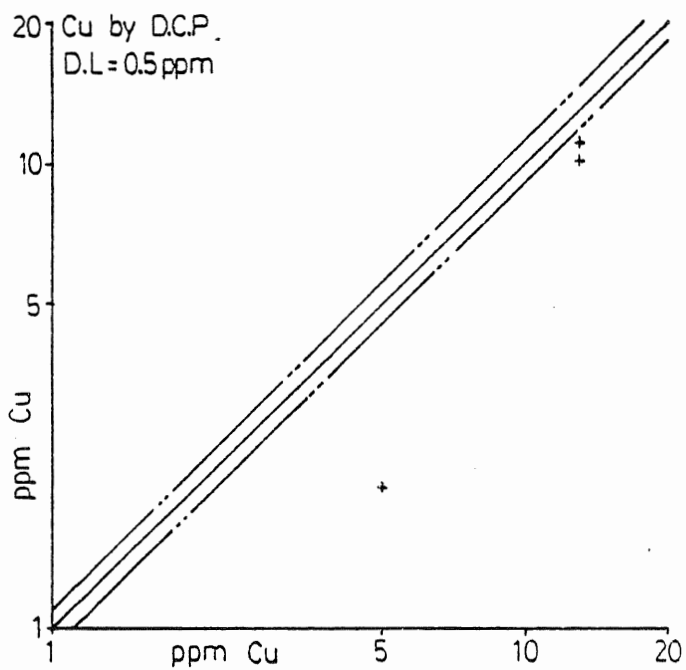
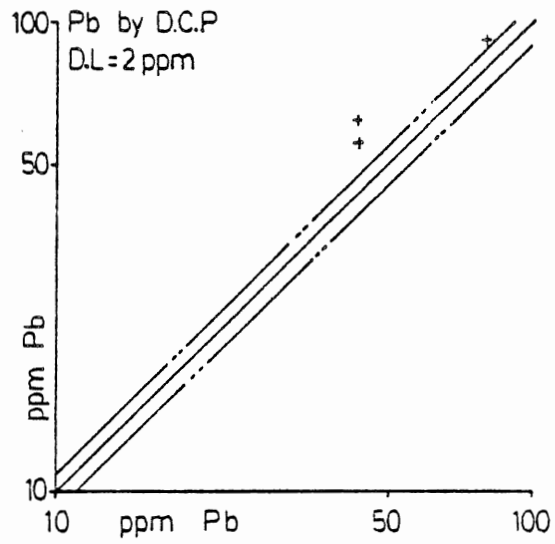
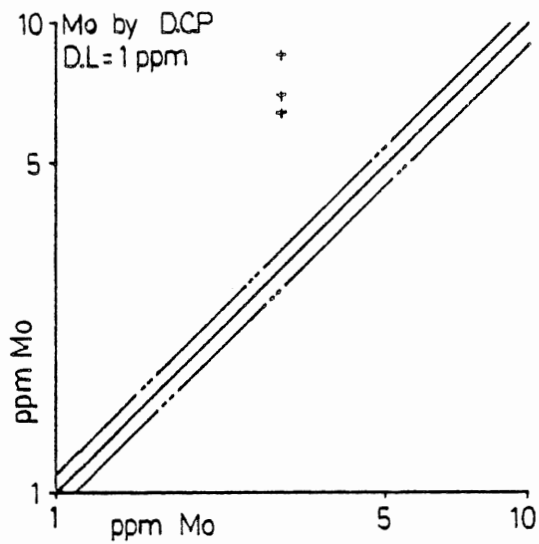
Table III-3 (Cont'd) Trace Element Duplicate Analyses

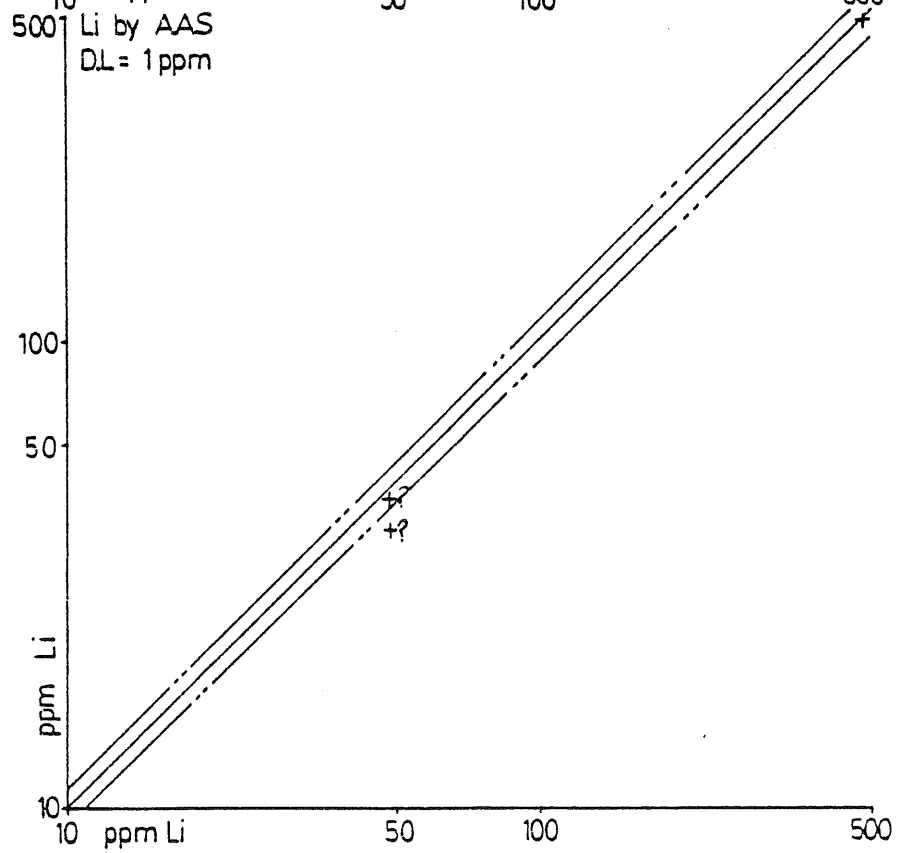
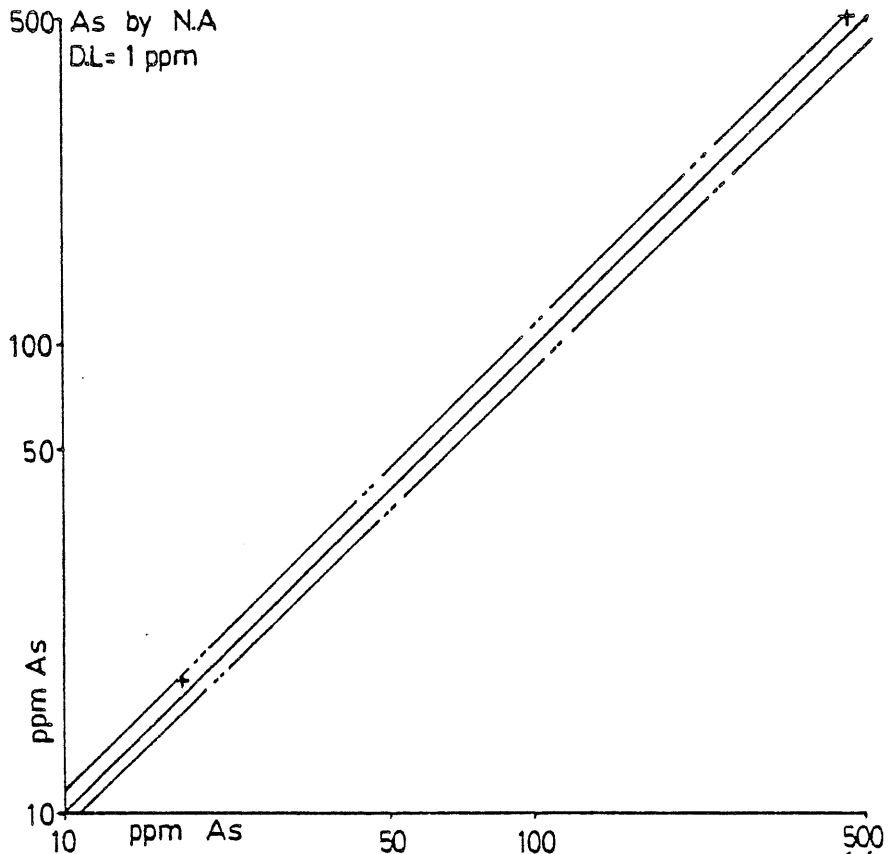
DD#	73-24	Duplicate	78-24	Duplicate	78-20	Duplicate	79-05	Duplicate	79-07	Duplicate	79-08	Duplicate	79-06	Duplicate
Depth (m)	44.6		92		53.88		51.60		70.66		72.93		85.30	
Rock Type	102		100		110		183		711		521		511	
Values in ppm except where noted														
Sn	3	5	3	5	5	5	15	25	360	340	25	20	7	5
W	3	<1	3	3	4	5	9	14	23	23	18	17	300	320
Mo	<0.5	<0.5	1.5	3.5	<0.5	<0.5	4.5	4.5	130.	120.	6.5	6.5	63.0	69.0
As	13	12	16	12	8	7	13	12	30	24	20	21	4	7
Cu	39.0	44.0	60.0	84.0	34.0	34.0	7.0	6.5	430.	410.	4.0	4.0	1.5	2.0
Pb	4	2	100	90	<2	<2	<2	2	8	8	4	4	6	6
Zn	110	110	130.	100.	43.0	72.0	97.0	96.0	2900.	2800.	21.0	22.0	16.0	17.0
Sb	0.7	0.5	0.9	0.2	0.3	0.4	0.3	0.4	0.4	0.3	0.4	0.8	<0.2	0.2
Bi	0.4	0.3	0.7	0.3	1.0	0.5	0.5	0.3	12.0	9.0	4.0	0.2	11.0	6.3
Li	31	37	48	52	52	55	150	130	55	170	57	57	26	25
F	320	310	420	420	350	480	2500	2200	2500	3500	860	1100	610	510
B	50	25	25	25	100	25	10	10	50	50	25	25	50	25
Cl	50	<50	<50	<50	<50	<50	<50	<50	<50	<50	<50	<50	<50	50

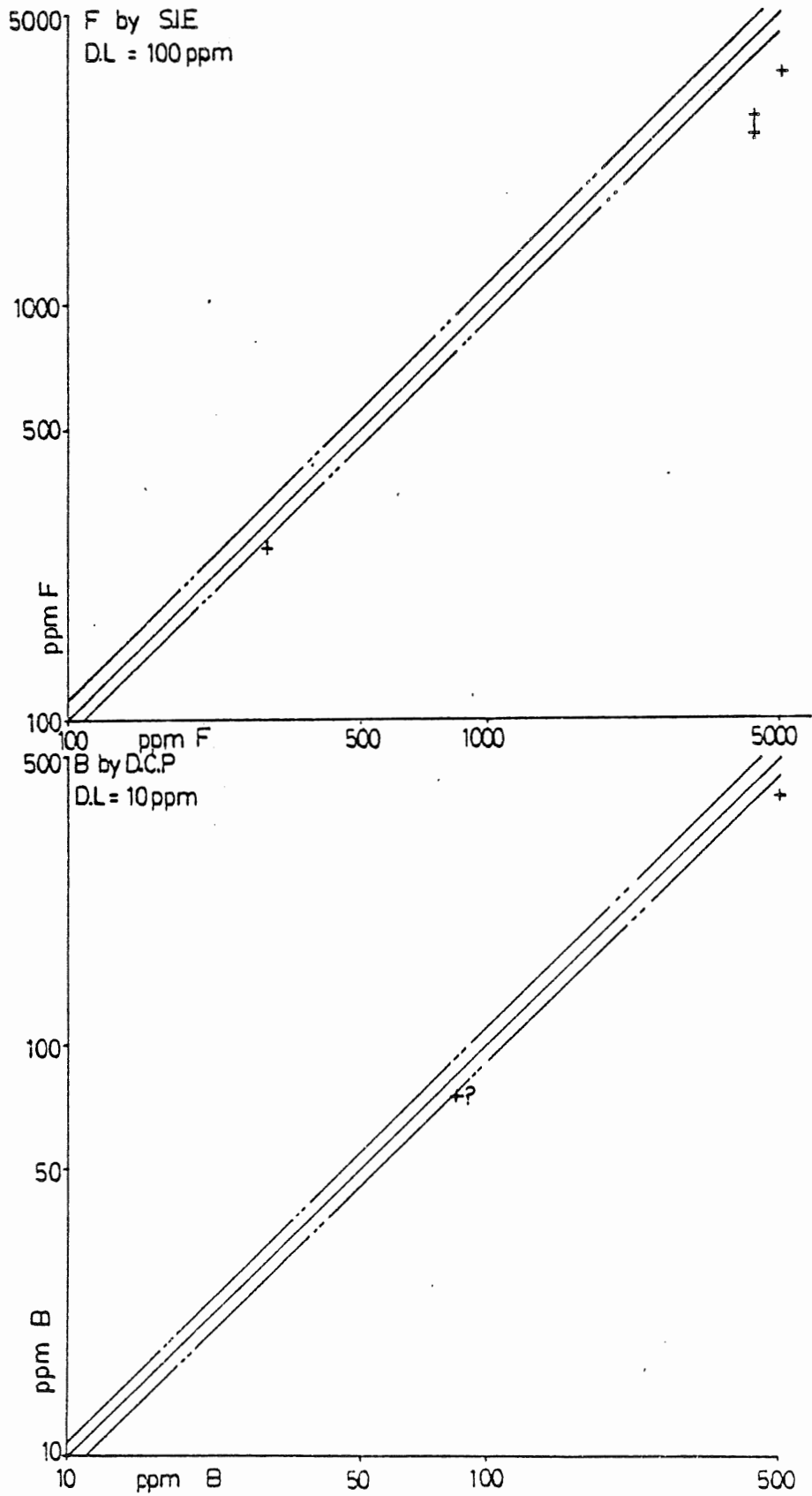
Figure III-1

Accuracy of trace element analyses using reference samples. Results of analyses are plotted against 'usable' values. Precision limits of $\pm 10\%$ are marked. Bi is not plotted as recommended values are unreliable or, in the case of GSE, Bi was not totally digested.









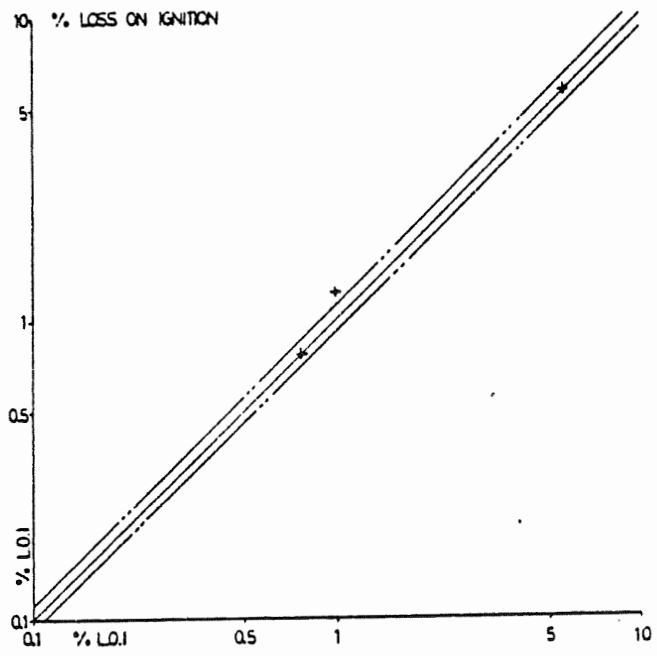
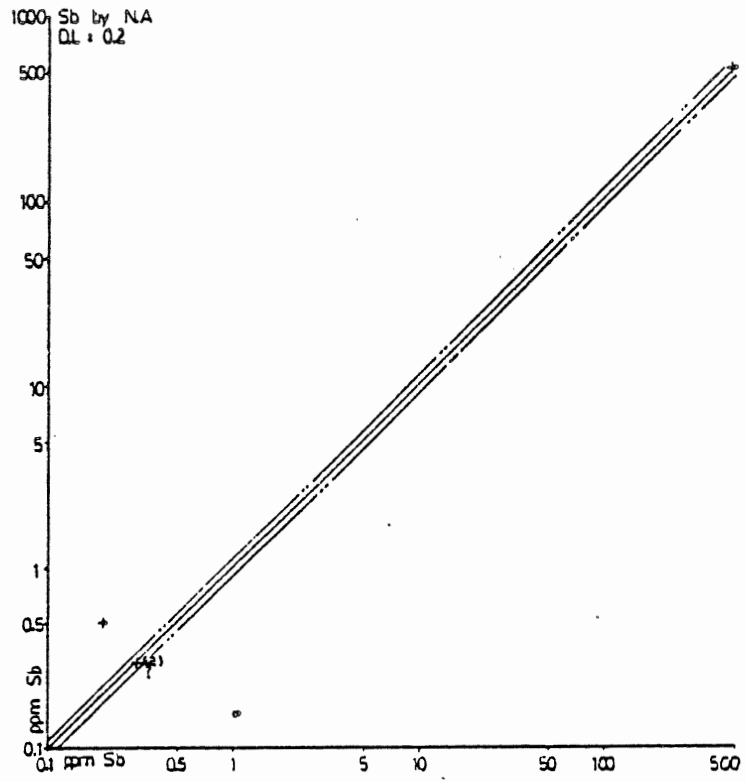
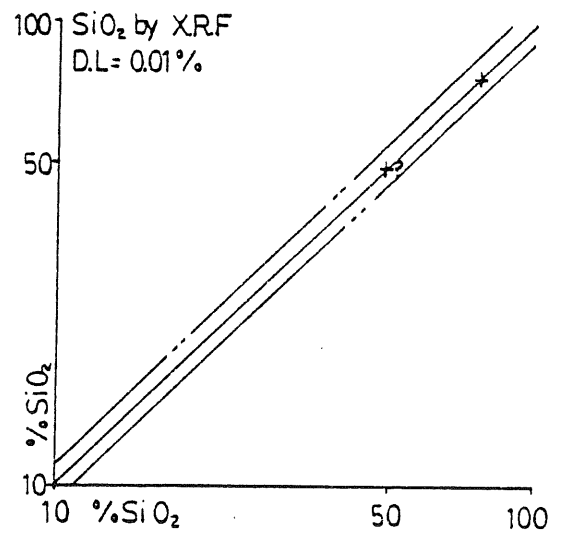
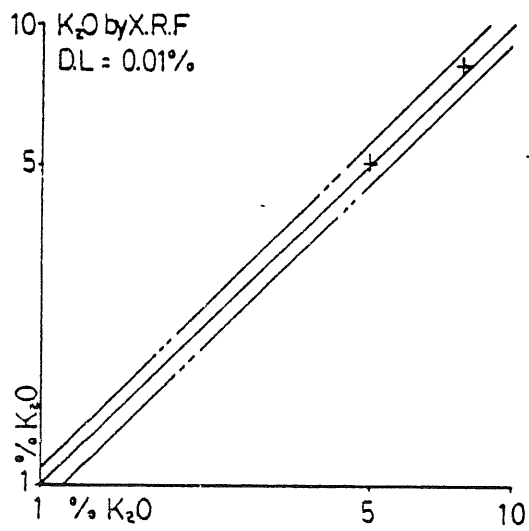
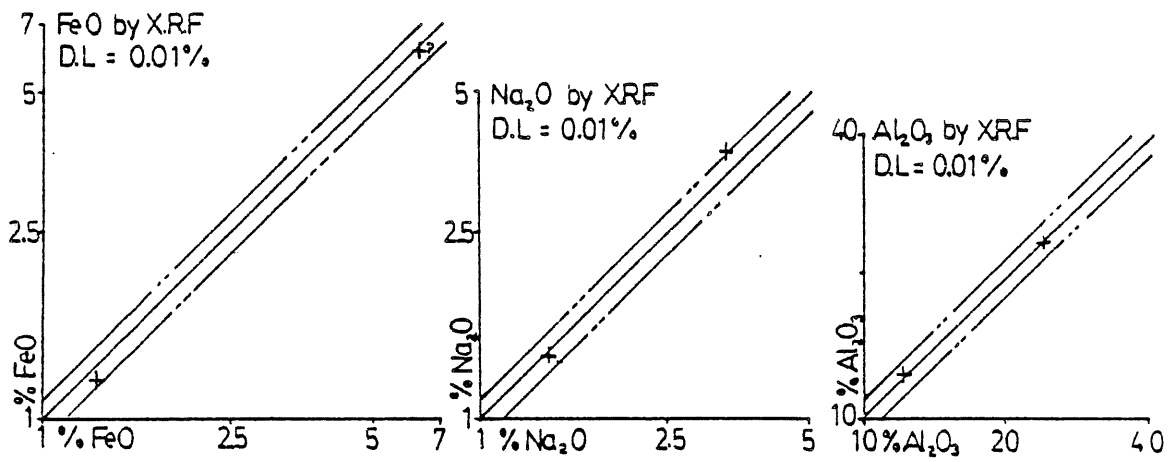
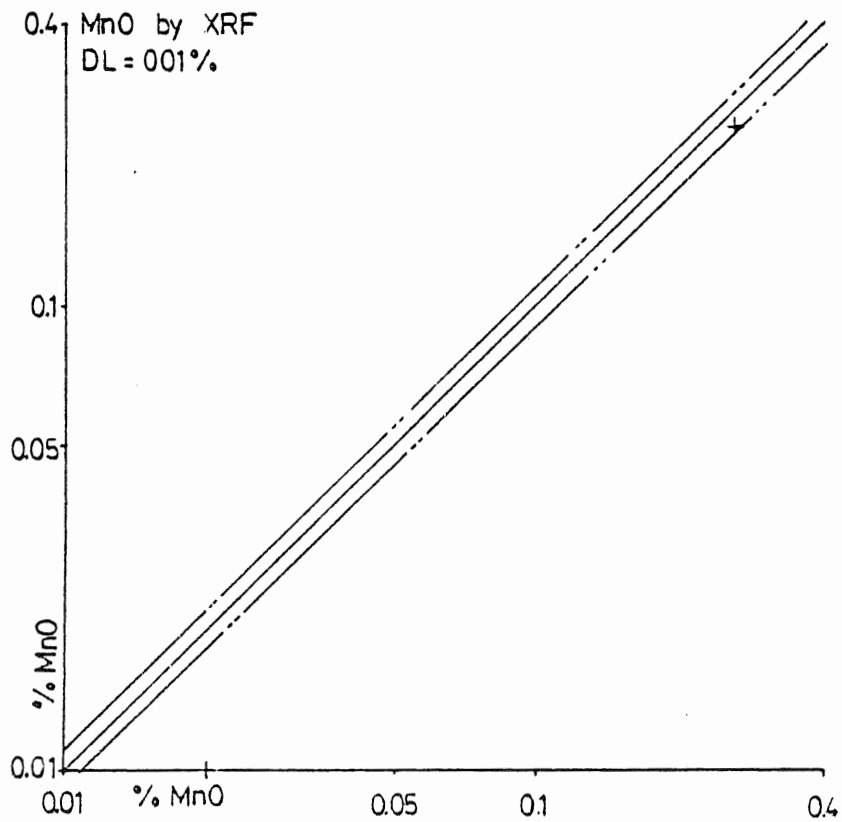
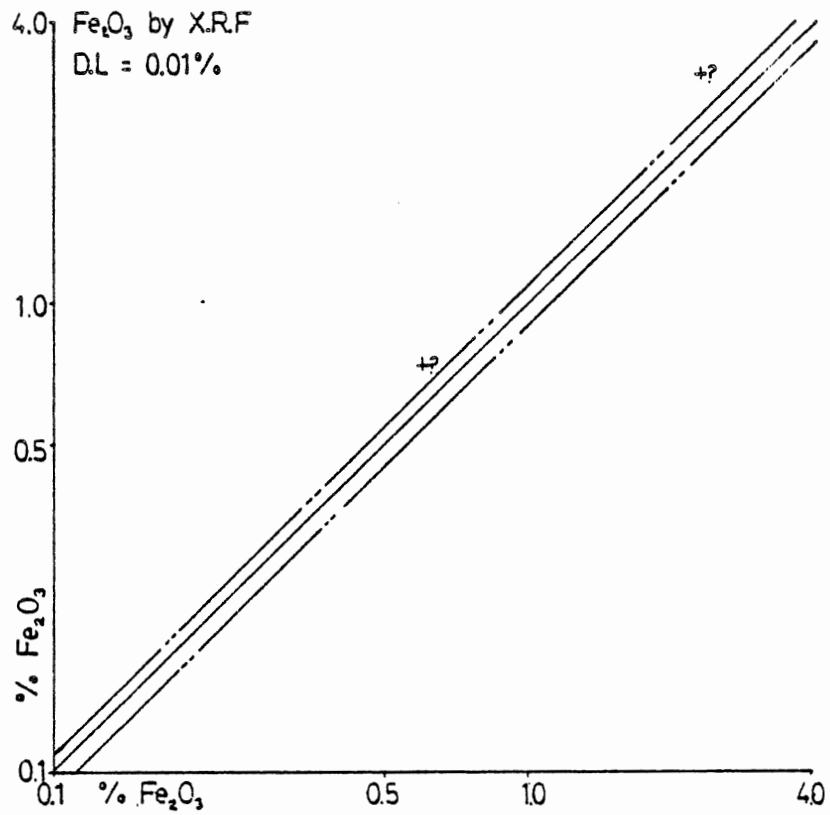
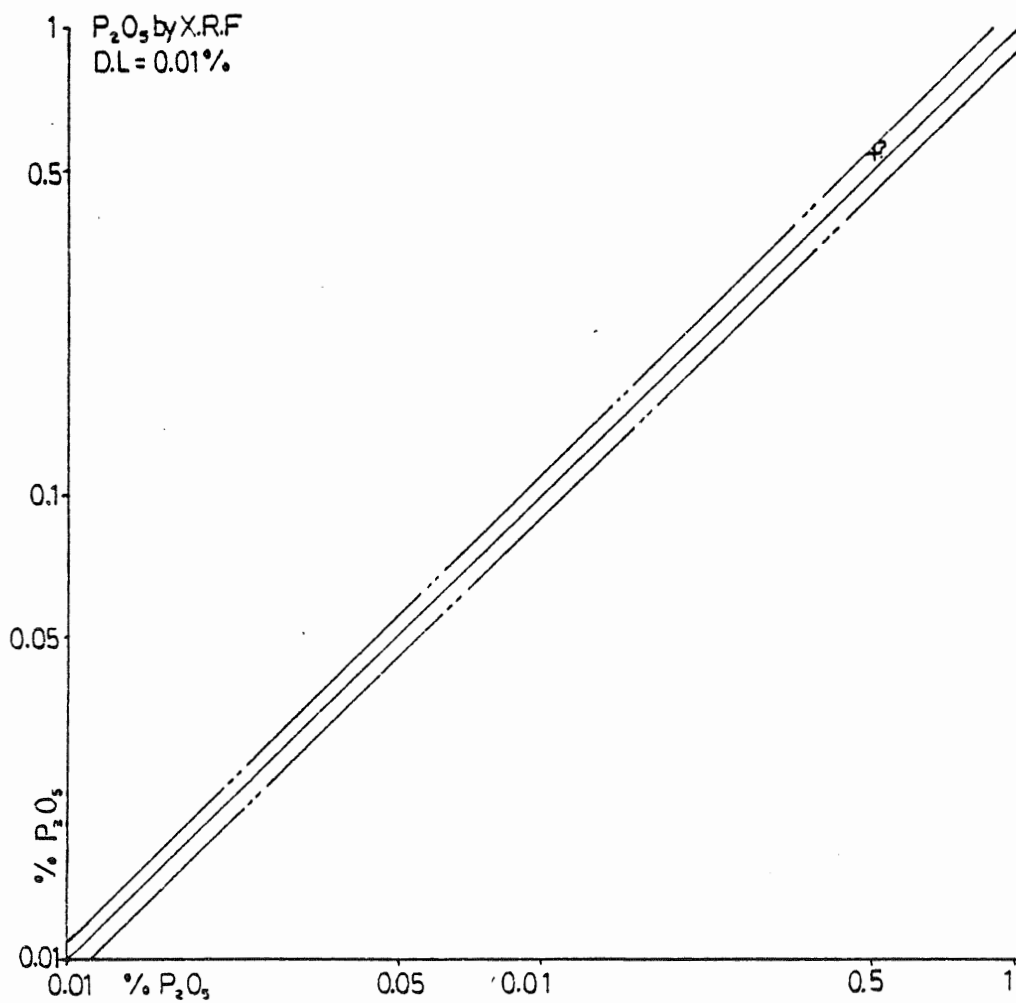
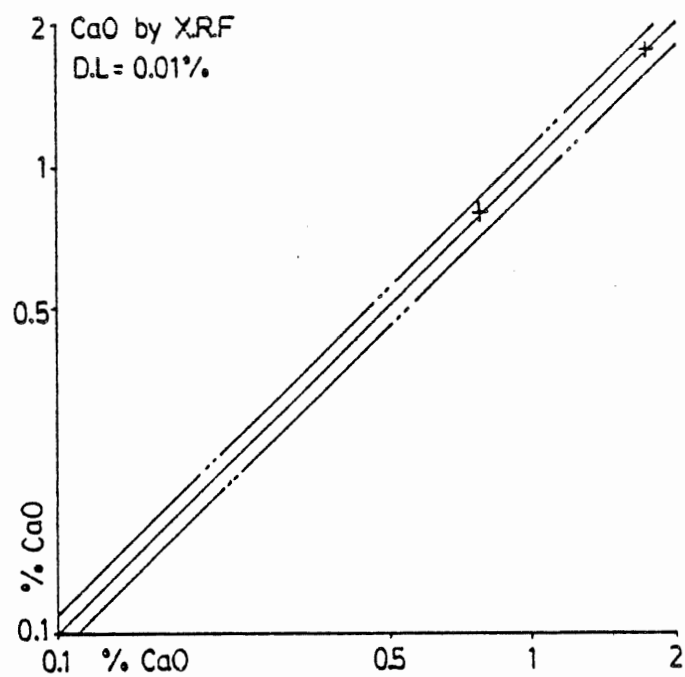


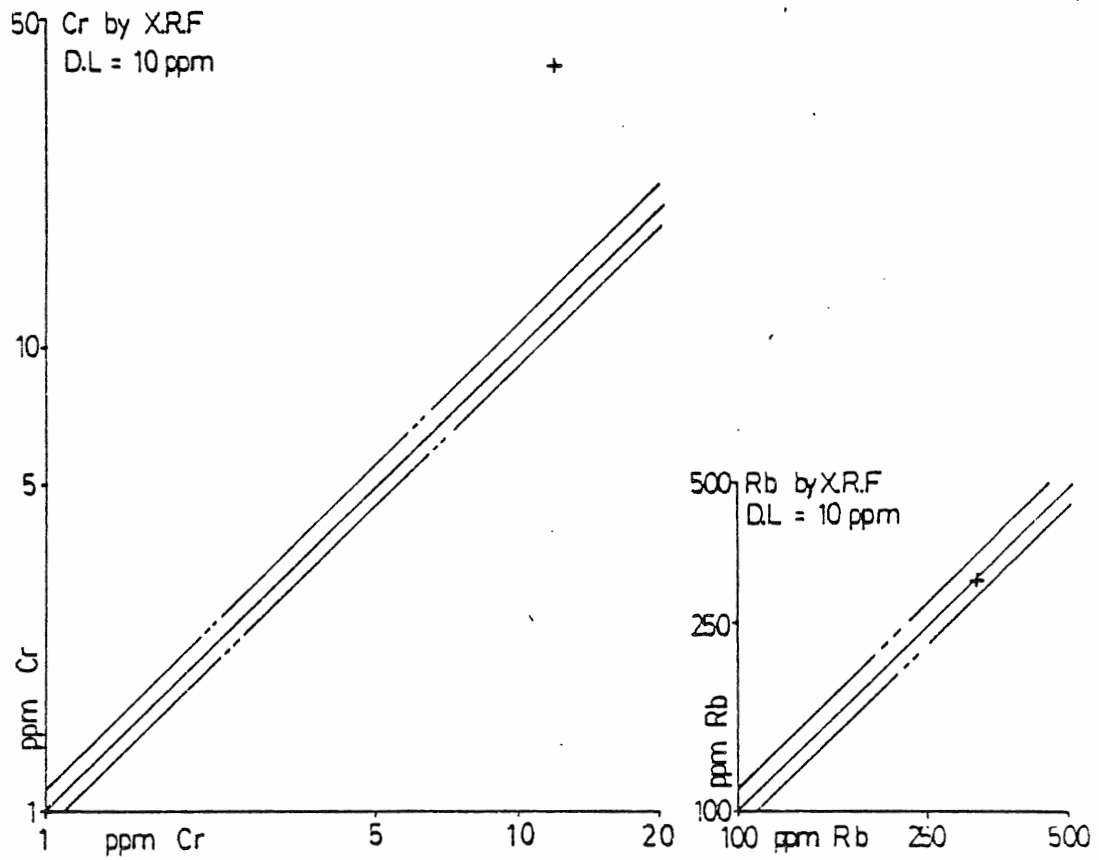
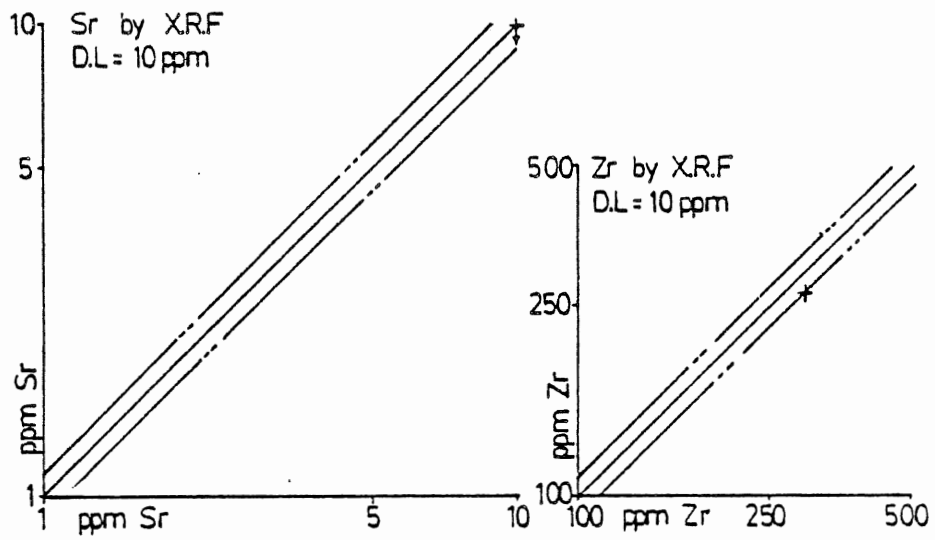
Figure III-2

Accuracy of whole rock analyses
using reference samples. Results of
analyses are plotted against
'usable' values. Precision limits
of $\pm 10\%$ are marked.









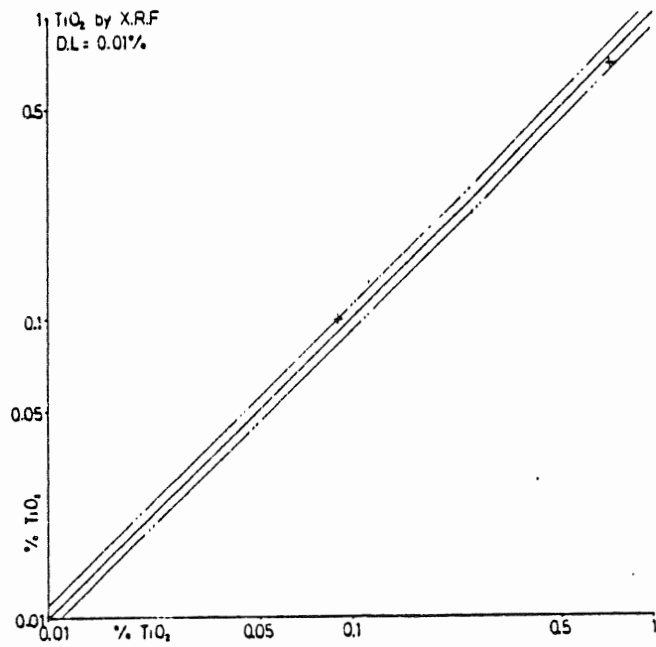
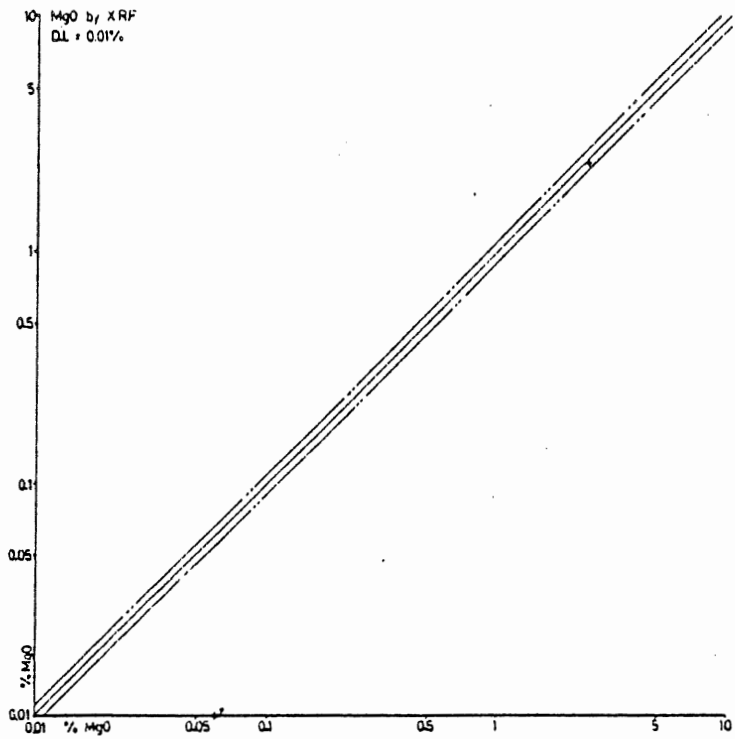
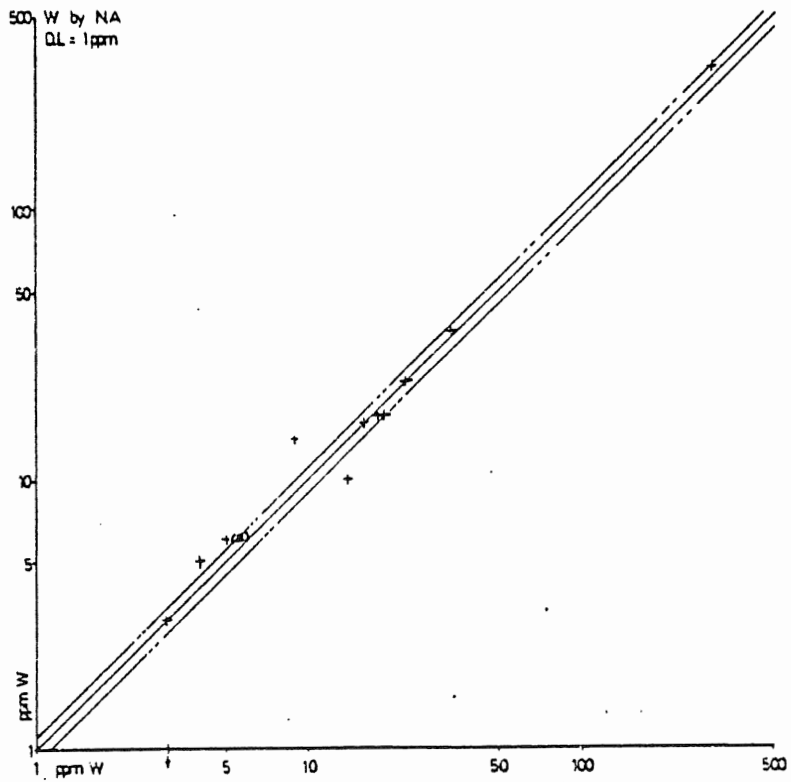
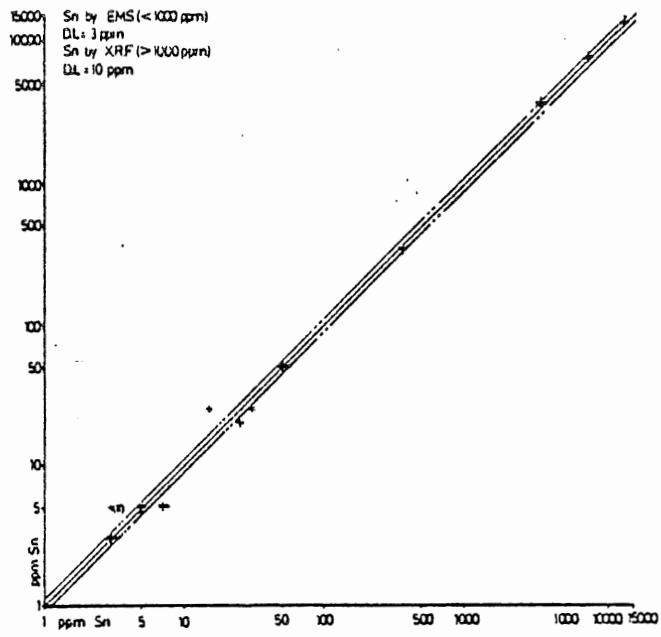
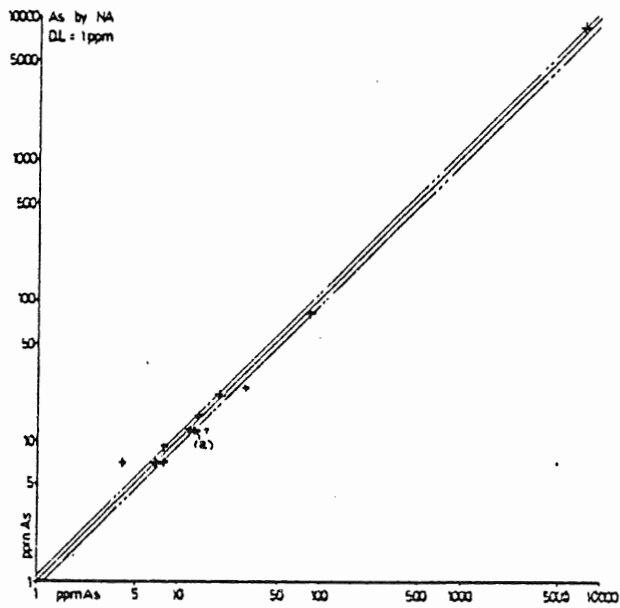
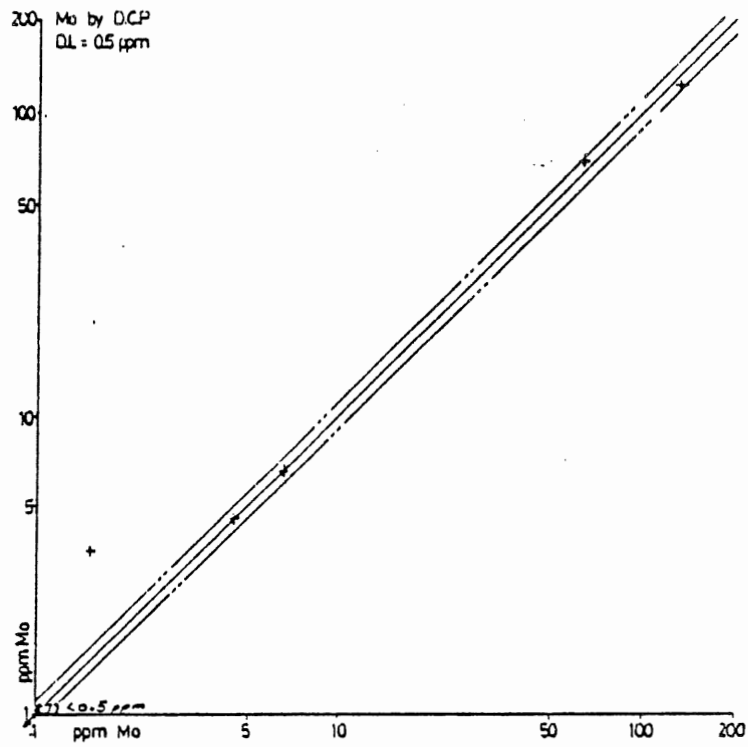
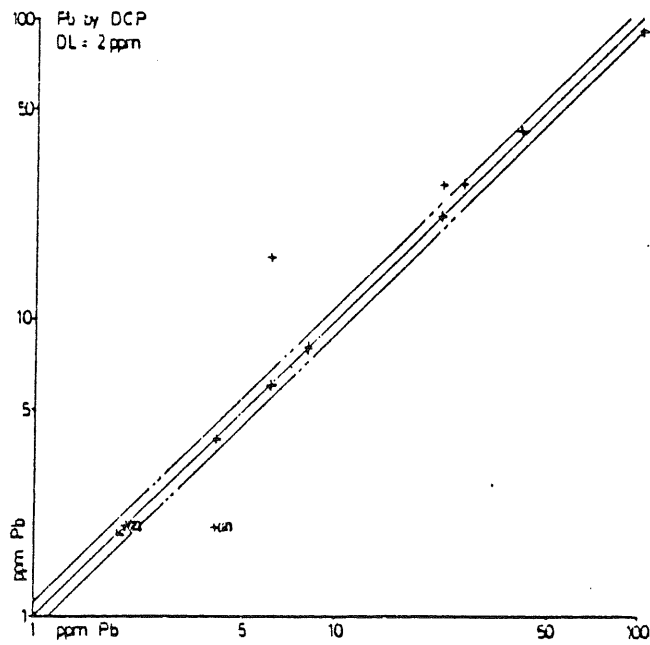
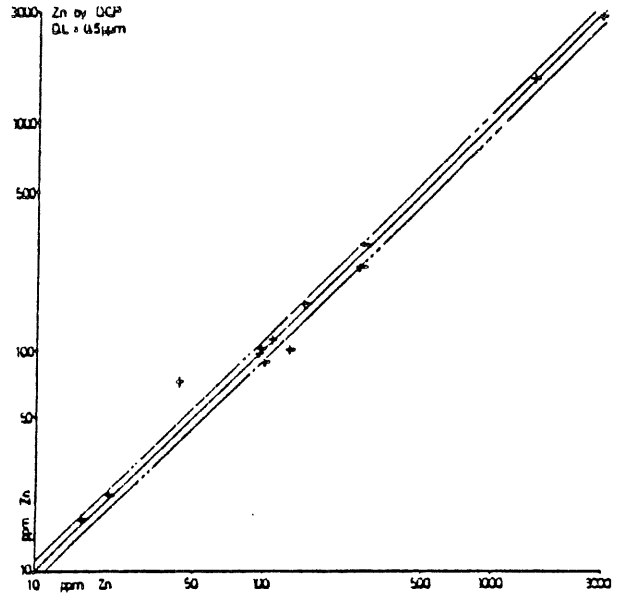
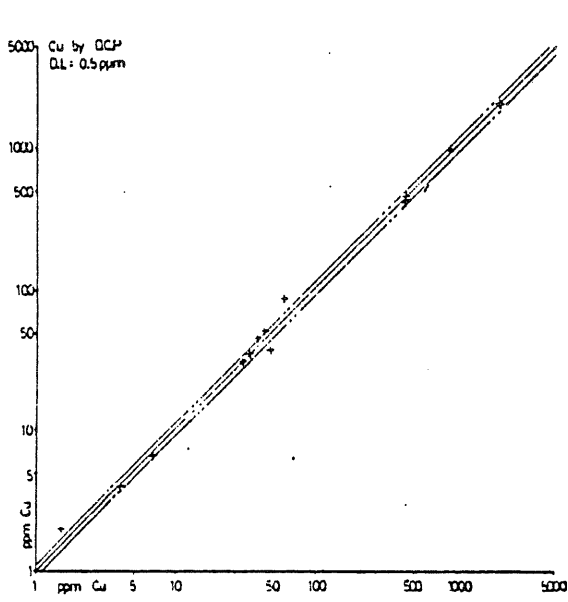


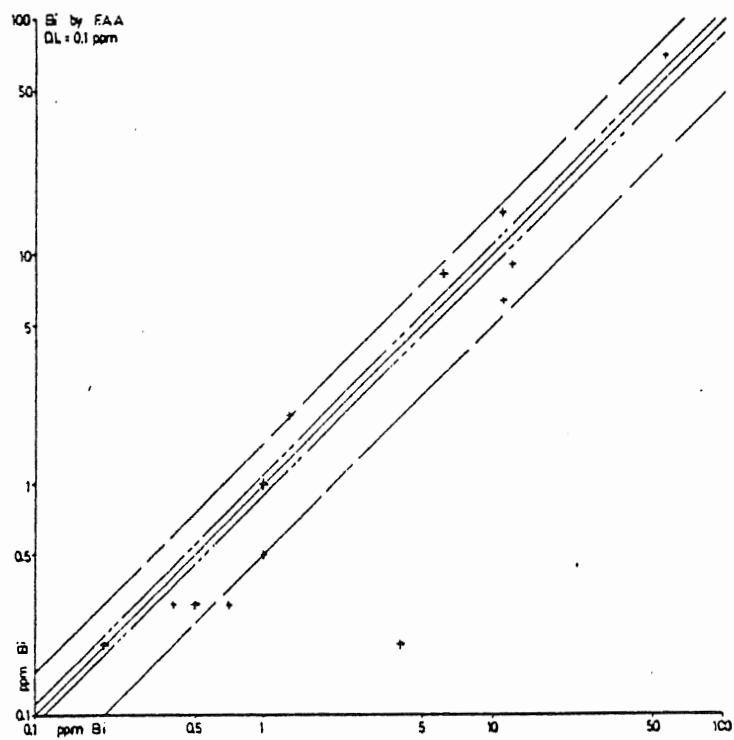
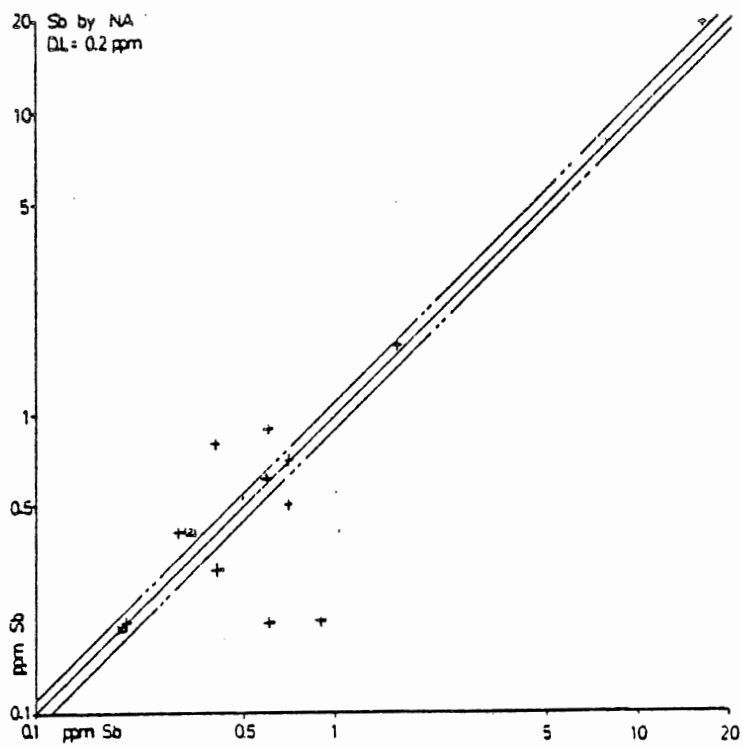
Figure III-3

Precision of trace element analyses using duplicate samples. Duplicate results are plotted against each other. Precision limits of $\pm 10\%$ are marked. In the graphs of Bi and Li, $\pm 25\%$ limits are also marked.









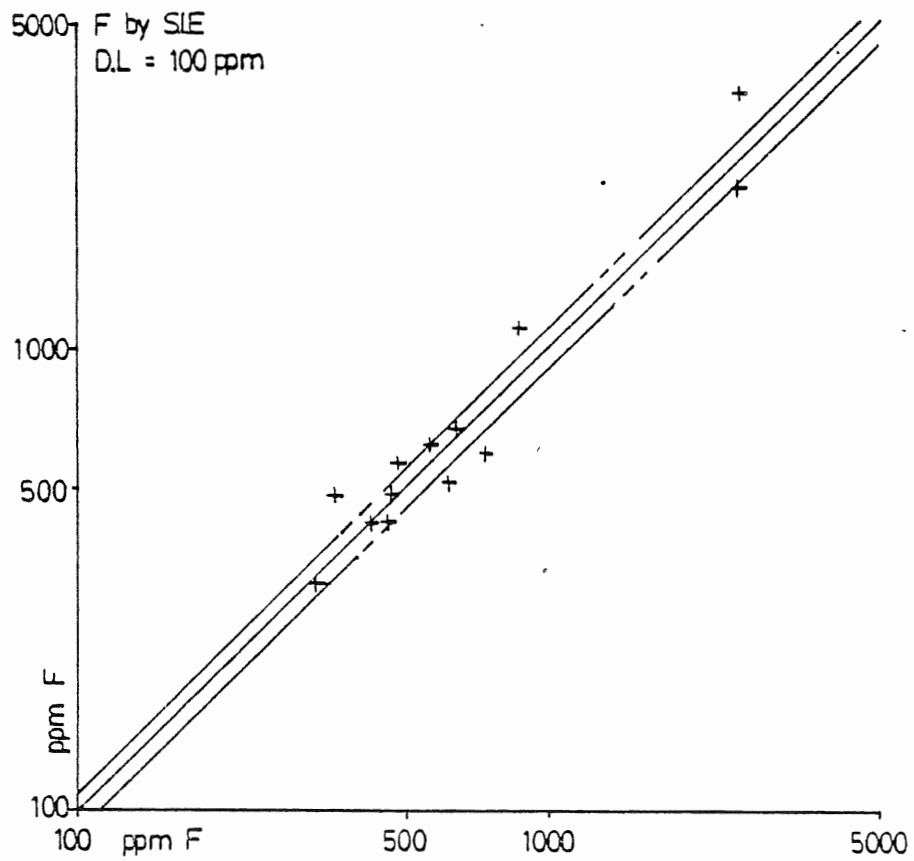
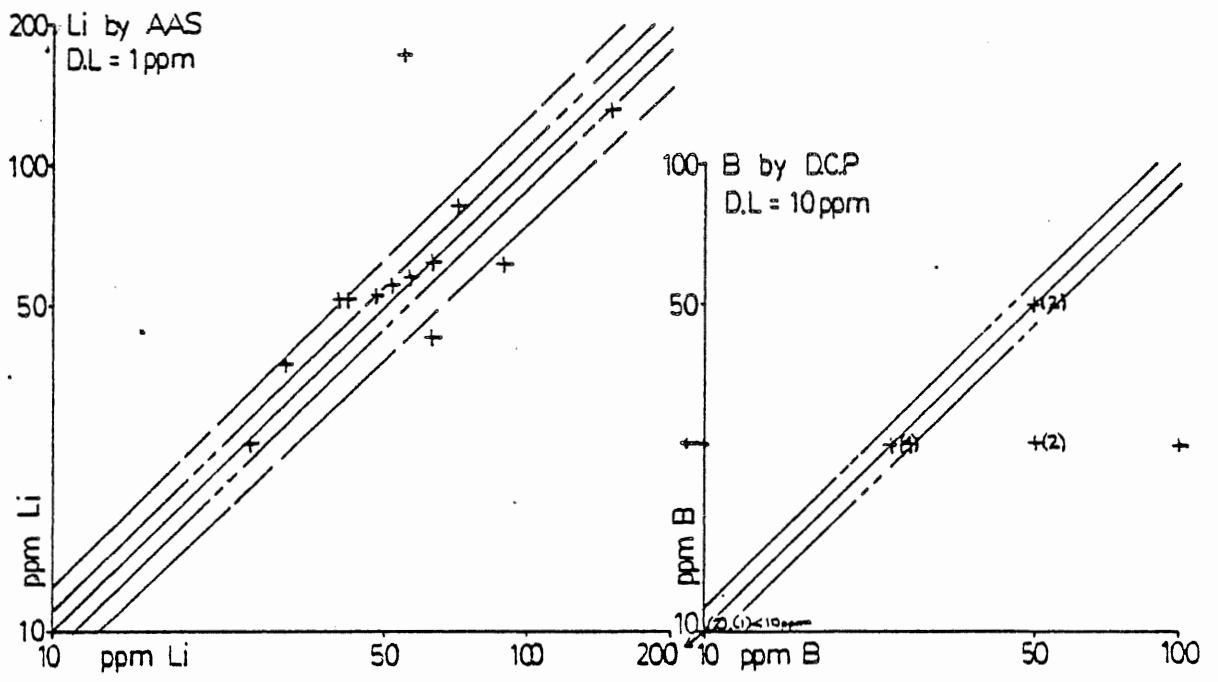
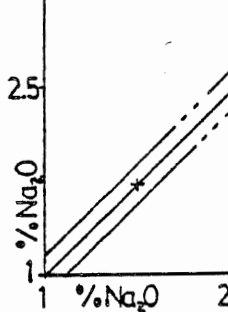


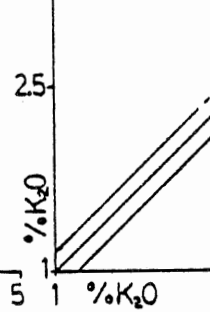
Figure III-4

Precision of whole rock analyses using duplicate samples. Duplicate results are plotted against each other. Precision limits of $\pm 10\%$ are marked.

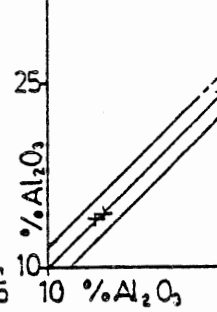
5 Na₂O by XRF
D.L. = 0.01%



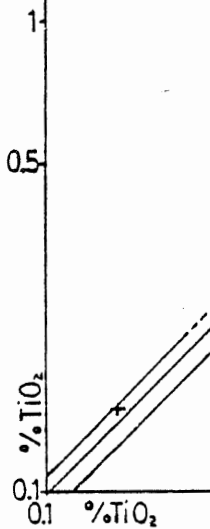
5 K₂O by XRF
D.L. = 0.01%



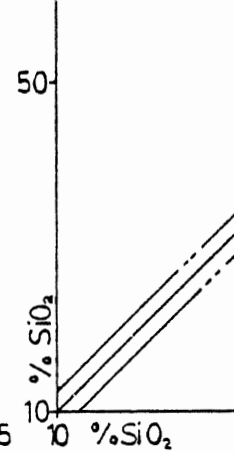
50 Al₂O₃ by XRF
D.L. = 0.01%



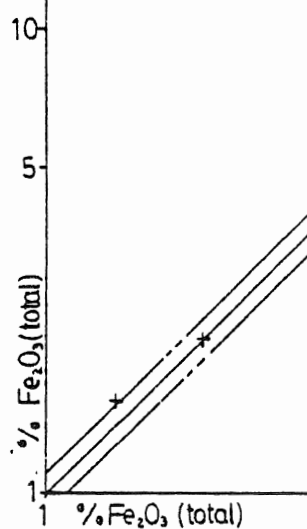
1.5 TiO₂ by XRF
D.L. = 0.01%



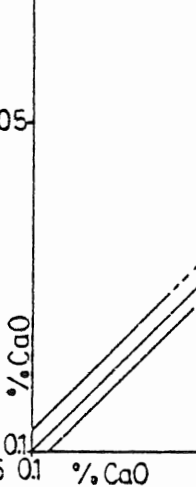
100 SiO₂ by XRF
D.L. = 0.01%

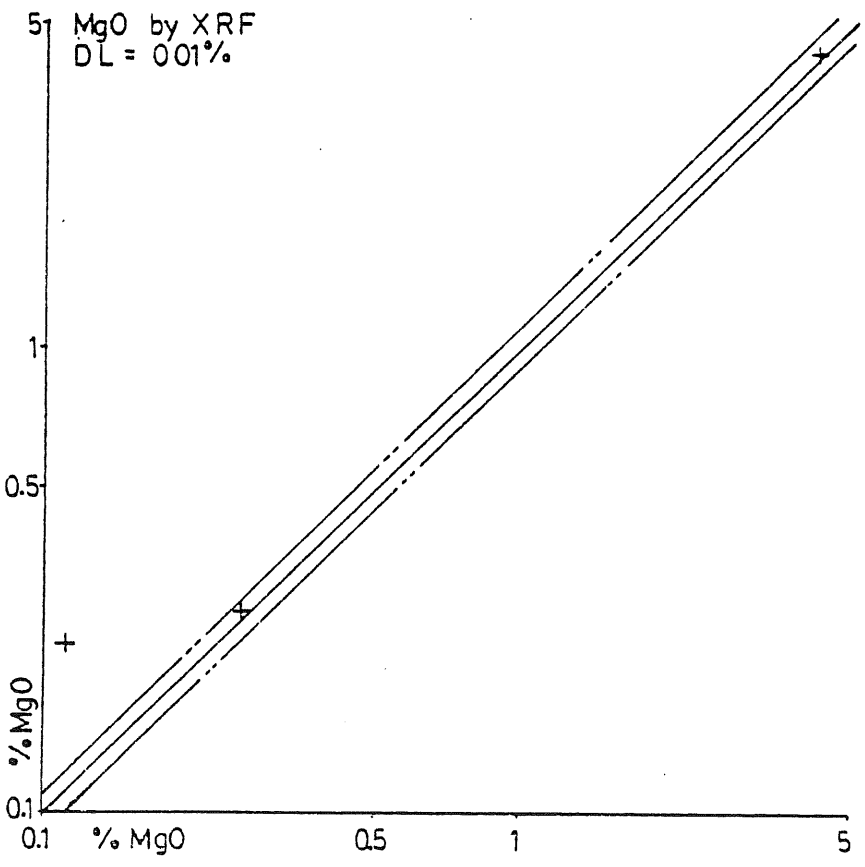
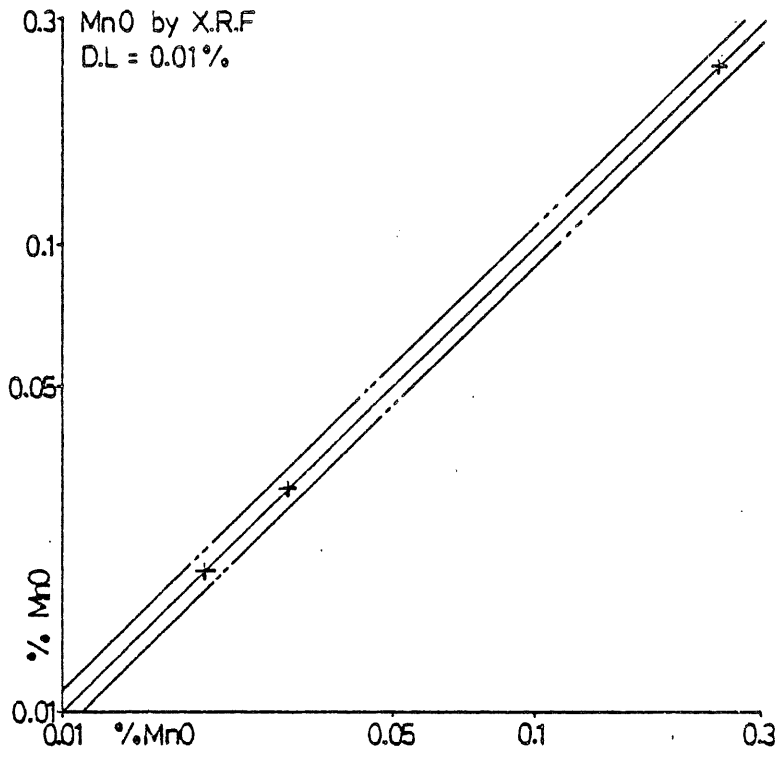


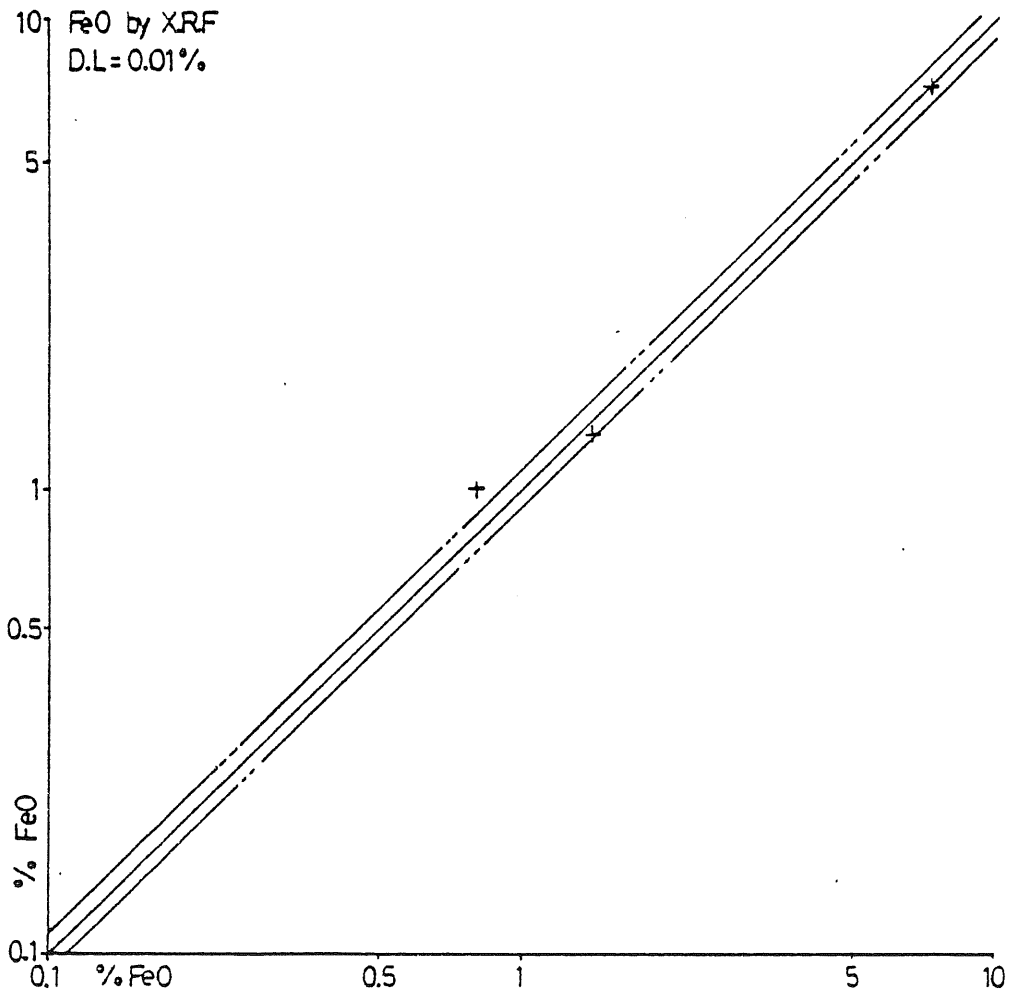
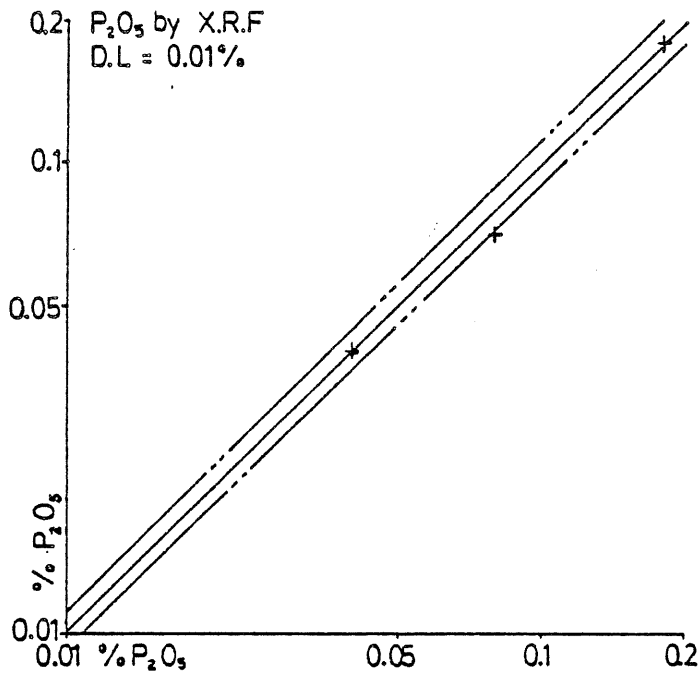
15 Fe₂O₃ (total) by XRF
D.L. = 0.01%

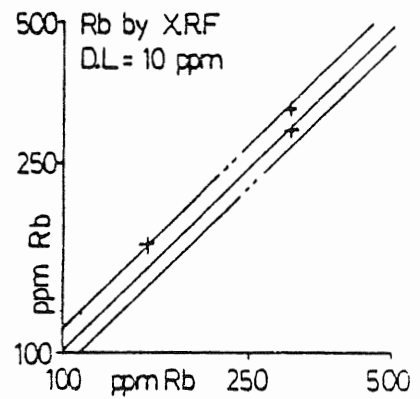
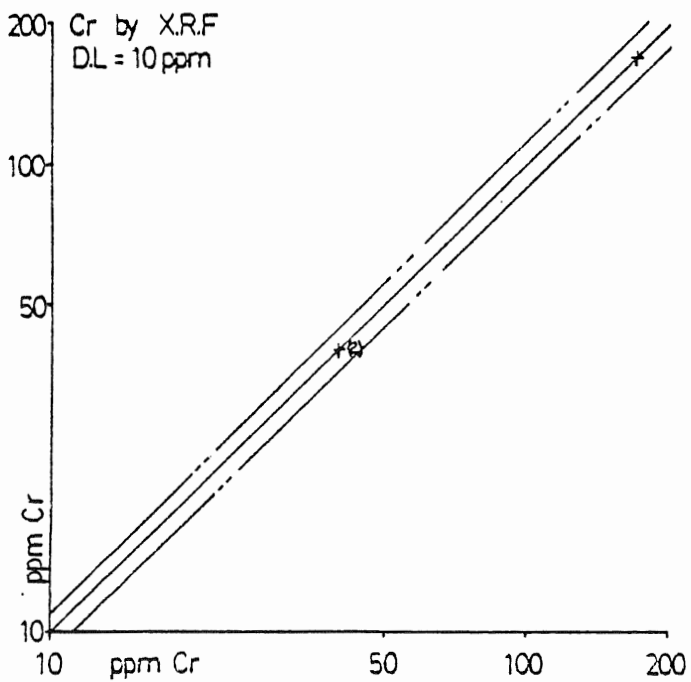
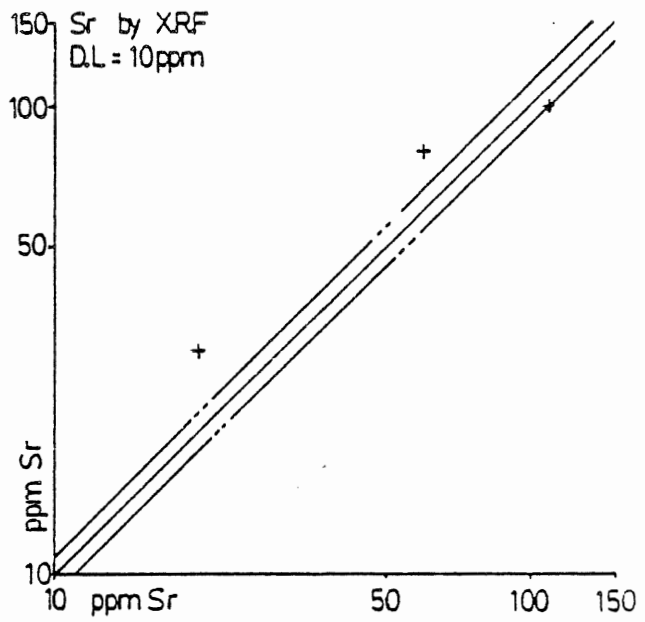
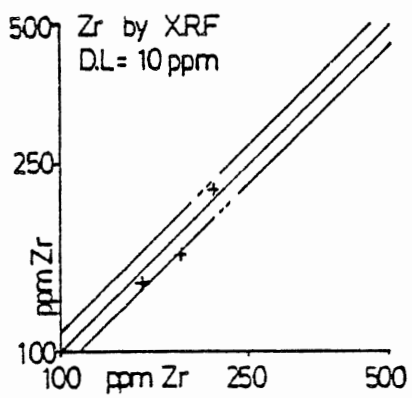


12 CaO by XRF
D.L. = 0.01%









APPENDIX IV

PARTITIONING OF POLYMODAL DISTRIBUTIONS

This section summarizes the procedures used by Sinclair (1974) to choose background and threshold values from a set of geochemical data. It is an arbitrary method of segregating the data into background and anomalous groups by partitioning a cumulative probability plot. Other methods (e.g. Levinson, 1974) established the mean (background) and standard deviation of a set of data, with the threshold arbitrarily chosen to correspond to the mean plus two standard deviations, i.e. the upper 2.25% of a normal population. This procedure is not recommended as it assumes that 2.25% of any sample population will be anomalous; also, the ranges of background and anomalous populations in a data set may overlap, so that the mean and standard deviation are actually obtained from the sum of two populations and thus would be of no use.

Sinclair's method uses lognormal probability paper, with a lognormal abscissa scale and an ordinate scale of cumulative frequency percent. A lognormal cumulative distribution of a single population will plot as a straight line; that of two populations will plot as a curve. The approximate proportions of each population is shown by a

change in curvature or slope, i.e., the inflection point. In an example taken from Sinclair (Fig.IV-1), 20 percent of the anomalous population A is combined with 80 percent of background population B. The slope of the combined populations changes at about the 20th cumulative frequency percentile, forming an inflection point. The less perceptible the change in slope, the greater degree of overlap in the populations.

To separate multiple populations in a data set, a cumulative frequency diagram must first be constructed. The steps are similar to those used for creating histograms and are presented here. An example using tungsten values in the monzogranite will be shown later.

1. Determine range of log values.

$$\text{Range} = \log(X_{\text{max}}) - \log(X_{\text{min}})$$

2. Determine width of each class interval by dividing the range by the number of intervals desired. Construction of a histogram may aid in deciding on the number of intervals.

$$\text{Width} = \text{Range} / \# \text{ of intervals}$$

3. List the ranges of each of the class intervals and their corresponding antilogs.
4. Record the number of samples in each interval and determine their percentages of the total.
5. Sum (cumulate) the percentages of samples in each class from the maximum to the minimum value and record the cumulative value for each class interval. This is done because of the poor precision of values in the lower ranges (due to poor sample preparation or analyses or both) and of the importance of the higher values in establishing the threshold. Cumulation from highest to lowest values will place

the lowest (and therefore less desirable) class interval in the 100 percent cumulative range, which will not be plotted due to the nature of the graph paper (Lepeltier, 1969).

6. Plot points at the antilog of the lower class limit of each class against the cumulative percentage for that interval. Draw a best fit line or lines through the points.

According to Koch and Link (1970) a small sample population (less than 100) gives a poor estimate of the metal content in a data set because the standard deviation is larger (giving a less precise confidence interval) than that of a population with more than 100 values. They have derived an arbitrary 'correction factor' to replace the cumulative frequency percentages by a 'plotting percentage' where,
$$\text{Plotting Percentage} = 100 * [(3(\text{Cumulative Frequency}) - 1) / (3n + 1)]$$
where n is the sample size.

This manipulation was accomplished in the course of population partitioning and an example is given with the usual cumulative frequency determination. It was found that there is not much difference between the two partition models. The background and threshold values changed slightly within the same order of magnitude, and so the plotting percentage formula was not used.

Figure IV-2 shows a graph for tungsten with both the cumulative and plotting percentage points. Note the existence of essentially two lines of different slopes. This implies the existence of two lognormal populations, a higher anomalous one and one of a lower background. Points

Figure IV-1

Two idealized hypothetical populations
A and B are combined in the proportions
 $A/B = 20/80$ to produce the dotted curve
with an inflection point at 20 cumulative
percent.
(Modified after Sinclair, 1974)

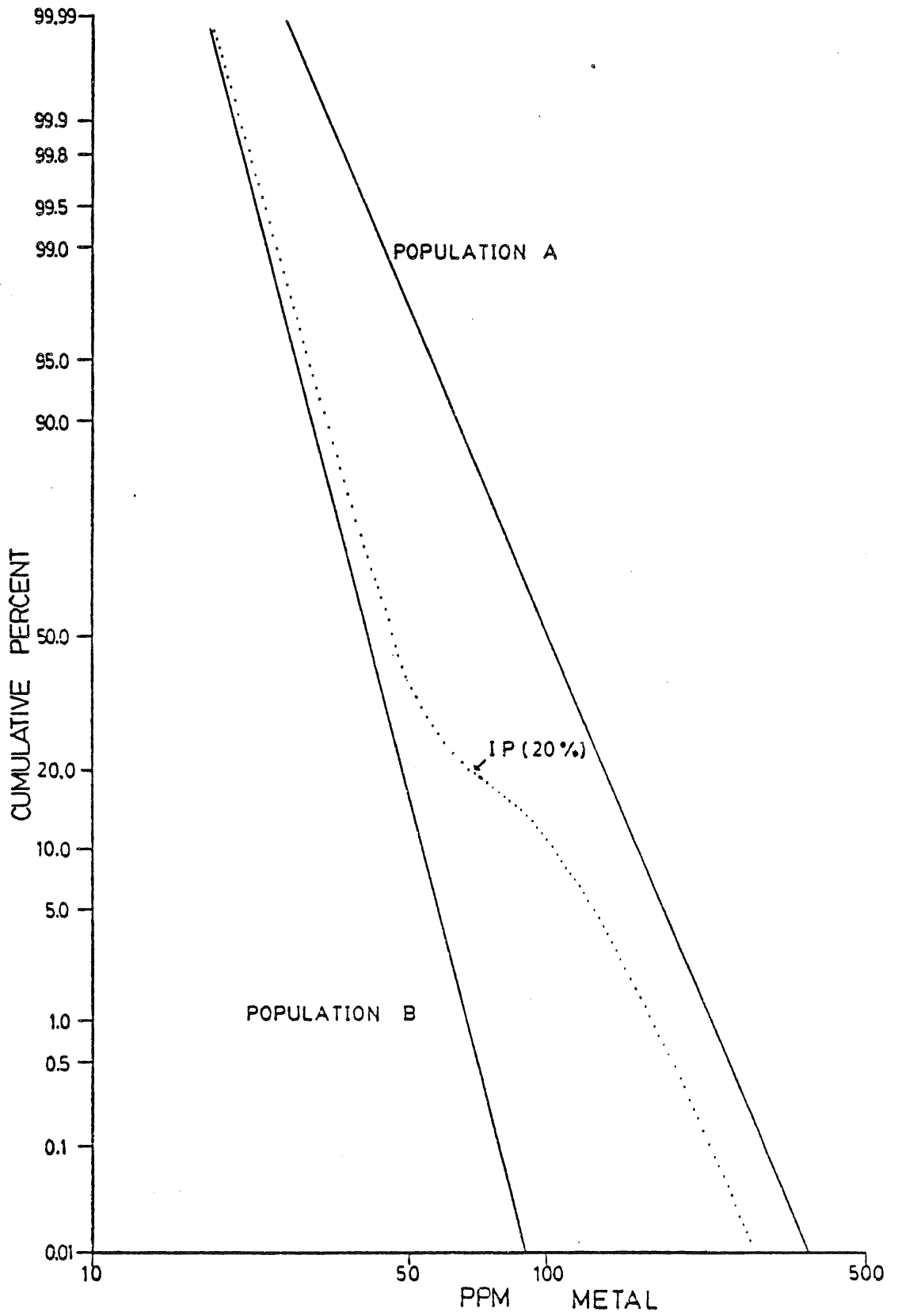
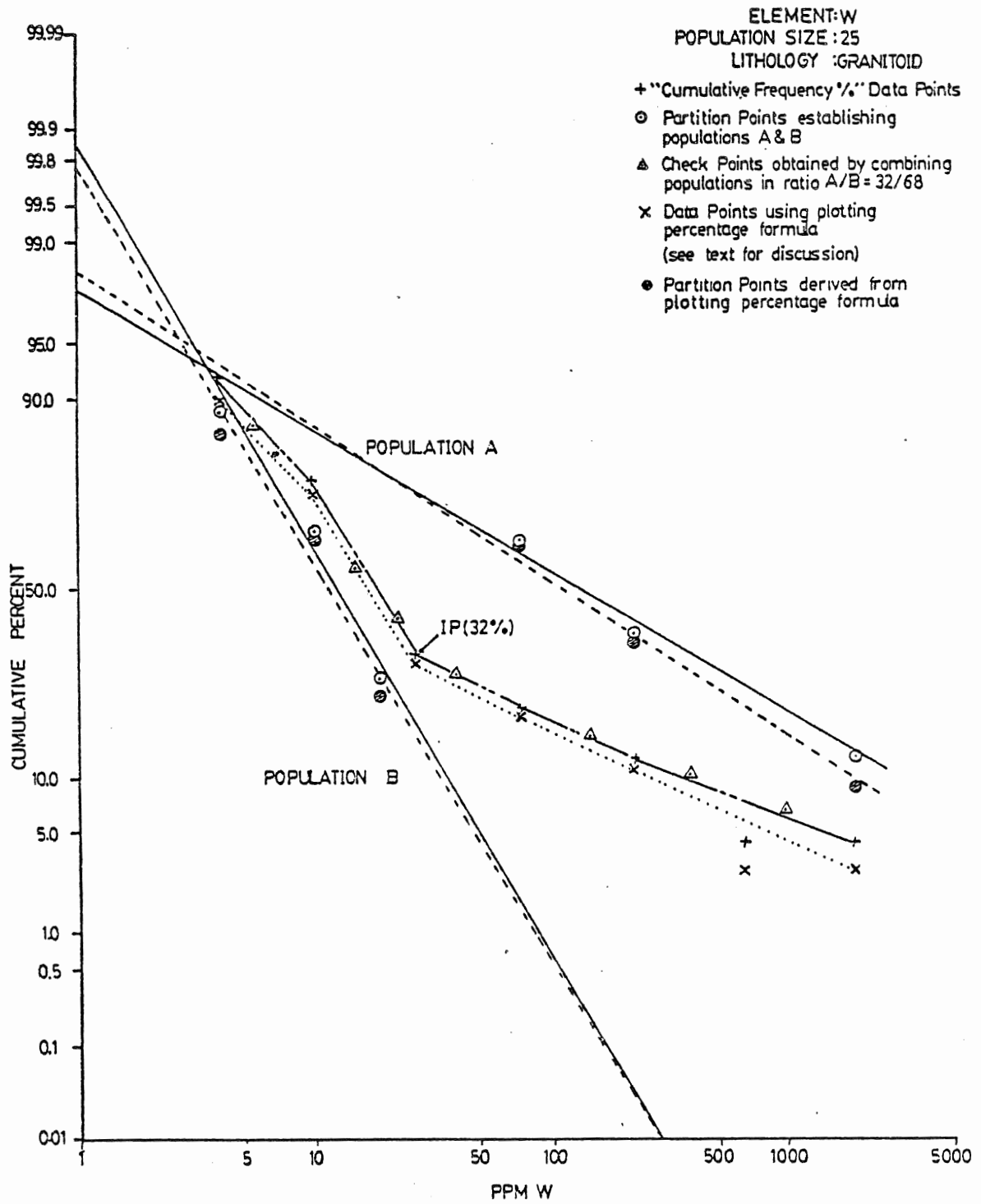


Figure IV-2

Cumulative frequency plot of 25 values of tungsten in plutonic samples, using both cumulative frequency and plotting percentage formulae. Solid lines denote cumulative frequency populations; dashed lines denote plotting percentage populations. There is little difference between the two methods.



representing class intervals accounting for 0 percent of the total population (e.g. 662-1950 ppm interval) are plotted but are not connected. The types of curves obtained in the study range from straight lines (one population) to smooth curves (more than one population) to ragged curves. Data points were connected by straight lines instead of smooth curves to facilitate drafting and this may account for some departure from a smooth curve. Other reasons for such departures include: incomplete sampling of the data set; non-lognormality of the distributions (although most trace elements have log-normal distributions (Levinson, 1974)) or; polymodality of data due to different bedrock types or change in element concentration by secondary dispersion effects (Parslow, 1974). Care was taken to ensure appropriate sample collection (unweathered) and adequate preparation of core before analysis, but errors can occur, resulting in poor cumulative frequency plots.

The graph can now be partitioned into its constituent populations. According to Sinclair (1974), the position of the inflection point indicates the relative proportions of the data set. If the populations are very different from each other (background vs. anomalous), there is a discernable change in slope of the curve, making the inflection point readily apparent. Less disparate populations or populations with a greater degree of overlap have more subtle slope changes, complicating establishment of

the inflection point. Paralow (1974) states visual estimation of the inflection point position may result in errors of \pm 5-10 percent; he also states that because most anomalous populations constitute a small portion of the total data set (less than or equal to 10 percent), this estimation may not compound any large error. It may be possible to formulate an equation of each cumulative frequency curve and, by using second derivatives obtain an accurate position of the inflection point. For the purposes of expediency, this was not done; instead, visual estimations were performed. Uncertainties in the inflection point position occurred, and so several different values were tried to obtain the 'best fit'. On the tungsten curve, the point was estimated at 32 cumulative percent, corresponding to 27 ppm on the abscissa scale.

Once the inflection point is obtained, each population of the data set can be defined. Each data point plotted on the graph represents a certain percentage of the total data, but also represents a certain cumulative percentage of one of the populations. For example, the last point plotted on the tungsten curve at the 1951 ppm abscissa level represents 4 percent of the total data. It also corresponds to $(4/32 * 100) = 12.5$ cumulative percent of population A, so a point is plotted at this ordinate level on the 1951 ppm level. This formula is repeated until there are enough points to draw a straight line, representing population A or until the points

start to curve. This would indicate the influence of the other population(s). The lines are fitted by regression analysis. One of the problems encountered were too few data points to effectively partition the population. Where this happened, points from the cumulative curves were used and an approximate line was drawn.

The second population (B) is derived in the same way, although the complements of the cumulative frequency scale are used instead, e.g., 30 cumulative percent on the A scale is equivalent to 70 cumulative percent on the B scale.

Defining three or more populations is more complex and is described in Sinclair (1974).

To ensure the method is correct, the two populations are recombined using their defined proportions (e.g. 32 cumulative percent of A plus 68 cumulative percent of B) at various abscissa levels. If these 'check points' do not plot close to the original curve, the process should begin with a new inflection point or different proportions of each population.

The geometric mean of each partitioned population is chosen at the 50th cumulative percentile. The background corresponds to the mean of the lower population. Choosing a threshold is more difficult. If the populations did not overlap too much, there would be a significant change in

slope and the threshold could be chosen at that point. Usually this does not happen and thresholds are often chosen arbitrarily from various cumulative percentiles. Threshold values were chosen arbitrarily by Sinclair (1974) at the 97.5 (or 98; or 99) and the complementary 2.5 (or 2; or 1) cumulative percentiles of the partitioned populations A and B, respectively. This divides data into three groups at the corresponding ppm levels, so that for example, 99 percent of population A (and 1 percent of population B) is above a certain ppm value, and 99 percent of B (and 1 percent of A) is below a certain level. See Sinclair for further information.

The purpose of choosing the threshold is to effectively segregate the anomalous values from the normal background data set. Sinclair's method of choosing a threshold value from each population divides the data into three groups. The upper group contains most of the anomalous population; the middle group contains a mixture of anomalous and background values; the lower group contains most of the background values. In this way priorities can be attached to the data for subsequent work: top values demand top priority for follow-up investigation, whereas those of the middle group are of secondary importance.

It is important to compare the values in each group with rock types, sample locations and topography - do not simply

look at the numbers. For example, those values in the middle group which occur in the same location as those of the anomalous group can be included in any follow-up examination.

The following is an example of constructing a cumulative frequency diagram using tungsten in monzogranite.

1. Range : <1 to 5400 ppm Use 1 in the computations, so that,
 $\text{Range} = \log 5400 - \log 1$
 $= 3.73$ Round to 3.75

2. Use 8 intervals; thus Interval Width = $3.75 / 8 = 0.47$

Interval Range	Antilog of Range(ppm)	Count	% Total	Cumul. %
0-0.47	1 ⁺ -3	2	8	100
0.47-0.94	4-9	4	16	92
0.94-1.41	10-26	11	44	76
1.41-1.88	27-76	3	12	32
1.88-2.35	77-224	2	8	20
2.35-2.82	225-661	2	8	12
2.82-3.29	662-1950	0	0	4
3.29-3.76	1951-5754	1	4	4
		----- TOTAL 25		

*1 includes values <1 ppm

Cumul. Freq.	Plotting %
25	97.4
23	89.5
19	73.7
8	30.3
5	18.4
3	10.5
1	2.6
1	2.6

Partition the population :

3. Inflection Point(visually) = 32 cumulative % (equivalent to 27 ppm)

Therefore, Population A consists of 32 % of the data set and, Population B consists of $(100 - 32) = 68$ % of the data set.

4. Partition Points of Population A

- i. at 1951 ppm level = 4 cumulative % = $4/32 * 100 = 12.5$ % of pop'n A
- ii. at 225 ppm level = 12 cumulative % = $12/32 * 100 = 37.5$ %
- iii. at 77 ppm level = 20 cumulative % = $20/32 * 100 = 62.5$ %

5. Partition Points of Population B

- i. at 19 ppm level = 50 cumulative %(A scale) = 50 cumul. %(B) = $50/68 * 100 = 73.5$ % (on B scale) = 26.5 % (A scale)
- ii. at 10 ppm level = 76 cumulative %(A scale) = 24 cumul. %(B) = $24/68 * 100 = 35.3$ % (B)
- iii. at 4 ppm level = 92 cumulative %(A scale) = 8 cumul. %(B) = $8/68 * 100 = 11.8$ % (B)

Plot partition points on graph; draw best fit lines through the points. Recombine the two populations in the proportions 32 percent A plus 68 percent B at various ppm levels to see how well the partitioned populations correspond to the original curve.

6. Check Point Calculations

Recombined Populations at a particular ppm level = "Point of Mixture"(Pm)

$$P_m = f_{A}P_A + f_{B}P_B$$

where $f_A = 32$ % or 0.32
 $P_A = A$'s cumulative % at any ppm level
 $f_B = 68$ % or 0.68
 $P_B = B$'s cumulative % at any ppm level

Thus:

- i. at 5.6 ppm level, $P_m = 0.32(90.5) + 0.68(84) = 86.1 \%$
- ii. at 15 ppm level, $P_m = 0.32(81.5) + 0.68(43) = 55.3 \%$
- iii. at 23 ppm level, $P_m = 0.32(78) + 0.68(24) = 41.3 \%$
- iv. at 40 ppm level, $P_m = 0.32(69) + 0.68(8.5) = 27.9 \%$
- v. at 150 ppm level, $P_m = 0.32(48) + 0.68(0.175) = 15.48 \%$
- vi. at 390 ppm level, $P_m = 0.32(32) + 0.68(0) = 10.24 \%$
- vii. at 1000 ppm level, $P_m = 0.32(20) + 0 = 6.4 \%$

The check points appear to closely correspond the original curve, so the partitioning is judged a success.

The above steps were repeated for the plotting percentage curve (not shown here) and similar populations were obtained.

	<u>Proportion</u>	<u>Proportion * N</u> (# of samples)	<u>Background</u> (50th %-ile)
Population A	32 %	8	~ 135 ppm
Population B	68 %	17	12 ppm

7. Arbitrary Thresholds

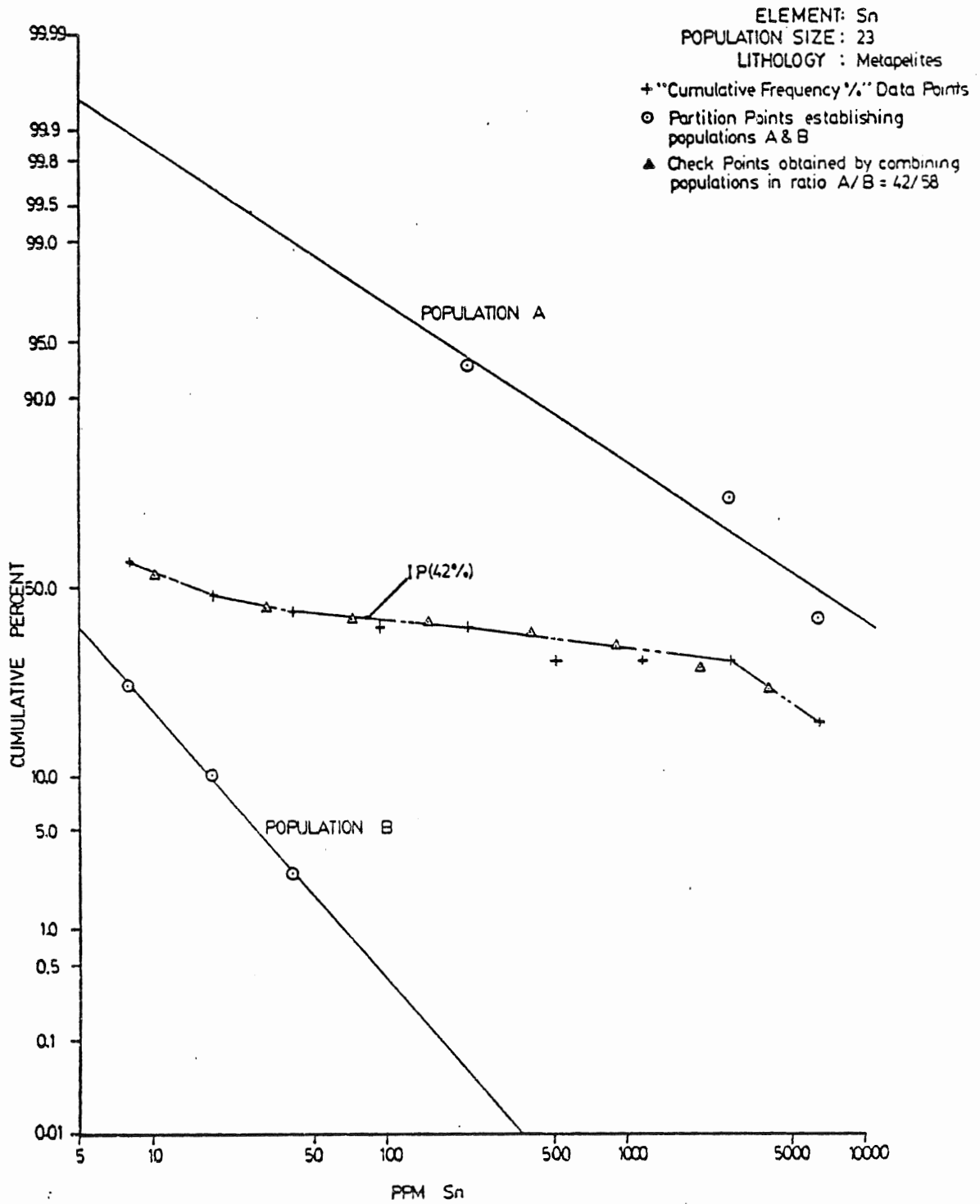
- i. By eye on graph; at inflection point = 27 ppm
Use as a 'lower threshold'
- ii. 99 cumulative % of population A = < 1 ppm
1 cumulative % of population B = 90 ppm
- iii. 98 cumulative % of population A = < 1 ppm
2 cumulative % of population B = 70 ppm
- iv. 2.5 cumulative % of population B = 65 ppm
Use as an 'upper threshold'

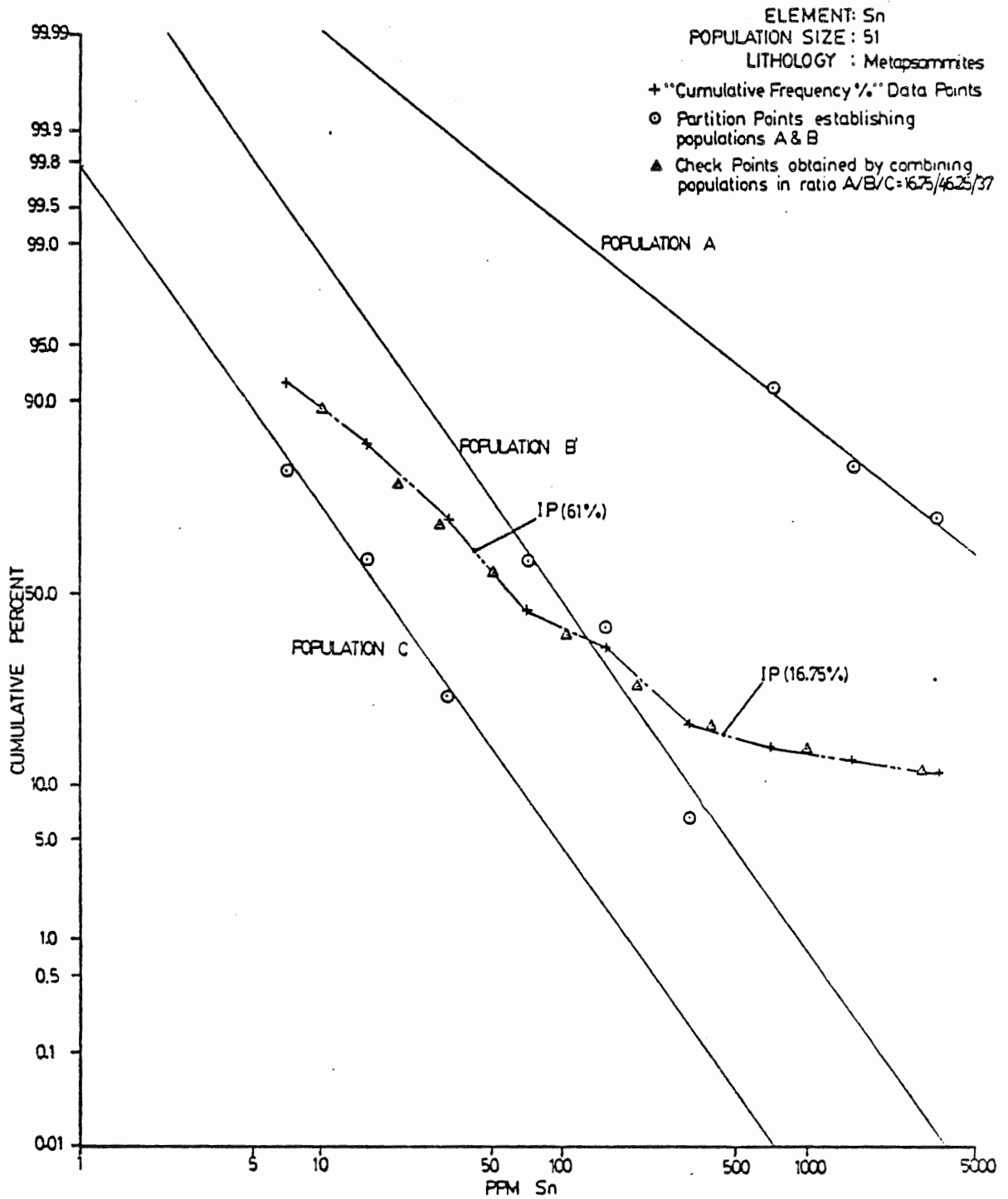
	<u># samples in group</u>
Group I <27 ppm	17
Group II >27 <65 ppm	3
Group III >65 ppm	5

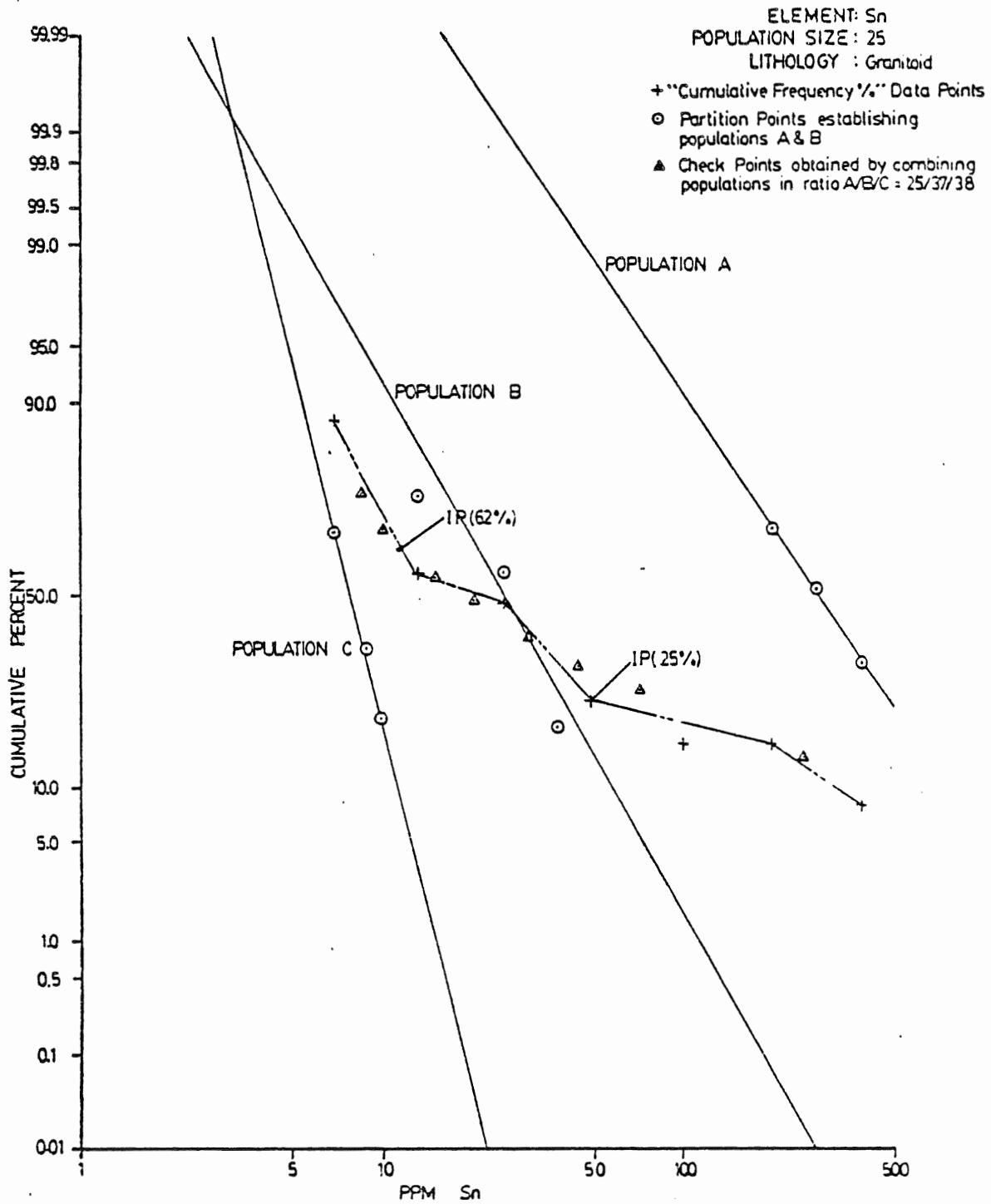
This appears to correspond well with the population partitioning. When compared back to the samples, those of groups II and III consist of 2 greisens and 6 'unmineralized'(with regard to tin) samples, containing rare to minor scheelite-bearing quartz veinlets. Tungsten does not appear associated with tin mineralization in greisens, but with other vein stages.

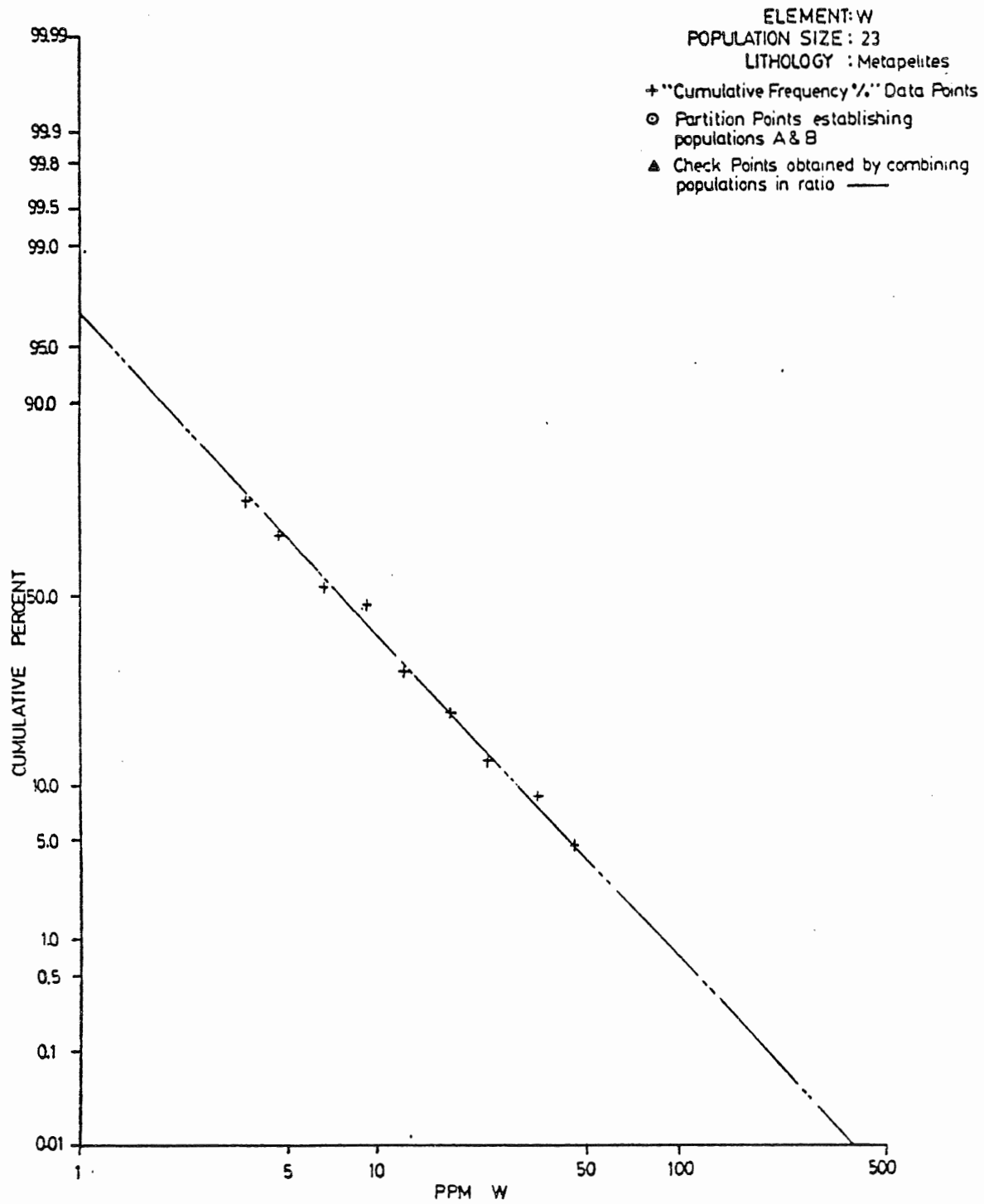
Figure IV-3

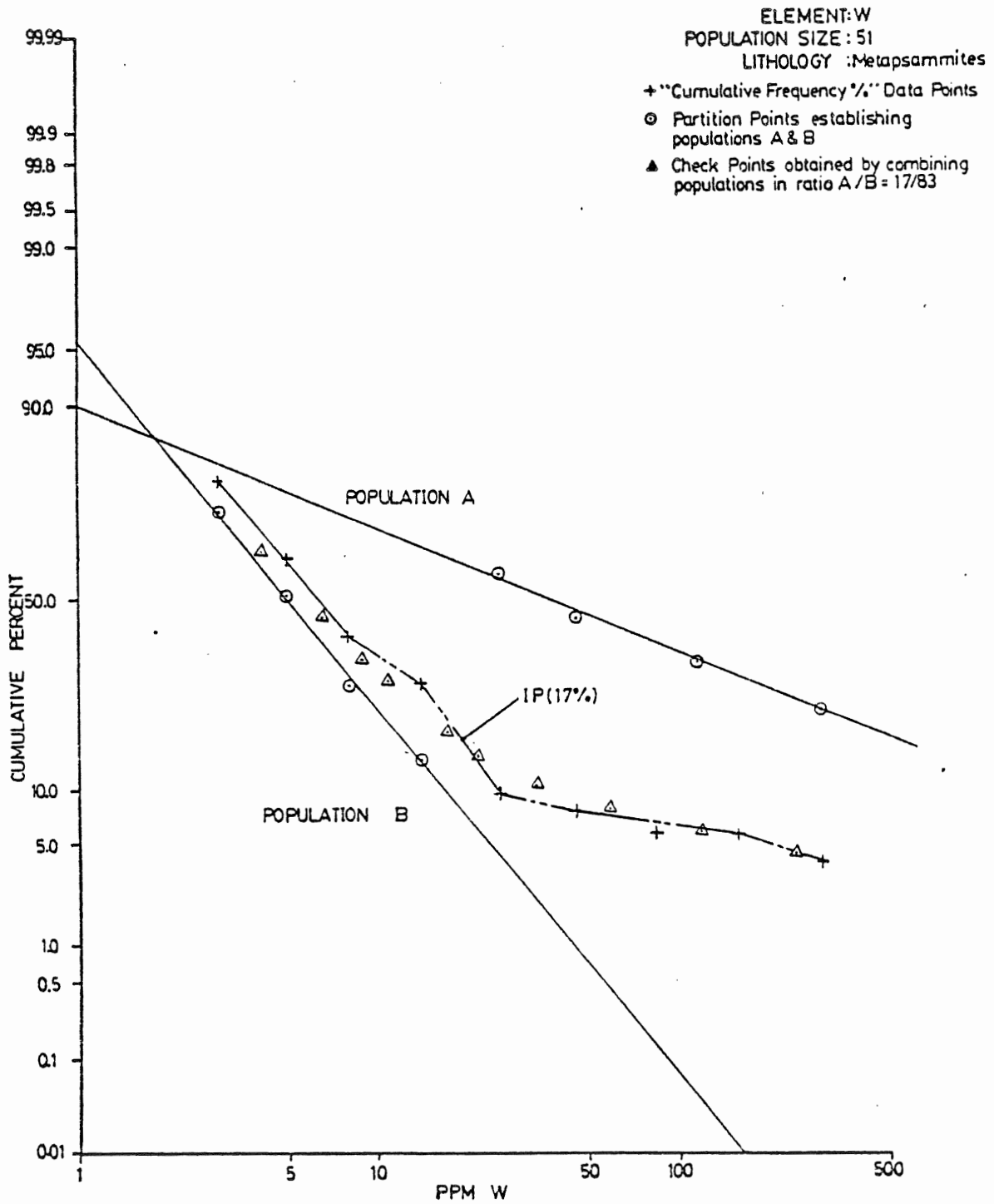
Cumulative frequency graphs of 11 elements
in 3 lithologies(33 graphs)

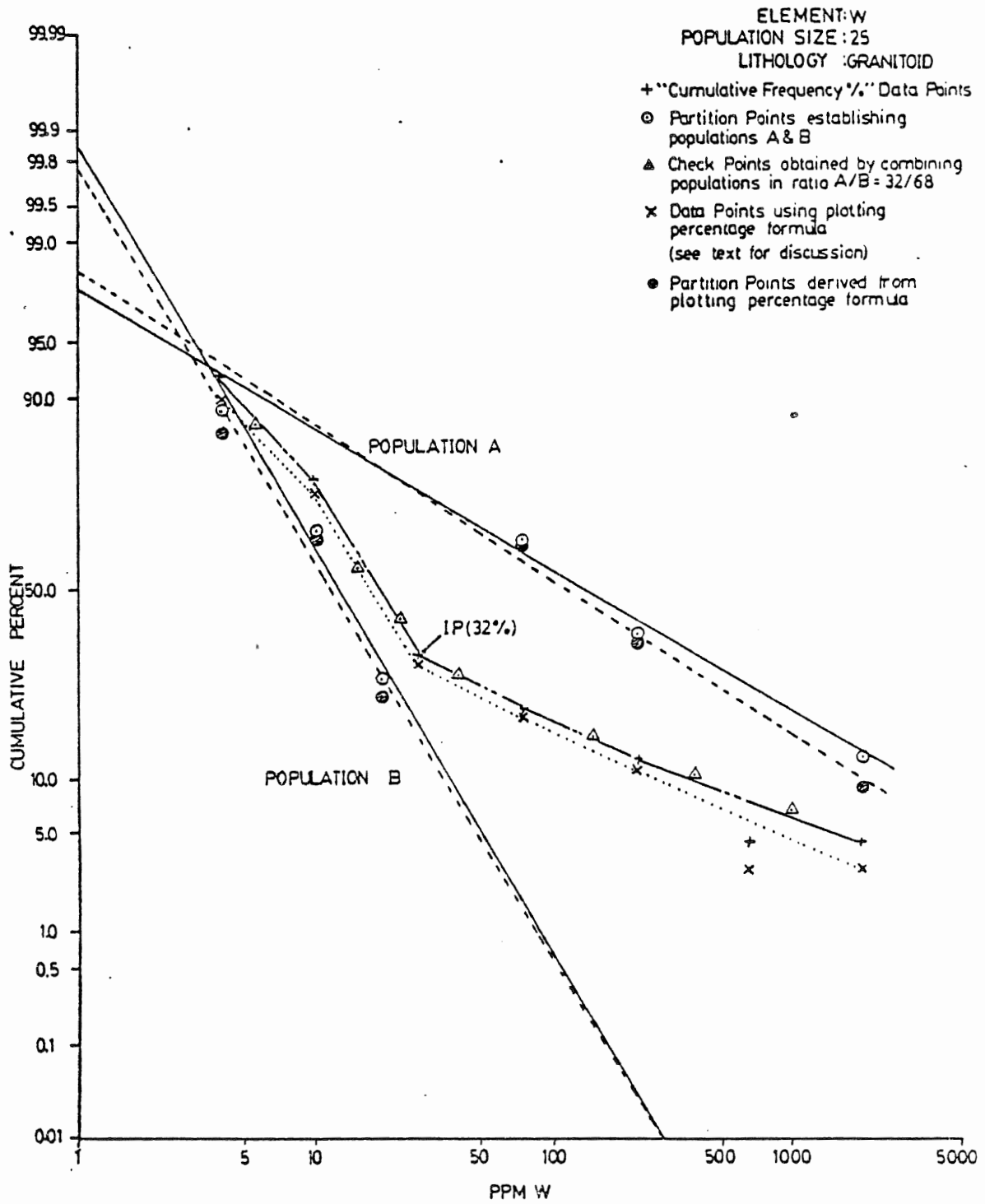




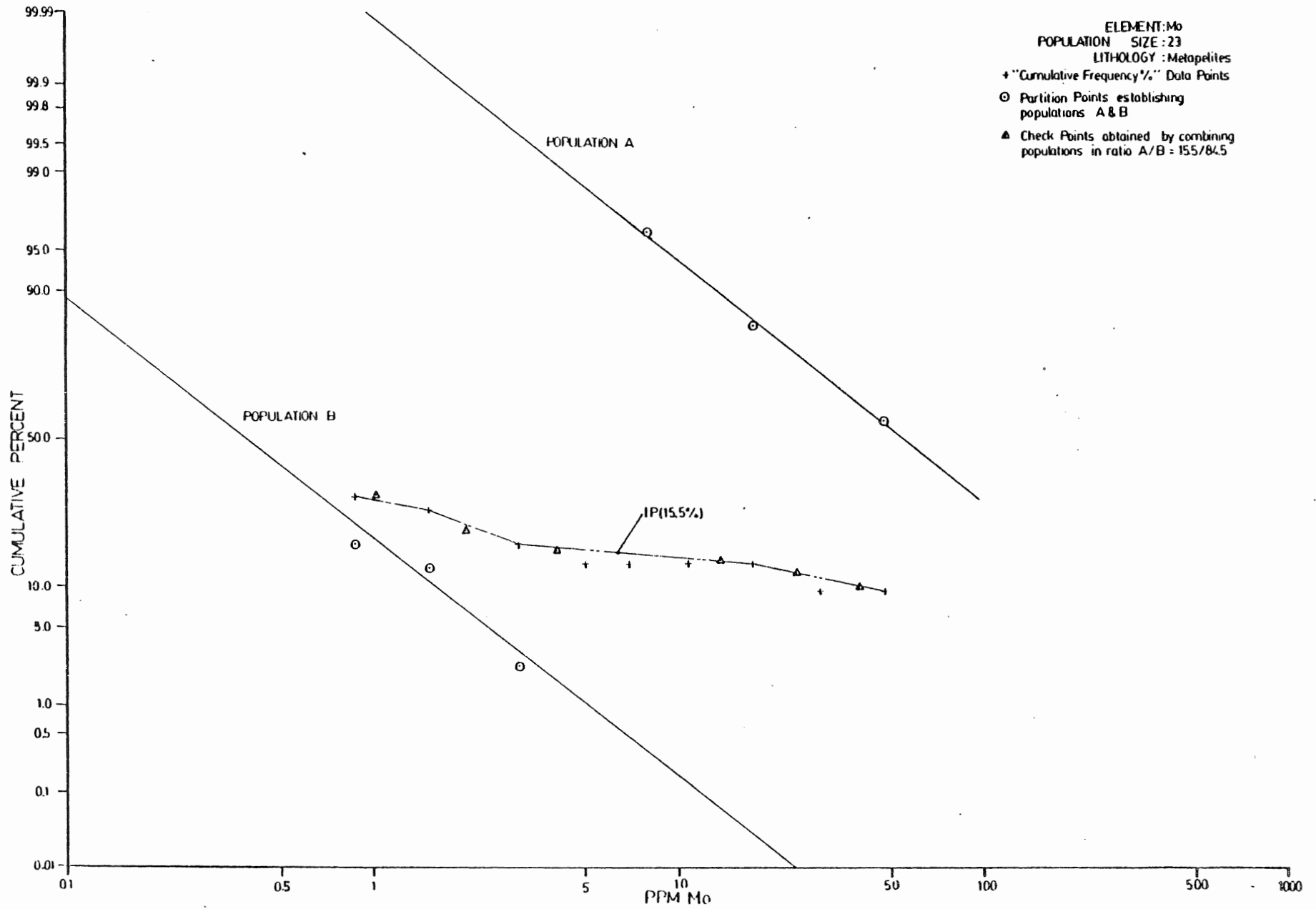


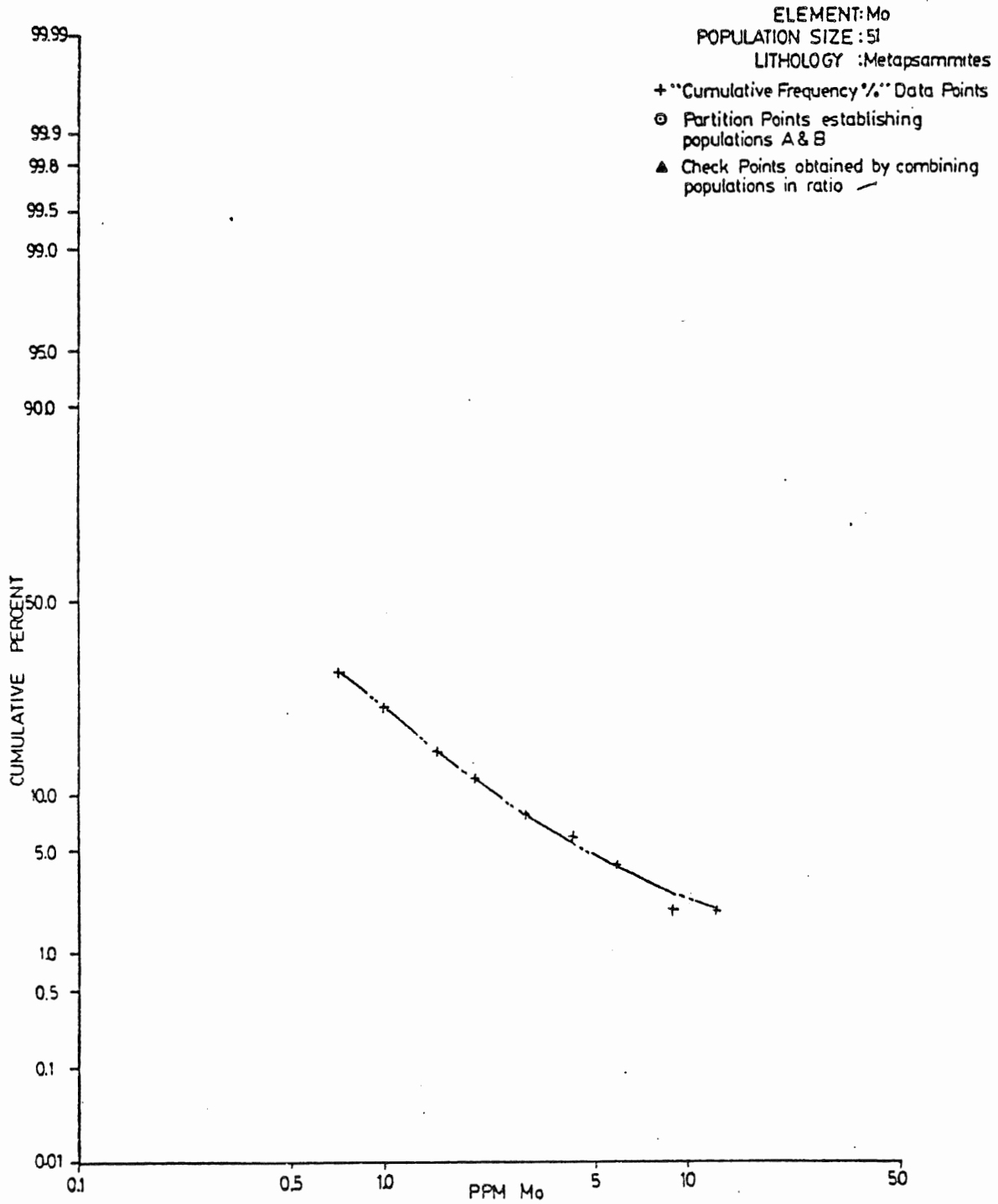


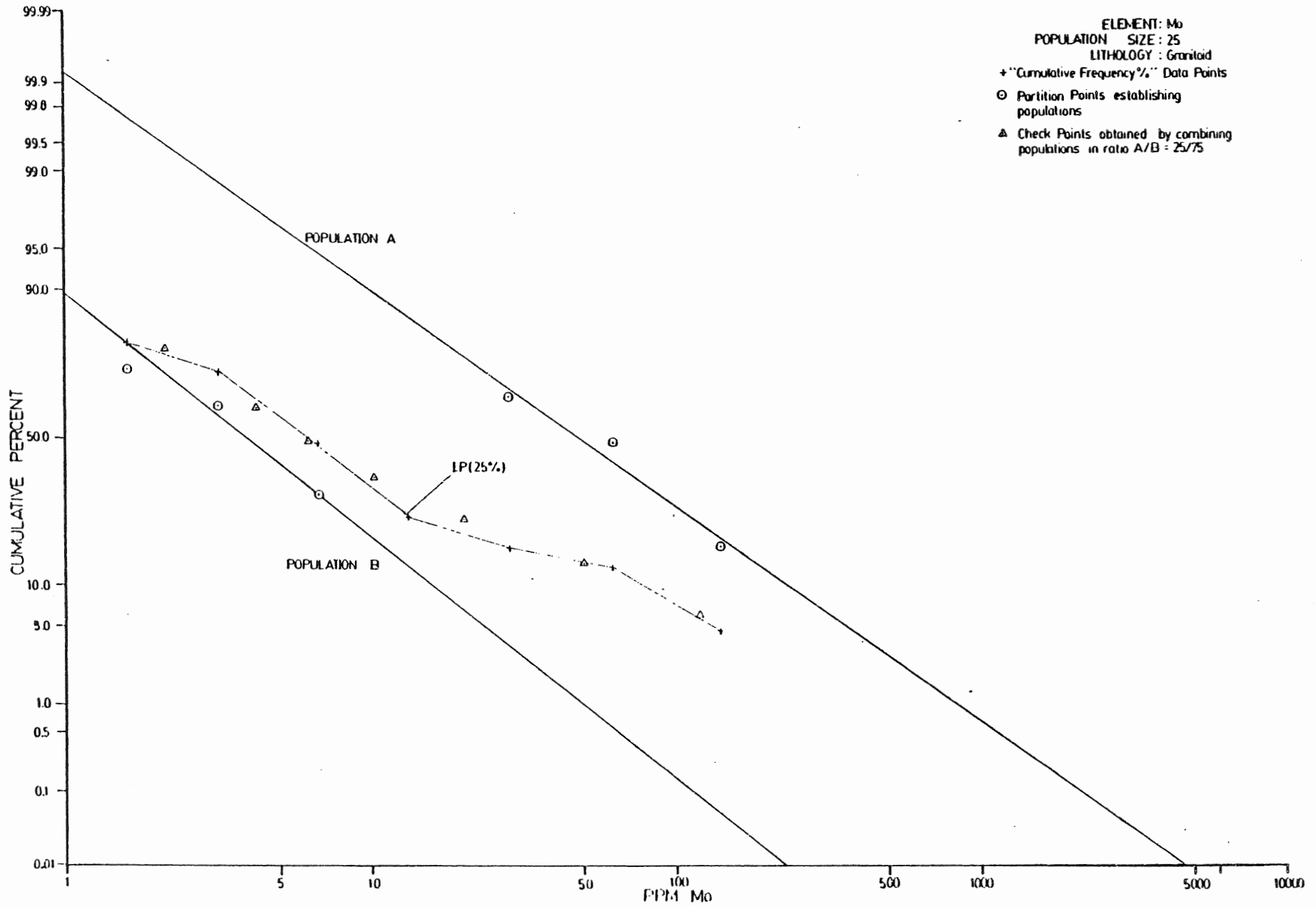


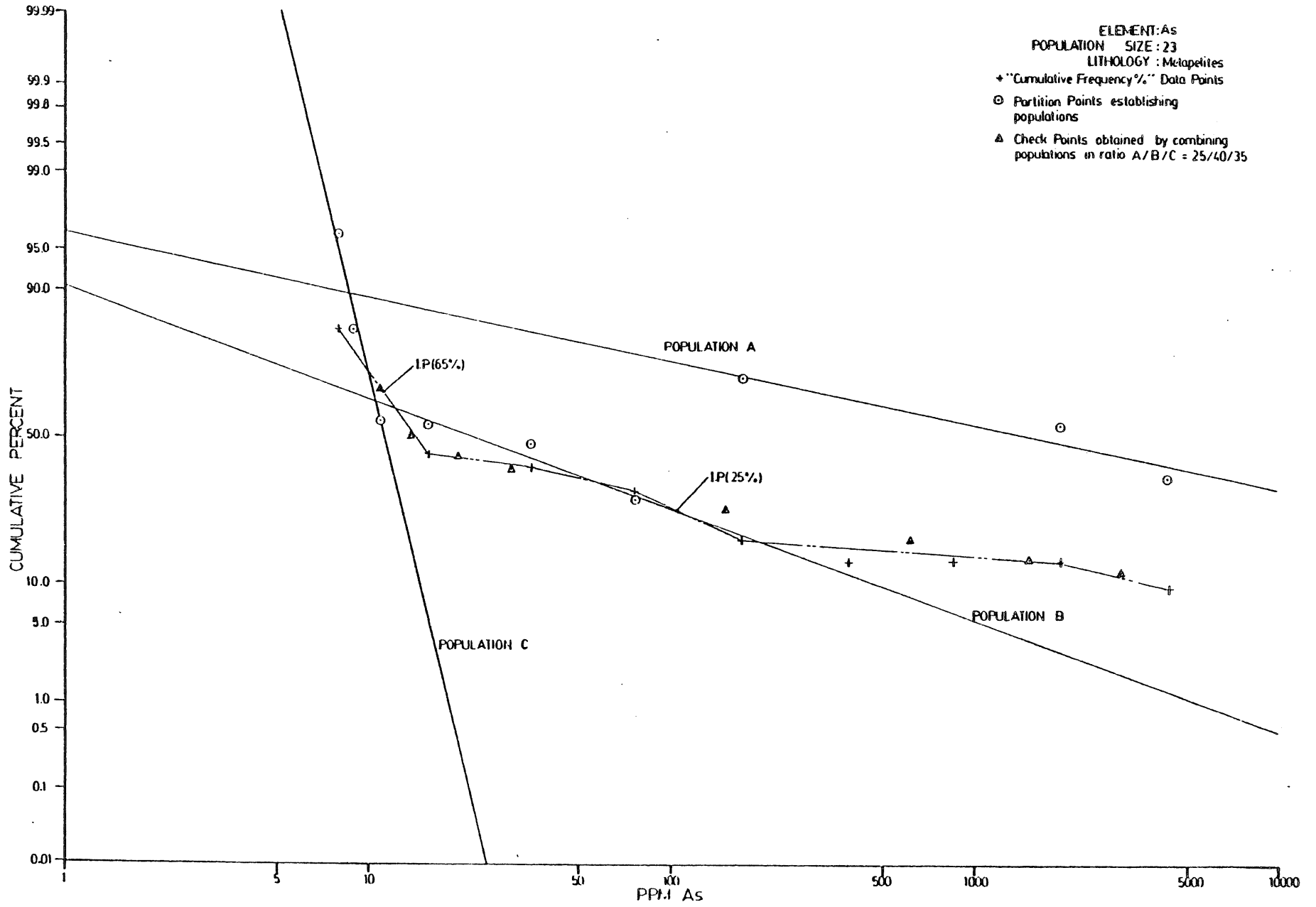


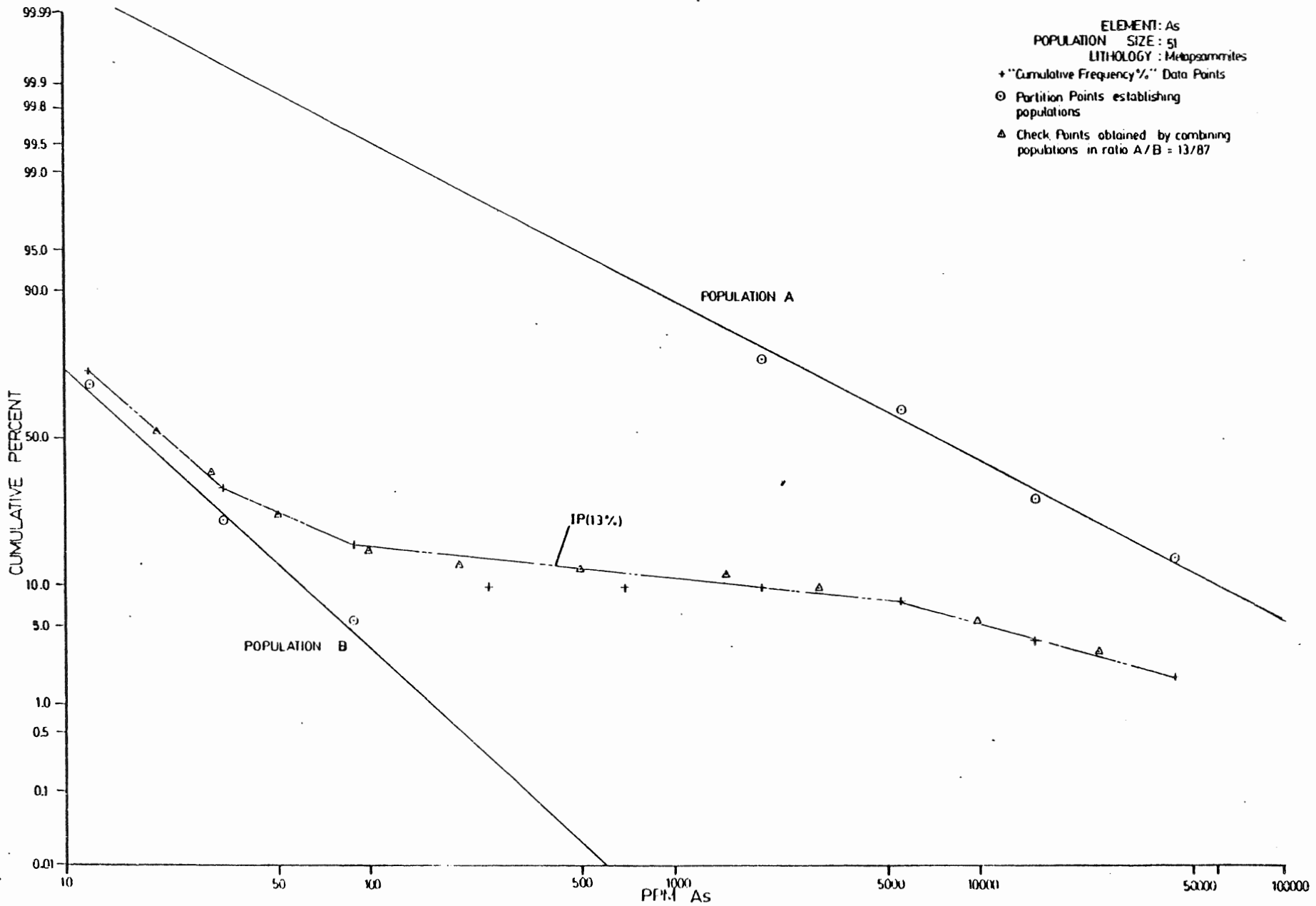
340



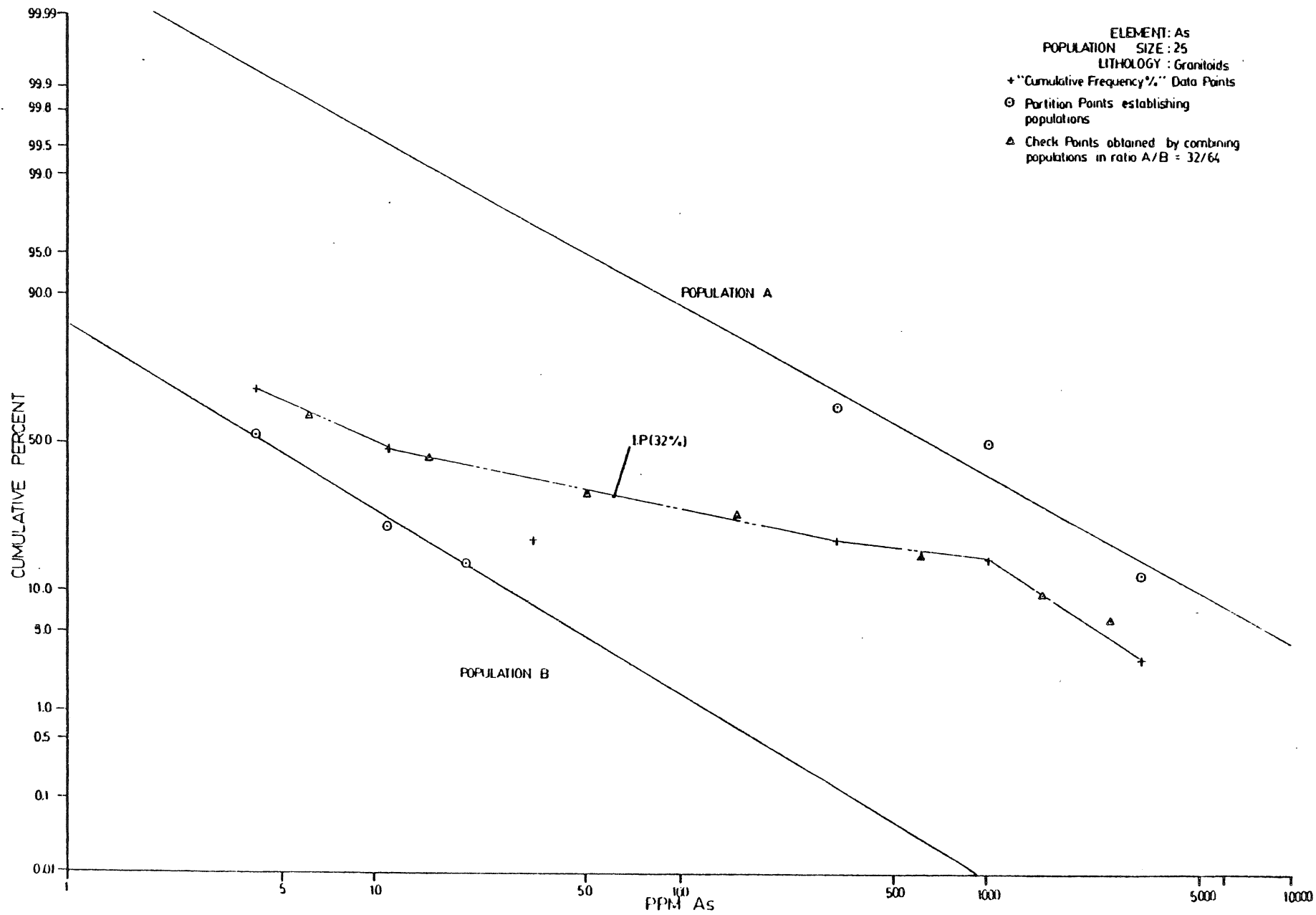


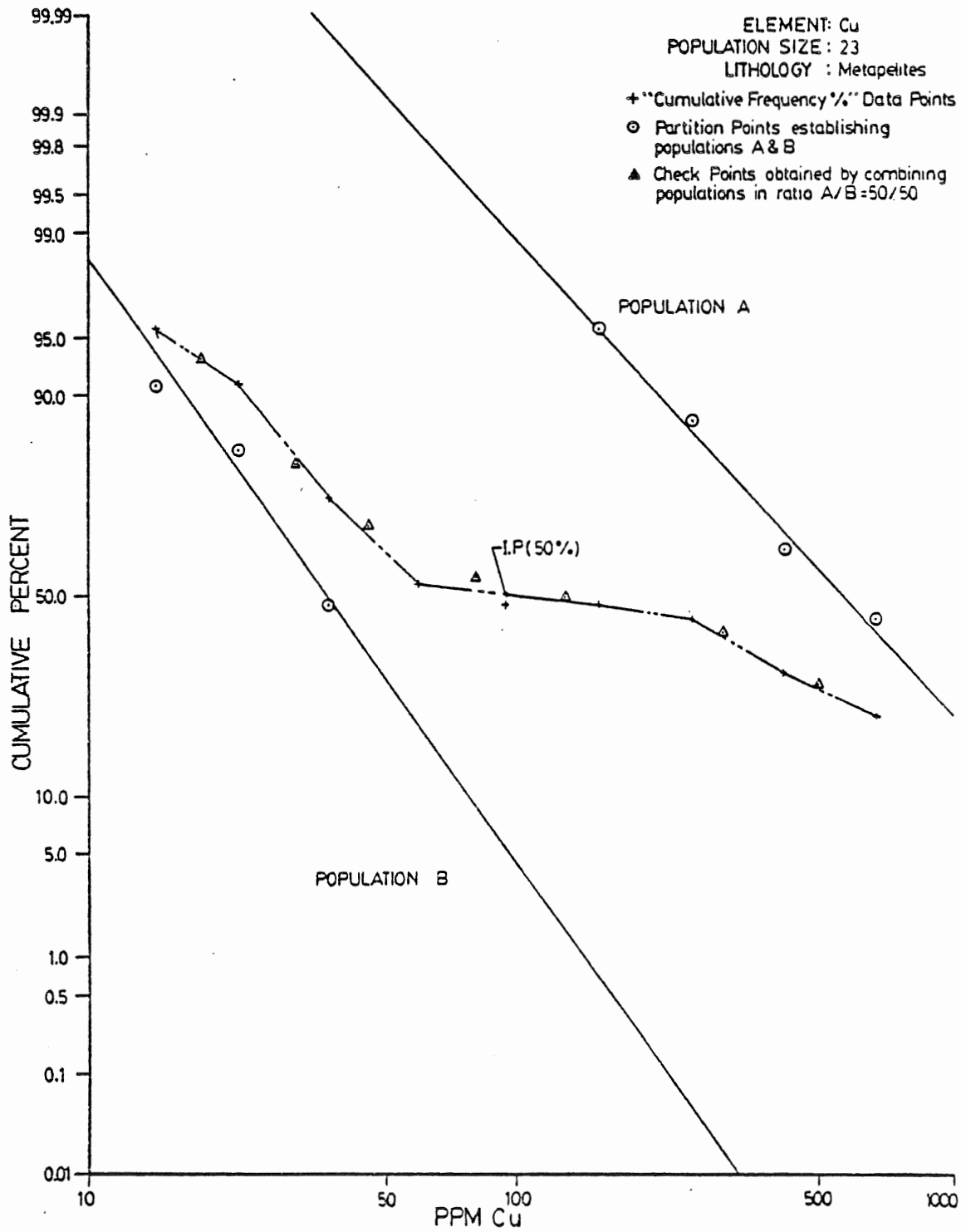




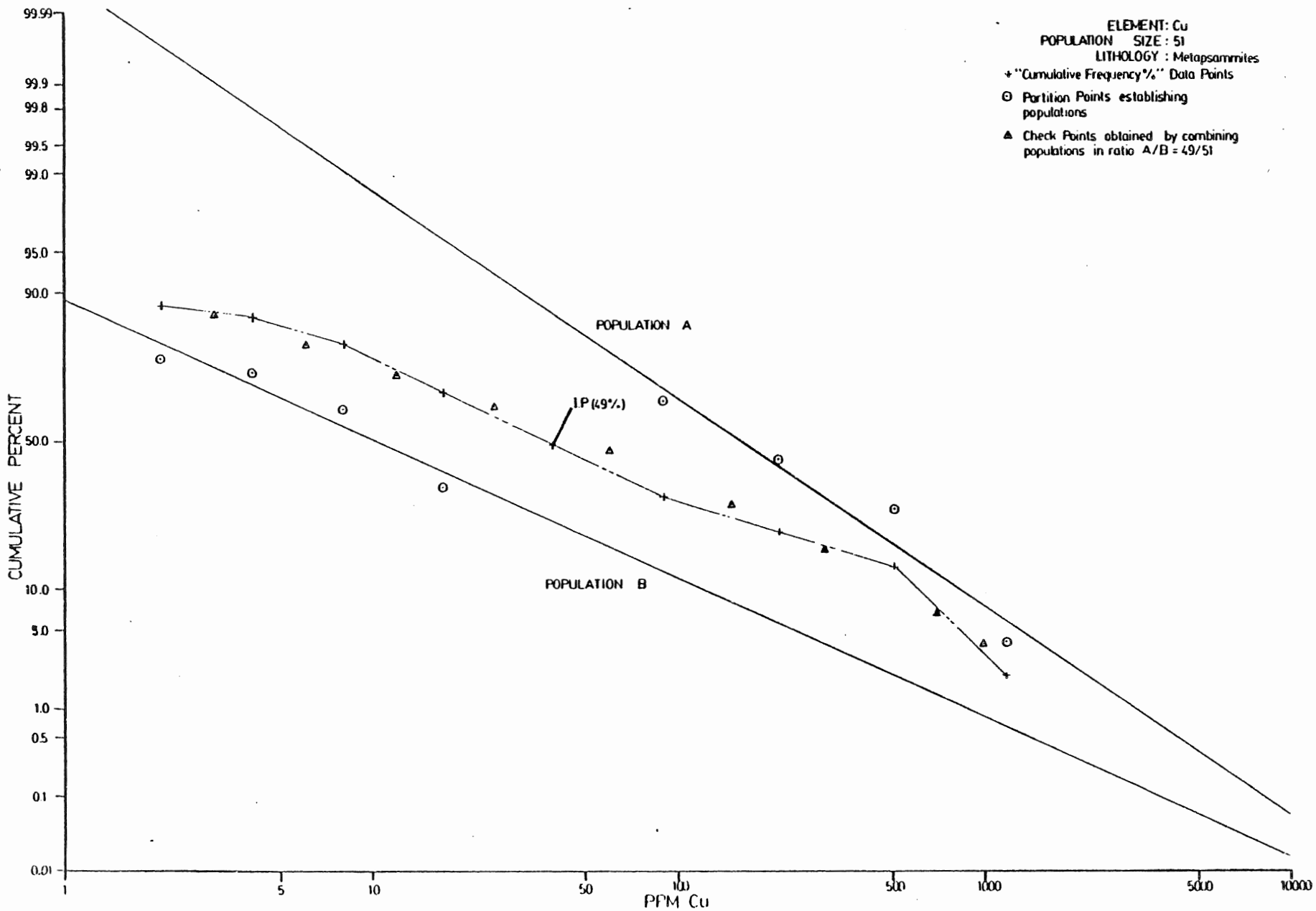


345

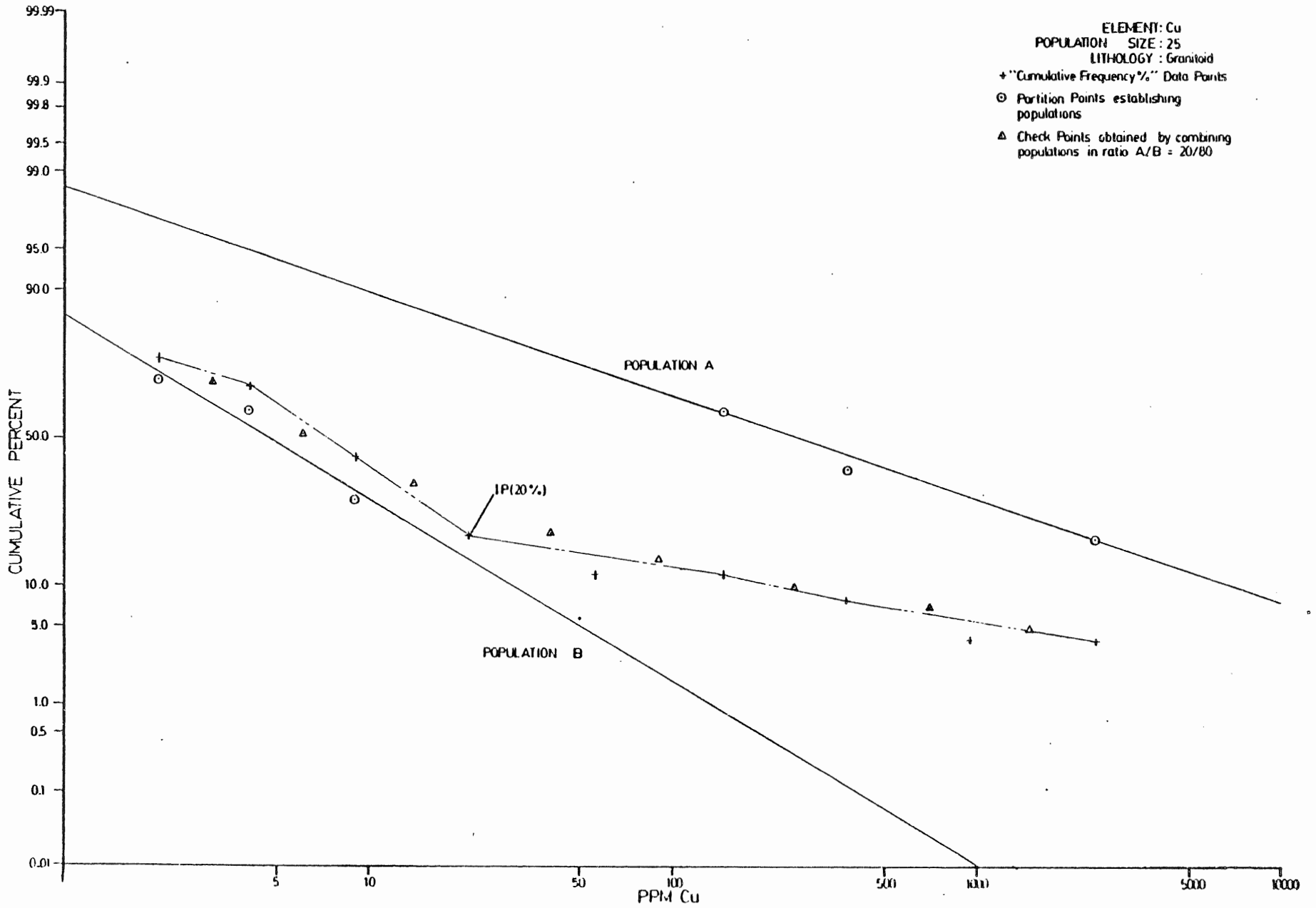




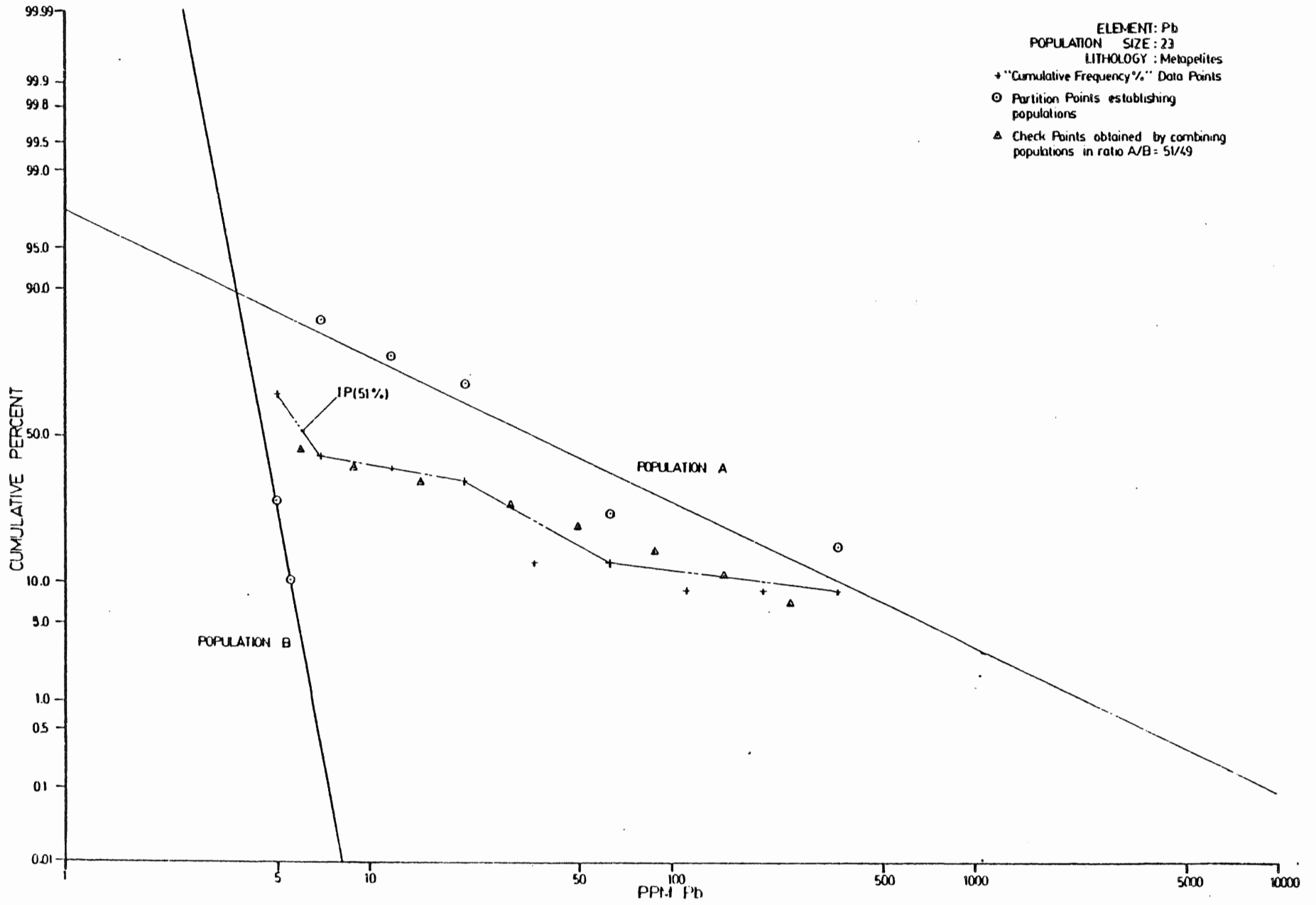
347



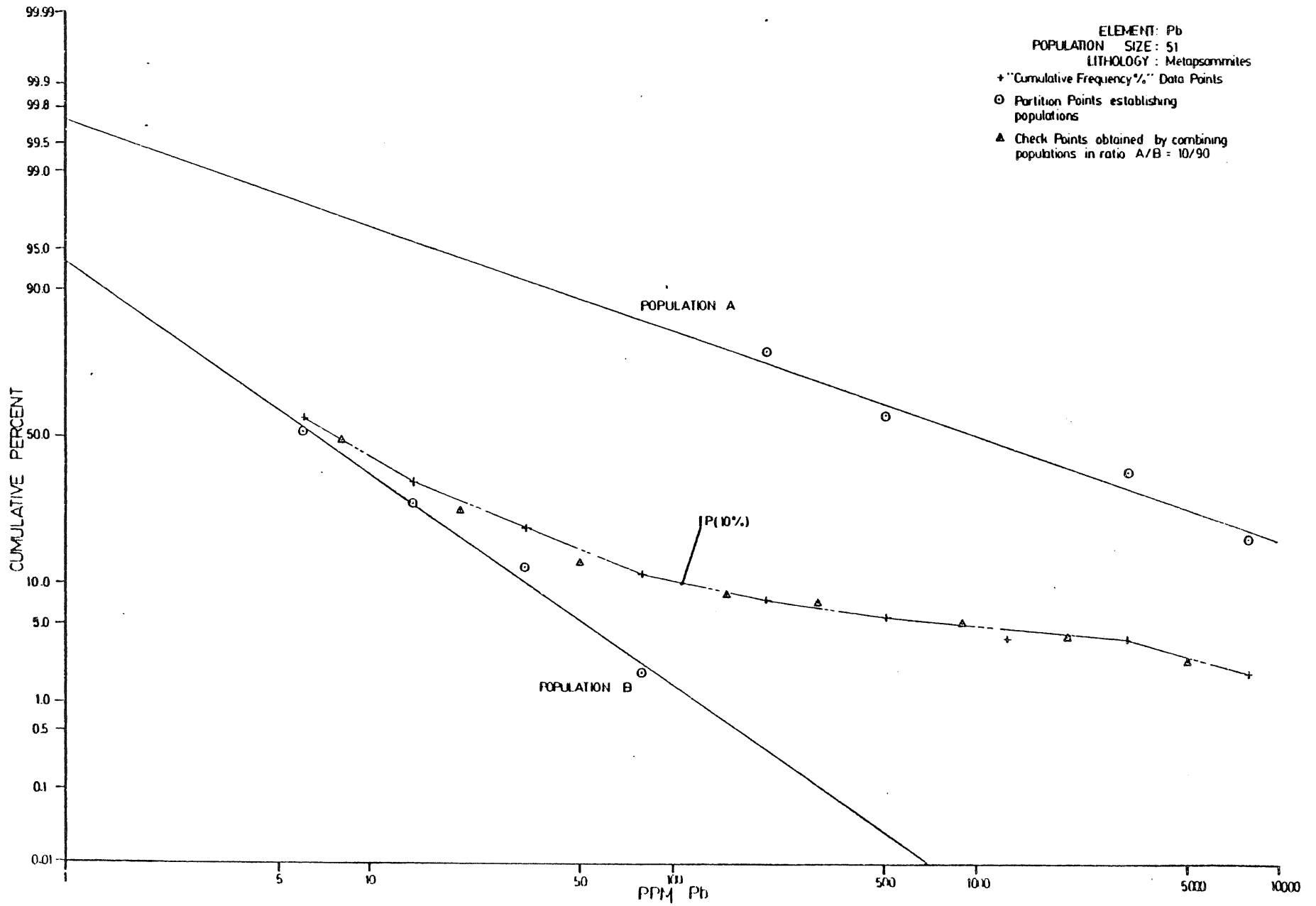
348

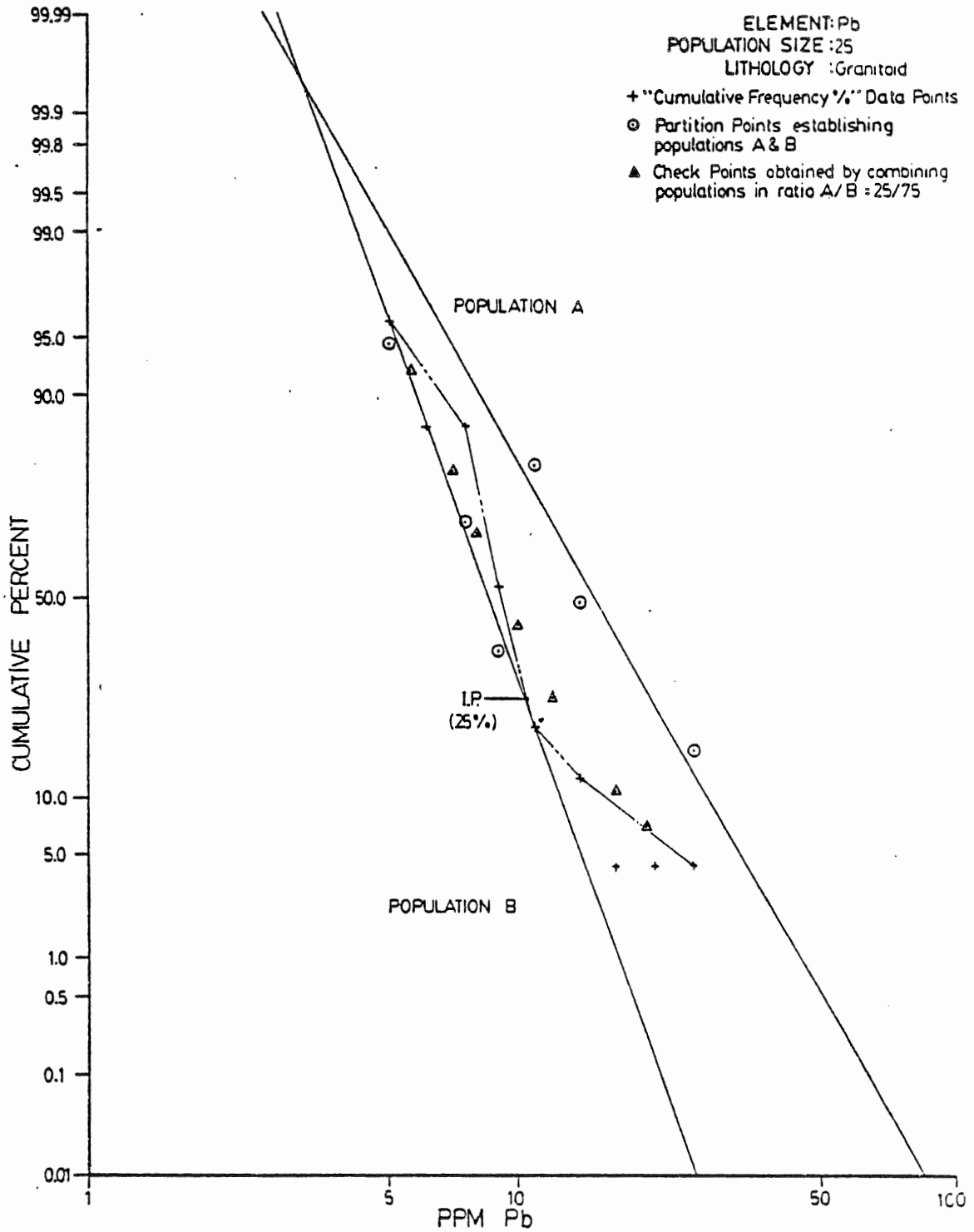


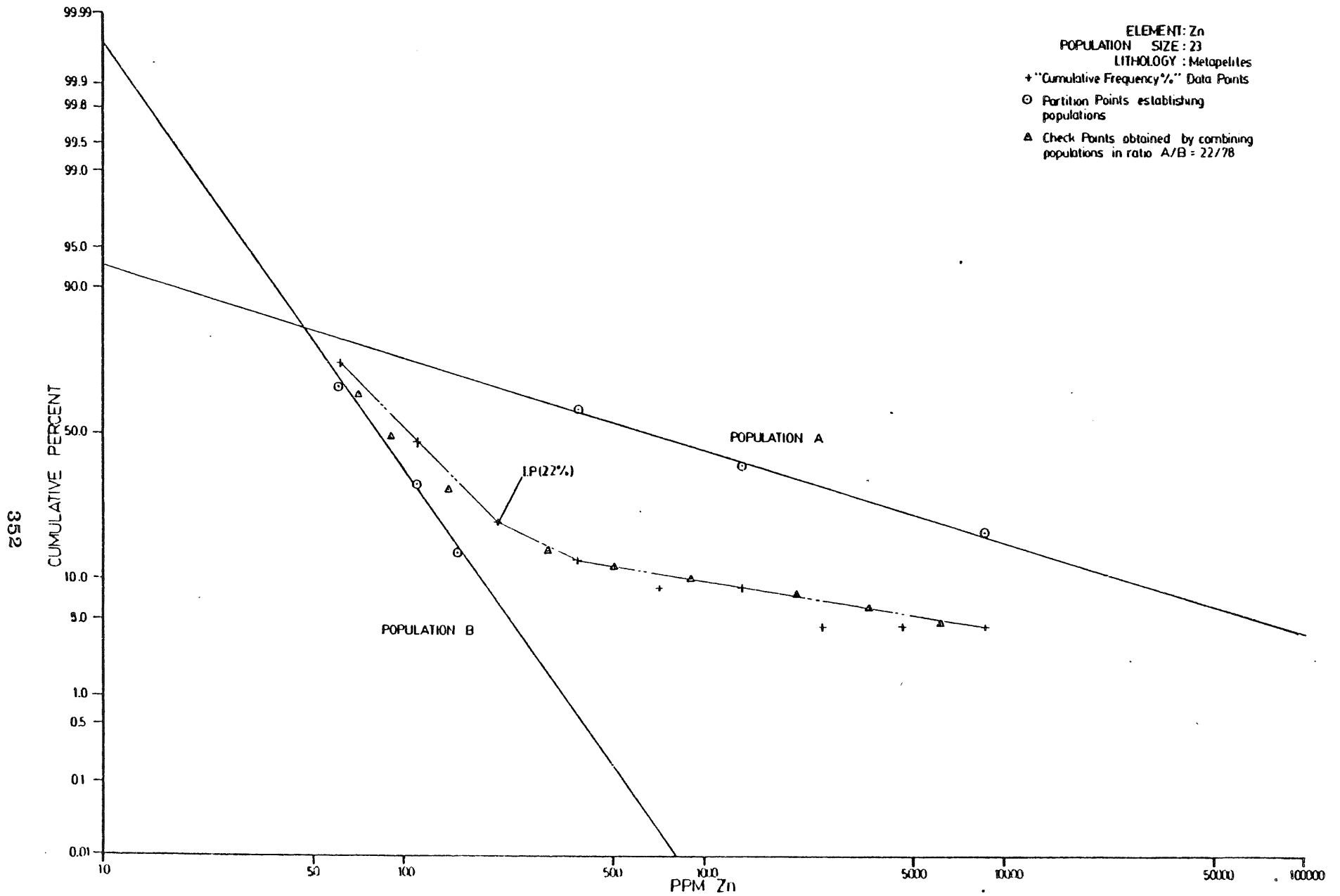
349

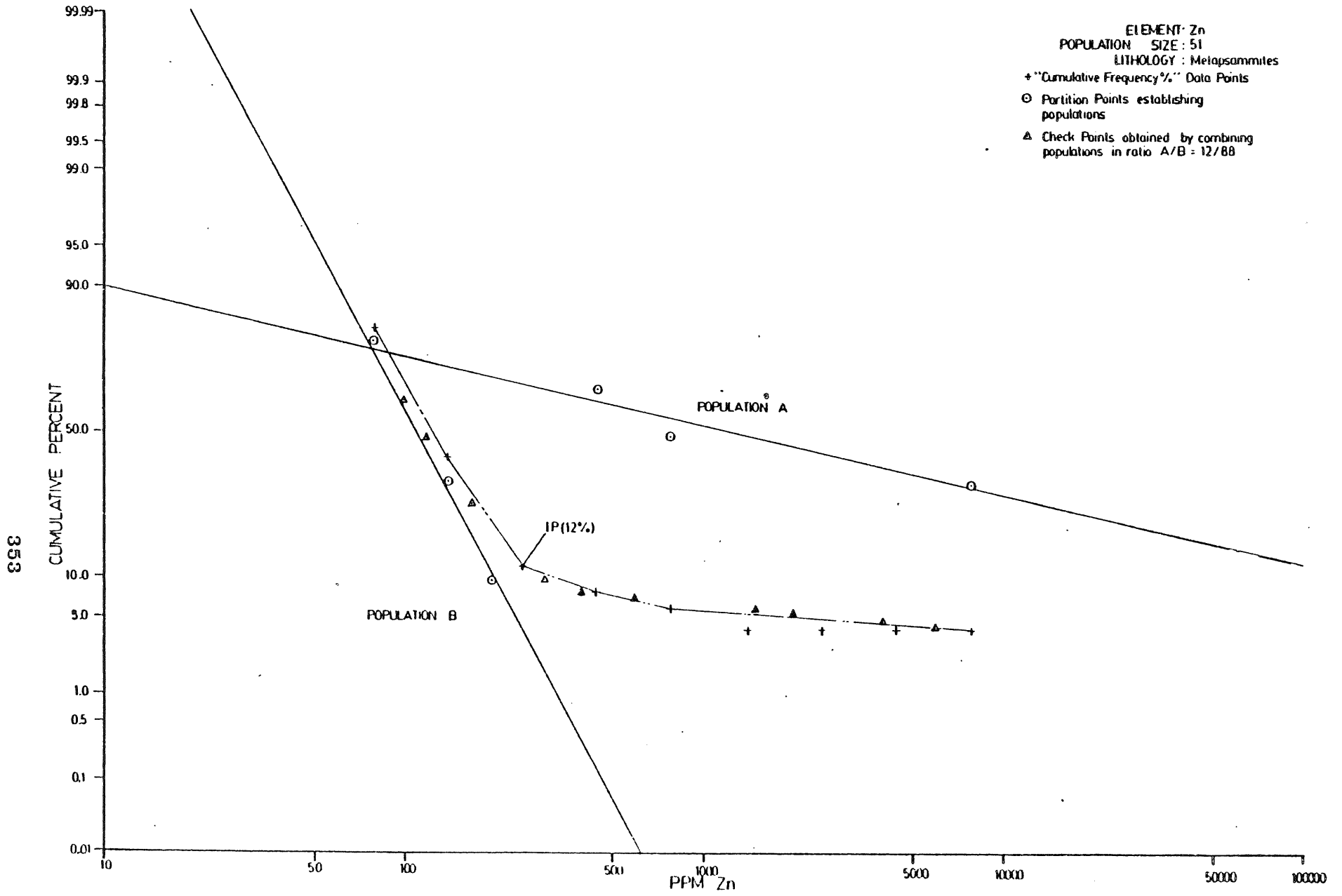


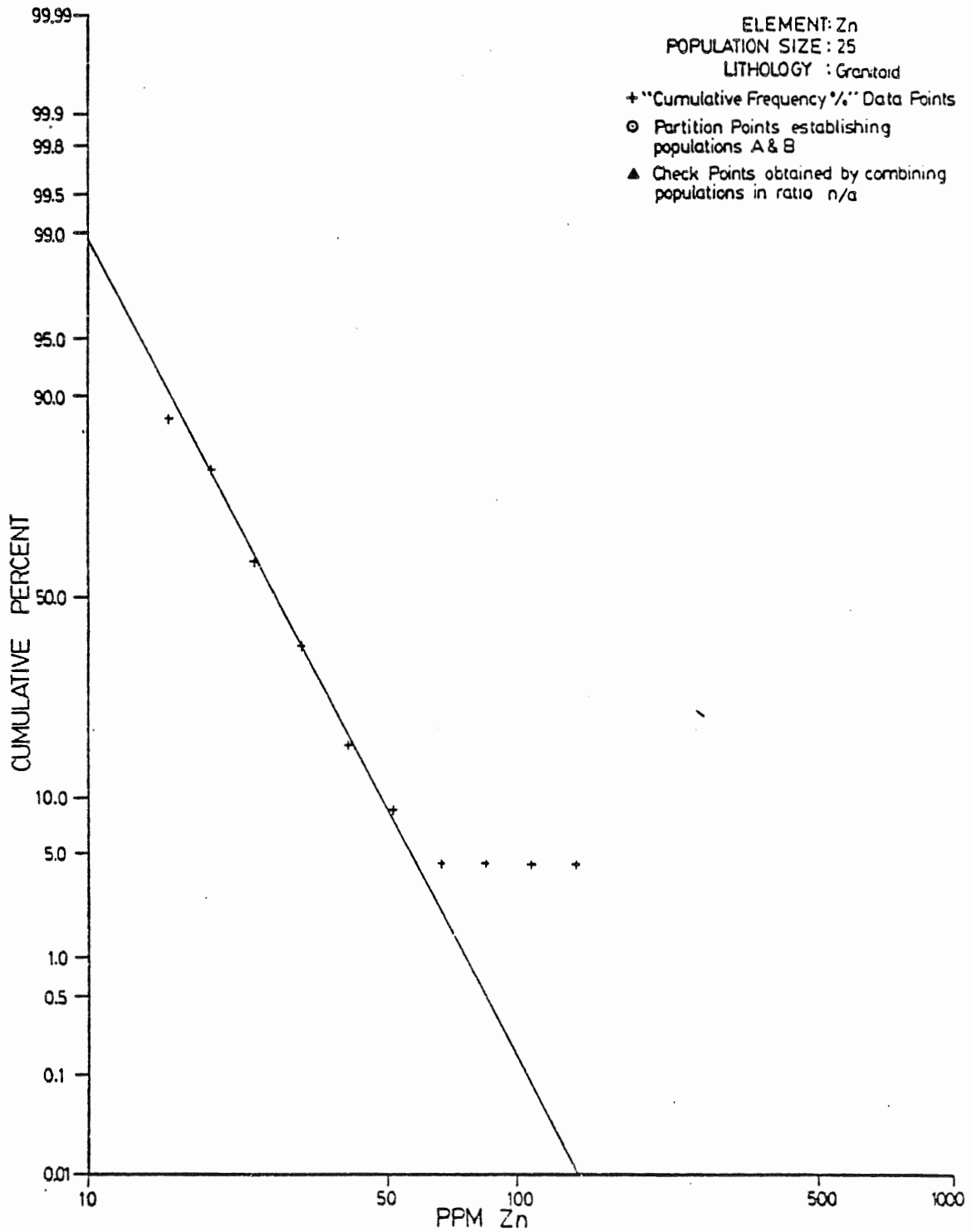
058

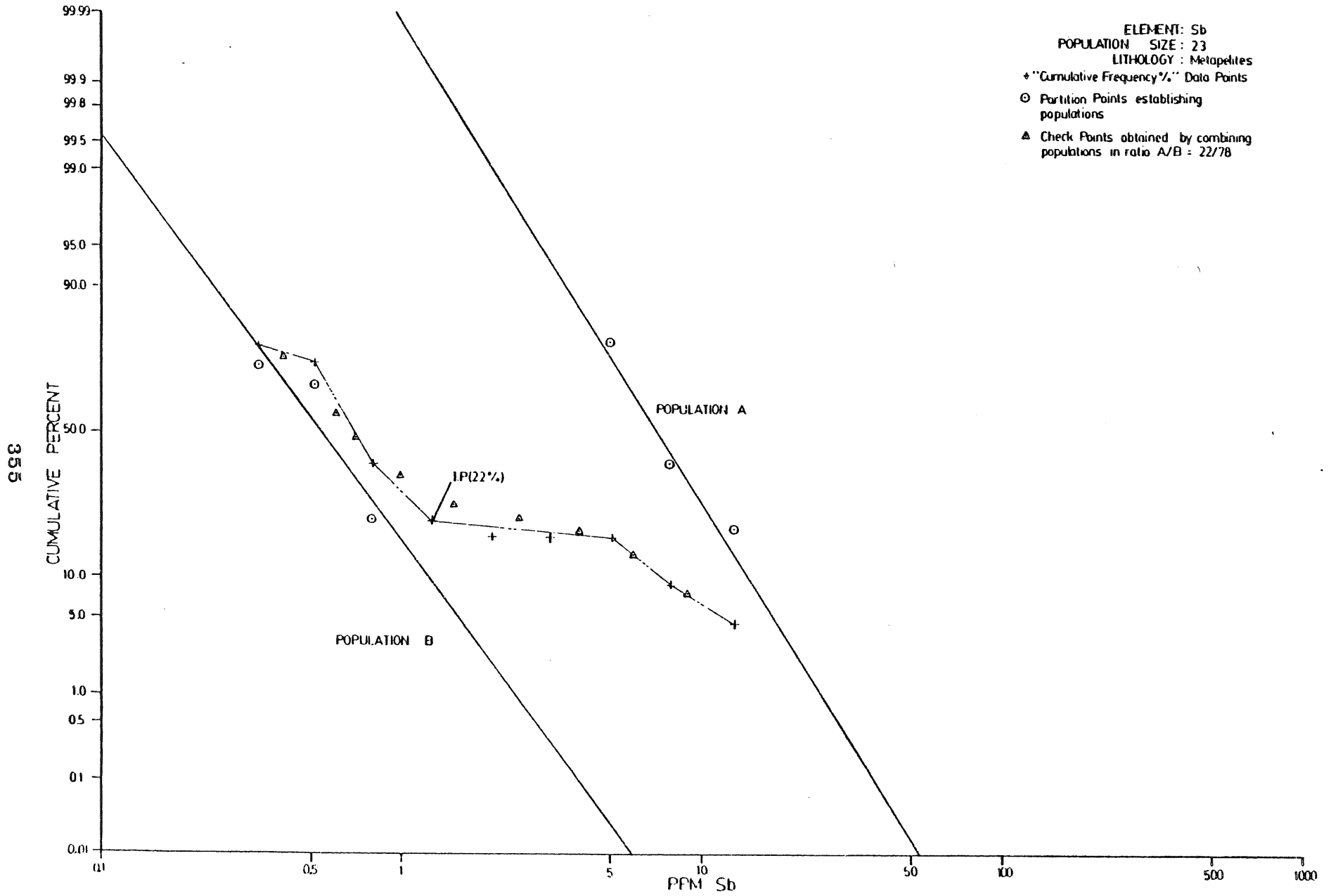




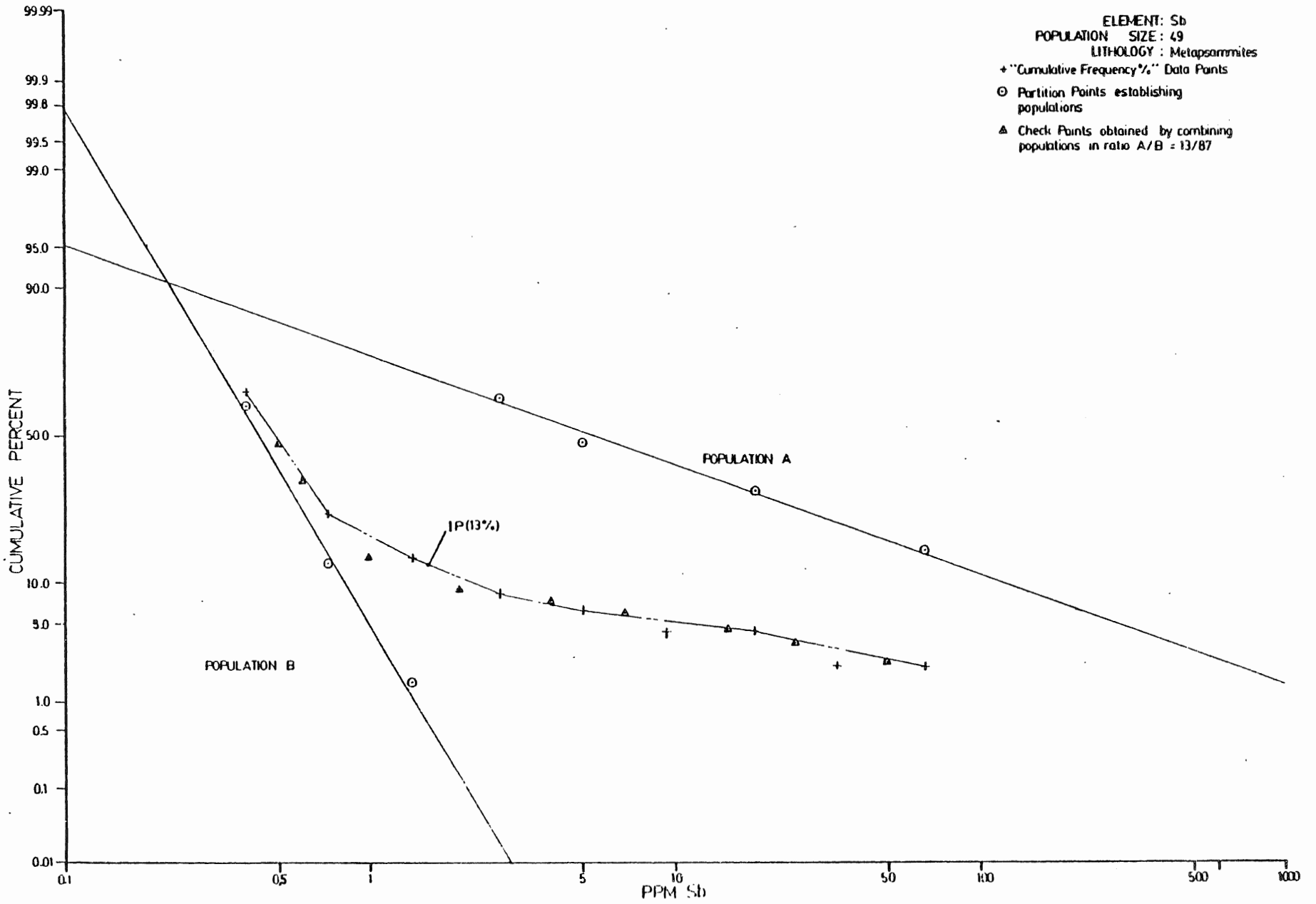




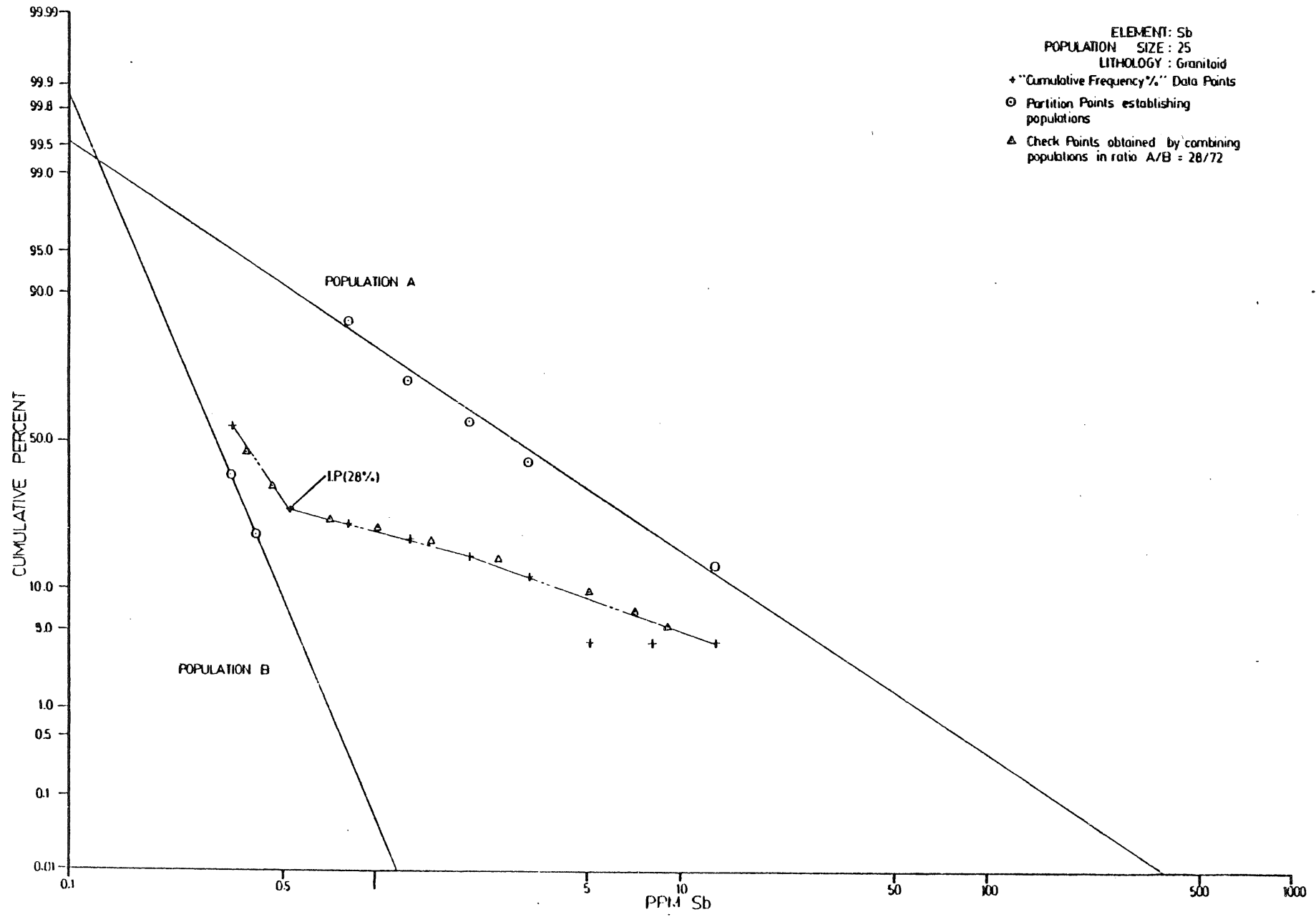


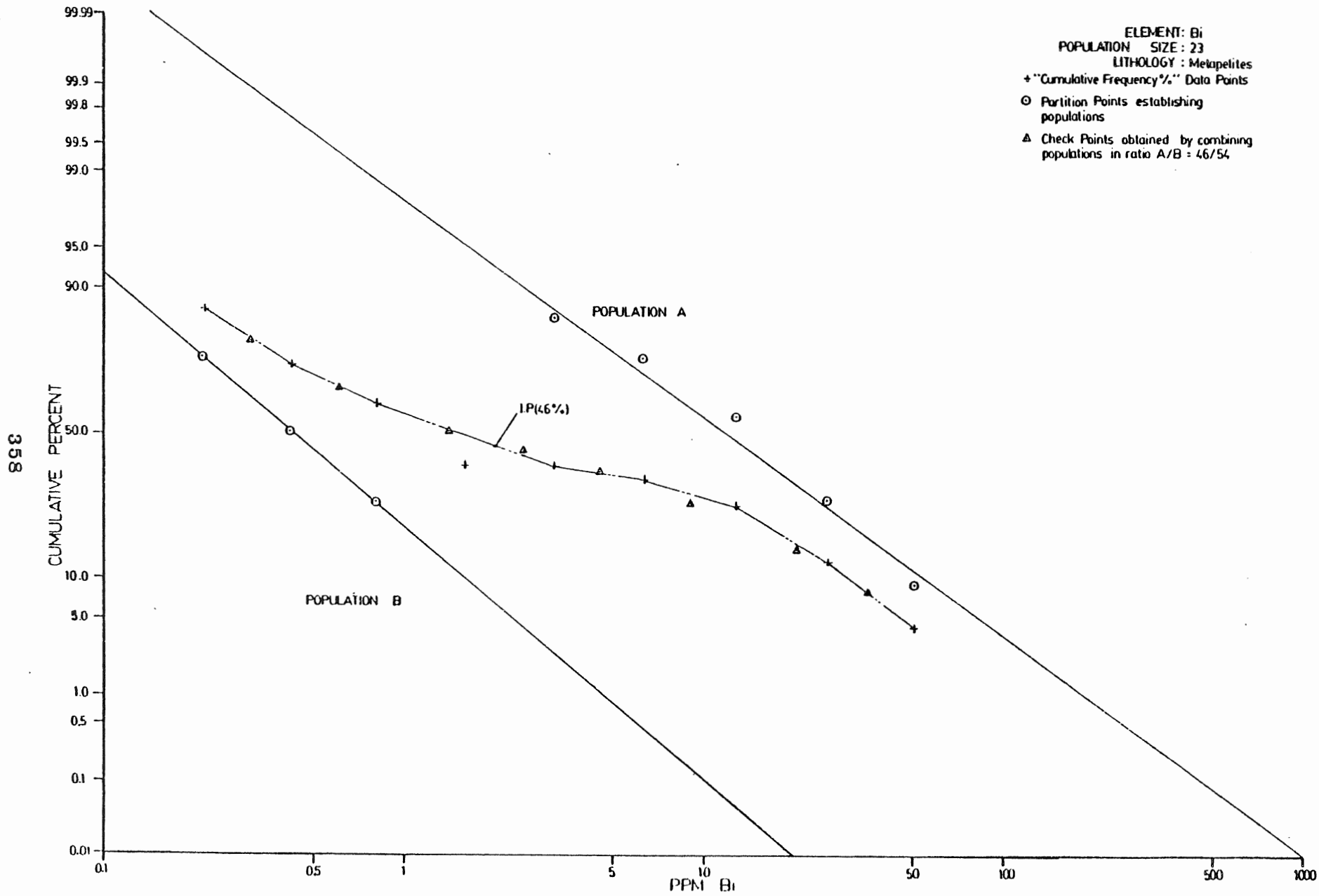


358

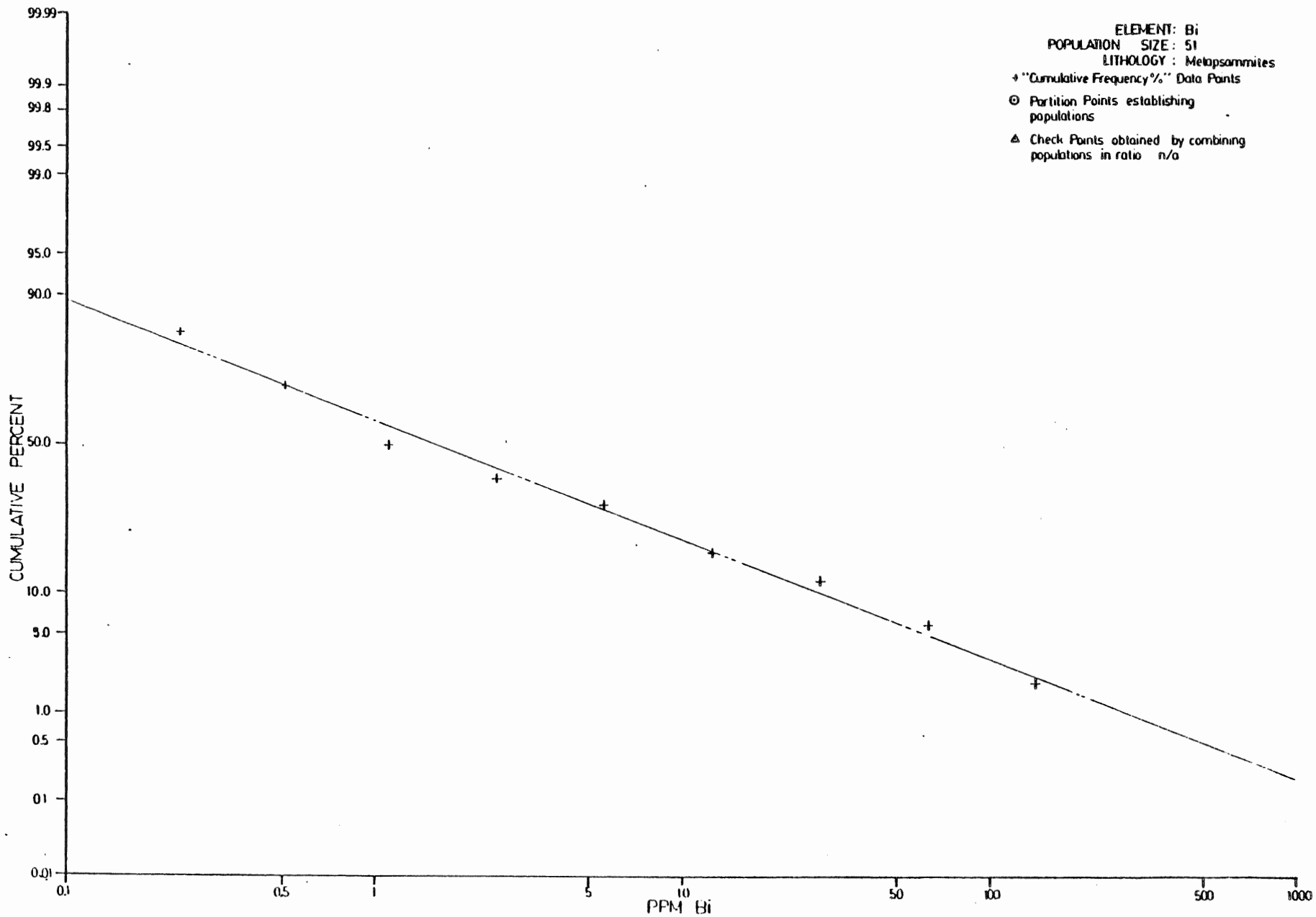


357

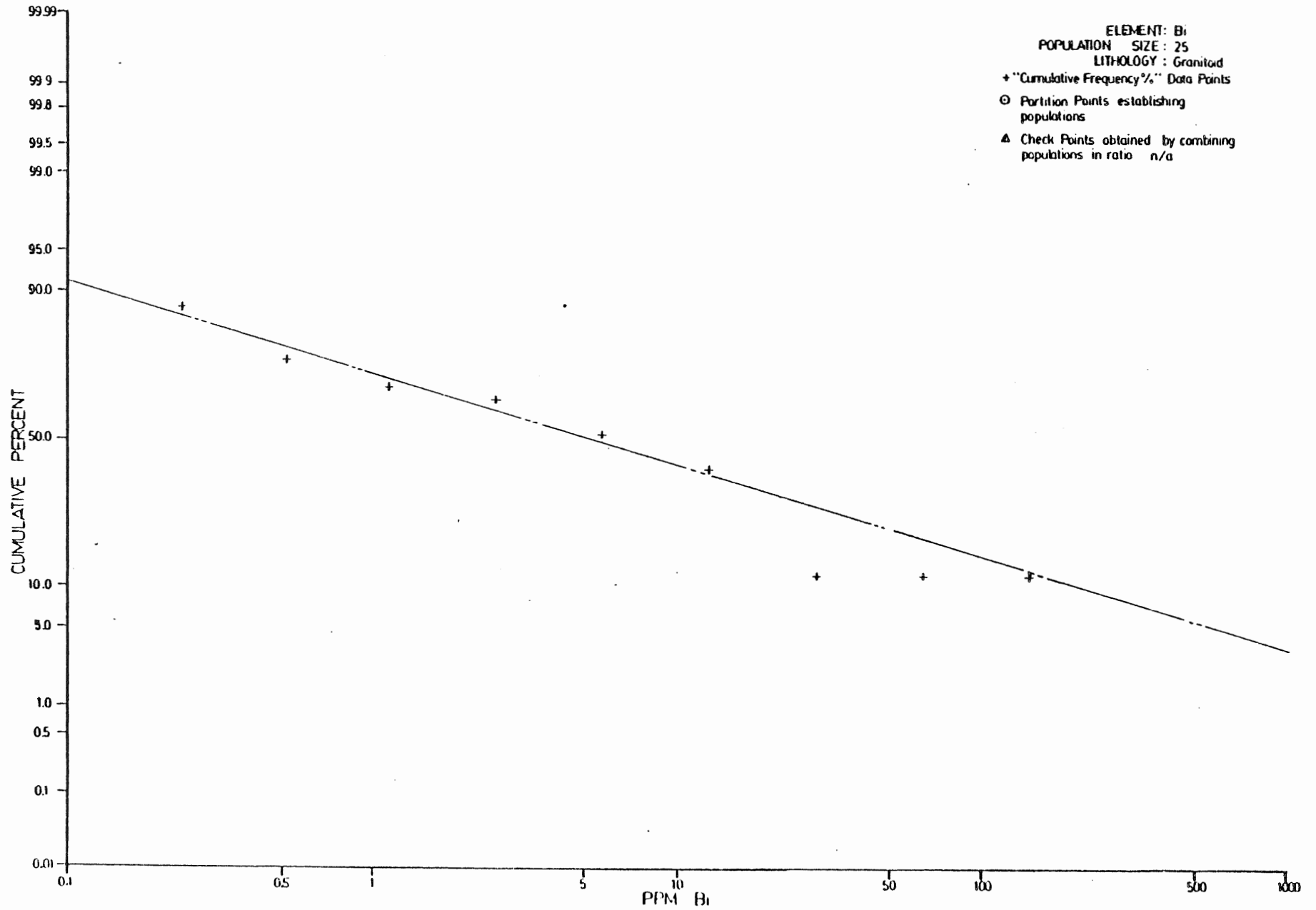


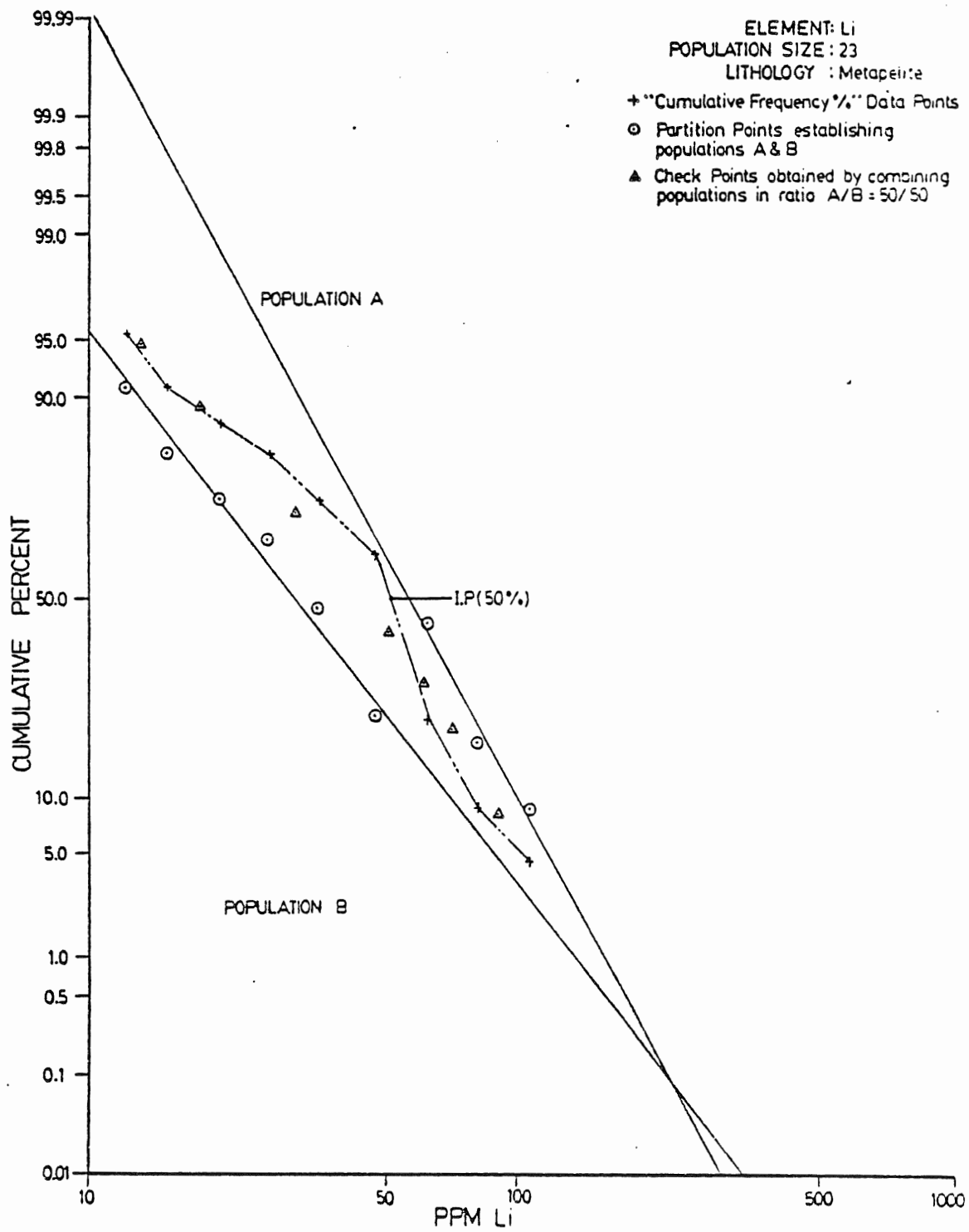


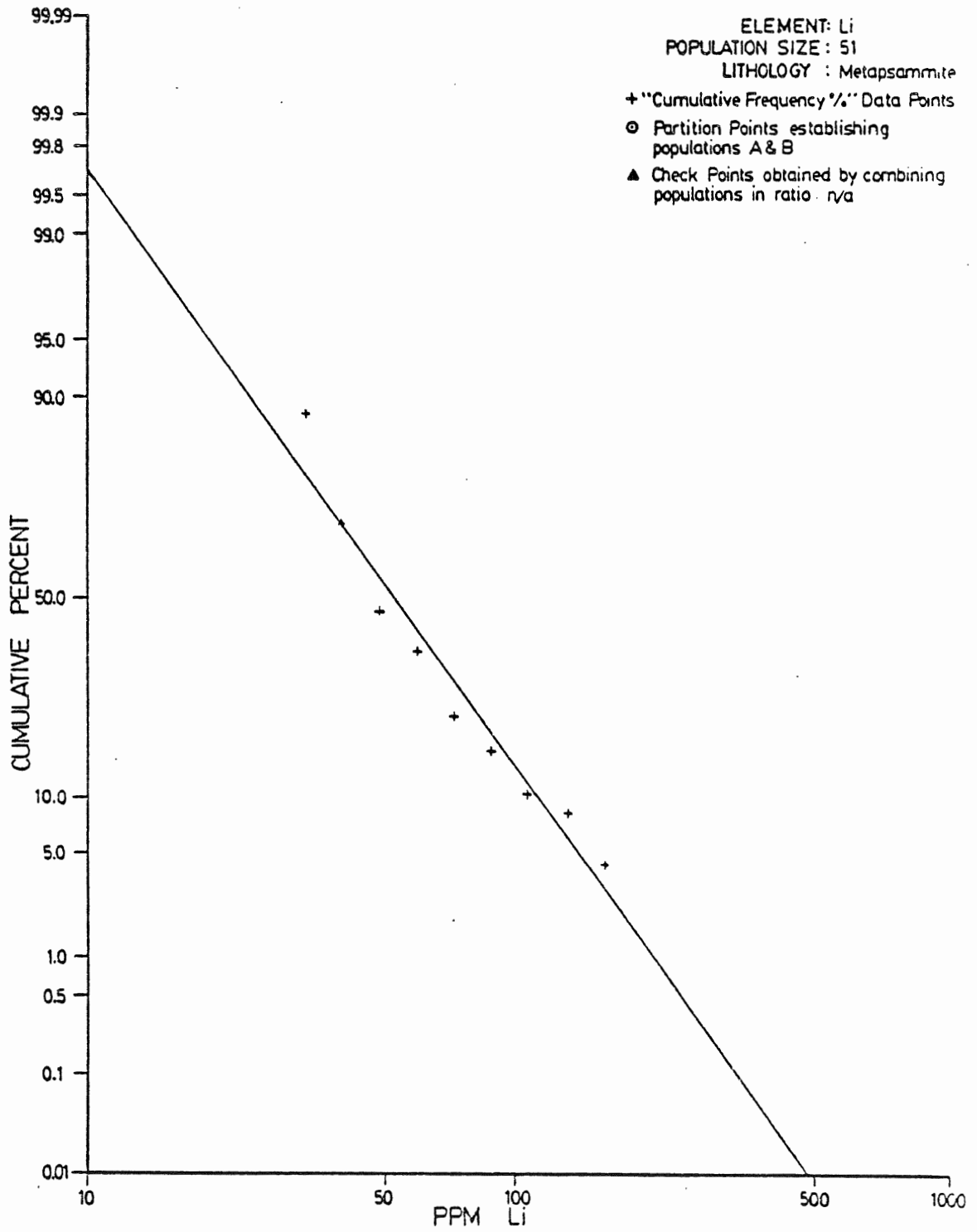
698

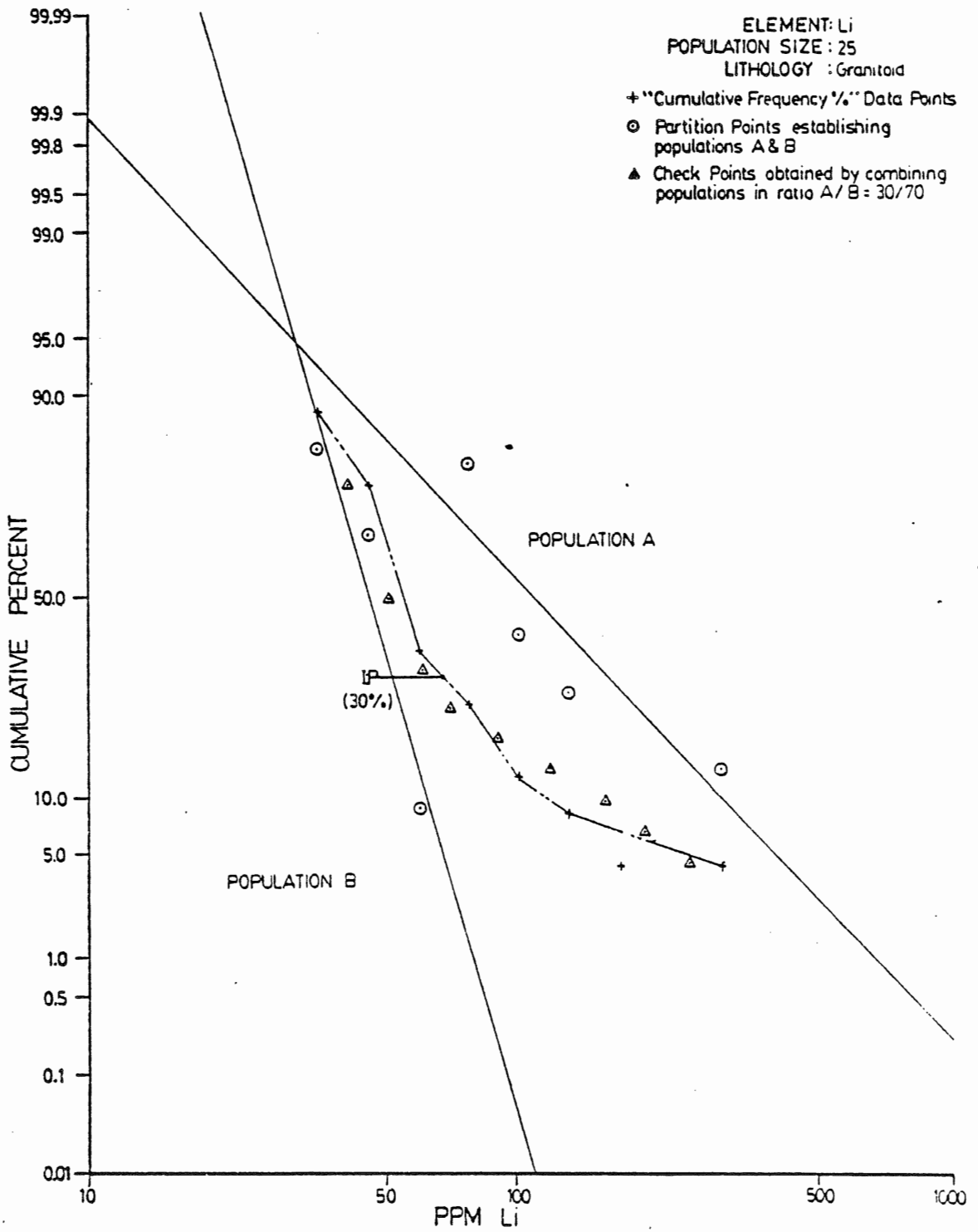


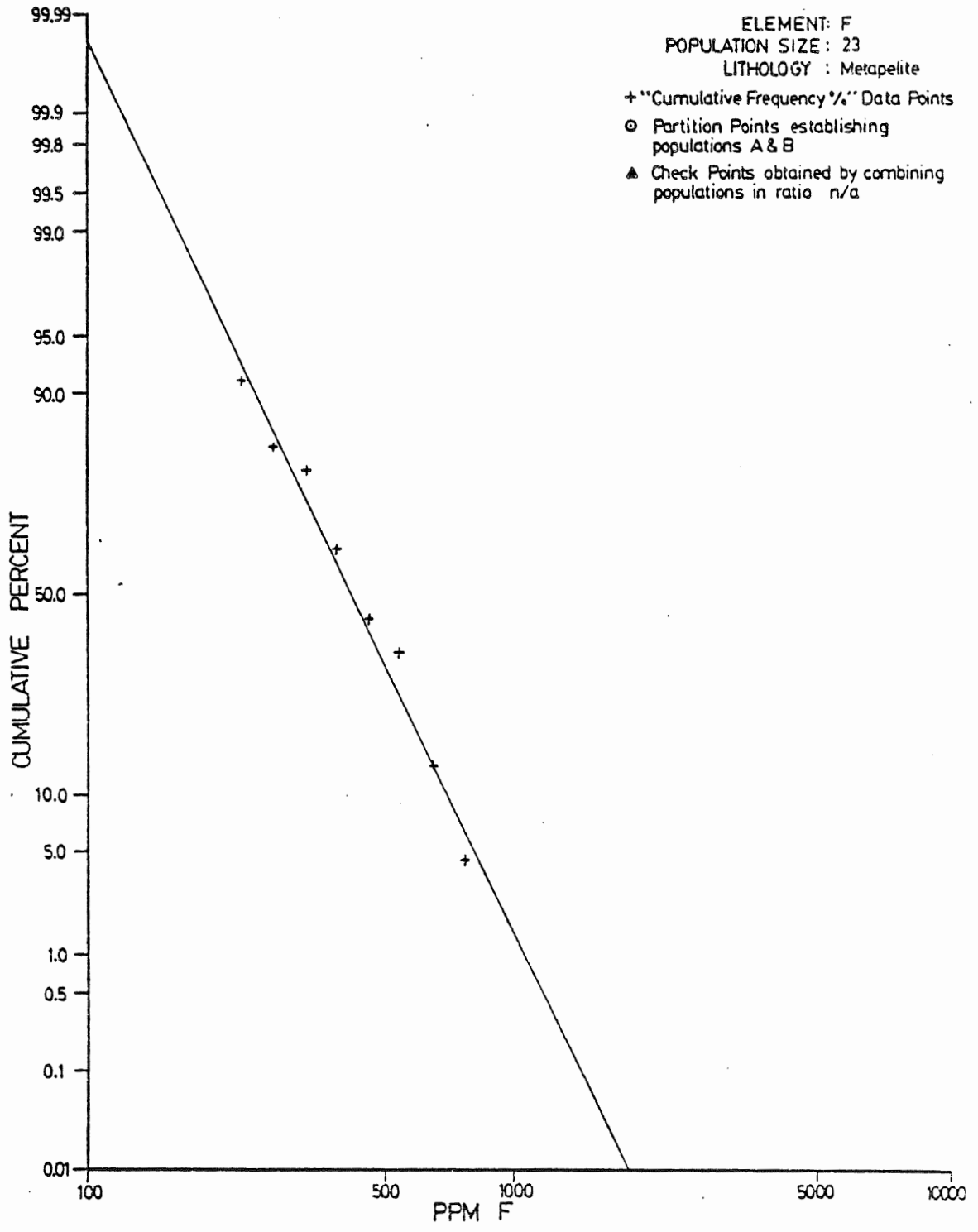
360

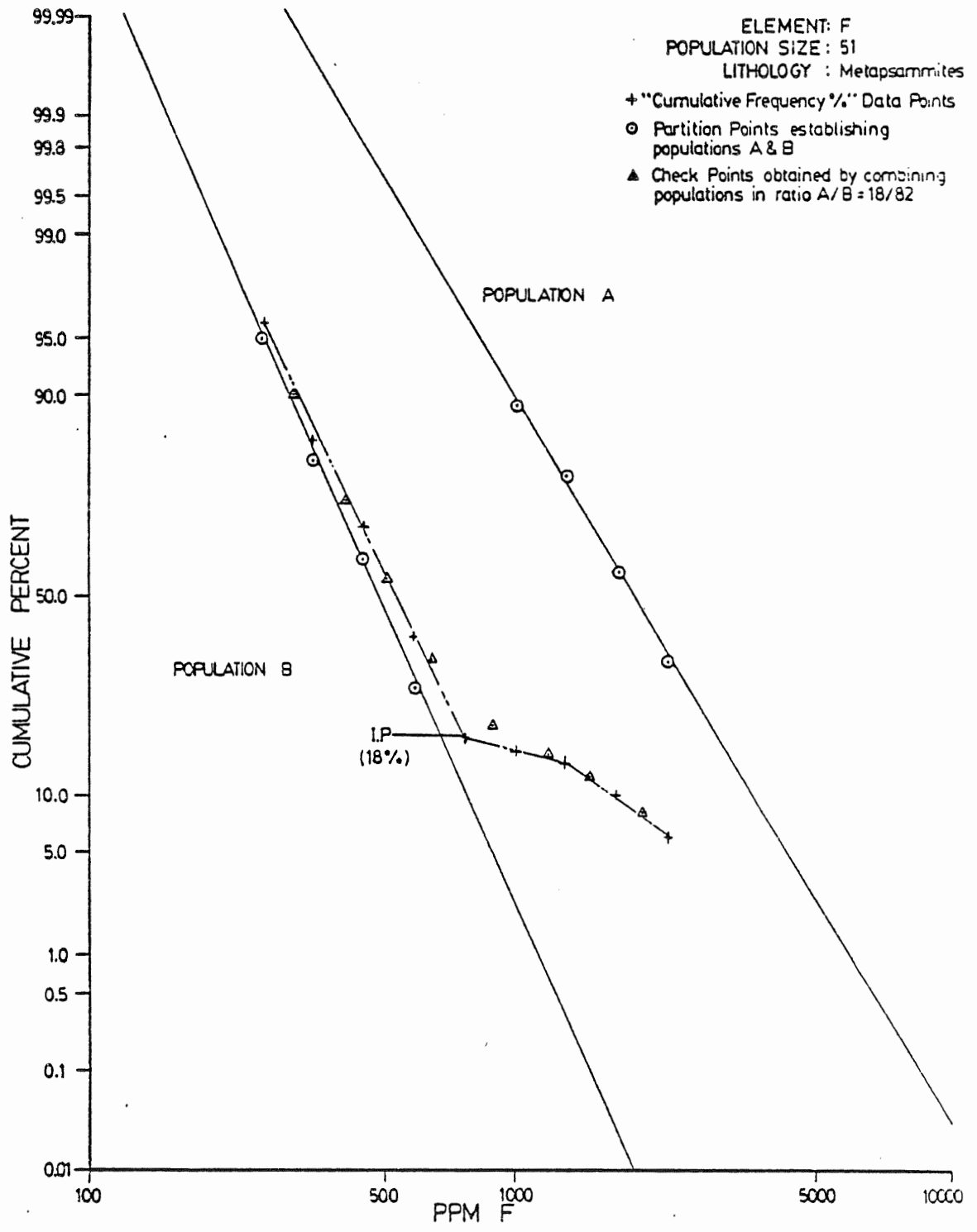


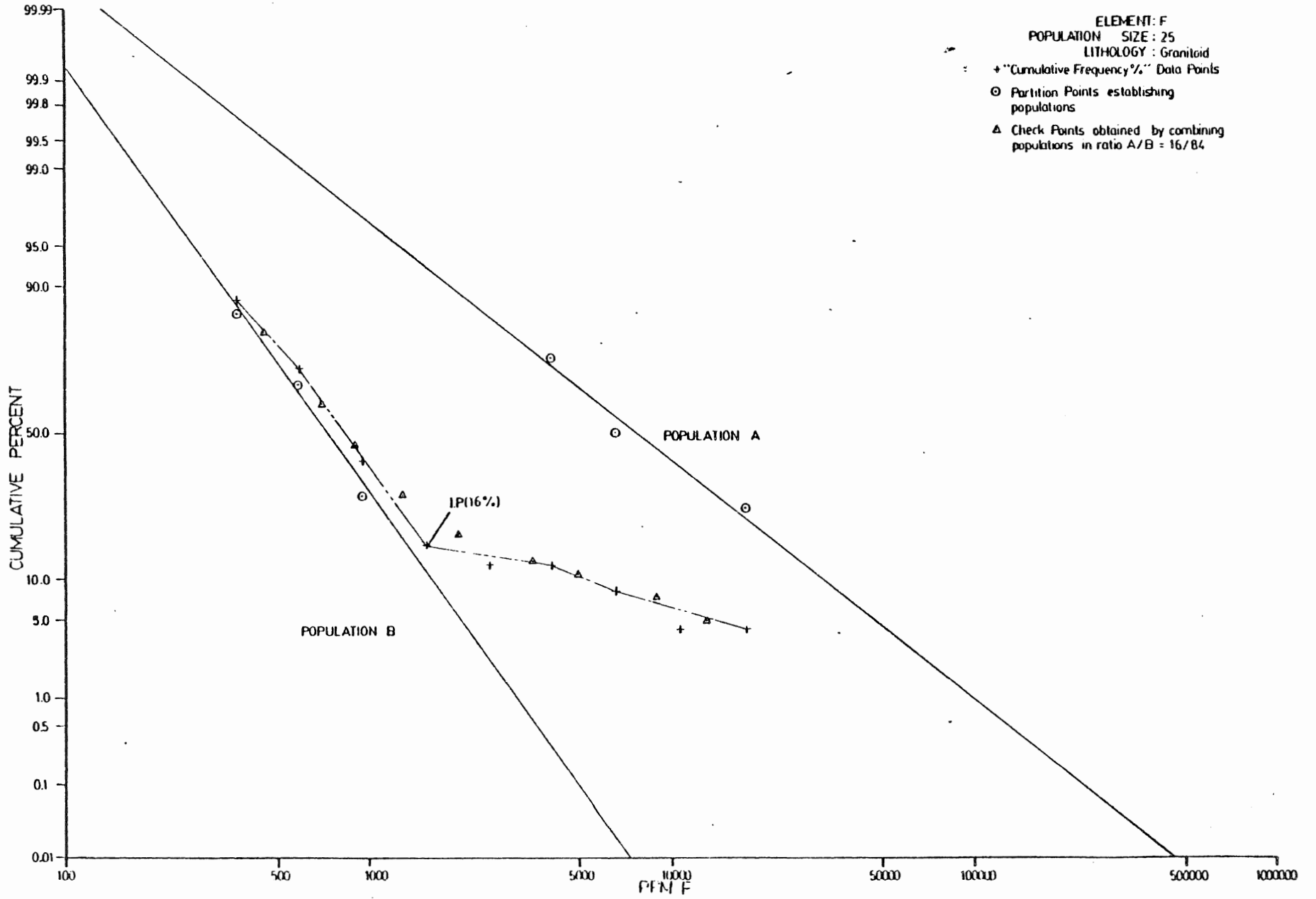












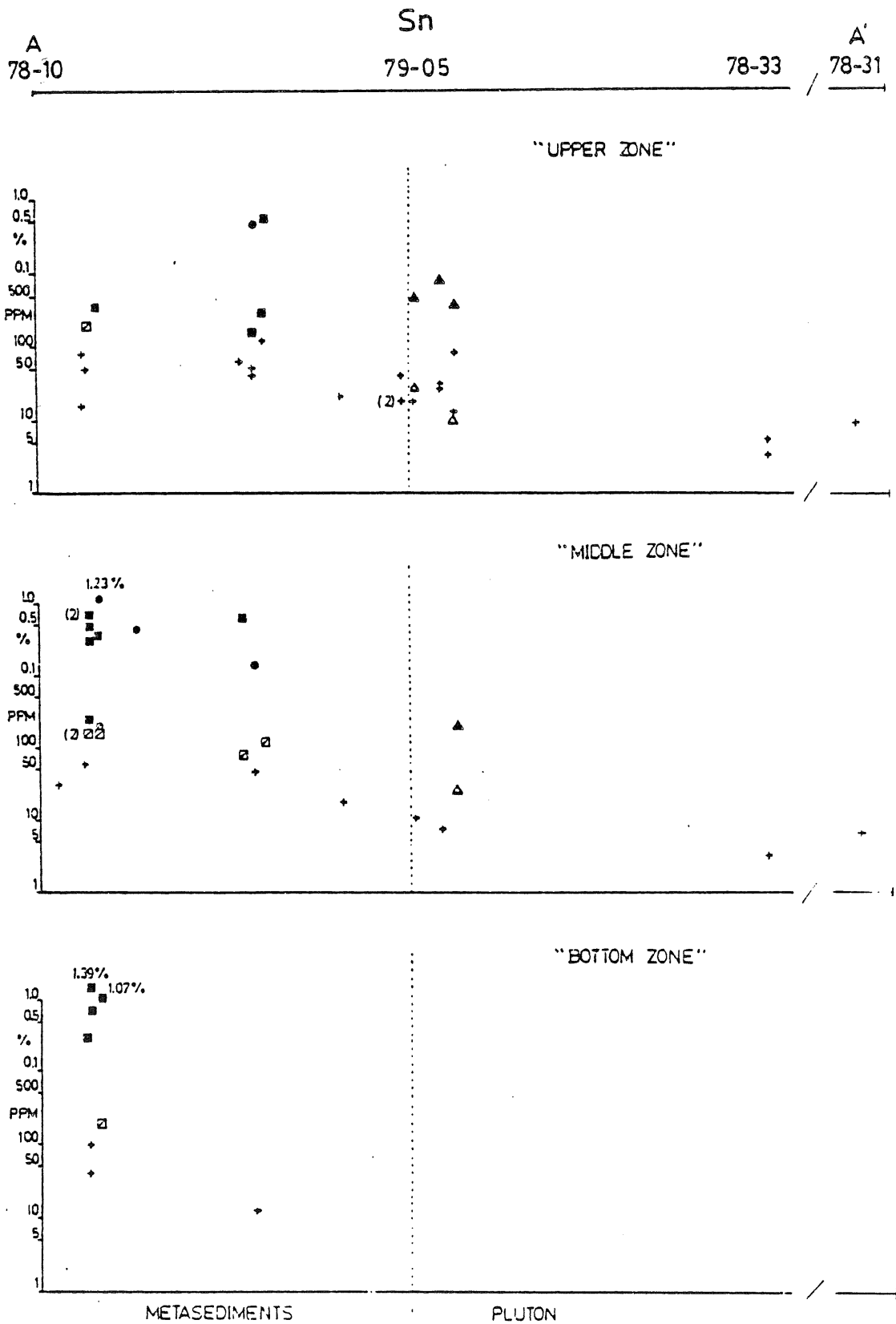
APPENDIX V

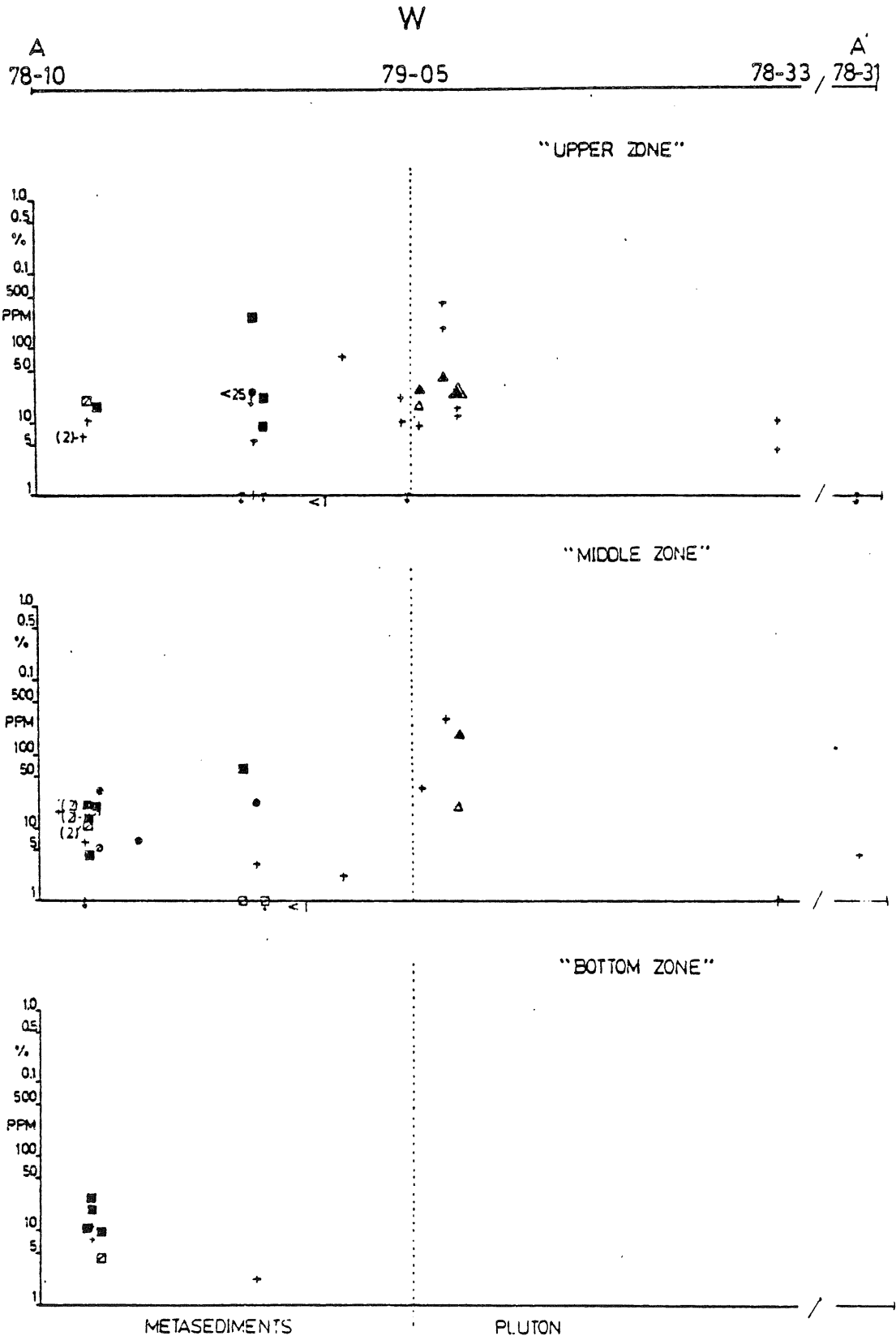
VARIATION OF TRACE ELEMENTS IN TWO CROSS-SECTIONS

Figure V-1

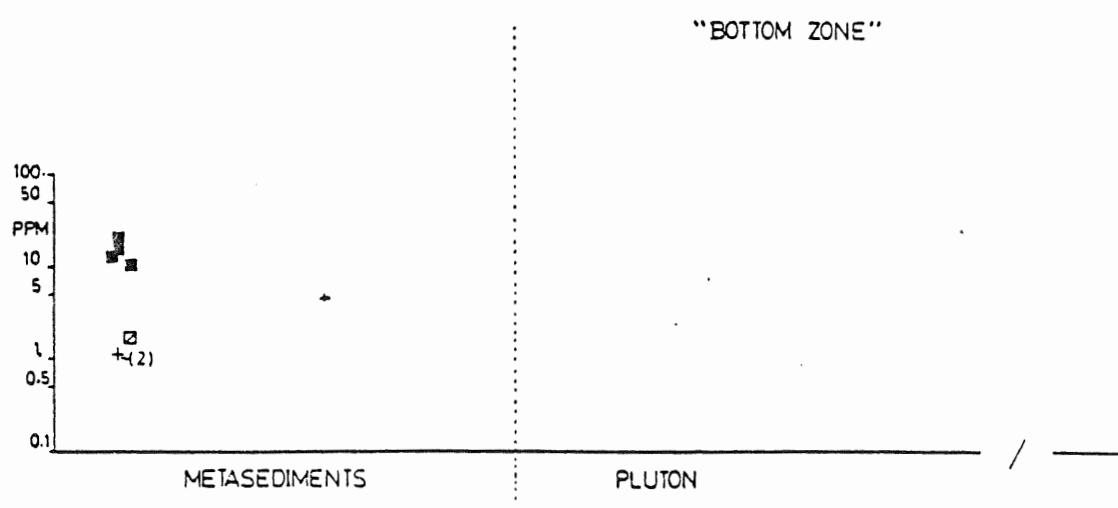
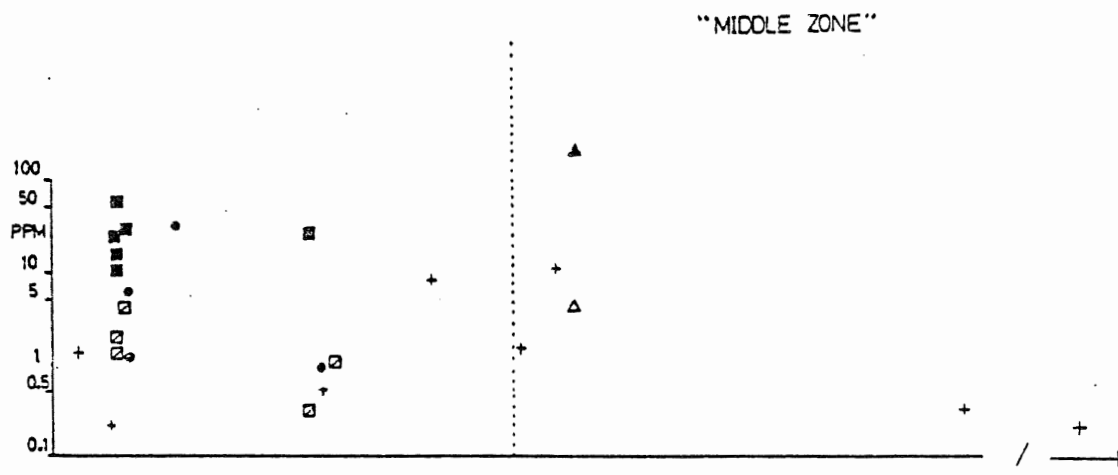
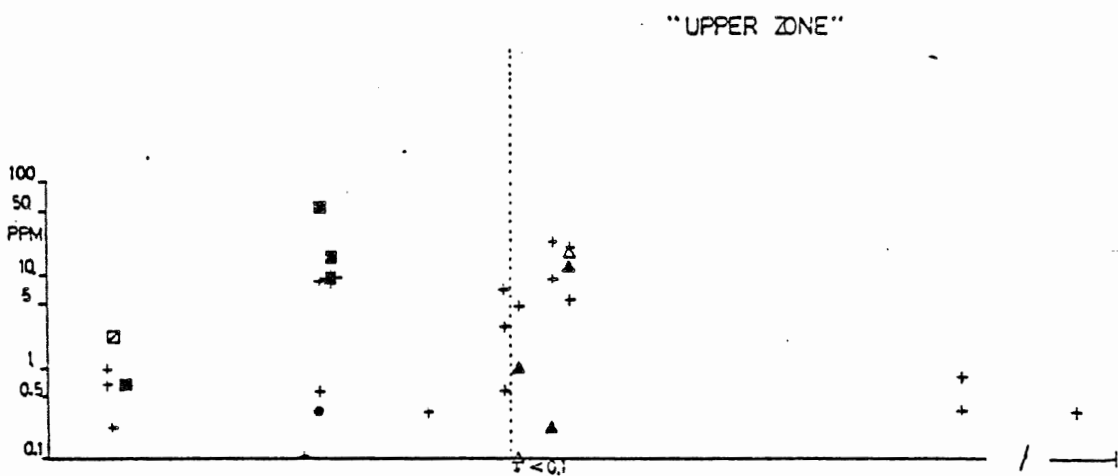
Variation of selected trace elements in two cross-sections, A-A' and B-B'. See Fig. 5.1 for location of cross-section lines. There are slight increases in trace element content of barren samples toward the pluton, but these appear due to thin veinlets containing those elements. There does not appear to be any variation in trace element content with depth, either in barren samples or mineralized 'patches'. However, there is an apparent variation of some elements (Sn, Zn) in metasediment veins with depth and distance from pluton (cross-section A-A').

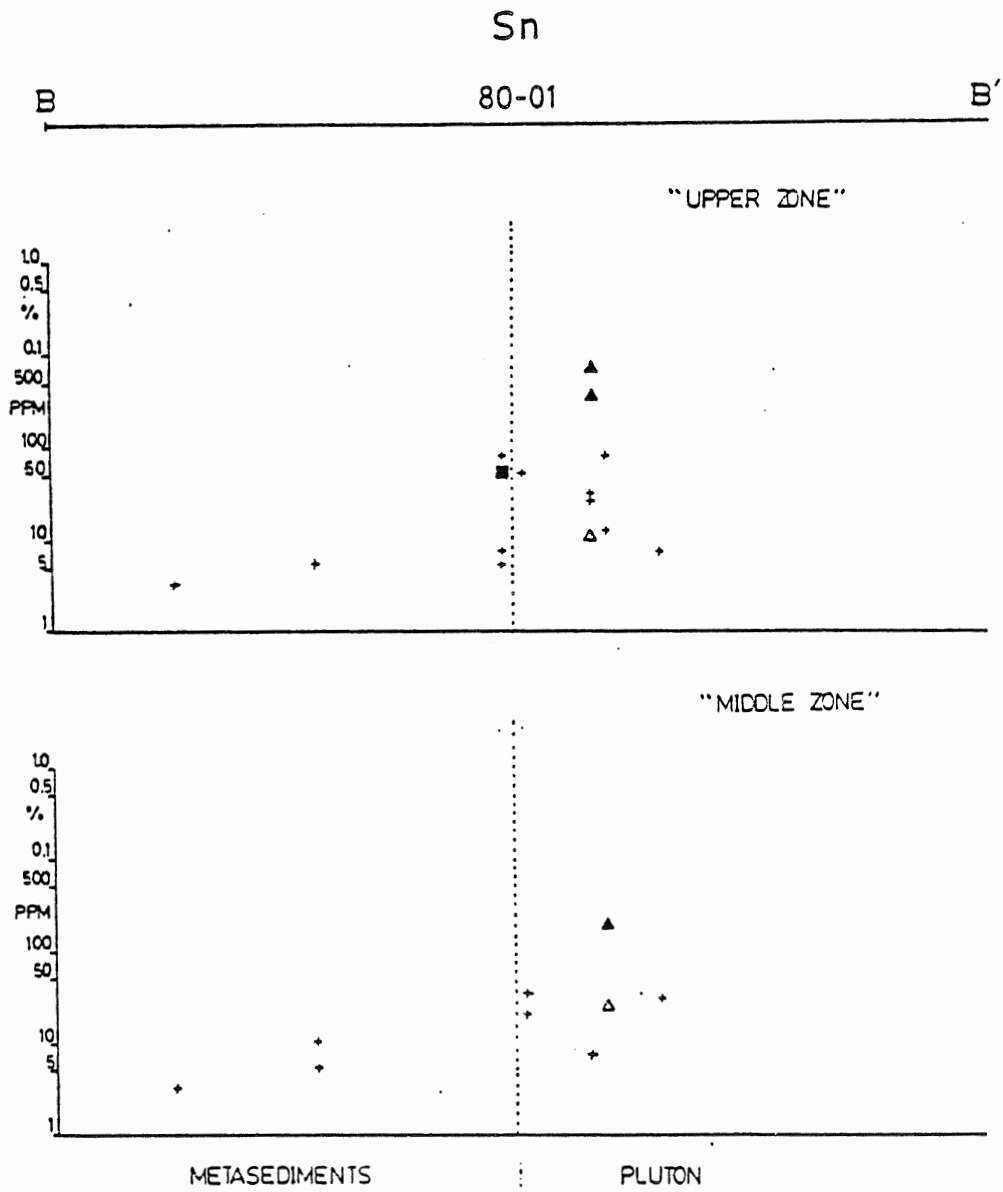
- + barren or unmineralized
- stratiform mineralized 'patch'
- ☒ adjacent mineralized 'patch' (cm to m distant)
- vein in metasediments
- sample adjacent vein
- ▲ greisen vein or alteration
- △ adjacent greisen
- ↓ below indicated detection limit (note: one vein has a high [As], complicating W analysis, so that W's detection limit is raised to 25 ppm; on section A-A')





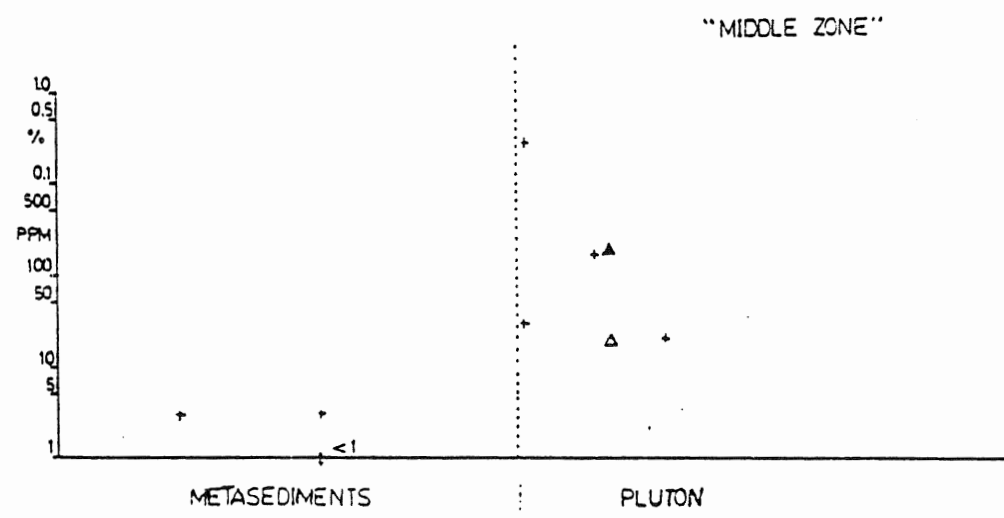
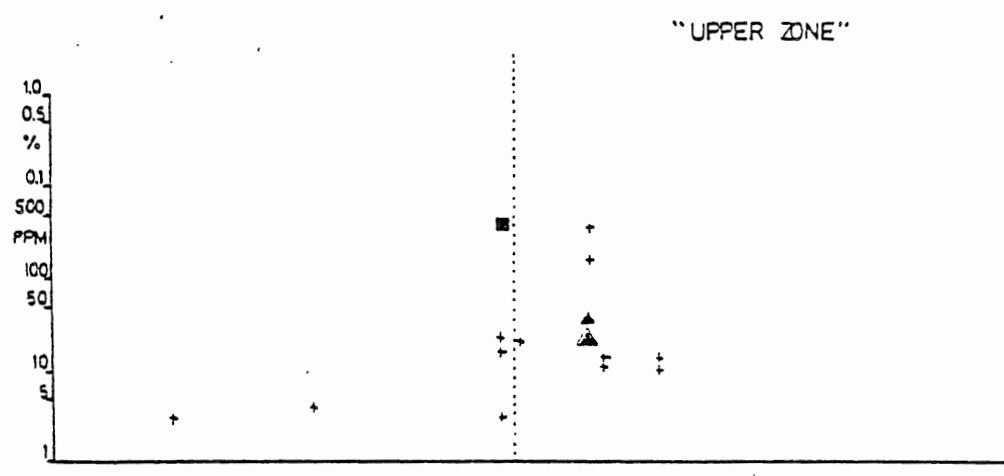
A 78-10 Bi 79-05 78-33 A' 78-31





W
80-01

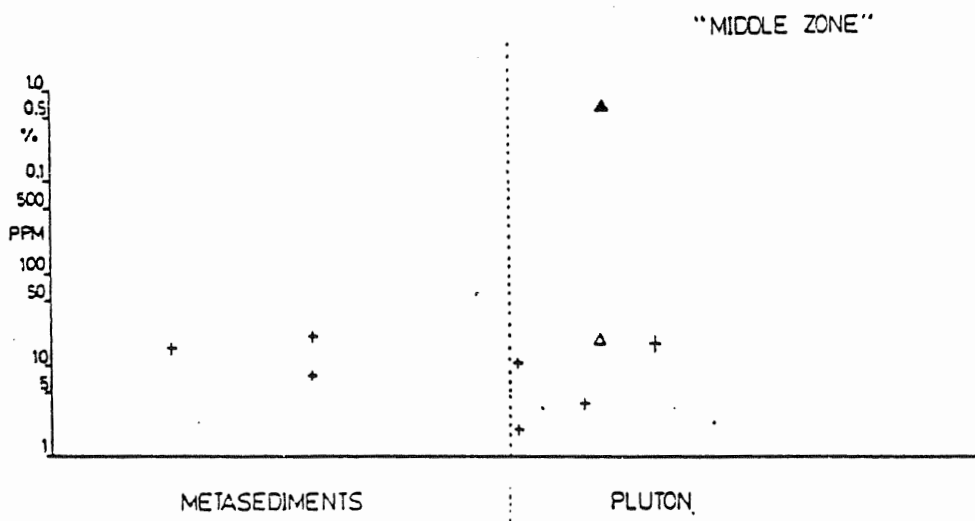
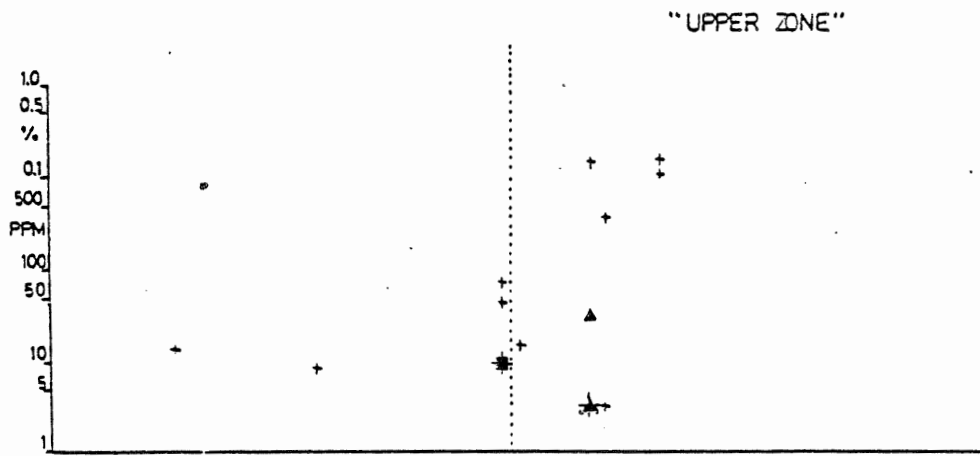
B B'



As

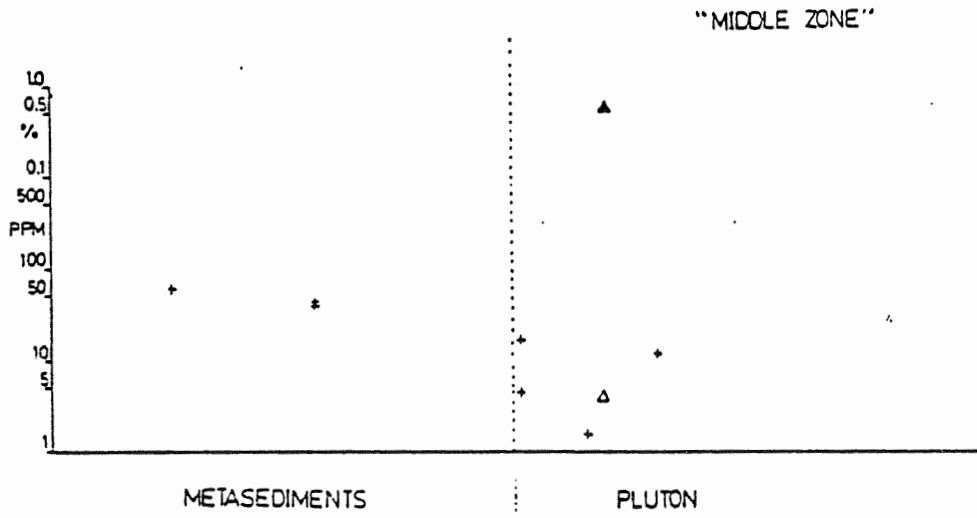
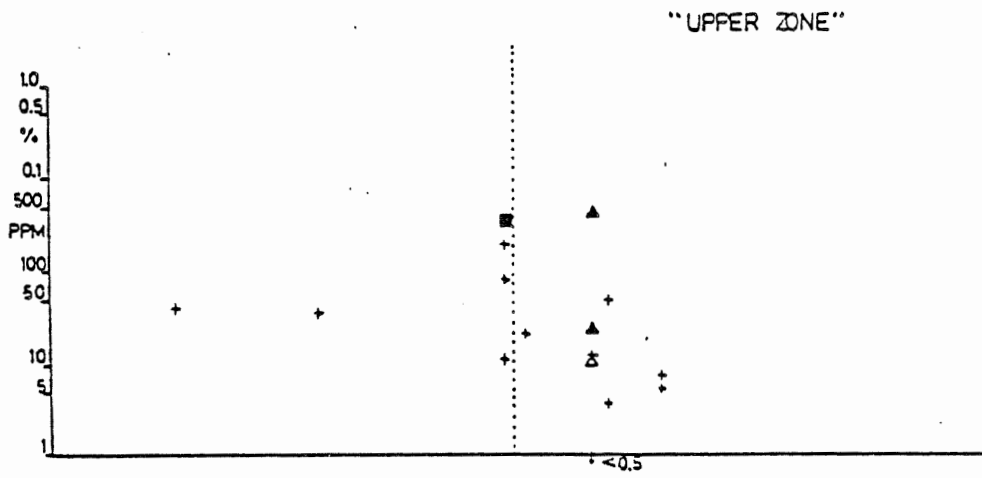
80-01

B B'



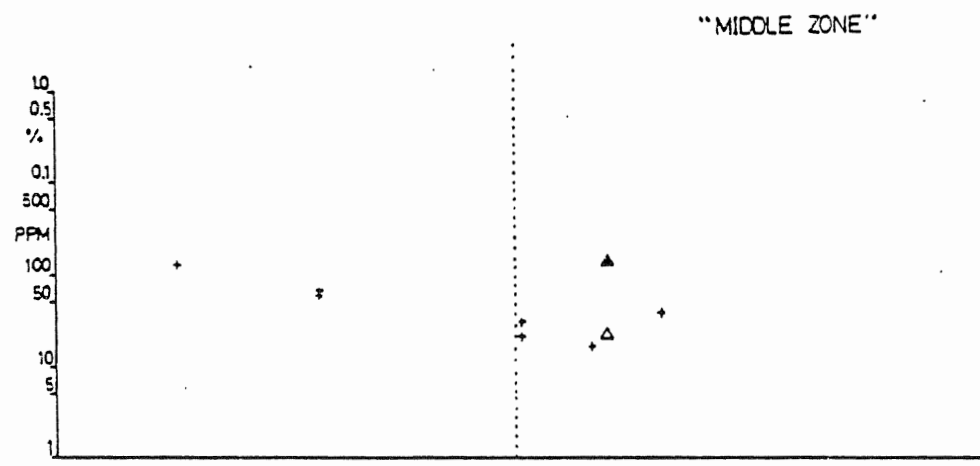
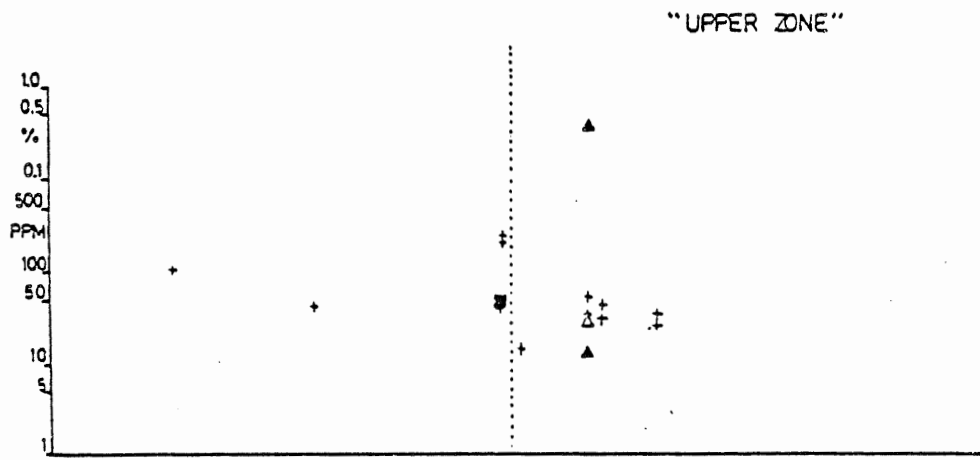
Cu
80-01

B ————— B'



Zn
80-01

B B'

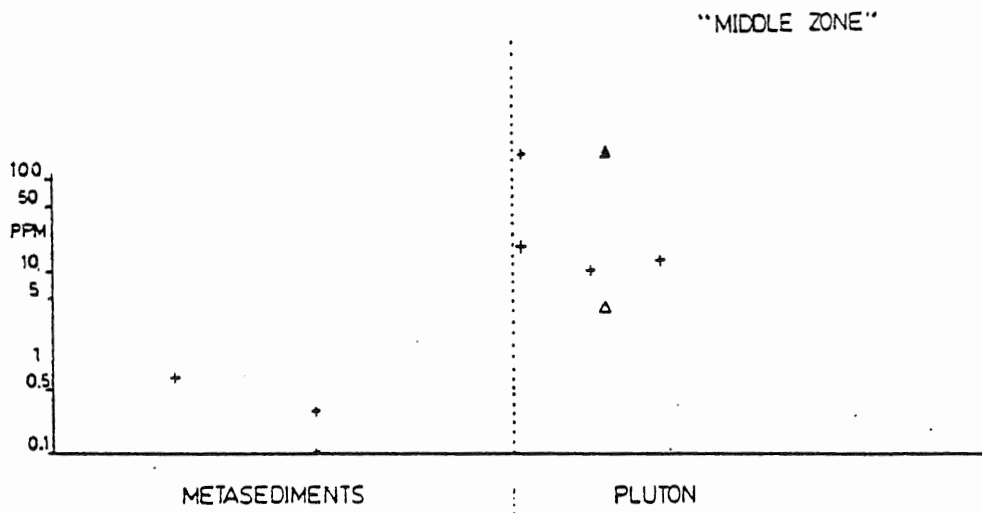
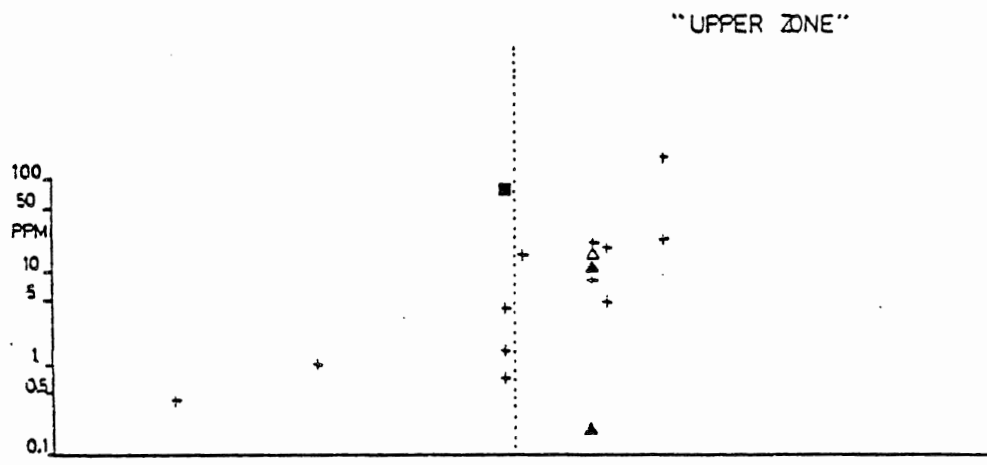


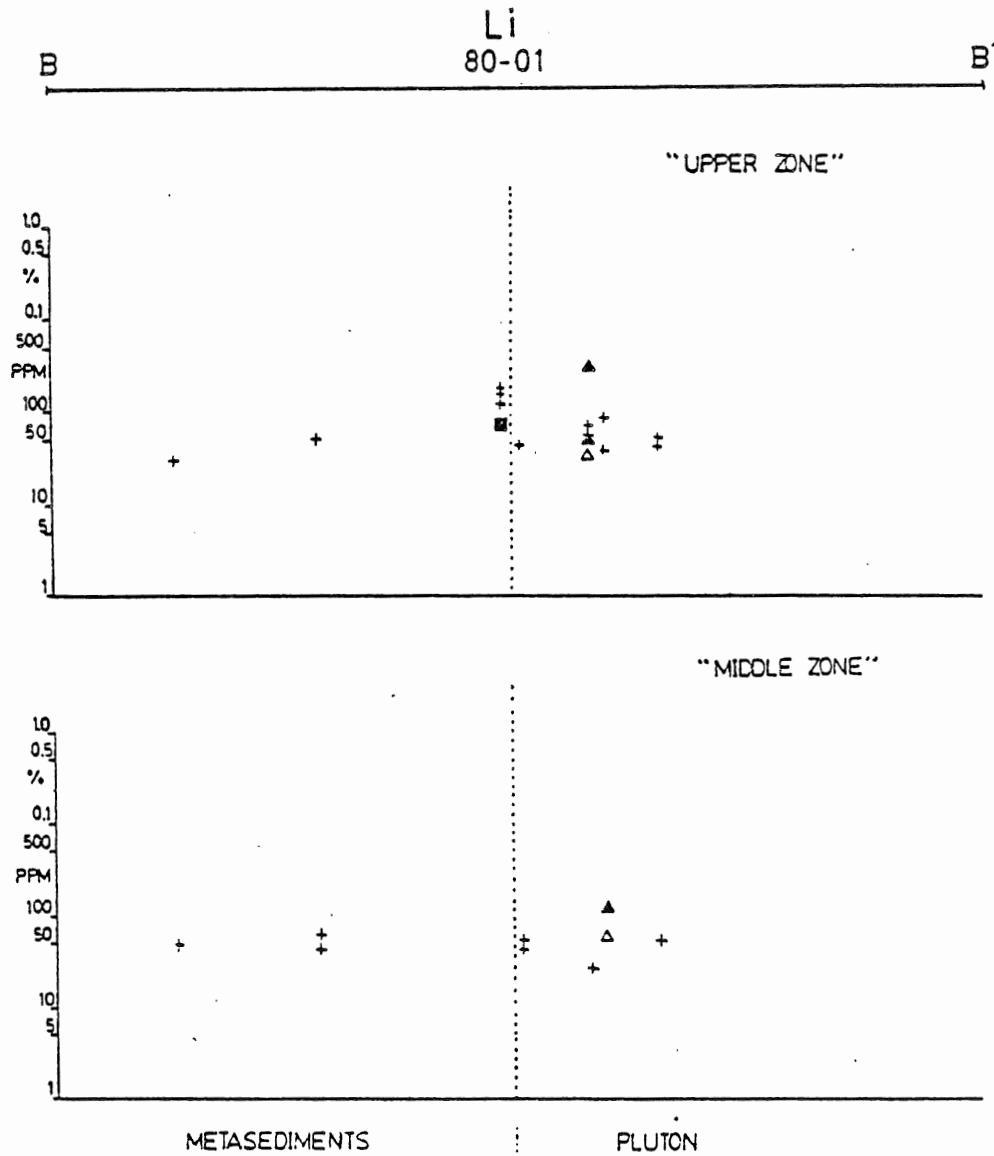
METASEDIMENTS

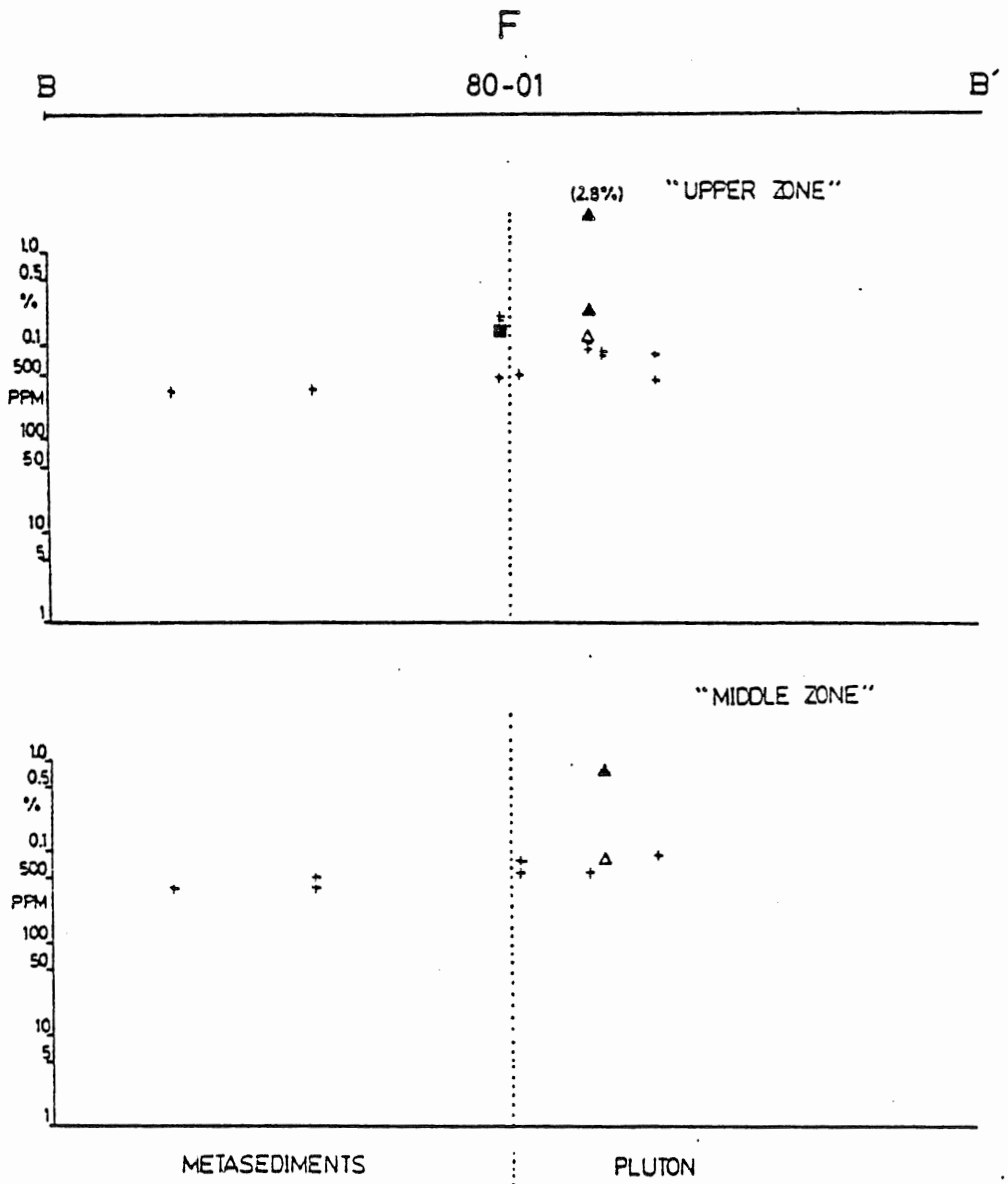
PLUTON

Bi
80-01

B B'







SELECTED BIBLIOGRAPHY

- Abbey, S., 1980, Studies in "standard samples" for use in the general analysis of silicate rocks and minerals. Part 6: 1979 edition of "usable" values: Geol. Surv. Can. Paper 80-14, 30 p.
- Bailey, J.C., 1977, Fluorine in granitic rocks and melts: a review: Chem. Geol., vol. 19, p. 1-42.
- Barnes, H.L., 1979, Solubilities of ore minerals: in H.L. Barnes, ed. Geochemistry of Hydrothermal Ore Deposits, 2nd edition: J. Wiley and Sons, New York, p. 404-460.
- Barr, S.M., 1982, Geochemistry of granitoid plutons of Cape Breton Island, Nova Scotia: in Y.T. Maurice, ed. Uranium in granites: Geol. Surv. Can. Paper 81-23, p. 55-59.
- Baumann, L., 1970, Tin deposits of the Erzgebirge: Trans. Inst. Min. Metall. B79, p. 68-75.
- and Tischendorf, G., 1978, The metallogeny of tin in the Erzgebirge: in M. Stempok, ed. Metallization Associated with Acid Magmatism(MAWAM): Czechoslovak Geol. Surv., vol. 3, p. 17-28.
- Berry, L.G. and Mason, B., 1959, Mineralogy: Concepts, Descriptions, Determinations: W.H. Freeman and Company, San Francisco, 630 p.
- Bischoff, J.L., Radtke, A.S. and Rosenbauer, R.J., 1981, Hydrothermal alteration of graywacke by brine and seawater: roles of alteration and chloride complexing on metal solubilization at 200° and 350° C: Econ. Geol., vol. 77, p. 659-676.
- Blatt, H. and Sutherland, B., 1969, Intrastratal solution and non-opaque heavy minerals in shale: Jour. Sed. Petrol., vol. 39, p. 591-600.
- , Middleton, G. and Murray, R., 1980, Origin of Sedimentary Rocks: Prentice-Hall Inc., New Jersey, 728 p.
- Boissavy-Vinau, M. and Roger, G., 1980, The TiO₂ /Ta ratio as an indicator of the degree of differentiation of tin granites: Mineralium Deposita, vol. 15, p. 231-236.

- Bromley, A.V., 1975, Tin mineralization of western Europe: is it related to crustal subduction?: Trans. Inst. Min. Metall. B 84, p. 28-29.
- Burnham, C.W., 1979, Magmas and hydrothermal fluids: in H.L. Barnes, ed. Geochemistry of Hydrothermal Ore Deposits, J. Wiley and Sons, New York, p. 71-136.
- and Ohmoto, H., 1980, Late-stage processes of felsic magmatism: Mining Geology Special Issue, no. 8, p. 1-11.
- Cant, J.W., Fisher, D.F., Wilson, B.H., Dickie, G.B. and Sarkar, P.K., 1978, Report of exploration in Yarmouth County, Nova Scotia, May 1976 to April 1978: Shell Canada Resources Limited, internal report, 54 p.
- , 1979, Report on an induced polarization survey and diamond drilling program, Plymouth area, Yarmouth project: Shell Canada Resources Limited, internal report, 13 p.
- Carmichael, I.S.E., Turner, F.J., and Verhoogen, J., 1974, Igneous Petrology: McGraw-Hill, New York, 739 p.
- Cathles, L.M., 1981, Fluid flow and genesis of hydrothermal ore deposits: Econ. Geol. 75th Ann. Vol., p. 424-457.
- Charoy, B. and Weisbrod, M., 1974, Interactions between rocks and solutions in mineralized greisens from St. Renan (Brittany, France): in M. Stemprok, ed. Metallization Associated with Acid Magmatism (MAWAM): Czechoslovak Geol. Surv., vol. 1, p. 254-261.
- Chatterjee, A.K., 1980, Polymetallic tin mineralization related to acid magmatism, southwestern Nova Scotia: in K.A. McMillan, ed. Nova Scotia Dept. of Mines and Energy, Mineral Resources Division, Report of Activities 80-1, p. 59-65.
- and Muecke, G.K., 1982, Geochemistry and distribution of uranium and thorium in the granitoid rocks of the South Mountain batholith, Nova Scotia: some genetic and exploration implications: in Y.T. Maurice, ed. Uranium in Granites, Geol. Surv. Can. Paper 81-23, p. 11-17.
- Clarke, D.B., Barr, S.M. and Donohoe, H.V., 1980, Granitoid and other plutonic rocks of Nova Scotia: in Proceedings, "The Caledonides in the USA", IGCP Project 27, p. 107-116.

- and Halliday, A.N., 1980, Strontium isotope geology of the South Mountain batholith, Nova Scotia: *Geochim. et Cosmochim. Acta*, vol. 44, p. 1045-1058.
- Collins, P.L.F., 1981, The geology and genesis of the Cleveland tin deposit, Western Tasmania: fluid inclusion and stable isotope studies: *Econ. Geol.* vol. 76, p. 365-392.
- Craig, J.R. and Vaughan, D.J., 1981, *Ore Microscopy and Ore Petrography*: J. Wiley and Sons, New York, 406 p.
- Craw, D., 1981, Oxidation and microprobe-induced potassium mobility in iron-bearing phyllosilicates from the Otago schists, New Zealand: *Lithos*, vol. 14, p. 49-57.
- Cullen, J.D., 1983, *Metamorphic petrology and geochemistry of the Goldenville Formation metasediments, Yarmouth, Nova Scotia*: Unpub. M. Sc. thesis Dalhousie University, 206 p.
- Deer, W.A., Howie, R.A. and Zussman, J., 1974, *An introduction to the rock-forming minerals*: Longman Group Ltd., London, 528 p.
- Dick, L.A. and Hodgson, C.J., 1982, The MacTung W-Cu(Zn) contact metasomatic and related deposits of the northeastern Canadian Cordillera: *Econ. Geol.*, vol. 77, p. 845-867.
- Dobson, D.C., 1982, Geology and alteration of the Lost River tin-tungsten-fluorine deposits, Alaska: *Econ. Geol.*, vol. 77, p. 1033-1052.
- Duursma, E.K. and Hoede, C., 1976, Principles of diffusion in sedimentary systems: in K.H. Wolf, ed. *Handbook of Strata-bound and Stratiform Ore Deposits*, vol. 2, *Geochemical Studies*: Elsevier Scientific Pub. Co., p. 29-51.
- Edmond, J.M., 1982, The chemistry of the ridge crest hot springs: *Marine Tech. Soc. Jour.*, vol. 16, p. 23-25.
- Einaudi, M.T., Meinert, L.D. and Newberry, R.J., 1981, Skarn deposits: *Econ. Geol.* 75th Ann. Vol., p. 317-391.
- El Sharkawi, M.A.H. and Dearman, W.R., 1966, Tin-bearing skarns from the north-west border of the Dartmoor granite, Devonshire, England: *Econ. Geol.*, vol. 61, p. 362-369.
- Gamble, R.P., 1982, *An experimental study of sulfidation*

- reactions involving andradite and hedenbergite: *Econ. Geol.*, vol. 77, p. 784-797.
- Garnett, R.H.T., 1966, Distribution of cassiterite in vein tin deposits: *Trans. Inst. Min. Metall. B* 75, p. 245-273.
- Germann, K., 1973, Deposition of manganese and iron carbonates and silicates in Liassic marls of the Northern Limestone Alps(Kalkalpen): in C. Amstutz and A.J. Bernard, eds. *Ores in Sediments*, IUGS, series A, no. 3, Springer-Verlag, p. 129-138.
- Ghisler, M., Jensen, Aa., Stendal, H. and Urban, H., 1980, Stratabound scheelite, arsenopyrite and copper sulphide mineralization in the Late Precambrian sedimentary succession of the East Greenland Caledonides: *Geol. Surv. Ireland Special Paper No. 5*, p. 19-24.
- Goncharov, G.N. and Filatov, S.K., 1972, The typical structural features of cassiterite from Sherlovaya Gora: *Geochem. Int.*, vol. 1971, p. 268-275.
- Graf, J.L., Jr. and Skinner, B.J., 1970, Strength and deformation of pyrite and pyrrotite: *Econ. Geol.*, vol. 65, p. 206-215.
- Grigoryan, S.V., 1974, Primary geochemical halos in prospecting and exploration of hydrothermal deposits: *Int. Geol. Rev.*, vol. 16, p. 12-25.
- Groves, D.I. and McCarthy, T.S., 1978, Fractional crystallization and the origin of tin deposits in granitoids: *Mineralium Deposita*, vol. 13, p. 11-26.
- Hanor, J.S., 1979, The sedimentary genesis of hydrothermal fluids: in H.L. Barnes, ed. *Geochemistry of Hydrothermal Ore Deposits*, 2nd edition, J. Wiley and Sons, New York, p. 137-172.
- Harris, I.M. and Schenk, P.E., 1975, The Meguma Group: in I.M. Harris, ed. *Ancient Sediments of Nova Scotia: Society of Economic Paleontologists and Mineralogists (Eastern Section) Guidebook, 1975 Field Trip: Maritime Sediments*, p. 17-38.
- Helgeson, H.C., 1964, *Complexing and Hydrothermal Ore Deposition*: Pergamon Press, New York, 128 p.
- Holland, H.D., 1972, Granites, solutions, and base metal deposits: *Econ. Geol.*, vol. 67, p. 281-301.
- Hosking, K.F.G., 1979, Tin distribution patterns: *Bull.*

- Geol. Soc. Malaysia, no. 11, p. 1-70.
- Hutchinson, R.W., 1979, Evidence of exhalative origin for Tasmanian tin deposits: CIM Bull., vol. 72, p. 90-104.
- , 1980, "Evidence of exhalative origin for Tasmanian tin deposits" - author's reply: CIM Bull., vol. 73, p. 167-168.
- , 1982, Geologic setting and genesis of cassiterite-sulphide mineralization at Renison Bell, Tasmania - a discussion: Econ. Geol., vol. 77, p. 199-202.
- Ishihara, S., Sawata, H., Arpornsuwan, S., Busaracome, P. and Bungbrakearti, N., 1979, The magnetite-series and ilmenite-series granitoids and their bearing on tin mineralization, particularly of the Malay Peninsula region: Bull. Geol. Soc. Malaysia, no. 11, p. 103-110.
- , 1981, The granitoid series and mineralization: Econ. Geol. 75th Ann. Vol. p. 458-484.
- Jackson, N.L., 1979, Geology of the Cornubian tin field "a review": Bull. Geol. Soc. Malaysia, no. 11, p. 209-237.
- , Halliday, A.N., Sheppard, S.M.F. and Mitchell, J.G., 1979, Isotopic and fluid inclusion evidence bearing on the polyphase metallogenic evolution of the St. Just District, Cornwall[abs.]: Problems of Mineralization Associated with Acid Magmatism; Mineral Studies Group Meeting, p. 4-5.
- Jeffery, P.G. and Hutchison, D., 1981, Chemical Methods of Rock Analysis, 3rd edition: Pergamon Press, New York, 379 p.
- Jenner, K.A., 1982, A study of sulphide mineralization in the Meguma Group sediments Gold Brook, Colchester County, Nova Scotia: Unpub. B.Sc. thesis, Dalhousie University, 60 p.
- Kelly, W.C. and Rye, R.O., 1979, Geologic, fluid inclusion, and stable isotope studies of the tin-tungsten deposits of Panasqueira, Portugal: Econ. Geol., vol. 74, p. 1721-1822.
- Koch, G.S., Jr. and Link, R.F., 1970, Statistical Analysis of Geological Data, vol. I: J. Wiley and Sons, New York, 375 p.
- Kodama, H., Longworth, G. and Townsend, M.G., 1982, A

- Mossbauer investigation of some chlorites and their oxidation products: *Can. Min.*, vol. 20, p. 585-592.
- Krauskopf, K.B., 1979, *Introduction to Geochemistry*, 2nd edition: McGraw-Hill, New York, 617 p.
- Kretschmar, U. and Scott, S.D., 1976, Phase relations involving arsenopyrite in the system Fe-As-S and their application: *Can. Mineral.*, vol. 14, p. 364-386.
- Kullerud, G. and Yoder, H.S., Jr., 1965, Sulfide-silicate reactions and their bearing on ore formation under magmatic, postmagmatic and metamorphic conditions: Symposium, Problems of Postmagmatic Ore Deposition, vol. II, *Czechoslovak Geol. Surv.*, p. 327-331.
- Lane, T.E., 1975, Stratigraphy of the White Rock Formation: in I.M. Harris, ed. *Ancient Sediments of Nova Scotia: Society of Economic Paleontologists and Mineralogists (Eastern Section) Guidebook 1975 Field Trip: Maritime Sediments*, p. 43-62.
- Lebedev, L.M., 1967, *Metacoloids in Endogenic Deposits*: Plenum Press, 298 p.
- Lehmann, B. and Schneider, H.-J., 1981, Strata-bound tin deposits: in K.H. Wolf, ed. *Handbook of Strata-bound and Stratiform Ore Deposits*, vol. 9, *Regional Studies and Specific Deposits*: Elsevier Scientific Pub. Co., p. 743-771.
- , 1982, Metallogeny of tin: magmatic differentiation versus geochemical heritage: *Econ. Geol.*, vol. 77, p. 50-59.
- Lepeltier, C., 1969, Simplified statistical trends of geochemical data: *Econ. Geol.*, vol. 64, p. 538-550.
- Levinson, A.A., 1974, *Introduction to Exploration Geochemistry*: Applied Pub. Ltd., Illinois, 614 p.
- Long, D.T. and Angino, E.E., 1982, The mobilization of selected trace metals from shales by aqueous solutions: effects of temperature and ionic strength: *Econ. Geol.*, vol. 77, p. 646-652.
- Love, L.G., 1969, Sulphides of metals in recent sediments: in C.H. James, ed. *Proceedings, Sedimentary Ores Ancient and Modern*, 15th Inter-University Geological Congress, 1967, Spec. Pub. No. 1, Dept. of Geology, University of Leicester, England, p. 31-60.

- Lufkin, J.L., 1977, Chemistry and mineralogy of wood-tin, Black Range, New Mexico: *Am. Min.*, vol. 62, p. 100-106.
- Marsh, B.D., 1982, On the mechanics of igneous diapirism, stoping, and zone melting: *Am. Jour. Sci.*, vol. 282, p. 808-855.
- Mason, R., 1978, *Petrology of the Metamorphic Rocks*: George Allen and Unwin, London, 254 p.
- Maucher, A. and Rehwald, G., 1961, Card Index of Ore Microphotographs: Verlag, W. Germany, 3 vol. (published continuously).
- McKenzie, C.B. and Clarke, D.B., 1975, Petrology of the South Mountain Batholith, Nova Scotia: *Can. Jour. Earth Sci.*, vol. 12, p. 1209-1218.
- Mercer, W., 1976, Minor elements in metal deposits in sedimentary rocks - a review: in K.H. Wolf, ed. *Handbook of Strata-bound and Stratiform Ore Deposits*, vol. 2, *Geochemical Studies*: Elsevier Scientific Pub. Co., p. 1-27.
- Meyers, A.T., Havens, R.G., Connor, J.J., Conklin, N.M. and Rose, H.J., Jr., 1976, Glass reference standards for the trace element analysis of geological materials - compilation of interlaboratory data: *Geol. Surv. Prof. Paper 1013*, 29 p.
- Michard, A., 1976, *Elements de geologie Marocaine*: Editions du Service Geologique du Maroc: Notes et Memoires du Service Geologique, no. 252, 408 p.
- Mitchell, A.H.G., 1979, Rift-, subduction- and collision-related tin belts: *Bull. Geol. Malaysia*, no. 11, p. 81-102.
- Miyahisa, M., 1968, Lattice constants of cassiterites: *Mineralogical Abstracts*, vol. 19, p. 141.
- Mookerjee, A. 1981, Ores and metamorphism: temporal and genetic relationships: in K.H. Wolf, ed. *Handbook of Strata-bound and Stratiform Ore Deposits*, vol. 4, *Tectonics and Metamorphism*: Elsevier Pub. Co., p. 203-260.
- Moore, F. and Howie, R.A., 1979, Geochemistry of some Cornubian cassiterites: *Mineralium Deposita*, vol. 14, p. 103-107.
- Morganti, J.M., 1981, Ore deposit models - 4. Sedimentary-

- type stratiform ore deposits: some models and a new classification: Geoscience Canada, vol. 8, p. 65-75.
- Mulligan, R., 1975, Geology of Canadian tin occurrences: Geol. Surv. Can., Econ. Geol. Rept. no. 28, 155 p.
- Nekrasov, I. Ya., 1971, Features of tin mineralization in carbonate rocks, as in Eastern Siberia: Int. Geol. Rev., vol. 13, p. 1532-1542.
- Newhouse, W.H. and Buerger, M.J., 1928, Observations on wood-tin nodules: Econ. Geol., vol. 23, p. 185-192.
- Nicolini, P., 1970, *Geologie des Concentrations Minerales Stratiformes*: Gauthier-Villars, Paris, 792 p.
- Pan, Y. and Ypma, P.J.M., 1974, Heating and recrystallization of wood-tin - an indication of low temperature genesis of cassiterite and wood-tin veins in volcanics (abs.): Geol. Soc. Am. Abstracts with Program, vol. 6, p. 62-63.
- Parslow, G.R., 1974, Determination of background and threshold in exploration geochemistry: Jour. Geochem. Explor., vol. 3, p. 319-336.
- Patterson, D.J., Ohmoto, H. and Solomon, M., 1981, Geologic setting and genesis of cassiterite-sulphide mineralization at Renison Bell, Tasmania: Econ. Geol., vol. 76, p. 393-438.
- , 1982, Geologic setting and genesis of cassiterite-sulphide mineralization at Renison Bell, Tasmania - a reply: Econ. Geol., vol. 77, p. 203-206.
- Pettijohn, F.J., 1975, *Sedimentary Rocks*, 3rd edition: Harper and Row, New York, 628 p.
- Plant, J., Brown, G.C., Simpson, P.R. and Smith, R.T., 1980, Signatures of metalliferous granites in the Scottish Caledonides: Trans. Instn. Min. Metall. B 89, p. 198-210.
- Plimer, I.R., 1980, Exhalative Sn and W deposits associated with mafic volcanism as a precursor to Sn and W deposits associated with granites: Mineralium Deposita, vol. 15, p. 275-289.
- Ramdohr, P., 1980, *The Ore Minerals and their Intergrowths*, 2nd edition: Pergamon Press, England, 1205 p.
- Reynolds, P.H., Kublick, E.E. and Muecke, G.K., 1973, Potassium-argon dating of slates from the Meguma Group,

Nova Scotia: Can. Jour. Earth Sci., vol. 10, p. 1059-1067.

----- and Muecke, G.K., 1978, Age studies on slate: applicability of the Ar/ Ar stepwise outgassing method: Earth Planet. Sci. Lett., vol. 40, p. 111-118.

-----, Zentilli, M. and Muecke, G.K., 1981, K-Ar and $^{40}\text{Ar}/^{39}\text{Ar}$ geochronology of granitoid rocks from southern Nova Scotia: its bearing on the geological evolution of the Meguma Zone of the Appalachians: Can. Jour. Earth Sci., vol. 18, p. 386-394.

Richardson, J.M.G., Spooner, E.T.C. and McAuslan, D.A., 1982, The East Kemptville tin deposit, Nova Scotia: an example of a large tonnage, low grade, greisen-hosted deposit in the endocontact zone of a granite batholith: Current Research, Part B, Geol. Surv. Can. Paper 82-1B, p. 27-32.

Rickard, D.T., 1969a, The microbiological formation of iron sulphides: in I. Hessland, ed. Stockholm Contributions in Geology, Univ. of Stockholm, vol. 20, p. 49-66.

-----, 1969b, The chemistry of iron sulphide formation at low temperatures: in I. Hessland, ed. Stockholm Contributions in Geology, Univ. of Stockholm, vol. 20, p. 67-95.

Rittenhouse, G., 1943, Transportation and deposition of heavy minerals: Bull. Geol. Soc. Am., vol. 54, p. 1725-1780.

Roedder, E., 1968, The noncolloidal origin of "colloform" textures in sphalerite ores: Econ. Geol., vol. 63, p. 451-471.

Rose, A.W. and Burt, D.M., 1979, Hydrothermal alteration: in H.L. Barnes, ed. Geochemistry of Hydrothermal Ore Deposits, 2nd edition: J. Wiley and Sons, New York, p. 173-235.

Sarkar, P.K., 1978, Petrology and geochemistry of the White Rock metavolcanic suite, Yarmouth, Nova Scotia: Unpub. Ph.D. thesis, Dalhousie University, 350 p.

-----, 1980, Assessment report, Plymouth, Yarmouth County, Nova Scotia: Shell Canada Resources Limited, internal report, 32 p.

Saxby, J.D., 1976, The significance of organic matter in ore genesis: in K.H. Wolf, ed. Handbook of Strata-bound and

- Stratiform Ore Deposits, vol. 2, Geochemical Studies: Elsevier Scientific Pub. Co., p. 111-133.
- Schenk, P.E., 1975, A regional synthesis: in I.M. Harris, ed. Ancient Sediments of Nova Scotia: Society of Economic Paleontologists and Mineralogists (Eastern Section) Guidebook 1975 Field Trip: Maritime Sediments, p. 9-16.
- and Lane, T.E., 1982, Excursion 5B: Pre-Acadian sedimentary rocks of the Meguma Zone, Nova Scotia - a passive continental margin juxtaposed against a volcanic arc: International Association of Sedimentologists Field Excursion Guidebook, 85 p.
- Schulling, R.D., 1967, Tin belts on the continents around the Atlantic Ocean: Econ. Geol., vol. 62, p. 540-550.
- Shcherba, G.N., 1970, Greisens: Int. Geol. Rev., vol. 12, p. 114-150, 239-255.
- Shneider, Yu. A., 1937, Morphological and genetic scheme of the habits of cassiterite: Chemical Abstracts, vol. 31, p. 5723.
- Sinclair, A.J., 1974, Selection of threshold values in geochemical data using probability graphs: Jour. Geochem. Explor., vol. 3, p. 129-149.
- Sinclair, P.E., 1978, An application of Pleistocene geology to mineral exploration in southwestern Nova Scotia: Unpub. B.Sc. thesis, Dalhousie University, 109 p.
- Smith, F.G., 1947, Transport and deposition of the non-sulphide vein materials. Part II. Cassiterite: Econ. Geol., vol. 42, p. 251-264.
- Solomon, M., 1980, "Evidence of exhalative origin for Tasmanian tin deposits" - a discussion: CIM Bull., vol. 73, p. 166-167.
- Spry, A., 1969, Metamorphic Textures: Pergamon Press, England, 350 p.
- Stanton, R.L., 1972a, Ore Petrology: McGraw-Hill, New York, 713 p.
- , 1972b, Sulphides in sediments: in R.W. Fairbridge, ed. The Encyclopedia of Geochemistry and Environmental Sciences: Van Nostrand and Reinhold Co., New York, p. 1134-1140.
- Steele, T.W., Wilson, A., Goudvis, R.G., Ellis, P.J. and

- Radford, A.J., 1978, Analysis of the NIMROC reference samples for minor and trace elements: Nat. Inst. Metall., Rept. no. 1945, 25 p.
- Stemprok, M., 1969, Geochemical association of tin: in W. Fox, ed. A Second Technical Conference on Tin, Bangkok, vol. 1, p. 159-176.
- , 1980, Tin and tungsten deposits of the west-central European Variscides: in J.D. Ridge, ed. Proceedings of the Fifth Quadrennial IAGOD Symposium, vol. I, p. 495-512.
- Stendal, H., 1982, Geochemistry and genesis of arsenopyrite mineralization in Late Precambrian sediments in central East Greenland: Trans. Inst. Min. Metall. B 91, p. 187-191.
- Streckeisen, A.L., 1976, To each plutonic rock its proper name: Earth Sci. Rev., vol. 12, p. 1-33.
- Strong, D.F., 1980, Granitoid rocks and associated mineral deposits of eastern Canada and western Europe: in D.W. Strangway, ed. The Continental Crust and its Mineral Deposits: Geol. Assoc. Can. Special Paper 20, p. 741-769.
- Sutherland, D.G., 1982, The transport and sorting of diamonds by fluvial and marine processes: Econ. Geol., vol. 77, p. 1613-1620.
- Takahashi, M., Aramaki, S. and Ishihara, S., 1980, Magnetite-series/ilmenite-series vs. I-type/S-type granitoids: Mining Geology Special Issue, no. 8, p. 13-28.
- Tauson, L.V., 1974, The geochemical types of granitoids and their potential ore capacity: in M. Stemprok, ed. Metallization Associated with Acid Magmatism(MAWAM): Czechoslovak Geol. Surv., vol. 1, p. 221-227.
- Taylor, F.C., 1967, Reconnaissance geology of Shelburne map-area, Queens, Shelburne and Yarmouth Counties, Nova Scotia: Geol. Surv. Can. Memoir 349, 83 p.
- Taylor, R.G., 1979a, Geology of Tin Deposits: Elsevier Scientific Pub. Co., New York, 543 p.
- , 1979b, Some observations upon the tin deposits of Australia: Bull. Geol. Surv. Malaysia, no. 11, p. 181-207.
- Terry, R.D. and Chilingar, G.V., 1955, Summary of

- "Concerning some additional aids in studying sedimentary formations" by M.S. Shvetsov: Jour. Sed. Petrog., vol. 25, p. 229-234.
- Tischendorf, G., 1973, The metallogenic basis of tin exploration in the Erzgebirge: Trans. Inst. Min. Metall., B 82, p. 9-23.
- , Schust, F. and Lange, H., 1978, Relation between granites and tin deposits in the Erzgebirge, GDR: in M. Stempok, ed. Metallization Associated with Acid Magmatism(MAWAM): Czechoslovak Geol. Surv., vol. 3, p. 123-137.
- Travis, R.B., 1955, Classification of Rocks: Quarterly of the Colorado School of Mines, vol. 50, 98 p.
- Turekian, K.K. and Wedepohl, K.H., 1961, Distribution of the elements in some major units of the Earth's crust: Bull. Geol. Soc. Am., vol. 72, p. 175-192.
- Valliant, R.I. and Barnett, R.L., 1982, Manganiferous garnet underlying the Bousquet gold orebody, Quebec: metamorphosed manganese sediments as a guide to gold ore: Can. Jour. Earth Sci., vol. 19, 993-1010.
- Vaughan, D.J., 1976, Sedimentary geochemistry and mineralogy of the sulphides of lead, zinc, copper and iron and their occurrence in sedimentary ore deposits: in K.H. Wolf, ed. Handbook of Strata-bound and Stratiform Ore Deposits, vol. 2, Geochemical Studies: Elsevier Scientific Pub. Co., p. 317-363.
- Wastnerack, J., Kuhne, R.K and Schulze, H., 1974, Late magmatic and high- to medium-temperature postmagmatic metasomatism in Saxonian Erzgebirge(GDR): in M. Stempok, ed. Metallization Associated with Acid Magmatism(MAWAM): Czechoslovak Geol. Surv., vol. 1, p. 228-231.
- White, D.E., 1981, Active geothermal systems and hydrothermal ore deposits: Econ. Geol. 75th Ann. Vol., p. 392-423.
- Whitehead, R.E., 1973, Environment of stratiform sulphide deposition; variation in Mn:Fe ratio in host rocks at Heath Steele Mine, New Brunswick, Canada: Mineralium Deposita, vol. 8, p. 148-160.
- Yeates, A.N., Wyatt, B.W. and Tucker, D.H., 1982, Application of gamma-ray spectrometry to prospecting for tin and tungsten granites, particularly within the Lachlan Fold Belt, New South Wales: Econ. Geol., vol. 77, p. 1725-1738.